CLIMATE VARIABILITY AND PREDICTABILITY IN TROPICAL SOUTHERN AFRICA WITH A FOCUS ON DRY SPELLS OVER MALAWI

Nicholas Dennis Mwafulirwa

A thesis submitted in fulfilment of the
degree of Master of Science

Department of Geography and Environmental studies

University of Zululand

August 1999

ABSTRACT

The climate variability and predictability in tropical southern Africa at inter-annual time scale is studied. Dry spells are identified using Malawi daily rainfall and circulation patterns are investigated at intraseasonal time scale. The study first examines the temporal and spatial variations of Malawi summer rainfall and relationships with global/regional environmental variables are established. Malawi summer rainfall shows that extreme weather has become more frequent in the last three decades. Three oscillations are identified in Malawi summer rainfall; these are the 2.4 and 3.8 year cycles followed by the 11.1 year cycle. These cycles may be associated with the Quasi-Biennial Oscillation (QBO), El Nino/Southern Oscillation (ENSO) and solar cycle respectively. The summer rainfall indicates strong correlation with Nino3 sea surface temperature and Indian Ocean outgoing longwave radiation (OLR), three to six months prior to the rainy season. Malawi pentad summer rainfall at intraseasonal time scale shows similarity in distribution with other regional pentad summer rainfall, (e.g., onset and cessation dates). Results from spectral analysis of daily rainfall indicate two major cycles, namely the 10-25 and the 30- 60 day cycles. Results from composite analysis, using the NCEP reanalysis data set, reveal distinct circulation patterns prior to occurrence of dry summers over Malawi. The circulation patterns prior to dry summer are dominated by westerly flow which changes latitude, causing subsidence. Below (above) normal sea surface temperatures are observed across the east Atlantic(central Indian Ocean), a pattern typical of El Nino conditions. Pronounced below normal geopotential heights occur during dry summers to the south of Africa and east of Madagascar with corresponding south westerly wind anomalies.

Results from case studies of dry spells at intraseasonal time scale indicate the prominence of deep low pressure cell east of Madagascar and the absence of a well defined Inter-tropical Convergence Zone (ITCZ) over southern Africa. Dry spells are dominated by high pressure cell over Botswana in conjunction with divergent southerlies and subsidence over southern Africa.

Results from composites reveal possible predictors for Malawi summer rainfall: zonal winds, geopotential heights east of Madagascar, SST in the central Indian Ocean and in the south east Atlantic Ocean, and low-level velocity potential over northern Madagascar.

Results from multivariate regression analysis show that lowest predictability is found

in early Malawi summer rainfall (NDJ) while highest predictability is found with FMA rainfall. The highest predictability for November-April (NA) Malawi summer rainfall is associated with sea surface temperature in the southeast Atlantic Ocean and Indian Ocean, sea level pressure over Indian Ocean and QBO in JAS months.

This study has contributed to the understanding of summer rainfall in tropical southern Africa. The knowledge gained can be used by decision makers, farming community, water resource managers for planning and operational purposes. Further statistical forecast models could be developed from precursors (predictors) identified in the study to assist in mitigating the negative effects of climate variability.

PREFACE

The economy of Malawi depends upon rain-fed agriculture. Power sources for almost all industries in the country rely upon hydroelectricity. There are times when the country may experience drought. The Government of Malawi has recognised the importance of climate variability. For example, the government does its budget calculations after the summer rains when crops have been sold. Generally a dry summer season is followed by a small budget for Malawi Government ministries.

These climate variations have not been studied and documented at all time scales in the country. It is therefore important that this be done and used for planning purposes in agriculture and optimum utilisation of water resources.

The intention of this thesis is to understand the kinematic and thermodynamics features associated with extreme summer climate conditions during November-April and their precursor periods May to October with a focus on predictability of dry conditions. These are investigated in this thesis at different time lags using various statistical methods. The study lays the groundwork for further analyses of predictability of summer rainfall over tropical southern Africa and the formulation of forecast models.

The specific objectives of the study are:

(a) To increase the understanding of the summer rainfall variability over tropical southern Africa by examining temporal and spatial characteristics of Malawi summer rainfall at interannual and intraseasonal time scales.

(b) To identify and establish statistical relationships between Malawi summer rainfall and other phenomena such as ENSO, Quasi-Biennial Oscillation (QBO), Sea Surface Temperature (SST), OLR, etc.

(c) To increase the understanding of characteristics of extreme climate conditions before and during summer with emphasis on dry seasons.

(d) To increase the understanding of circulation controls over tropical southern Africa associated with dry spells, as identified in Malawi daily rainfall, at intraseasonal time scale.

(e) To develop statistical forecast models for Malawi summer rainfall.

The lay-out of chapters is as follows:

The study is divided into 7 chapters and maps/diagrams are generally appended at

the end of each section. Chapter 1 provides a motivation and background on rainfall variability and climate over southern Africa with special focus on Malawi, including a literature review. The study is motivated by recurring drought and the absence of any studies undertaken for Malawi in respect of the circulation patterns associated with these dry conditions at any time scale. The hypotheses to be tested are outlined at the end of the chapter after briefly defining drought. Chapter 2 presents the source and use of data and methods of analyses.

Chapter 3 concentrates on investigating the temporal and spatial pattern of Malawi summer rainfall. Malawi seasonal, monthly and pentad/daily rainfall distributions are described, and Malawi rainfall index is presented and its spectral character is described. This chapter also investigates statistical associations between Malawi summer rainfall and other global phenomena such as QBO, SOI, Southern Atlantic SST and pacific SST. The objective of this chapter is to increase the understanding of the summer rainfall variability over tropical southern Africa and to identify possible predictors for forecasting Malawi summer rainfall. The Chapter also touches on intraseasonal oscillations. Here an approximate onset date of Malawi summer rainfall is identified using pentad data and the intervals between wet spells is defined. The chapter presents daily analyses of rainfall and spectral analyses for each season (December-March) covering the1972-1993 period. Dominant oscillations in Malawi daily rainfall are revealed.

Chapter 4 dwells on the composite analyses of dry summers as identified by Malawi summer rainfall (November-April). Precursors are presented in terms of anomaly fields of selected meteorological variables, subsequently used to identify predictors in chapter 6.

Chapter 5 concentrates on two case studies of dry spells in 1980 and 1992. Horizontal and vertical cross-sections are analysed and presented for each case and circulation patterns for each dry spell are shown in terms of anomaly fields of selected meteorological variables. Chapter 6 identifies and presents common precursors and possible predictors from composite analyses of chapter four. The stepwise regression technique is used to select best possible predictors, from a pool of candidates, for Malawi summer rainfall and subsequently statistical forecasting models are developed. Chapter 7 gives the significant findings of each chapter and general conclusions of the entire thesis.

Acknowledgements

I would like to thank my supervisor, Professor Mark R. Jury of the Geography Department and Environmental Studies, University of Zululand, for his tireless guidance and support throughout my research period. This research is partly funded by Water Research Commission of South Africa, World Meteorological Organization (WMO) of United Nations and Malawi Government. I extend my sincerely thanks to them. Special thanks are extended to staff in the Department of Geography and Environmental Studies, University of Zululand, namely Dr. Dube, Mrs. Kozakiewicz, Messrs Mulder, Mthembu, Mpeta, Mwandla and Nhlabathi for their friendliness and making the working environment suitable for research. My special thanks goes to E. Mpeta who made his personal computer programmes available for use. My special thanks also goes to NCEP for making available data in the Internet for public use. The thesis is a contribution to the CLIVAR Africa project of the World Climate Research Programme (WCRP).

Last, but not least, I wish to extend my thanks to the Government of Malawi through Malawi Meteorological Department for allowing me to further my education and the support rendered to me while on training by enjoying all privileges.

CONTENTS

CHAPTER 7: SUMMARY AND CONCLUSIONS

List of figures

Page

List of Tables

Page

Chapter 1

INTRODUCTION AND LITERATURE REVIEW

1.1 Introduction

1.1.1 Rainfall variability over southern Africa

Climate is one of the most important factors determining the agricultural potential of any region. The economies of most countries of southern Africa are heavily dependent on agriculture and most of the crops are rain-fed and the food security in these countries revolves around climate as a resource. Water is a limited commodity. Rainfall over southern Africa shows a high degree of inter- and intra- annual variability. Southern Africa experiences periods of dry or wet of varying lengths ranging from days to decades. Therefore a contribution to an understanding of the climate variability and predictability of summer rainfall at inter-annual and intraseasonal time scales is of great importance to the region experiencing recurring droughts and floods. The knowledge will be of great help to farming community, water resource managers and agriculturalists in the proper planning endeavours for effective management of water resources.

Southern Africa has been plagued by recurrent drought in recent years. The devastating drought of 1982 to 1984, for example, caused the maize crop yields south of 15°S to decline to 10% of historical values and numerous sources of water dried up (Jury and Levey, 1997). The southern region as a whole lost livestock amounting up to 90% in the 1982/83 drought (Makarau, 1995). Similarly in the1992 summer, rainfall was 50% of normal over southeastern Africa which surpassed the drought of 1982-1983 in severity (Jury and Lutjeharms, 1993). The collapse of February rainfall during the 1992 El Nino led to a ten-fold decline in maize yield and large stock losses in Botswana, South Africa, Zimbabwe and Namibia (Jury and Pathack, 1995). Zhakata (1996) reported that the drought of 1981-1985 caused severe social, political, economical and environmental constraints in Zimbabwe and the government had to declare the drought a national disaster and a number of drought recovery programmes were introduced. According to Zhakata (1996) the 1982/83 season was one of the worst on record since 1901 for Zimbabwe. He further reported that in the 1991/92 rainy season 90% of inland dams dried up and crops withered and livestock perished in thousands in Zimbabwe.

According to Dilley (1996) 300, 000 metric tons of food (Maize) was provided by USAID food for peace (FFP) to Malawi during the1992/93 drought. In summary droughts caused social-economic hardships, reduced harvests, negative economic growth rates and even political instability.

The recurrence of droughts over southern Africa in recent years has contributed to an increased interest in the research scientists to focus more attention on the study of climate variability and its predictability. Due to fluctuations of rainfall with its associated floods and droughts over Africa, many researchers have focused their attention on Africa with the aim of understanding and predicting the inter-annual variations of the atmosphere-Ocean system. International programs such as Tropical Ocean Global Atmosphere (TOGA) and World Climate Research Program of Climate Variability and Predictability (CLIVAR, 1995) have been formed in an effort to understand climate fluctuations and their predictability.

Several studies of rainfall variations over southern Africa have focused on the spatial and temporal aspects of these variations. These studies have been made at different time scales. Generally most of the precipitation occurs during the period November to April over southern Africa with highest peaks during the period December to March (Mulenga, 1998). Many of these studies have used monthly or seasonal data to investigate interannual variability. Tyson (1984, 1987) studied the decadal cycles of rainfall while Matarira and Jury (1992) and Levy (1993) have studied the characteristics of rainfall at intraseasonal time scale. Some studies have related variability in rainfall over southern Africa to changes in atmospheric circulation (Tyson, 1981, 1986; Taljaard, 1986b). Other studies have emphasised the significance of relationships between rainfall and circulation forcing (Harrison, 1986; Lindesay, 1988; Harangozo and Harrison, 1983; Lindesay and Jury, 1991). Dry and wet spells of a few days have been studied by Hofmeyr and Gouws (1964); Taljaard *et al* (1987); Lindesay and Jury (1991); Barclay (1992); Matarira and Jury (1992). Rainfall characteristics at large scale over southern Africa have been examined by many researchers (e.g., Hulme, 1992; Diaz, 1996). Temporal cycles of rainfall have been linked to regional circulation adjustments involving interactions between Ocean and atmosphere such as the global phenomenon ENSO (Nicholson and Entkhabi, 1987; Lindesay, 1988).

Climate variability in southern Africa may be recognised by variations in frequency of below or above normal rainfall. Relationships with rainfall events have been investigated. Some studies focus on understanding the circulation patterns during multi-day dry periods (Shulze, 1984; Jury and Lyons, 1992). Rainfall variability over southern Africa has been characterised by Hulme *et al.* (1996) in terms of a regional index. Most parts of southern Africa have registered a decrease in rainfall. Poor rainfall had been noted in the1980's and early 1990's (Mason, 1996) and is thought to be inter-decadal variability. Pronounced decreases in rainfall were noted over Zimbabwe, eastern South Africa and northern Botswana from the late 1970's (Nicholson, 1993, Hulme, 1996). Rainfall over southern Africa tends to be quasi-cyclic. A rainfall periodicity of 18-20-year's is found in northeast South Africa (Tyson, 1986); besides the 10-12 year cycle which accounts for more than 30% of the inter-annual rainfall variance along the south coast of South Africa. Similar findings have been reported by Jury *et al.* (1992) for Botswana and Ngara *et al.* (1983) for Zimbabwe.

The motivation of the research, the problems to be investigated and general objectives of the study are outlined below.

1.1.2 Motivation

The economy of Malawi is dependent on rain-fed agriculture. Malawi (figures 1.1a and 1.2) has been experiencing drought in recent years like most other countries in Southern Africa. During the drought of the1991/92 season, for example, maize production decreased by almost 50 percent (Malawi Ministry of Agriculture Report, 1993) and the Malawi government had to import food to feed the population because of below normal rainfall. Drought returned in1993/94 and 1994/95 seasons with ill- effects.

The total rainfall received determines the type of farming and which crops can be cultivated. Consequently a failure of rains for more than one month in a single year adversely affects agriculture and the economy of Malawi. The time to perform any agriculture related activity is regulated by the seasonal rainfall distribution over the country. Subsequently any fluctuations in total crop yields are attributed to inter-annual rainfall variability.

The farming community and politicians have demanded explanations from meteorologists/climatologists for the causes of these droughts. They require forecasts for the quality of an incoming summer rainfall season. Malawi meteorologists, lacking a detailed scientific understanding of rainfall variability and its predictability in Malawi, could not give a proper explanation with confidence. No serious attempts have been made to understand rainfall variability in Malawi. Atmospheric circulation patterns associated with extreme weather conditions over the country have not been studied. The precursors for dry and wet years for Malawi summer rainfall are unknown and operational statistical forecasting models applied in the prediction of seasonal precipitation in the country are unverified. No detailed studies on relationships (teleconnections) between Malawi summer rainfall and other distant meteorological variables have been done. Therefore this study seeks to address some of these problems by investigating climate variability and its predictability at seasonal and intraseasonal time scales to lay the foundation for further future studies on climate fluctuations in the country. The study will further contribute considerably to the understanding of climate variability over tropical Southern Africa in general and subsequently enhance the ability to predict atmospheric weather conditions at medium and long-range time scales thus mitigating the adverse effects of climate fluctuations. Knowledge gained from the study of climate variability will also contribute to understanding of other environmental related problems such as preservation of ecosystems, environmental degradation or

desertification, optimum food production and pollution. In order to utilize natural resources efficiently, the climate variability should be understood at various time scales. Variations of climate should be accepted by policy makers and economists in order to achieve more sustainable production. In this study the investigation of the variations of the climate over tropical Southern Africa, with a focus on dry conditions over Malawi, will be done at inter-annual and intraseasonal time scales. Drought can not be stopped, but the timely availability of a scientifically based early indication of the most probable nature of the forthcoming rainy season would assist in making contingency plans for coping with it.

The general objective of the study is to identify precursors for dry summers and possible predictors for forecasting Malawi summer rainfall. From these foundations, statistical forecast models are developed.

1.1.3 Malawi climate background and rainfall variability studies

1.1.3.1 Climate background

The domain of study will be from 20°N to 40°S and 30°W to 90°E but with a focus on Malawi (figure 1.2) within tropical southern Africa. Malawi, covering an area of 118,484 square kilometers, is a land-locked country lying between latitudes 9 and 17°S and longitudes 32 and 36°E. Lake Malawi is 571.5 kilometres long and 470 metres above sea level and covers two thirds of the length of the country in the east. It is also a part of the Great African Rift valley. The altitudes of different areas vary from near sea level to more than 1,500 metres in some plateaus and up to about 2,500 metres in mountainous areas rising to 3,000 meters at Mt. Mulanje in southern Malawi.

Malawi experiences a tropical type of climate with two seasons, namely the rainy season and the dry season. The rainy season is experienced from November of one year to April of the next year while the dry season is experienced from May to October. Summers are generally hot and wet while winters are cool and dry. According to Torrance (1972) the climate of Malawi depends on the ITCZ, the subtropical high pressure belt in the south between 25° and 35°S, and its topography.

Malawi is usually being affected by a broad belt of a strong convective activity during the rainy season (figure 1.3). This ITCZ belt, which is the main rain bearing system, marks the converging point of northeasterly monsoon of the Northern Hemisphere and

the southeasterly trade winds of the Southern Hemisphere. The belt is known as Inter-Tropical Convergence Zone (ITCZ), lagging behind the sun by a month or so (Hsu and Wallace, 1976; Kidson, 1977). It invades the country from the north on its southwards movement to its southern limit in February and then moves back to the north. During the rainy season the ITCZ may oscillate over the southern tropical areas in sympathy with pressure changes usually across South Africa. The other main rain bearing system for Malawi weather during the rainy season is the Congo Air Boundary (CAB) which marks the confluence between the Indian Ocean southeast trades and recurved South Atlantic air that reaches Malawi as northwesterly airmass through the Democratic Republic of Congo. This system brings well-distributed rainfall over the country and even floods may be experienced in some areas especially if it is associated with the ITCZ. There are times when the country is affected by tropical cyclone originating from the Indian Ocean. Depending on its position over the Indian Ocean, a cyclone may result in having either a dry or a wet spell over Malawi. The other weather features of significance are easterly and westerly waves, and temperate weather systems. The extra tropical waves are believed to be active during the start and end of the rainy season. During winter Malawi is influenced by a divergent southeasterly airmass driven by high pressure cells southeast of Africa. A strong high pressure cell over the eastern South African coast draws a cool moist easterly airmass into the country causing overcast conditions with drizzle over highlands and east facing escarpments near Lake Malawi, locally called "chiperoni". These weather conditions usually last for two to three days.

1.1.3.2 Past studies of climate variability in Malawi

Literature on the study of climate variability specifically on Malawi is almost non-existent at all time scales. Consequently this study will serve to fill the gap for Malawi. However, a few localised studies on rainfall variability have been attempted.

Nkhokwe (1996) reported that there was strong positive correlation between Malawi summer rainfall of southern areas, central lakeshore and northern areas of the country with Ethiopia/Eritrea rainfall. However, according to Nkhokwe (1996), rainfall over central inland areas of the country indicated poor correlations. Localised associations were observed between summer rainfall and stratospheric QBO and monthly phases of the SO from July to December was significantly correlated with JFM and FMA rainfall for most stations. Nkhokwe (1996) used Malawi monthly station rainfall covering the

period 1957-1987 from 20 stations. Monthly data were binned into overlapping three monthly averages from which normalized indices for each station were created. Similarly the indices were created from Ethiopia/Eritrea (Northern Hemisphere summer period) monthly rainfall. The aim of the analysis was to find out if Malawi summer rainfall could be predicted from Ethiopia/Eritrea rainfall. Nkhokwe (1996) applied multi-variate correlation technique to develop some statistical forecasting models one for each station. However, their validations have not been operationally tested with independent data in the country.

Kamdonyo (1993), using a percentile technique adopted from Australia researchers, attempted to demarcate the spatial and temporal extent of Malawi's cyclical drought. He used rainfall in the analysis but no attempt was made to investigate circulation patterns at all time scales. In this thesis, the focus is on the entire season November-April and on the entire country. The common precursors for extreme weather conditions (dry and wet summers) are identified using composite analysis. The circulation features associated with extreme weather conditions are identified through analyses of NCEP data at seasonal and intra-seasonal time scales.

The section that follows gives a brief description of the observed climate of southern Africa through literature review. There are several research papers on climate variability studies but only selected papers, especially those documenting SST, ENSO, circulation patterns and satellite OLR, will be cited in an attempt to focus the research. It should be noted that most climate variability studies consider multi-month periods, within summer. In this study, the focus is on November-April (NA) Malawi rainfall at inter-annual time scale and December to March (DJFM) at intraseasonal time scale.

1.2 Literature review

Major rain-bearing systems over southern Africa

The circulation patterns and climate over southern Africa have been explained in several publications (Tyson, 1984, 1986; Lindesay and Vogel 1990; Matarira and Jury 1992; Jury and Levy 1993). The climate of southern Africa is characterized by a high degree of intra- and inter-annual variability and rainfall is erratic in both time and spatial distribution. The seasonality of rainfall can best be understood in the context of the wind and pressure systems (Nicholson *et al.*, 1988). According to Theron and Harrison (1990)

the thermodynamic characteristics of the underlying subcontinent are responsible for influencing the mean circulation patterns over southern Africa. They note that convective heat fluxes have greater influence in the upper troposphere while the mechanical forcing tend to dominate in the lower atmosphere.

The climate of southern Africa is influenced by the position of the subcontinent in relation to the major circulation features of the southern hemisphere (Torrance, 1972; Tyson, 1986; Preston-Whyte and Tyson, 1988). Southern Africa is generally under the influence of a sub-tropical anticyclone throughout the year. The region usually experiences one rainy season starting in late October and extending to early April with the exception of the southern Cape Province which gets rainfall mainly in winter. The influences of the ITCZ are more evident within latitudes 0-20°S than beyond where temperate weather systems become more dominant. Mason (1997) argued that statistically significant mid-latitude response to boundary-layer forcing, in temperate latitudes, could not be identified easily due to the high degree of internal atmospheric variability and that climate extremes could occur even in the absence of forcing. Consequently areas south of 20°S are influenced by interaction of temperate and tropical features, with rainfall decreasing from east to almost complete aridity in the Namib desert further west (Tyson, 1986). An interior thermal low and moist north-easterly flow deepen during early November (Matarira and Jury, 1992). Upper westerly waves are prevalent during early summer and their influence tapers off as the season progresses to mid summer. Subsequently inland troughs and tropical easterly systems become most active weather features. In other words, convective rainfall is prevalent during austral summer over southern Africa. During this time of the year, a heat low (tropical low) develops over Botswana while an inter-Tropical Convergence Zone (ITCZ) lies over the southwestern Indian Ocean along about 10°S. Pronounced easterly flow extends from the edge of the South Indian Ocean anticyclone into Southern Africa then recurving southwards into a low pressure cell over Botswana. A maximum convective rainfall band may develop in the northwest-south east direction and shifts position in sympathy with pressure changes across South Africa.

Variations in the atmospheric pressure, in conjunction with changes in wind field, modulate the occurrence of extended dry and wet spells over Southern Africa. During the period of a few dry days surface pressures tend to be above normal while during wet days they tend to be below normal over the region (Preston-Whyte and Tyson,1988).

Preston-Whyte and Tyson (1988) reported that on the scale of about a month during a period of dry spells, negative surface pressure anomalies tended to occur in the Gough Island region and positive anomalies occupied over Marion Island and over land. They found opposite tendencies during period of wet spells. They further observed that in the middle level (500 hPa) a quasi-stationary trough developed in the westerlies over the west coast region, leading to wetter conditions over the summer rainfall region of southern Africa. Analyzing and comparing months in two near-decadal spells of dry and wet spells they noted that at the 500 hPa level the pressure anomaly fields showed distinctive regional gradients and opposite patterns. In the middle troposphere during wet conditions, negative pressure anomalies occurred over the interior whilst strongest positive deviations were observed over the south-western Ocean area in the region of Gough Island. Weaker positive deviations occurred over the adjacent southern and south-eastern Ocean areas (Preston-Whyte and Tyson, 1988). They noted an opposite gradient during dry conditions. It should, however, be argued that rainfall generating systems over Southern Africa and indeed elsewhere vary from one part of the country to another (Dyer,1979).

Southern Oscillation and Walker Circulation influence on rainfall

The Southern Oscillation and Walker Circulation have a strong influence on rainfall variability over southern Africa (Lindesay *et al.*, 1986). Generally below normal rainfall is experienced over southern Africa during ENSO year and above normal rainfall during non El Nino year (Nicholson and Entekhabi, 1986; Lindesay, 1988). Dry years are characterised by anomalously easterly wind regime at low levels and westerly winds at higher levels over the tropics. During wet years westerly winds are dominant at lower levels and are associated with easterly winds at the higher levels. The meridional flow increases equatorward during ENSO years (dry years) and increases poleward during La Nina (wet years) over southern Africa. The ascending branch of the Walker Cell in the Indian Ocean is located over tropical Africa during La Nina years with the consequence of enhanced convection over these areas. The meridional cell (Hadley circulation) becomes more dominant. This configuration contributes to a pronounced Inter-Tropical Convergence Zone between temperate and tropical synoptic systems (around 20°S) whilst the subtropical anticyclone intensifies near 30°S. Subsequently, according to Harrison (1986), easterly flow strengthens due to the strong pressure gradient between

north and south. The easterly flow is being controlled (modulated) by zonal circulation (Walker circulation) carrying moisture into the Inter-Tropical Convergence Zone over Africa (Tyson, 1986). Wet years over southern Africa are associated with an enhanced Walker circulation. Weather systems shift during warm ENSO years. During this period there is a general eastwards shift of locations of maximum convection. The cloud bands (the tropical-temperate troughs) are located frequently to the east of the southern Africa with the consequence that latent heat and water vapour are transported to the higher latitudes over the South Indian Ocean and Madagascar. In other words cloud bands are observed over and east of Madagascar during dry summers over the African subcontinent (D'Abreton, 1992; Vanden Heever *et al.*, 1997). Detailed information about the Walker Circulation and its influences on southern African rainfall may be found in Tyson (1986); Preston-Whyte and Tyson (1988) and in many other papers.

Circulation regimes and associations

Preston-Whyte and Tyson (1988), by identifying time changes in pressure gradients between specific stations in the southern African region, correlated changes in geostrophic flow patterns to changes in rainfall over the region. They developed correlation fields, using period 1958 -1978, for the relationship between 500 hPa wind anomalies with some rainfall data over southern Africa. They observed that the occurrence of tropical easterly flow and easterly waves could be inferred from the Durban-Bulawayo pressure index and Alexander Bay-Windhoek index respectively. They noted that both indices showed positive correlation with rainfall and indicated that at an annual scale an increase in rainfall over northern parts of South Africa followed tropical easterly flow at 500 hPa. Rainfall increases over western regions as pressure rises over the Gough Island region and an upper trough develops over the west coast. Analyzing various flow types at both 850 and 500 hPa and subsequently extracting dominant controls which contribute to annual rainfall, Preston-Whyte and Tyson (1988) concluded that the predominant annual circulation controls of southern Africa's rainfall are at the 500 hPa level, save for the far northeastern Transvaal where a localized Indian Ocean Anticyclone control is important. They linked Marion Island blocking to both blocking and the occurrence of tropical-temperate cloud bands which brings a north-west to south-east band of rain to Africa.

In an effort to examine the spatial and temporal modes of meteorological variables, Dyer (1981) used PCA technique to create unrotated eigenvectors of monthly mean sea level pressure covering period from 1951 to 1977 over the South Atlantic Ocean and Indian Ocean. Tyson (1981), interested in finding causes of extended dry and wet spells, investigated circulation patterns using surface pressure for the area extending from 20°S to 40°S and 10°W to 60°E at resolution 10° by 10 ° and upper air data for the period 1956 to 1977. He found that wet spells were associated with low pressure over the interior of the subcontinent and higher pressure near Gough Island. The 18-year rainfall cycle over Southern Africa was thought to be controlled by wave number one in the circumpolar westerlies. Consequently north-south shifts in the location of the anticyclone in sympathy with wave number one may result in dry or wet conditions over southern South Africa.

According to Tyson (1984) differences in annual rainfall from year to year may be associated with tropospheric circulation patterns. It was noted, after examining the differences in annual geopotential heights at 850 hPa and 500 hPa levels between 16 stations across southern Africa and surrounding Oceans, that variations in rainfall were linked to fluctuations in low latitude easterly winds the disposition of troughs. Tyson (1984) observed that easterly waves with a pronounced trough axis appearing over Botswana appeared to cause wet conditions. Miron and Tyson (1984) observed that wet spells were associated with pressure anomalies: negative over central areas of the subcontinent and positive deviation over south-western Ocean areas in the proximity of Gough Island.

Jury and Pathack (1991) observed areal averaged rainfall departures exhibit 6.25 year cycles in NE Madagascar and 12.5 and 18.75 year cycles in SW Madagascar and Zimbabwe respectively. They found that summer rainfall and meridional winds in Northeast Madagascar and Zimbabwe are out of phase and negatively correlated (Jury and Pathack, 1991). They used Hovmoller-type satellite imagery composites to investigate the presence of synoptic weather systems. They found that convective structure was dominated by transient easterly wave in the 10-20°S latitude belt with 15-20 days as a common period.

According to Lindesay and Jury (1991) the coupling between tropical easterly waves, an Anticyclone centred over Mozambique channel and westerly waves in mid-latitudes

resulted in the flood of February 1988. Interaction between the upper westerly waves and the ITCZ over Zambia was also similarly identified by Kumar (1978).

Barclay *et al.* (1993) investigated differences in the convective potential of troughs passing over southern Africa in the early summer using synoptic weather data and radiosonde time height sections. The study area was 20-30°S, 20-30°E. Wet and dry cases were chosen on the basis of the intensity and distribution of rainfall, sharp thermodynamics changes across the plateau and the passage of geopotential wave. The aim of their study was to understand the weather controls in October and November and to identify differences in the convective potential of early summer transient westerly troughs over southern Africa. They observed that the 500 hPa structure obtained by differencing wet and dry composites was dominated by low geopotential height and cyclonic vorticity over the plateau near 25°S, 25°E and high geopotentials and anticyclonic vorticity to the south over the Oceans near 40°S, 30°E. In this study, insight on climate variability has been similarly assessed..

Jury and Majodina (1997) investigated the climatology of southern Africa extreme weather during the period 1973-1992 in the domain 15-40°S, 5°W, 60°E using daily weather maps. Using strict criteria: rainfall > 70 mm/day and temperature > 38°C . They analysed extreme cases. Temperatures showed increasing trend in all regions with 1992 having highest temperatures. They found that rainfall north of 30°S was negatively correlated with lows and winds over the sea to the south. Thus a year with more frequent and intense mid-latitude lows coincided with drought in the subtropics.

Preston-Whyte and Tyson (1988) have analyzed rainfall variability in terms of dry and wet spells of different time scales over Southern Africa. They used October-September to analyze percentage of mean rainfall for different designated dry and wet spells. They found that 1971/72-1980/81 was dominated by wet spells on a subcontinental scale notably in central South Africa, Southern Botswana, Namibia and Zimbabwe. They noted that this was the most persistent wet spell with six consecutive years experiencing above normal rainfall. They further observed that 1962/63-1970/71 was dry over the whole subcontinent. They found that dry spells are more persistent than wet spells and have greater areal extent and spatial homogeneity. The circulation patterns associated with either dry or wet conditions have been determined and have been correlated with global circulation (Tyson, 1986). Tyson (1986) reported that enhanced rainfall is associated with winds of a northerly component over the interior, while southerly winds

enhanced rainfall over the coastal areas of south eastern South Africa. According to Tyson (1986) the occurrence of dry conditions over a summer rainfall region of southern Africa has been associated with weakened easterly winds while wet conditions with strengthening of the tropical easterly wind regime. The occurrence of rains from a specific synoptic situation may be modulated by planetary controls such that their frequency of occurrence, intensity and speed of passage may produce an excess or absence of rainfall over periods of days.

Regional teleconnections

The study of relationships between meteorological variables and rainfall variability over a region are useful because the knowledge obtained from such findings may assist in explaining the characteristics of weather and climate. Conceptual models could be formulated. Most of research work to date has assumed that the climate variability over the whole southern region is homogeneous and weather responses to teleconnections are then constant (Makarau, 1995).

Significant work has been done on rainfall variability in the region as related to ENSO events. Walker (1924), looking for predictors for Indian rainfall, observed that the fluctuations of monsoon rainfall are significantly correlated to the phenomenon known as the Southern Oscillation (SO) which is a large- scale see-saw of atmospheric mass between the Pacific and east Indian Oceans in the tropics (Montgomery, 1940; Abu-Zeid *et al.*, 1992). Changes in pressure between these Oceans is measured from observations at Tahiti and Darwin, quantified by the Southern Oscillation Index (SOI); the difference in standardized monthly mean in sea level pressure between Tahiti (17.5°S, 210.4°E) and Darwin (12.5°S, 131°E).

El-Nino is characterised by anomalous warming of the equatorial eastern Pacific waters off the coast of Peru and Ecuador. Generally weak warm currents develop off the coast of Peru and Ecuador around Christmas every year. The SO and El-Nino are closely related phenomena and are referred to as El-Nino/Southern oscillation (ENSO) which may be defined as a low frequency phenomenon arising from the instability of the coupled tropical Ocean-atmosphere system. The Southern Oscillation has been studied extensively since the pioneering works of Walker and Bliss (1937)after identifying teleconnections from the Pacific by Bjerknes (1966, 1969).The Walker Circulation atmospheric cells tend to be zonal and are directly responsive to sea surface temperatures

over the eastern and western Pacific Ocean (Preston-Whyte and Tyson, 1988). The Ocean gains maximum radiative heat over the area where the SST is lowest whilst ENSO is associated with surface wind stress and cloud frequency (Kilonsky and Ramage, 1976). Rainfall is concentrated in the zones of maximum surface wind convergence and upper air divergence, along the ITCZ off the equator.

Southern Oscillation Index (SOI) correlations

Climate variability in southern Africa has been linked to the Walker circulation and Southern Oscillation. Lindesay (1987), using seasonal and annual rainfall covering a period 1935-1983, found a definite pattern of spatial correlation between rainfall and the Southern Oscillation Index. Events initiated in the South Pacific Ocean play a role in determining pressure, temperature and wind anomalies and subsequently rainfall over southern Africa through sub-tropical wave trains.

The relationship between the Southern Oscillation Index (SOI) and rainfall in Southern Africa has been investigated (Nicholson and Entekhabi, 1986; Lindesay, 1986; Hastenrath, 1995). According to Helpert and Ropelewksi (1992), below normal surface temperatures occur from June through August prior to the onset of good summer rainfall for southern Africa (La Nina) while above normal temperatures during the same period proceed El Nino years. Consequently observed warmer (cooler) winter temperatures in southern Africa are associated with below (above) normal rainfall the following summer. Other studies dwell on the relationships between Southern Oscillation Index (SOI) and circulation indices of southern Africa (e.g. Tyson,1984; Lindesay, 1986). Relationships between rainfall across South African and atmospheric circulation variables associated with SOI have been investigated by Lindesay (1988). After determining the correlation between SO and rainfall across South Africa, Lindesay (1988) correlated fluctuations in SOI with the circulation and other meteorological variables over southern Africa during the period 1957 to 1983. Results showed that during the early months of October and November correlations of both signs were observed over South Africa. Lindesay (1988) found that the correlations were rather poor and there was no spatial coherence in the distribution of oppositely correlated areas. Positive correlations, with spatially coherent areas, were found over central parts of South Africa during the months December, January and February while an opposite pattern was found over the south-west Cape province. It was observed that a zone of high positive correlations was

oriented in the north-west to south-east direction during the months December-March which was probably due to tropical and temperate trough influences. It was found that SOI accounted for only 20 percent of rainfall variability over central South Africa. According to Lindesay (1988) the results of spectral analyses of central South African summer rainfall at periods of the Southern Oscillation confirm the thermodynamics that connect phase changes of the oscillation with changes in circulation over southern Africa.

According to Harrison (1984) the Southern Oscillation modulates the occurrence and preference in location of strong convection which contribute a large part of summer rainfall over South Africa. However, ENSO is associated with above normal rainfall over East Africa (Ogallo, 1987).

Preston-Whyte and Tyson (1988) reported that Southern Africa rainfall is inversely correlated with rainfall over the equatorial belt of Africa. Detailed discussions on spatial and temporal fluctuations of rainfall over Africa may be found in Nicholson (1986) and Janowiak (1988). Temporal characteristics of rainfall anomalies over Southern Africa indicate a significant peak at a 5-6.3 year cycle over Malawi, Zambia, Western South Africa and southern Namibia (Nicholson, 1986). Significant coherence with El Nino Southern Oscillation in this range was identified over Malawi, northern South Africa, Angola and southern Zambia.

Some earlier and detailed description of the ENSO phenomenon can be found in the works of Horel and Wallace (1981); Rasmusson and Carpenter (1982); Kousky *et al.* (1984); Cane, Zebiak and Dolan, (1986); Ropelewski and Halpert (1987); Philander (1989) and Asnani (1993).

Quasi-Biennial Oscillation (QBO) correlations

Some studies have related stratospheric QBO phases to rainfall variability. QBO refers to a zonal wind in the equatorial stratosphere which changes direction from easterly to westerly and vice versa with a periodicity of about 28 months (Naujokat, 1986). These wind regimes propagate downwards at a rate of 1.2 km per month and they have a maximum amplitude at about 20 hPa level. The easterlies persist for a longer period at higher level than westerlies, and are stronger than westerlies. There is a time lag within 30 and 50 hPa for the change in the phase from westerlies to easterlies. The easterlies are slower to propagate downwards than westerlies. According to Naujokat (1986) these

alternating descending stratospheric wind regimes have been noticed in all equatorial some areas such as Kenya, Singapore and Canton Island.

The QBO phases have been associated with inter-annual variability of summer rainfall in southern Africa. QBO enhances rainfall when it is in a westerly phase, providing other factors particular to ENSO, are favourable and enhances drought if it is in an easterly phase and the other ENSO factors are negative (Mason and Tyson, 1992). According to Jury *et al* (1993) there is a significant negative correlation between OLR over East Africa in November and 30 hPa QBO at 0 to +2 months lag. Jury *et al.* (1994) have determined that upper tropospheric winds are correlated with QBO over southern Africa yielding easterly flow within which an anticyclonic gyre lies southwest of South Africa and a cyclonic gyre lies over Zimbabwe at 200-500 hPa level.

According to Ogallo (1984) during short rains (October to December) and long rains (March to May), the association between stratospheric westerly winds and above normal rainfall over East Africa is 80% while the association between the stratosphere easterly wind and below normal rainfall during short and long rains were respectively 71% and 75%. According to Ogallo (1984) results from cross-correlation analysis does not give statistically significant correlations between rainfall and patterns of stratospheric zonal winds. Ogallo (1993), using Kenya upper wind data, investigated the QBO over tropical eastern Africa and confirmed the relationship with seasonal rainfall. Westerly and easterly wind regimes were observed at 30 hPa to propagate downwards at a rate of 1.2 km per month, in agreement with findings of Plumb (1984). Results from spectral analysis showed dominant peaks around 28 months.

There is relationship between the stratospheric QBO and the onset and maintenance of cold and warm ENSO events. Mukherjee, *et al.* (1985) have pointed out that a westerly phase of QBO is associated with an active monsoon over India while an easterly phase is associated with a weak monsoon. Some characteristics of QBO can be found in Holton and Lindsen (1972); Trenberth (1980); Gray *et al.* (1991) and Knaff *et al.* (1991). It should be pointed out that no clear mechanisms are yet defined for interaction between the QBO, the troposphere circulation and convection over Africa.

Sea surface temperature (SST) and OLR correlations

Many studies have related African rainfall variability to sea surface temperature (SST) over the Atlantic, Indian and Pacific Oceans. The relationship between SST in the tropical Atlantic and African rainfall has been studied by Hirst and Hastenrath (1983) for Angola. Nicholson and Entekhabi (1987) looked into rainfall variability in equatorial and southern Africa in relation with SST along the southwest coast of Africa. Nicholson and Entekhabi (1987) observed that a warm central Indian Ocean was associated with enhanced rainfall over East Africa but found weak correlations between East African rainfall and global signals such as SOI and QBO. Ogallo (1987) observed that the highest correlations between East African rainfall and SSTs during northern winter were concentrated over the Indian Ocean.

Nyenzi (1988) looked into the relationship between East African rainfall variability and SST over both the Atlantic and Indian Oceans. It was observed that fluctuations of SST off Angola were often out of phase with other global signals (for example SST in Indian Ocean). Using an annual series of Sahel rainfall formulated by Nicholson (1985) which were divided into 5 driest and 5 wettest years covering July to September from 1950 to 1980, Folland, Palmer and Parker (1986) found that the dry years had substantially higher SST in the Indian Ocean, South Atlantic and the southeast tropical Pacific but lower SST in the North Atlantic, North Pacific and the Mediterranean. They further found a strong statistical relationships between seasonal rainfall in the Sahel and global SST and formulated patterns to force the global atmospheric general circulation of the U.K. Meteorological office. They, however, argued that the discovery of relationships between SST and African rainfall should not preclude the importance of local effects from the earth's surface on the seasonal time scale.

Walker (1989) found that rainfall is enhanced when SST in the subtropical belt of the eastern Agulhas current is above normal during and prior to La Nina years. She used monthly SST and surface wind of gridded ship data over the southeast Atlantic and south-west Indian Oceans in correlation analysis with South African plateau rainfall. It was observed that in normal years significant correlation is found between rainfall with Benguela and Agulhas SST. In wet years surface wind composites showed increased easterlies in the subtropical belt especially to the east of Madagascar. Walker (1989) recognised the importance of Agulhas current area to the south of Africa and observed that the difference between composite wet and dry summers showed that SST over the

area were 10% above normal during wet years. She proposed that a warmer than usual Agulhas current enhances links between tropical and temperate troughs over South Africa.

Nicholson and Nyenzi (1990) used empirical orthogonal function (PC) and spectral analysis to study the spatial and temporal patterns of SST variations in the Indian and Atlantic Oceans. Their results showed that the variations in SST were coherent over most of the tropical the Oceans in the 5-6 year range. It was observed that anomaly fields of SST appeared to move eastwards from northeast of Brazil with the Indian Ocean lagging the western Atlantic SST by four to eight months and the eastern Atlantic lagging the western Atlantic by two to six months. The greatest coherence of SST anomalies was identified from 20°N to 35 °S in the Indian Ocean and from 10°N to 30°S in the Atlantic Ocean and appeared to be approximately in phase.

Mason (1992) identified links between SST in the surrounding Oceans over southern Africa and rainfall variability over South Africa. It was argued that areas over the Ocean with greatest variability in SST may not necessarily have the greatest influence on rainfall. Mason (1992) applied PCA technique on U.K. Met Office marine data at 5 ° interval and considered the South West Indian Ocean and South Atlantic Ocean. Using the SST data for the period 1910 to 1989 eight principal components were identified. Mason (1992) observed that after ranking the response of rainfall to SST variability over all years in the period 1953 to 1989 in terms of statistical significance for the whole summer region, the SST changes in three areas, namely Central South Atlantic Ocean (PC5), South Atlantic Subtropical Convergence region (PC8) and western equatorial Indian Ocean (PC4) have strongest influence on rainfall of South Africa. Mason (1992) further observed changes in SST in these regions do not have a unique atmospheric response probably due to the modulating effect of QBO over southern Africa (Mason, 1992; Jury and Pathack, 1993). Mason (1992) performed correlation analysis on rainfall and SST with easterly or westerly QBO and found that the Ocean region associated with greatest rainfall response was the Indian Ocean south east of South Africa (QBO easterly). It was followed by south Atlantic Subtropical Convergence region with westerly QBO and lastly Benguela system (South East tropical Atlantic) with westerly QBO.

Mason *et al.* (1993) have reviewed the fluctuations in atmospheric circulation that produce drought over South Africa including links between regions of homogeneous

SST variation in the surrounding Oceans around South Africa. They noted that the variability of South African climate may be due to changing synoptic conditions and pressure patterns from scales of weeks to years.

The influence of the Indian Ocean on Africa climate has drawn the attention of many researchers. Ogallo (1987) observed that the highest correlations between East Africa rainfall and SSTs during northern winter were concentrated over the Indian Ocean.

SST over the central Indian Ocean (0-10°S, 60-80°E) has been associated with southern African rainfall (Pathack, 1993). It was observed that the correlation was as high as -0.6 at lags of -3 and -6 months.

Jury (1996) found that SST in the equatorial Indian Ocean correlated significantly with South African rainfall ($r < -0.6$) at -2 and 0 month lags and were associated with the El Nino. He observed that SSTs of the central Indian Ocean modulates the overlying monsoon trough. He noted that a centre of convective action alternates between southern Africa and the south-west Indian Ocean from year-to-year. Area-averaged summer rainfall indices were used from station data for north-central South Africa, northeast Namibia and Zimbabwe. These were correlated with gridded fields of seasonal indices (3-months means) of SST covering the period 1955-1988. Positive correlations were observed at lag -2 months with South Africa in the Atlantic Ocean while negative correlations were found over south of India in the central ocean basin and off the east African coast with Zimbabwe and Namibia. Strongest correlations of $r \approx -0.4$ were found in the region 5°N-5°S, 70-85°E with Zimbabwe ans Namibia (Jury, 1996).

According to Jury and Pathack (1991) the correlation between SSTs and convection (Outgoing Longwave Radiation) shows that a warming of waters within the cyclogenesis region northeast of Madagascar triggers decreased rainfall to Southeast Africa. The circulation pattern may be explained as follows: Low pressure is formed over warmer SSTs northeast of Madagascar, consequently south easterlies and northeasterlies tend to converge there thus depriving southern Africa of moisture. The result is that southern Africa experiences drought. According to Jury *et al.* (1991), the increased low level westerly anomalies off the northern tip of Madagascar reduces the inflow of moisture and subsequently limits rainfall over southern Africa. Likewise low-level easterly anomalies south of Madagascar in the region 25-35°S, 40-55°E, result in cyclonic centred over Madagascar in dry summers and oppose convective outflows. Strong

convective activity across equatorial eastern Africa, northeast Madagascar and the Southwest Indian Ocean matches with below normal convective activity across southern Africa. The importance of low level pressure anomalies over Madagascar was also reported by D'Abreton (1992) who used ECMWF data to identify dry and wet spells. D'Abreton (1992) reported that daily seasonal convective variability was governed by responses to anomalies of SST in the west Indian Ocean.

Using COADS data, Rocha (1992) investigated regional teleconnections controlling rainfall variability over southeast Africa and found that central Indian Ocean SST is important to southern Africa summer rainfall. Rocha (1992) utilized COADS gridded data and results of the correlation analysis and General Circulation Model (GCM) experiments indicated the greatest influence of central Indian Ocean SST to Southeast African summer rainfall. The global PC1 SST variance was related to the ENSO signal in the eastern equatorial Pacific Oceans and central Indian Ocean. Warming in the eastern Pacific Ocean was in sympathy with the warming in central Indian Ocean (0-10°S, 60-80°E) in dry years.

Jury *et al.* (1996) investigated climate determinants of summer drought over northern South Africa. They used 25 stations covering the period 1950-1988.They correlated January-March normalized rainfall with regional patterns of OLR and SST for countries such as Namibia, Botswana and Zimbabwe; results of which showed statistically significant correlation of greater than +0.6. Convection over southern Africa is modulated by common climatic processes. They observed significant correlation coefficients of greater than -0.5 between SST in the central Indian Ocean and February rainfall from 0 to -9 months lags. The strong statistical associations lead to the conclusion that the strong convection and SST in the central Indian Ocean precedes and sustain late-summer drought over Southern Africa.

Jury and Pathack (1991) studied the variability of summer convection and circulation over the tropical Southwest Indian Ocean. They used satellite derived OLR data at a resolution of 5° interval, area- averaged rainfall and SSTs. Inter-annual trends were examined by analysing January-February zonal and meridional wind indices from Zimbabwe, Madagascar and Mauritius. SST indices covered the period 1949-1984 and OLR was of shorter period. They observed areas of lowest OLR was associated with the ITCZ. Their correlation results show correlation of -0.9 between OLR and rainfall

departures in January and February which lie across the 10°S latitude extending further south in the proximity of Madagascar. They observed that maximum convection was greatest in the longitude 20-35°E over northern Zambia and reduced over the SW Indian Ocean. They found that circulation variability was dominated by quasi-decadal cycles and a trend of increasing westerlies.

Pathack (1993), using the COADS SST data has shown that early summer (November) rainfall over South Africa is correlated positively with central Atlantic SST. Cooling in the central Indian Ocean stimulates February rains. Pathack (1993) found there was strong correlation (r = +0.9) between February rainfall and preceding October OLR in the central Indian Ocean (0°S, 70°E).

Jury and Pathack (1993) investigated climate patterns associated with extreme modes of summer rainfall over southern Africa using composite techniques. Composite differences between the wet summers of 1970s and the dry summers of the early 1980s were analysed. They used composite differences between the four wettest and four driest summers (January and February) over the period 1975 -1984. Composite difference fields were analysed for OLR, SST and upper and lower tropospheric wind. Their results for OLR difference field indicated the widespread nature of convective variations with a consistent sign in the domain 15-33°S, 0-40°E. An opposing sign was observed over the southwest Indian Ocean, representing a dipole whereby wet summers over southern Africa coincide with dry summers over the adjacent Ocean. The dipole characteristic was regarded as a primary mode of inter annual climatic variability over southern Africa. Composite differences of SST were negative over large areas of the central equatorial Indian Ocean and SE Atlantic Ocean and positive to the south of Africa where the Agulhas Current is active. Wind composites showed distinct different circulation patterns during the extreme summers: upper westerly and lower easterly circulation anomalies occurred over the tropical zone off the east coast of Africa and a pronounced anticyclonic gyre was positioned over positive SST differences SE of Africa.

Similar methods are employed in this study in chapter six.

Jury and Levey (1992) have analysed the climatology and characteristics of drought in the eastern Cape of South Africa. In order to quantify the cycles of drought and background climatic forces, they initially used monthly rainfall data from two stations covering the period 1877-1987 and seven stations covering 1969-1987 (March and

October) over the domain 10-41°S, 0-60°E and constructed yearly standardized indices. Spectral analysis was performed on rainfall data and the index was correlated with the SOI and other climatic variables in surrounding areas. The background circulation of drought was studied using regional wind from the Climate Analysis Centre (CAC), and SST and OLR from COADS. They used composite analysis to the selected three driest and three wettest March and October months. According to Jury and Levey (1992) results of composite analysis showed that the droughts of 1950s and 1960s were more sustained than the 1982-1984 drought. The wet periods of 1974 and 1976 were similar to those of early 1950s. They observed that the highest spectral peak from two stations with long period was in the range 16.6-20 years cycles. Another distinct cycle was at 3.5 years. Drought in March was associated with cool SST to the south-west and east in the Indian Ocean and an intense anticyclonic gyre in the south-west Indian Ocean, and stronger westerlies in mid-latitudes. Drought in October was associated with a NW-SE band of reduced convection extending from tropics to mid latitudes.

Jury *et al.* (1992) employed correlation analysis between OLR and a standardized summer rainfall index over Botswana using a short1975-1984 data set for January-February period when convective activities are at a maximum. Rainfall data were for Zambia, Zimbabwe, Mozambique, South Africa, Namibia and Botswana obtained through Nicholson of Florida State University. Their results showed statistically significant correlations across the region 20-33°S, 20-30°E ($r = -0.67$) and $r = -0.93$ at 24°S, 25°E: a sympathetic pattern. Positive correlations were observed over Madagascar and along 10°S. Jury *et al.* (1992) investigated the 'dry', 'wet' and 'wet-dry composite' patterns. The wet-dry composite illustrated that convection over southern Africa (24°S, 25°E) is offset by sinking motions over equatorial Africa and the south-west Indian Ocean. It was observed that an east-west oriented dry anomaly extended from Namibia to Malawi during the 1980 summer. The dry anomaly extended northwards toward India from East Africa.

Jury (1996) reported that summer rainfall departures over southern Africa correlates positively with convection in the central and western Indian Ocean during November According to Jury (1996) the relationship shows that the reduced (increased) convection in the spring time monsoon transition corresponds with the above (below) normal rainfall in the following summer over southern Africa. It was noted that rainfall indices

displayed a sympathetic area over southern Africa with distinct NW-SE alignment consistent with a forced cloud band of the subtropics. In this thesis, Malawi summer rainfall is correlated with field OLR at -6, -3 and 0 months lag.

Research on Intra-Seasonal Oscillations (ISO)

Rainfall fluctuations are driven by changes in circulation. There are fluctuations in rainfall associated with the east wind regime (seasonal) and others which are driven on shorter time scales. ISO in the atmosphere are generally defined as convective fluctuations with periods longer than synoptic scale but shorter than seasonal time scale, usually of the order of 10-60 days (Makarau, 1995). A lot of research has been done on ISO since discovery of the global 40-60 day oscillation in the equatorial areas by Madden and Julian (1971). These were characterised as planetary-scale eastward-propagating zonal circulation cells along the equator. The oscillations are generally called the Madden and Julian Oscillation (MJO) and are studied using various methods. Detailed discussions of MJO can be found in Knutson and Weikmann (1987); Rui and Wang, (1990); Madden and Julian (1994) amongst others.

Dry/wet spells fluctuations

Climate variability over southern Africa at intraseasonal scale has been investigated for selected dry and wet spells (Tyson, 1981; Taljaard, 1986; Matarira and Jury, 1992; Levey, 1993; Jury, 1996; Hargraves and Jury, 1997; Nassor and Jury, 1997).The findings from these studies have identified common features of predominant dry and wet spells. According to studies by Harangozo (1989) and Barclay (1992) baroclinic westerly waves are the dominant weather system during early summer, while mainly barotropic atmospheric structure is important during late summer.

The significance of tropical air flow in enhancing rainfall over Southern Africa was identified by using the frequency method (Miron and Lindesay, 1983). They grouped rain-bearing winds and rainfall amounts in categories and related the results to patterns of airflow for wet spells and extended dry spells. In this study the frequency method is used to identify the onset date of Malawi summer rainfall using pentad.

Jury *et al.* (1991) observed transient convective waves in the SW Indian Ocean that moved eastwards in 1980 for example while others propagated westwards in 1972, 1974, 1977,1981 while many others were quasi-stationary in 1978 and 1984. Their study indicated that in the 10-20°S band there is no common zonal propagation.

Matarira and Jury (1992), using daily rainfall data for 33 stations in Zimbabwe, investigated contrasting meteorological structure of intraseasonal wet and dry spells using ECMWF composites. Circulation patterns for each case of dry and wet spells were studied. They observed that dry spells showed an increase in mid-latitude cyclones off the south-west coast of Africa and also and tropical cyclones near Madagascar. In dry spells mid-tropospheric troughs were positioned over the east and west coasts of Africa near 25°S and increased anticyclonic vorticity over Zimbabwe.

Levey (1993) in his analysis of precipitation pentad time series for central South Africa during austral summer, observed a 20-35 day oscillation while Makarau (1995) identified 10 to 25 and 30 to 50 days cycles when studying dry and wet spells in Zimbabwe from summer pentad rainfall. Time-longitude analysis (Hovmoller plots) of selected meteorological variables between 1987 and 1992 in the tropics (Levey,1993) showed that 21% of cases were stationary, 50% moved eastwards, 12% moved westwards while 18% of patterns were indeterminate.

Studies on vertical structure over southern Africa may be found in Harangozo (1989). Many of these analysis methods are applied here using NCEP data.

Nassor and Jury (1997) studied intraseasonal climate variability over Madagascar using ECMWF and daily summer rainfall data. 16 cases were identified for a composite analysis of flood events defined by rainfall > 70 mm per day. They performed the spectral analysis and results showed the maximum spectral peak at 40.7 days in 1989 and 1991 which is near the period of the MJO. They observed that 10-20 day cycles were very common in many summers and were attributed to transient easterly waves. Results also indicated the variation from longer peaks (1987, 1990) to shorter chaotic cycles (1988, 1992) and revealed an interplay between monsoon surges, easterly waves, tropical cyclones, African tropical troughs and subtropical westerly waves (Nassor and Jury, 1997).

1.3 Hypothesis

The hypotheses to be tested will be that:

(i) The circulation patterns and embedded weather systems some months before dry seasons behave differently. The analysis will attempt to determine common predictors for dry years.

(ii) Dry summers over Malawi are related more to the circulation features south of 10°S than north of it.

(iii) Dry spells have unique circulation patterns associated with them.

The above hypotheses will be tested by examining circulation patterns of selected dry spells using NCEP reanalysis data covering the period 1962-1995.

1.4 Summary

The main objective of this chapter was to illustrate the research problem, and to review similar studies on climate variability. The research problem is to identify climate variability and its predictability in tropical southern Africa using drought in Malawi as an example. According to Allan (1995) drought affects water users as well as those involved in allocation period, policy development on water usage and its management and implementation/influence economic prosperity. Predictability is to be achieved by identifying precursors/predictors formulating statistical forecasting models for Malawi summer rainfall, and thereby understanding the climate variability at inter-seasonal to intraseasonal time scales. Temporal variations are to be analysed for Malawi summer rainfall and associations with the circulation at large will be established using correlation analysis. Some climatic impacts of rainfall variability and past attempts to understand its variability have been cited and the climate of Malawi in the context of southern Africa has been described briefly. The hypotheses to be tested have been presented, the results of analysis are given in chapter 4 and 5. Up to 1998, Malawi did not have in-house climate prediction capability, and the country relied on seasonal forecasts issued by outside institutions. Hence this study seeks to fill a gap so that Malawi can contribute more to regional efforts geared at improving seasonal forecasts in southern Africa.

The objectives of the study are achieved through methods described in the next chapter.

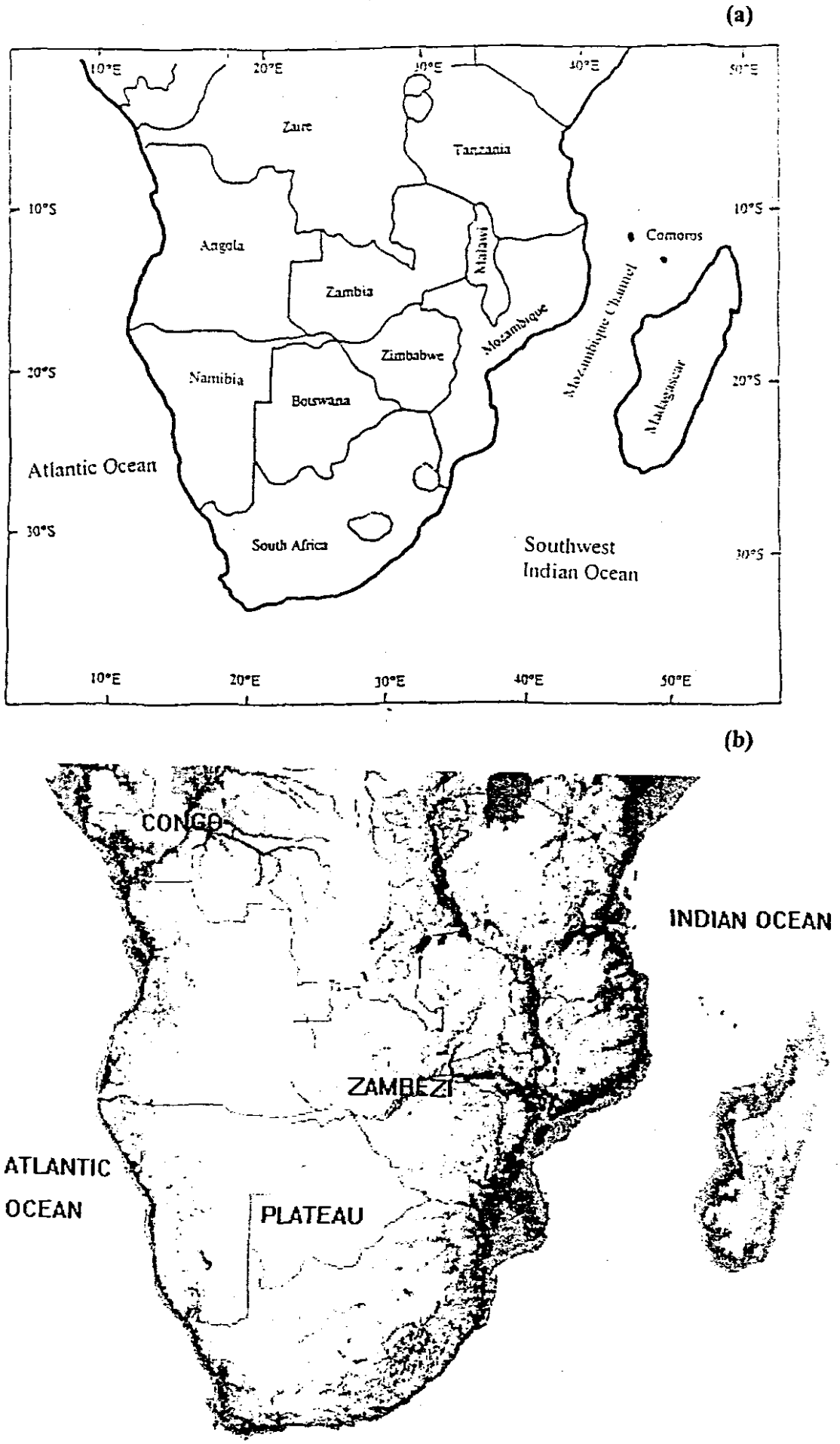

Figure 1.1: (a) Map of southern Africa showing position of Malawi lying within 10-20°S, 30-40°E belt. (b) *Topographic map of southern Africa. Dark shaded areas* are generally <1000 metres and light shaded are generally > 1000 metres.

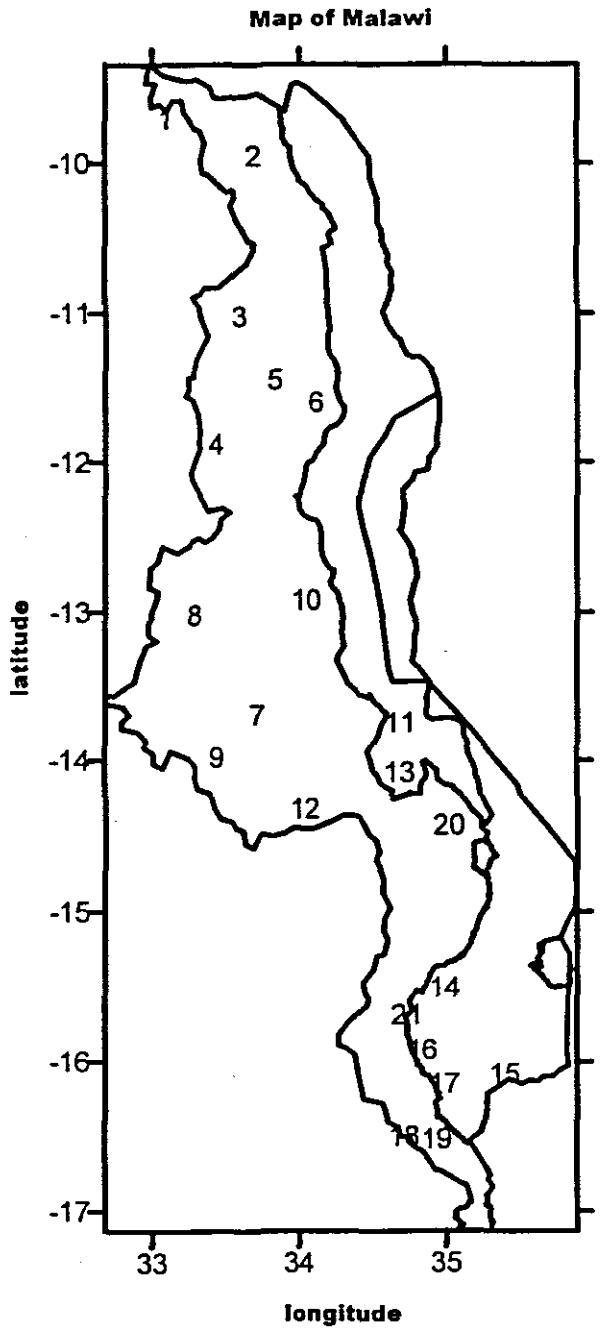

Malawi stations used in the study:

1 Chitipa
2 Karonga
3 Bolero
4 Mzimba
5 Mzuzu
6 Nkhata Bay
7 Dowa (agr.)
8 Kasungu*
9 Chitedze*
10 Nkhotakota
11 Salima
12 Dedza*
13 Monkey Bay
14 Makoka*
15 Mimosa
16 Bvumbwe*
17 Thyolo*
18 Ngabu*
19 Makhanga*
20 Mangochi*
21 Chileka*

(A station with a star is also used in daily rainfall analysis).

Figure 1.2: Map of Malawi showing stations used in the study. Stations from 1 to 6 are from northern region; from 7 to 12 are from central region and the rest are from southern region.

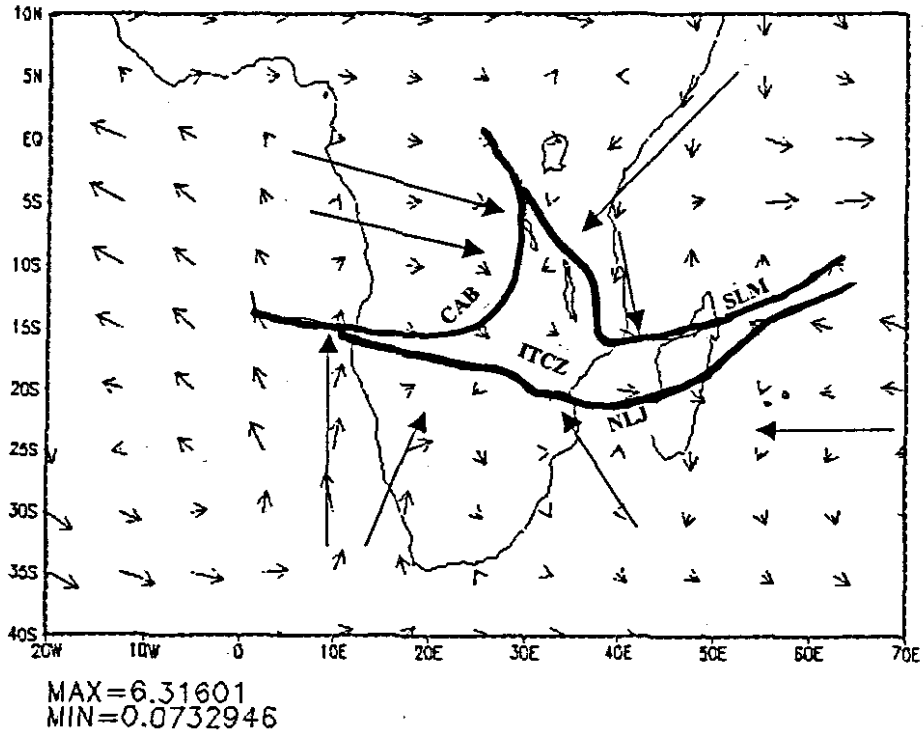

Figure 1.3: Approximate mean position of Inter-Tropical Convergence Zone (ITCZ) in January with associated wind circulation. Wind vector pattern is extracted from NCEP monthly longterm mean (1968-1996) averaged over 1000-700 hPa and for DJF. Approximated Southern limit of monsoon (SLM). northern limit of Trades (NLT) and Congo Air Boundary (CAB) have been indicated.

Chapter 2

DATA AND METHODS

2.1 Introduction

Our understanding of climate dynamics can be facilitated using raw observed data interpreted using sound methods of analyses. The objective of this chapter is to briefly explain types of data, sources and methods to be used. The Malawi station data used in the research are daily, pentad and monthly rainfall in correlation with other meteorological fields and for selection of dry years used in seasonal composite analyses. Precursor and rainy season patterns are computed for sea level pressure, geopotential height, wind, OLR, SST, precipitable water, temperature, streamfunction and velocity potential. In the intra seasonal analyses, pentad rainfall data are used in identifying an onset date of summer rainfall and the in-season fluctuations observed. Results are compared with other findings in the region. Daily rainfall data are used in spectral analysis and in the selection of case studies of in-season dry spells. The circulation patterns are elucidated by visualising NCEP daily anomalies of geopotential height, wind vector, zonal and meridional wind components, OLR and relative humidity (RH).

2.2 Data and sources of data

The summer rainy season in Malawi and across southern Africa is considered to be from October of one year to April of the following year (Lindesay, 1988; Rocha, 1992; Jury *et al.*, 1992). Most of the thesis is based on data obtained from the NCEP weather and climate reanalysis data set, with others derived from the Comprehensive Ocean-Atmosphere data set (COADS), both originating from the National Oceanic and Atmospheric Administration (NOAA). These are in addition to rainfall data and other local variables as described below.

2.2.1 Rainfall data

Monthly summer rainfall data originate from the Malawi Meteorological Department. The data covers the period from1961/62 to1994/95, November to April of each season. The quality control was done according to WMO standard.

Initially 23 stations were selected and monthly rainfalls were formulated into their standardised departures using the historical means and standard deviations for each. Hence, the seasonal cycle was removed based on averages calculated for the period 1962 to 1995. The standardized data have a mean of zero and a variance of one. In this way diverse stations could be combined into indices and compared. The time series of selected stations was cross-correlated and those stations showing strong positive values significant at better than 95% confidence level were retained. Initially it was thought that the Malawi rainfall data should be divided into north and south regions. However, after creating independent averages, the cross correlation was found to be statistically significant at 99% level. Hence stations data for the whole (small) country could be combined. The time series for the remaining 21 stations (figure 1.1b) was averaged to create a single rainfall index for Malawi (November-April). This areal index is used to identify dry and wet years. Monthly indices were further sub-divided into three monthly bins. The rainy season is characterised by highest rainfall in the January month. Here the focus is mainly on Malawi, the six month season (NA), following the work of Preston-Whyte and Tyson (1988) who regionally-aggregated data from 33 stations to create South African rainfall index for the October-September rainfall year from 1910/11-1983/84 and Jury and Pathack (1993) who used rainfall from number of countries to investigate composite climatic patterns associated with extreme modes of summer rainfall over southern Africa.

A daily rainfall index was created from ten Malawi stations covering the period 1972-1993. These stations are indicated with an asterisk in figure 1.2. Monthly rainfall data for Kwazulu-Natal (Jury, 1997) have also been used in correlation analysis in chapter 3. Malawi monthly maximum temperatures, supplied by the Malawi Meteorological Department, are also used in the study to analyse the intensity of dry spells.

2.2.2 Sea surface temperature (SST) and Sea level pressure (SLP)

The SST and SLP data were derived from the comprehensive Ocean Atmosphere Data Set (COADS) of the National Oceanic and Atmospheric Administration (NOAA). These data were obtained as monthly mean values for the period 1962-1995 in 10 x 10 °grid boxes. This was partly to reduce the dimensionality of the data set. These cover the area from 20°N to 40°S and 20°W to 90°E. The COADS data are representative of the

marine environment frequented by ships and the data quality is controlled (Makarau, 1995; Rocha, 1992). The monthly data were grouped into overlapping three monthly values, namely May-July (MJJ); July-September (JAS); September- November (SON) and December-February (DJF). The fields time series are correlated with Malawi summer rainfall. Indices formed from SLP are correlated with Malawi summer rainfall and results are presented.

2.2.3 SOI data

Southern Oscillation Index (SOI) data were obtained from NOAA as differences in standardized monthly mean in sea level pressure between a Pacific island of Tahiti (17.5°S, 210.4°E) and Darwin (12.5°S, 131°E). The indices have been used by other researchers (e.g., Lindesay, 1988; Jury and McQueen, 1993). The SOI data were grouped into three monthly overlapping averages from which indices were created. These indices together with other monthly indices were correlated with Malawi summer rainfall and results significant at the 95% significance level are retained.

2.2.4 QBO, OLR and Wind

QBO data were obtained from NCEP as 30 hPa zonal wind departures for the tropical band. The QBO is used in correlation analysis in the succeeding chapter. The outgoing longwave radiation (OLR) is used as a proxy for rainfall over the study region and the surrounding Oceans where negative values refer to convective activities and positive values for the a non-convective situation. The OLR data are used in two analyses and from two sources. OLR estimates are used for composite analysis from the NCEP reanalysis data set. More accurate satellite-derived OLR data were provided by Dr. Waliser of Institute for Terrestrial and Planetary Atmospheres of State University of New York, U.S.A and are corrected for satellite bias. These are utilised in correlation analysis with Malawi summer rainfall. The data are in a form of departures and later standardised covering the period 1975 to 1995 (e.g., Liebmann and Hartman, 1982). Surface wind at 10° horizontal resolution were derived from COADS as zonal(u) and meridional (v) wind components. COADS wind data used in the study come from ships in the domain 20°N to 40°S and 20°W to 90°E. Three months averages are calculated, namely MJJ, JAS, SON and DJF for the period 1962-1995. Area indices formed from

these months are correlated with the Malawi Rainfall Index. Those indices that are statistically significant at 95% significance level are included as candidate predictors in the step-wise regression analysis. The wind component correlations are recombined into vector fields and their results are presented in chapter 3. The aim is to search for predictors for Malawi summer rainfall using different methods. The models formed from these data will be used to develop long-range forecasts of summer climate impacts for southern African users.

2.2.5 Data from the National Center for Environmental Prediction (NCEP)

The NCEP Climate Data Assimilation System (CDAS) of atmospheric fields are used to determine the circulation regimes over tropical Southern Africa. These are used in the inter-annual and intra seasonal analyses in terms of monthly mean and anomalies as departures from 1968 to 1996 means. The meteorological fields utilized at inter-seasonal time scale are sea level pressure, vector wind, zonal and meridional wind components, geopotential height, OLR, SST, precipitable water, air temperature, relative humidity, velocity potential and streamfunction. NCEP reanalysis data (Kalnay *et al.*, 1996) have been used by many researchers and their good qualities have been documented (WMO/TD-NO. 876, 1998).

The following examples show that NCEP reanalysis data are of suitable quality.

Cavalcanti *et al.* (1998) studied years of contrasting characteristics using NCEP reanalysed data. Their analysis was based on anomaly fields of precipitation, zonal and meridional components of the wind at 200 hPa, outgoing longwave radiation and specific humidity. Moisture divergence and transport were calculated in the layer 1000 hPa to 300 hPa. They analysed four periods of summer and autumn seasons of the dry years 1983 and 1993 in the Northeast Region of Brazil and wet years 1984 and 1994. They observed that results of circulation patterns during these opposite cases were consistent in terms of precipitation observed over Brazil. They further observed that the main features of atmospheric circulation over South America are well explained by the reanalysis data. The differences in atmospheric variables between dry and wet periods defined clearly the characteristics of the atmosphere.

Mo *et al.* (1998) used NCEP reanalysis data and forecasts to examine the atmospheric circulations associated with California rainfall anomalies in the U.S.A. They used

global gridded analysis of OLR from NCEP covering the period 1973-1995. Their results showed that the reanalysis six hour precipitation forecasts are able to capture signals associated with inter annual variability. Composited OLR data gave good relationships between precipitation over the western United states and tropical convection.

According to the report from the first World Climate Research Programme (WCRP) international conference on reanalysis that was held at NOAA, USA, NCEP reanalysis data are of high quality and undertaken with fixed state-of-the art data assimilation/analysis methods to provide multi-year global data sets for a range of investigations of many aspects of climate, particularly inter-annual variability and for model validation and predictability studies. The large spurious effects present in operational analyses arising from changes in assimilation systems are absent from these data sets which thus provide a more homogeneous time series for precipitation, diabatic heating, surface fluxes and other components of the hydrological cycle (WWO/TD-NO. 876, 1998). In brief the reanalyses represent the most valuable resource that can be used with confidence in any research work, not only in meteorology but also in other related fields as well.

However, one problem with the NCEP reanalysis methodology is the assimilation of surface data over Africa. Evidently, to reduce artificial boundary layers in the model-observed fields, only station pressure data are incorporated. Wind, temperature, rainfall and other valuable inputs are ignored. Upper air radiosonde, aircraft and satellite data are incorporated; but the radiosonde network is very sparse over Africa. Hence further model improvements could bring a greater degree of realism to the reanalysis fields.

Some global monthly data have been obtained from NCEP webs in the Internet and utilized in correlation analysis with Malawi summer rainfall. These are monthly SSTs for the Southern Atlantic Ocean (0-20°E, 30°W-10°E), Nino3 region of Pacific (5°N-5°S, 150°W-90°W), Nino1&2 (0-10°S, 90-180°W) and Nino 4 (5°N-5°S, 160°E-150°W).

2.2.6 European Centre for Medium Range Weather Forecasting (ECMWF)

The daily water vapour flux, derived from primary parameters of specific humidity and wind components obtained from the European Centre, have been used in this thesis to study dry spells. Results are presented as anomaly fields. The data set cover the period

from 2 February 1992-12 March 1992 and 11 January 1980-27 January 1980 (periods of dry spells) in the domain 20°N-45°S, 20°W-90°E. The data are at resolution of 2.5 by 2.5° displayed at regular latitude/longitude grids . ECMWF data have been employed in a number of studies (e.g. Parker, 1994). Detailed information on the ECMWF data can be found in World Climate Research Programme Report (WMO/TD-NO. 876, 1998) and ECMWF (1989).

2.3 Methods

This section focuses on the various methods that have been utilized to further understand climate variability and predictability at inter-annual and intra seasonal time scales. Many are standard methods which have been used by other researchers. Composite and hovmoller techniques, and empirical orthogonal function (EOF)and cross spectral analysis are employed. Methods should be chosen with care because some may have difficulties in describing characteristics of oscillations at different stages.
In this study the composite technique has been utilized to study the circulation patterns that are associated with dry seasons. The sectional analysis method (e.g., hovmoller plots, longitude-height, latitude-height plots) and correlation technique have been used extensively in this study.

2.3.1 Inter-annual variability analysis

2.3.1.1 Creation of a Malawi Rainfall Index

The normalization method is a way to produce averages of observations from stations with different characteristics, especially in the tropics, where rainfall is convective. Normalization minimises differences in received rainfall owing to terrain elevation. An index created in this manner has unit variance and zero mean. The creation of the Malawi Rainfall Index (hereafter MRI) was based on 21 selected stations with continuous records.
Data for each station for each month were normalized with respect to the individual means and standard deviation according to the equation

$$Z_i = \frac{1}{k}\sum_{i=1}^{k}\frac{(Xi - Ui)}{\sigma i}$$

Where Z_i represents the individual standardized departure of values (monthly data over k years); Xi (i=1, 2,.., k) is the observed individual monthly value, *Ui* is the long-term mean monthly (or seasonal, etc) rainfall, σi is the long-term standard deviation. In this way, three and six month totals were obtained from monthly values for each station starting for November to April (summer) from 1961/62 to1994/95. The overlapping months were NDJ, DJF, JFM, FMA and NA. Rainfall for each station and season were subsequently averaged over all stations following confirmation of significant cross-correlation. An index formed in this way from monthly data is free of seasonal cycles. The MRI is used to compare with other variables formed in a similar manner via pair-wise correlation (Yarnal, 1993). The MRI NA index is used to select dry years using the following criteria:

Dry year: $\frac{(xi - u)}{\sigma} \leq -0.5$

Using the MRI, six years are initially identified as dry years as per criterion. Further analysis is done with all selected dry years before embarking on composite analysis. This is to find out if these years may be composited together. This is done by using NCEP meteorological anomaly fields. Three areas are used, one in the Indian Ocean and others in the Atlantic Ocean. The September to November (SON) period is used and variables are as indicated in table 2.1. Largest values are evaluated from each selected window for each variable and year. Results indicate that 1965 may be dropped from the list because it shows inconsistent signs with most of other variables. Therefore the composite analysis is subsequently based on five dry years. In subsequent chapters, these years are utilized in composite analyses: Low rainfall years are 1968, 1970, 1983, 1992 and 1995, the focus of research.The contribution from each year is further estimated using the t-test (see section 2.3.1.3 below). Some observed characteristics, considering all three areas in general, for the 5 driest years are:

(a) It appears all years contribute consistently for each variable with respect to their common mean at each selected area.

(b) The precursor year 1967 show the largest zonal wind anomaly value (+4.0 m/s) at 0-15°S, 0-15°E. Largest values are also found over an area 30-40°S, 5-20°E (> 2.8 m/s) in precursor years 1969, 1982 and 1991.

(c) Statistically significant OLR anomalies (> 5.0 w m^{-2}) are found at 15-30°S, 40-70°E

in precursor years 1967, 1969 and 1994. Significant OLR values (> 3.9 w m $^{-2}$) are also found at 0-15°S, 0-15°E in precursor years 1967, 1969, 1982 and 1991.

(d) largest anomalies of precipitable water (> 2.9 kg m $^{-2}$) occur in the precursor year 1994.

Period SON	u-wind (m/s) at 850 hPa level	SST °C	OLR w m $^{-2}$	Precipitable water (PW) kg m $^{-2}$	SLP hPa
Area 1 Indian Ocean	15-30°S 40-70°S	→			
1967	+0.8	+0.4	-10.0*	+0.5	+0.4
1969	+0.9	+0.5	-5.3*	+1.5	+1.5
1982	+1.3	+0.9	-2.0	+1.5	+0.2
1991	+0.8	+0.8	-0.4	+0.5	+0.1
1994	+1.2	+0.7	-5.2*	+0.3	+0.5
Mean	+1.0	+0.7	-4.5	+0.9	+0.4
Area 2 Atlantic Ocean	0-15°S 0-15°E	→			
1967	+4.0*	-0.6	-4.0*	+1.1	+0.4
1969	+0.5	-0.2	-5.0*	+0.5	+0.5
1982	+0.3	-1.1	-9.0*	+0.8	+0.6
1991	+1.5	-1.0	-5.0*	+0.2	+0.5
1994	+2.5	-0.6	-1.5	+3.0*	+0.8
Mean	+1.8	-0.6	-4.9*	+1.1	+0.6
Area 3 Atlantic Ocean	30-40°S 5-20°E	→			
1967	+0.2	+0.3	+0.3	+0.3	-0.2
1969	+3.0*	+0.4	+0.2	+0.1	-0.4
1982	+3.0*	+0.2	+0.2	+0.4	-0.4
1991	+5.0*	+0.4	+0.4	+0.4	-0.4
1994	+1.2	+0.6	+0.7	+1.5	-0.1
Mean	+2.5	+0.4	+0.4	+0.5	-0.3

Table 2.1: Characteristics of selected dry years in terms of departures for SON period.
* = statistically significant contribution > 95% level.

2.3.1.2 Spectral analysis

Meteorological and geophysical phenomena often display rhythmic variations. Spectrum analysis is used to describe the tendency of a series to show oscillations of a given frequency. The time series of a variable is represented as a sum of sines curves of different period. This procedure uses the Fast Fourier Transform which works on equally spaced values and plots the squared amplitude of the sinusoids. Spectral analysis is a modification of Fourier analysis so as to make it suitable for stochastic process. Periods or cycles in meteorological data may be due to non-linearity or interactions between high frequencies. Therefore caution should be taken when applying spectral analysis method in identifying cycles or periods. A possibility of adding artificial periods to the data set may be encountered with filtering. The periodogram represents hidden cycles in a series. In this study spectral analyses, utilizing the Statgraphics software package, has been applied to Malawi monthly, seasonal and daily rainfall to identify periodicities.

2.3.1.3 Composite analysis

Composite analysis is one of the techniques applied to study common features and patterns in selected fields. The group of cases are averaged according to a strict selection criteria. The technique reduces the number of maps thus making the analysis easier to handle and interpret. The other advantage is that the density of observed data is enhanced (Jury, 1997), an important consideration in tropical Africa and over the adjacent Atlantic and Indian Oceans. However, the disadvantage of the method is that specific details of individual cases are missed and the problem of mixing different climate types occurs. The method has been used by many researchers in the fields of meteorology and climatology such as (Rui and Wang, 1990; Matarira and Jury,1992; Jury and Pathack, 1993; Nassor,1994; Majodina,1995; Jury, 1996; Levey and Jury, 1996; Mpeta,1997; Nassor and Jury, 1997; Jury and Levey, 1997; Naeraa and Jury, 1998). To increase our understanding of mechanisms underlying inter-annual climate variability many researchers have analysed area-averaged rainfall and developed dry and wet scenarios using the composite technique (Miron and Lindesay, 1983; Tyson, 1984). Hargraves and Jury (1997) used the composite method in their study to highlight meteorological features of flood events over the eastern mountains of South Africa.

The technique consist of summing together the selected climatic fields and dividing by the total number of cases (sample size) to get the average value at each grid point. In this thesis composite analyses are employed using selected meteorological parameters of dry years as identified by the MRI. The results are presented in chapter 4. Mathematically the seasonal composites (averages) of the mean of individual sample (variable) are given by the average:

$\overline{X} = \frac{1}{N}\sum_{i=1}^{N} Ai$ where Ai is one of the total (N) individual seasonal averages

in the sample formed from the selected dry summers. Composite anomalies are formed by subtracting from the individual composite mean of the long-term average based on1968-1996 data set. The statistical significance of individual contributions to the composite (table 2.1) of each variable is estimated using the t- test at 95% significance level. The composite value (taken as mean for each variable and each year) of September-November over each window is used and a standard deviation of the entire anomaly composite over the same window is calculated. The aim is to identify years which contributed the most, to the overall composite pattern of each field. The calculated t-values outside the critical values of t-distribution with respect to each individual year are significant at 95% level using the two- tailed test. The values are also compared with their common five years average for each variable. T-values are calculated from (Cayan *et al.*, 1993):

$T = \frac{\overline{x}}{\sigma}(n\text{-}1)^{0.5}$ Where $\overline{x}$ is the composite average value

of September-November (SON) of each individual year for a particular variable over a particular area, σ is the standard deviation of the entire anomaly composite over the same window and $n-1$ is the number of degrees of freedom (here n = five dry years). The composite analysis, for five selected dry summers, has been done for NCEP anomaly fields, namely sea level pressure, geopotential height, vector winds, sea surface temperature, outgoing longwave radiation, precipitable water, temperature, streamfuction and velocity potential. The periods are November-April (NA) and the precursor period May-October (MO).

2.3.1.4 Regression and Correlation Analyses

The strength of association among variables is assessed by linear pair-wise and multiple correlation. The tool should be used with care because the method does not distinguish cause and effect, hence it is very easy to draw inappropriate conclusions. It should be noted that a correlation of zero value between variables may not necessarily imply that there is no relationship. This may be caused by difference between simple correlation coefficient that relates predictand to one of several predictors that influence it and partial correlation coefficients which yield relationships between variables keeping others constant.

Multiple regression is generally used in developing long range forecasting models (e.g., least squares). Correlations are performed in the succeeding chapter to identify predictors to include in forecast models. The step-wise multiple regression method is used within the Statgraphics software package. Malawi summer rainfall is the 'target' predictand.

A multiple regression is of the following form:

$R = a + bX + cY + dZ$

where R is the predicted Malawi seasonal rainfall anomaly, a is a constant, b, c, d are the regression coefficients for the predictors X, Y, Z. The number of predictors is restricted to three. The f-value and the r^2, coefficient of variance, are employed to choose useful models that could be used operationally. In step-wise multiple regression, the selection procedure here is forward to control the entry of variables into the model. Variables are entered with the aim of obtaining a model with a high degree of fit with the least number of predictors. This procedure is recommended in model formulation especially if one is not sure which variables are likely to be included from the candidate pool. The forward selection procedure starts by adding the new variable with highest partial correlation. The software package checks and compares at each stage to see whether the previously selected variables are still significant if they can be replaced or removed. The method has been employed by many researchers in climatology. Jury (1997) used the method to develop multi-variate linear regression models for South African summer rainfall covering the period 1971-1992. Hastenrath *et al.* (1995) has reported on empirical studies and found the important predictors to be the SOI, zonal wind over Singapore at 50 hPa, an index of October-November surface winds over the equatorial Indian Ocean and an index of November SST in the southwestern Indian

Ocean in respect of summer rainfall over southern Africa. In this study, models are developed for Malawi summer rainfall for groups of months namely NA, NDJ and FMA. The multi-variate algorithms are based on 32 years (1962-1993) data. Models which explain > 40% of variance are tested for their reliability. The predictors are also scrutinised for co-linearity. Prediction experiments (reliability test) are done using early portions of 1962-1986 (25 years) as a training period and tested against remaining later years 1987-1993. The procedure is repeated by using 1969-1993 to develop a model to predict the early years 1962-1968. Model validation is an important component of model construction (Mason, 1998). The reliability test seeks to reveal how the model might have performed in an operational situation. The method of finding the predicted values is similar to jack-knife skill test which involves the deletion of each year in turn from the training period and prediction based on the remaining observations. Only that here seven consecutive years are left out and their predicted values are based on the same model constructed by the remaining 25 years data. Colinearity in predictors corrupts models and is to be screened out particularly to eliminate conspiring El Nino signals and reduce artificial skill (Jury *et al.*, 1997). Consequently the identification of co-linearity in predictors is done in this study by calculating variance inflation factor (VIF) as recommended by Chatterjee and Price (1977) and adopted by Hastenrath *et al* (1995). The predictors in each developed model are considered and each one of them in turn is regressed on the remaining predictors and coefficient of determination (r_i^2) substituted in the equation

Variance inflation factor (VIF) = $\frac{1}{(1-r^2)}$. According to Chatterjee and Price (1977)

the presence of co-linearity in the estimation of coefficients of predictors is deduced when the value of VIF is greater than ten. The developed models in this study confirm this criterion. The independence assumption has been confirmed using the Durbin-Watson test for first-order autocorrelation in the residual errors. What is required is that error terms should be random. Negative autocorrelation exists if the Durbin-Watson statistic is increasing towards 4, while the independence exists if the Durbin-Watson statistic is about 2. Values below 1.5 indicate positive autocorrelation and the model should be rejected.

Correlation analyses have been used to establish associations between Malawi summer rainfall and other variables such as SST, OLR, Natal rainfall, QBO, SOI, Nino 3 SST, Nino 1&2 SST, OLR, sea level pressure, surface zonal and meridional wind components. The analysis period for OLR is short, 1975-1995, and correlation results are presented at lags -6, -3 and 0 month. Other correlation results cover period 1962-1995 and are presented at -7, -5, -3 and 0 months lags.

2.3.2 Intra-seasonal variability analysis

The year to year variability of summer climate over Southern Africa is primarily expressed as intra-seasonal wet and dry spells with varying characteristics.

2.3.2.1 Pentad analysis

The Malawi daily summer rainfall data is binned into 5-day averages to reduce noise associated with day to day variability. Each season ranges from 28 October to 31March, making 31 pentads in accordance with WMO format. From pentad data, a seasonal average is determined and subsequently standardized anomalies are computed (figure 3.3a). Cross-correlation analysis was performed and a subset index comprising ten inter-correlated Malawi stations was computed. These ten stations (figure 1.2, with asterisk) cover the central areas where maize is grown and the southern areas where commercial farming is popular, but where extreme weather conditions are prevalent.The same stations will be used in case studies of selected dry spells in chapter 5. This index has been used to identify onset, duration and cessation of the rains. The identification of troughs of dry and wet spells is done using pentad anomaly plots in the period1972-1993. The selection was based on the following criteria. The normalized departure for a dry spell has to be

$$\frac{(x-\mu)}{\sigma} \leq -0.5$$

where x is the pentad value, μ is the pentad long-term mean and σ is a long- term standard deviation.

2.3.3 Cross-sectional analysis

The sectional analysis is useful in studying circulation changes over the chosen domain. In this study, longitude-time analyses (hovmoller plots) have been used to investigate the horizontal circulation of selected dry summers at intra-seasonal time scale using NCEP reanalysis anomaly fields, averaged over the latitudes 10-17.5°S in the summer period November-April from 10°W to 70°E. The selected anomaly fields are zonal and meridional wind components at 850hPa and 200 hPa levels, temperature at 850 hPa and precipitable water. The spatial and temporal patterns are observed from the plotted graphs. Vertical cross-section plots for selected variables are analysed in height-longitude and height-latitude format. For the former, each variable is averaged over latitudes 10-17.5°S and November-April each dry summer for the 1000-100 hPa levels and plotted from 10°W- 70°E. For the height-latitude plot, each anomaly variable is averaged over 30-37.5°E and plotted from 10°N to 40°S in the same layer 1000-100 hPa averaged over the same period November-April. The anomaly fields used in the vertical section analyses are zonal wind and meridional wind to investigate the vertical structure associated with dry conditions. The study also investigates the circulation patterns during selected short-lived dry spells. These are done by plotting anomaly fields of daily NCEP reanalysis data obtained by subtracting mean climatology (1979-1995).

2.3.4 Mathematical Definitions of derivative parameters

This section gives the mathematical definitions of some derived parameters which may assist in understanding the circulation patterns. Parker (1994) pointed out that the creation of secondary derived parameters is useful to describe meteorological kinematic and thermodynamic structure. Divergence and vorticity are defined and related to velocity potential and streamfunction, which describe the divergent and rotational component of atmospheric circulations.

2.3.4.1 Stream function and velocity potential

A horizontal wind vector V in two dimension can be separated into a non-divergent part (rotational) and an irrotational part (divergent). These components can be applied to describe zonal and meridional circulations.

Thus:

$V = k * \nabla\Psi + \nabla\chi$ (From Helmholtz theorem).....Eq 2.9a

where ψ = a horizontal stream function (non-divergent part)

χ = a horizontal velocity potential (divergent part)

∇ = a gradient operator

κ = a unit vertical vector

The relationship with divergence and vorticity may be seen from these equations:

$$\varsigma = \nabla\psi \quad \text{.....Eq 2. 9b}$$

$$D = \nabla\chi \quad \text{..... Eq 2. 9c}$$

By convention usually anticlockwise circulation is taken as positive. For stream function winds travel clockwise (cyclonic) around maximum values in Southern Hemisphere. Positive values of streamfunction indicates cyclonic circulation and negative values shows anticyclonic circulation. Positive velocity potential is associated with convergence and negative values are associated with divergence. These parameters have been used by many researchers (for example, Knutson and Weickmann, 1987; Pathack, 1993; Makarau, 1995; Nassor and Jury,1997). The sign convention for the irrotational part (velocity potential) is that wind flows from small to higher values of velocity potential and perpendicular to the contours. Larger divergence may be produced when strong flow is created due to tight contour gradient. Chen and Tzeng (1990) pointed out that irrotational component part is important in identifying sources and sinks of atmospheric moisture and convection.

2.3.4.2 Divergence

Divergence measures the overall expansion of the wind velocity field (V). In other words the diffluence experienced by the air in the local horizontal plane. The divergence in the x, y plane is defined (Barry and Perry, 1973; Bluestein, 1992) as:

$$D = \nabla h.V = \frac{\partial u}{\partial x} + \frac{\partial v}{\partial y} \quad \text{.....Eq 2.10}$$

Where u = wind component in the zonal direction

v = wind component in the meridional direction

x = zonal distance (longitudinal)

y = meridional distance (latitudinal)

2.3.4.3 Vorticity

Vorticity (i.e. circulation per unit area) is the measure of rate of spin experienced by a vortex of air around a local vertical axis. The sense of sign of vorticity in the Southern Hemisphere is given as: Negative for cyclonic and positive for anticyclonic vorticity. Anticyclonic vorticity is associated with divergence while cyclonic vorticity is associated with low level convergence.

$$\varsigma = \frac{dv}{dx} - \frac{du}{dy} \quad \text{.....Eq 2.11}$$

There are several ways of expressing the content of water vapour of moist air in the atmosphere. Some of variables that are used in meteorology or climatology are defined below.

2.3.4.4 Precipitable water

The moisture content of the troposphere is represented by precipitable water (PW), defined as the depth of water that would be obtained if all that water in the column were condensed onto a lower horizontal surface of unit area. It is integrated between levels 1000 and 300 hPa (Chen and Tzeng, 1990).

Mathematically it is defined as:

$$PW = \frac{1}{g}\int_{P_1}^{P_2} q\,dp \quad \text{.....Eq2.12}$$

Where q is the mean specific humidity between pressure levels

g is the acceralation due to gravity

and P_1 is 1000 hPa and P_2 is 300 hPa.

2.3.4.5 Water vapor flux (Q)

Atmospheric humidity is determined by the exchange of moisture between the surface and the atmosphere and by advection of vapor by eddy diffusion. It usually involves latent heating due to phase changes (Preston-Whyte and Tyson, 1988). Water vapor flux (q) may be defined as the transport of moisture by the horizontal wind and is determined through vertical integration. In this study the integration is between 1000 hPa over the ocean (850 hPa over the African plateau) to the 500 hPa levels. Most of the horizontal transfer of water vapor is near 700 hPa in the tropics (Newell, *et al.*, 1972). It is presented mathematically

$$Q = \frac{1}{g}\int_{P_1}^{P2} qVdp \quad \text{.....Eq 2.13}$$

Where q = specific humidity in gm kg $^{-1}$

V = velocity at a particular level in m s $^{-1}$

P_1 and P_2 are respectively 1000 hPa and 500 hPa. Otherwise p1 is taken as 850 hPa over the African plateau. In this thesis, the resultant moisture flux vector is indicated for case studies of the dry spells of 1980 and 1992 in chapter 5.

2.3.4.6 Relative humidity

Relative humidity (RH) is defined as the ratio of observed mixing ratio to that which would prevail at the same temperature expressed as a percentage (Byers, 1974, p.110). The mixing ratio (W) is the amount of water vapor contained in mixture with dry air of unit mass expressed in grams per kilogram. RH has no dynamical relationship. It is not conserved, provides no gradient information and generally has small spatial scales due to its noisy character. Ebisuzaki *et al.* (1998) has argued that the humidity analyses are considered the most inaccurate of the primary fields. In this study RH will be used in chapter 5 when analyzing case studies of dry spells.

$$RH = \frac{W}{Ws}(100\%) \quad \text{.....Eq 2.14}$$

2.4 Summary

The data sources and nature, and analysis methods that will be used in the study have been described. The study will be conducted with respect to Malawi summer rainfall, representing tropical southern Africa. Correlation techniques will be intensively used in identifying possible predictors for forecasting the summer rainfall. The composite method will be used to study circulation patterns of extreme climate scenarios and in identifying precursors.

The next chapter analyses temporal and spatial modes of Malawi summer rainfall and relationships with other meteorological variables, by applying these methods.

Chapter 3

SPATIAL AND TEMPORAL MODES OF MALAWI SUMMER RAINFALL

3.1 Introduction

Spatial and temporal fluctuations of the Malawi summer rainfall at inter-seasonal and intra-seasonal time scales are investigated. The statistical relationships between Malawi summer rainfall and other meteorological variables/phenomena are identified. The aim is to fulfill one of the specific objectives of the study of identifying and establishing relationships for predictive purposes between Malawi summer rainfall and other meteorological variables. Thereafter, variables with significant statistical correlations are used as candidates in the development of statistical forecast models. Statistical associations are the prerequisites for the formulation of statistical forecasting models. November to April averaged Malawi rainfall index (MRI) for the period 1962 through 1995 is presented in figure 3.1a. The index is referred to in subsequent analyses to isolate dry years for composite analyses. The seasonal cycle is also given (figure 3.1b). To identify the periodicity of Malawi summer rainfall, spectral analysis is performed (figure 3.2). A knowledge of rainfall periodicity is of value for identifying possible physical causes of rainfall behaviour.

The MRI is correlated with QBO, SOI, Pacific Nino 3 SST (5°N-5°S, 150-90°W), Pacific Nino 1&2 SST (0-10°S, 90-180°W), Atlantic Ocean SST (0-10°S, 10°W-10°E) and KZ Natal rainfall and results are presented in table 3.1. In the subsequent sections, correlation results are presented between MRI and other field variables such as SST, sea level pressure (SLP) and surface winds. The correlations are shown at -7, -5, -3 and 0 months lags. Correlation results for bias-corrected satellite OLR is presented at -6, -3 and 0 months lags as mentioned in chapter2.

Section 3.2 presents results of rainfall time series analysis at inter-annual time scale while section 3.3 the analysis is at intra-seasonal time scale using daily and pentad rainfall. Section 3.4 concentrates on correlation analysis after summarising significant findings from daily rainfall analysis.

3.2 Results of rainfall time series analysis

3.2.1 Seasonal and monthly time series analysis

MRI (Figure 3.1a) shows low anomaly values during late 1960's and early 1970's (lowest 1967/68). A notable biennial high frequency fluctuation is evident. Similarly, low values are observed from 1979 to 1984 and again after 1989. Fluctuations are 4-6 years and of a lower frequency character illustrates the seasonal cycle of rainfall pattern whereby Malawi mostly gets unimodal rainfall (figure 3.1b) from November of one year to April of the following year with a highest peak in January. Even in dry years, the area averaged rainfall is 700mm. The autocorrelation at +1 year lag is + 0.1, which means that the sample size is equivalent to the degrees of freedom.

3.2.2 Results of spectral analysis

Spectral analysis of Malawi summer rainfall shows the highest peak at 3.8 years followed by 2.4 and 11.1 years cycle (figure 3.2). These cycles may be associated with ENSO, Quasi Biennial Oscillation (QBO) and the solar cycle respectively. The results are similar to findings by other researchers for southern Africa. For example, Makarau and Jury (1997), using a 90 year record of Zimbabwe rainfall, found a pronounced spectral peak at 2.3 years possibly associated with QBO. Results are also similar to those found by Jury and Pathack (1996) from the spectral analysis of February rainfall over northern South Africa using 25 stations covering 1950-1988. Significant spectral peaks were observed at 18.6, 4.2 and 2.4 years associated with the a luni-solar tide, the ENSO and QBO. Results (not shown) of correlation for each Malawi station and SOI indicate highest positive correlations in southern Malawi from lag - 6 months (JJA). Correlations become weaker toward the north. This suggests that northern Malawi lies in a transition zone between southern Africa ($r > 0$ for SOI) and East Africa rainfall ($r < 0$). Malawi rainfall is generally with Southern Africa's atmospheric response (dry in El Nino) as described further below.

3.3 Results of pentad rainfall analysis

Here the mean onset date and rainfall progression of Malawi summer season using pentad data are analysed, similar to the approach of Makarau (1995). The knowledge of rainfall within each summer season may assist in maximizing the effective use of

water resources and agricultural activities even though mean dates may vary in the season. The pentad period is from 28 October of one year through 31 March of the following year making 31 pentads each season from 1972 to 1993, taking into consideration the time span of other indices. The same data are utilised in the succeeding chapter to identify dry spells for subsequent study.

Results from pentad analysis show that Malawi first experiences a first major wet spell by pentad 8 (2-6 December) plus or minus two pentads (figure 3.3). This date differs slightly from Makarau (1995) who found that the appropriate date for Zimbabwe was 22-26 November. The second peak is observed at pentad 11 (17-21 December) taking about 15 days from the first peak. Malawi should generally expect its longest dry spell between pentad 11 (17-21 December) and pentad 17 (16-20 January). The separation from the date Malawi starts experiencing its longest dry spell to next maximum rainfall peak is about 35 days. Another peak is at pentad 20 (31 January-4 February) then at pentad 25 (25 February-1 March) whereafter declining trend is noted. The seasonal distribution is similar to Zambia, Zimbabwe and Madagascar (Makarau, 1995). The duration of each wet spell rarely goes beyond 15 days before being punctuated by a dry spell. It appears there is little relationship between the start of rainfall and the spread of rainfall within the season.

3.4 Results of correlation analyses

3.4.1 Malawi summer rainfall verses QBO and SOI

Correlation results between the MRI and JAS QBO indicates significant association at better than 95% significance level (r = +0.35), with QBO explaining 12.3% of total rainfall variance. Correlation between SON QBO verses MRI is also significant at 95% significance level (r = +0.33), 11% of variance. Malawi rainfall increases with a westerly phase of QBO. The result is in agreement with several findings over southern and eastern Africa (Jury *et al.*, 1994). The correlation results between MRI and SOI are presented in table 3.1. The correlations start picking up from -7 months lag (r = +0.29) to reach r = +0.48 at lags of -4 and -3 months then decreasing slightly to correlation coefficient of +0.42 at 0 months lag. SOI may explain up to 23% of a total variance of Malawi summer rainfall.

3.4.2 Malawi summer rainfall verses satellite OLR

OLR is responsive to cloud depth, cloud top temperature and rainfall (Jury and Pathack, 1995). Low OLR values in the tropics and summer subtropics show convective weather systems but warm cloud-free regions indicate high values. Results at lag -6 months (figure 3.4a) show weak negative field correlations over southern Africa with a centre over Malawi extending in the northwest direction to the Guinea coast. Positive correlations are found over the tropical Oceans with highest correlations to the north of Madagascar and west of Angola. Correlation at lag -3 months (figure 3.4b) shows highest positive values to the north east of Madagascar (central Indian Ocean) with correlation coefficient of 0.5 and a second one west of Angola. Marked negative correlation passes across Malawi in the north westward direction from southern Madagascar towards the Congo. Correlations at lag 0 (figure 3.4c) show the dominance of negative correlations over southern Africa, oriented in north east to southwest direction from Tanzania to South Africa with a pronounced centre over Zimbabwe. OLR in the tropical south Indian Ocean is positively correlated with Malawi summer rainfall. Hence increased convection initially north, and later east of Madagascar is associated with dry spells over Malawi.

3.4.3 Malawi summer rainfall verses SST

The field correlation pattern between SST within the domain 20°N, 35°S and 20°W, 90°E over the Atlantic and Indian Oceans and MRI (figure 3.5) shows the predominance of positive correlation coefficients over the tropical east Atlantic Ocean at all lags -7 to -3 months. Positive significant correlations (r = +0.3) are also found south east of Madagascar at lags -5 and -3 months. Negative correlations are observed to the north of 18°S in the Indian Ocean peaking at -7, -5 and 0 months lags (r = -0.3) at 5°S, 65°E and are bounded by positive correlations to the south along 25°S. Positive correlations are statistically significant (r > + 0.3) in the Atlantic Ocean within the 0-10°S, 10°W-10°E band. In the Indian Ocean positive correlations extend to the coast of East Africa in the northwest direction bounded by negative correlations on the eastern side with reduced spatial extent, at lags -3 and -5. Spatial distributions of positive correlations in the Atlantic Ocean gradually decrease at -3 months lag north of 11°S latitude with a centre off Angola and Gabon. The negative correlations to the south of 11°S cover a wider

area. Positive correlations in the Indian Ocean are maintained particularly south of Madagascar. Negative correlations become more predominant to the north of this positive band with a centre remaining near 5°S, 65°E. The pattern at zero lag indicates dominance of negative correlations to the north-east of Madagascar in the Indian Ocean and a reduced area of positive correlation to the south of this belt. Negative correlations in the Atlantic Ocean are located in the southern Atlantic Ocean, elsewhere values are positive.

As a result of the analysis, a useful predictor index has been created from SST values at 5°S, 5°E plus 25°S, 45°E then subtracting values at 5°S, 65°E. The correlations values are shown in table 3.1 (3AI) for Malawi NA summer rainfall. The values show the increasing trend from -7 months lag up to -3 months lag. A statistically strong correlation has been found between Malawi early summer rainfall (NDJ) and this index at -5 months (JAS) with correlation coefficient of +0.53. There are also strong correlations between this index at -3 months (SON) and Malawi DJF and JFM rainfall (r = +0.52). Results suggest that early, mid and late summer rainfall may be predicted from SST at least seven months in advance. This is a suitably long lead time for advance warning of weather prior to start of the season.

3.4.4 Malawi rainfall verses vector wind field correlations

The wind correlations are represented as vectors by recombining component correlations of zonal (u) and meridional (v) winds. These correlation wind vectors have been constructed at each grid point of 10° interval from correlation coefficients between Malawi summer rainfall (NA) and individual zonal (u) and (v) wind correlations. Large statistically significant correlation wind vectors on the map refer to wet minus dry conditions over Malawi.Winds would flow in the opposite direction in dry years. The lagged indices (wind components) created from identified key areas may be correlated with Malawi summer rainfall. The spatial extent and coherence of the correlation coefficient pattern are considered a test of predictive value and generally at least four adjacent grid points should exceed 95% confidence level for some credible teleconnection to be interpreted (Jury *et al.*, 1994).

'Wet-dry' conditions years are associated with the following features at each lag:

The pattern (figure 3.6a) at lag -7 months (MJJ) shows diverging southeasterly wind over the central Indian Ocean. The configuration of westerly winds south of India is

related to cool ENSO phase when rising motion is found around Indonesia region with a warm tongue of SST near Malaysia. Statistically significant westerly winds are observed south of Madagascar while onshore southwest winds are found along western coast of Africa from Congo to South Africa.

The pattern (figure 3.6b) at lag -5 months (JAS) indicates statistically significant NE monsoon flow anomalies (absent at -7 months lag) and onshore wind along southwest coast of South Africa and Namibia. The pattern also shows marked cyclonic flow at 30°S, 65°E over the Indian Ocean.

The pattern (figure 3.6c) at -3 months (SON) lag shows statistically significant equatorward wind east of Madagascar. This is in agreement with the finding of Makarau and Jury (1995) who found a reduction of equatorial northeasterly monsoons with respect to increased Zimbabwe summer rainfall. The configuration of strong westerly winds south of India indicates the situation during La Nina scenario whereby a convective belt is over Indonesia region. There is marked anticyclonic flow at 30°, 10°W in the Atlantic Ocean. The period September-November is the time when rain-bearing systems have gradually started to become active. The southeasterly and northeasterly winds are expected to become equally effective over tropical southern Africa.

The pattern (figure 3.6d) at 0 months (DJF) lag shows pronounced easterly winds north of Madagascar. There is a converging line of southeasterly and northwesterly winds passing over South Africa aligned in the northwest-southeast direction.

In summary Malawi rainfall is associated with:

(a) Westerly winds south of India, diverging southeasterlies over the central Indian Ocean, and westerly winds south of Madagascar at -7 month lag.

(b) NE monsoon and an onshore southwesterly wind regime along the southwest coast of South Africa and Namibia at -5 months lag.

(c) Marked diverging winds along 60°E, with strong westerly winds to the south of India indicating La Nina situation and anticyclonic flow south of 15°S in Atlantic Ocean at -3 months lag.

(d) Pronounced converging axis over the southwest coast of South Africa and easterly flow north of Madagascar.

Overall, the wind flow is diffluent over the central Indian Ocean in respect of increased rainfall over Malawi.

3.4.5 Malawi summer rainfall verses sea level pressure

Correlations have been mapped between MRI and pressure in the Atlantic and Indian Oceans at different lags. Positive correlations suggest high pressure over the Ocean, hence increased rainfall over Malawi.

The correlation pattern (figure 3.7a) between MRI and sea level pressure at -7 months lag indicates statistical significant negative correlations east of 80°E within 0-10°S belt in the Indian Ocean. Another significant band is found within 10-20°S band in the Atlantic Ocean.

Correlation between MRI and sea level pressure at -5 months lag (figure 3.7b) shows the dominance of negative values (r = -0.3) from northeast of Madagascar to the east Indian Ocean. The correlation coefficient is significant at 95% significant level. and indicates that occurrence of lower pressures during July-September in the Indian Ocean is a precursor for good rainfall over Malawi.

Correlation values at lag of -3 months (figure 3.7b) indicate persistence of negative values to the east of 70°E from south of India eastward. Positive values are observed within 50-70°E from the Horn of Africa to the south Indian Ocean. A strong E-W gradient is maintained across the centre Indian Ocean. Incoherent patterns are observed in the Atlantic Ocean. During wet years the E-W dipole helps to create zonal overturning and sinking motions over the west and central Indian Ocean.

Negative values increase south of India at zero lag (figure 3.7c). Negative values are dominant in the Atlantic Ocean. Positive values are found near Mauritius.

A predictor index of SLP created at 5°S, 85°E (EIp, see table 3.1) covering an area 10°N-10°S, 70-90°E shows significant correlation with Malawi NA rainfall. It has also been found that Malawi late summer rainfall (FMA or JFM) may be associated seven months in advance (MJJ) using this sea level pressure index (r = 0.42).

3.4.6 Malawi summer rainfall verses Natal rainfall

The correlation has been done between Malawi rainfall and KZ Natal rainfall. The aim of the analysis is to establish whether Malawi rainfall is associated with KZ Natal rainfall. The correlation is statistically significant between Malawi February rainfall and KZ Natal February rainfall, explaining 16% of a total variance. Malawi April rainfall can be predicted from October Natal rainfall explaining about 31% of Malawi rainfall

variations. Correlations between Malawi NA rainfall and SON and DJF KZ Natal rainfall are generally low.

3.4.7 Malawi summer rainfall verses Atlantic Ocean SST (ATs)

Correlations between Malawi summer rainfall and Atlantic Ocean SST (0-10°S, 10°W-10°E) monthly sea surface temperature (SST) indicate some significant relationships. The highest correlation > +0.45 is observed with JAS SST, explaining 20.3% of rainfall variance. The Malawi JFM summer rainfall correlates with JJA SST at (r = +0.38) more than 95% confidence level with 32 degrees of freedom. Results are indicated at selected lags in table 3.1 for NA Malawi rainfall.

3.4.8 Malawi summer rainfall with Pacific Nino 3, Nino1&2 and Nino 4 SST

An above normal Pacific SST Nino3 index signals that an El Nino may be developing and that southern Africa rainfall may receive inadequate rainfall (Dilley, 1996). MRI correlates with MJJ and JJA Nino 3 SST at 99% significant level (r = - 0.50 lags -7 , -6 months). Significant correlations are also observed between MRI and SON Nino 3 SST with correlation coefficient of -0.51 at lag -3 months. Malawi JFM with OND Nino 3 SST gives the correlation coefficient of -0.52. High correlations are also observed at 0 months. The Malawi JFM summer rainfall shows high correlation of -0.51 which is also statistically significant at 99% significance level. This shows Malawi rainfall may be predicted seven months in advance using Pacific ENSO conditions. Some of these results are shown in table 3.1.

Correlation results for Nino 1&2 and Nino 4 are presented in table 3.1 below. Nino 4 SST shows strong and increasing correlations as from -3 months lag (r^2 ~20%).

Period (month) Lags	MJJ -7	JAS -5	SON -3	DJF 0	AREA
SOI	8.4	**22.1**	**23**	**23**	Tahiti-Darwin pressure
QBO	8	12.3	11	10.8	Singapore Zonal wind at 30 hPa
Nino 3 st (SST)	**28.1**	19.4	**23**	**31.4**	5°N-5°S 150-90°W
Nino1 & 2 SST	9.6	11	14	14.4	0-10°S 90-180°w
Nino 4 SST	18.5	**20**	**23**	**27**	5°N-5°S 160°E-150°W
ATs	12.3	**20.3**	11.8	3.6	0-10°S 10°W-10°E
EIp	**21**	19	15	7	10°N-10°S 70°-90°E
3AI (3 area SST index)	**21**	**27**	**35**	14	5°S-5°E plus 25°S-45°E subtract 5°S-65°E

Table 3.1: Variance explained (r^2 %) for November-April (NA) Malawi seasonal rainfall and three month averages of other parameters at indicated lags for the period 1962-1995. $r^2 > 9\%$ is significant at 95% level and values ≥ 20% are bold.

The correlation values indicate that generally Indian Ocean variables die off at zero lag. 3AI gradually increases from lag -7 to -3 months lag then decreases rapidly thereafter. SOI is best as from -5 months while Nino 3 SST is best at -7 months and at zero lag.

3.5 Discussion and Summary

The objectives of this chapter were to investigate temporal and spatial fluctuations of Malawi summer rainfall at inter-annual time scale and to identify statistical relationships between summer rainfall and other meteorological variables. These have been achieved based on the available data. The MRI shows long dry periods from the early 1960's to early 1970's. Thereafter dry conditions became worse after 1991 (figure 3.1a).

It appears four out of five years dry years correspond with El Nino. This may be an indicator that, though the coefficient of determination explains at most 23% (table 3.1) of the total rainfall variance, ENSO has an influence on Malawi rainfall variability consistent with southern Africa. The ENSO variables yield consistent relationships at all lags and Nino 3 SST shows highest correlations at 0 lag with Malawi rainfall. The figures from the table suggests that the best ENSO variables for long-range prediction are, in order SOI, Nino 3 and Nino 4. The 3AI predictor is useful at shorter lead times. The rainfall spectral analysis shows the maximum peak at 3.8 years which is within ENSO period.

Results from lag correlations of OLR indicate that Malawi summer rainfall could be predicted six months in advance from OLR off the coast of East Africa (north of Madagascar) and over an area near 2°N, 65°E (r= +0.55) over the central Indian Ocean. All areas north of 30°S latitude, in the Indian Ocean, show correlation coefficients greater than 0.35. Maximum positive values show that Malawi should expect below normal rainfall when preceding Oceanic monsoon convection is enhanced. There is a positive correlation band within 0-15°S over the Atlantic Ocean (r > +0.35), another precursor area for extreme weather conditions over Malawi.

Results from SST lag correlations with Malawi summer rainfall show significant correlations from lags -7 to - 3 months off the coast of Angola. These positive values are indicators of wet conditions over Malawi at this lag. Maximum correlations are also centred at around 5°S, 65°E in the Indian Ocean at all lags with weak correlation at -3 months lag.

The Malawi summer rainfall is associated with Atlantic Ocean SST of JAS which explains about 20.3% of the total variance of Malawi rainfall. The correlation is significant at more than 95% significance level.

Some few selected brief summaries, among others, are listed below:

(1) Malawi summer rainfall time series shows that relatively dry conditions are more

frequent than in 1960's.

(2) Malawi summer rainfall shows a 2.4, 3.8 and 11.1 year cycles.

(3) Malawi summer rainfall correlated positively with OLR over the central Indian Ocean.

(4) SOI and QBO explain16% and 9% respectively of total variance indicating there are other factors contributing to the fluctuations of Malawi summer rainfall.

(5) KZ Natal February rainfall accounts for 16% of Malawi February rainfall but KZ Natal October rainfall may explain about 31% of Malawi April rainfall, suggesting northward propagation.

(6) Negative correlations with SLP are persistent at all lags to the east of 70°E in the Indian Ocean.

(7) The wind correlation vector fields have shown that winds to the south of India at -7 to-3 months lag is a key area to examine the quality of incoming rainy season.

In table 3.1 an index 3AI (3 area index of SST) is related to wind and sea level pressure and is important because it incorporates SST in both Atlantic and Indian Oceans. Usually SST over two selected areas 5°S, 5°E and 25°S, 45°E are in phase. Both these areas are anti-phase with the area 5°S, 65°E. Positive SST anomalies (negative SST anomalies) over these areas are associated with low pressure (high pressure) and hence cyclonic flow (anticyclonic flow). Dry conditions over tropical southern Africa may be associated with situation when negative anomalies of SST are found over areas 5°S, 5°E and 25°S, 45°E and positive over area 5°S, 65°E (e.g. figure 4.9b). Relatively warm moist air is transported away from tropical southern Africa towards centres of positive SST anomalies in the central Indian Ocean. An opposite sign of anomalies over these areas describes wet conditions over tropical southern Africa with onshore wind flow. Therefore the 3 area index (3AI) shows that there is interaction between these marine areas and atmospheric conditions over tropical southern Africa.

In an effort to further contribute to understanding climate variability and its predictability over tropical southern Africa, the next chapter utilises a composite analysis technique to investigate the circulation patterns associated with extreme weather conditions in a season and patterns some months prior to drought.

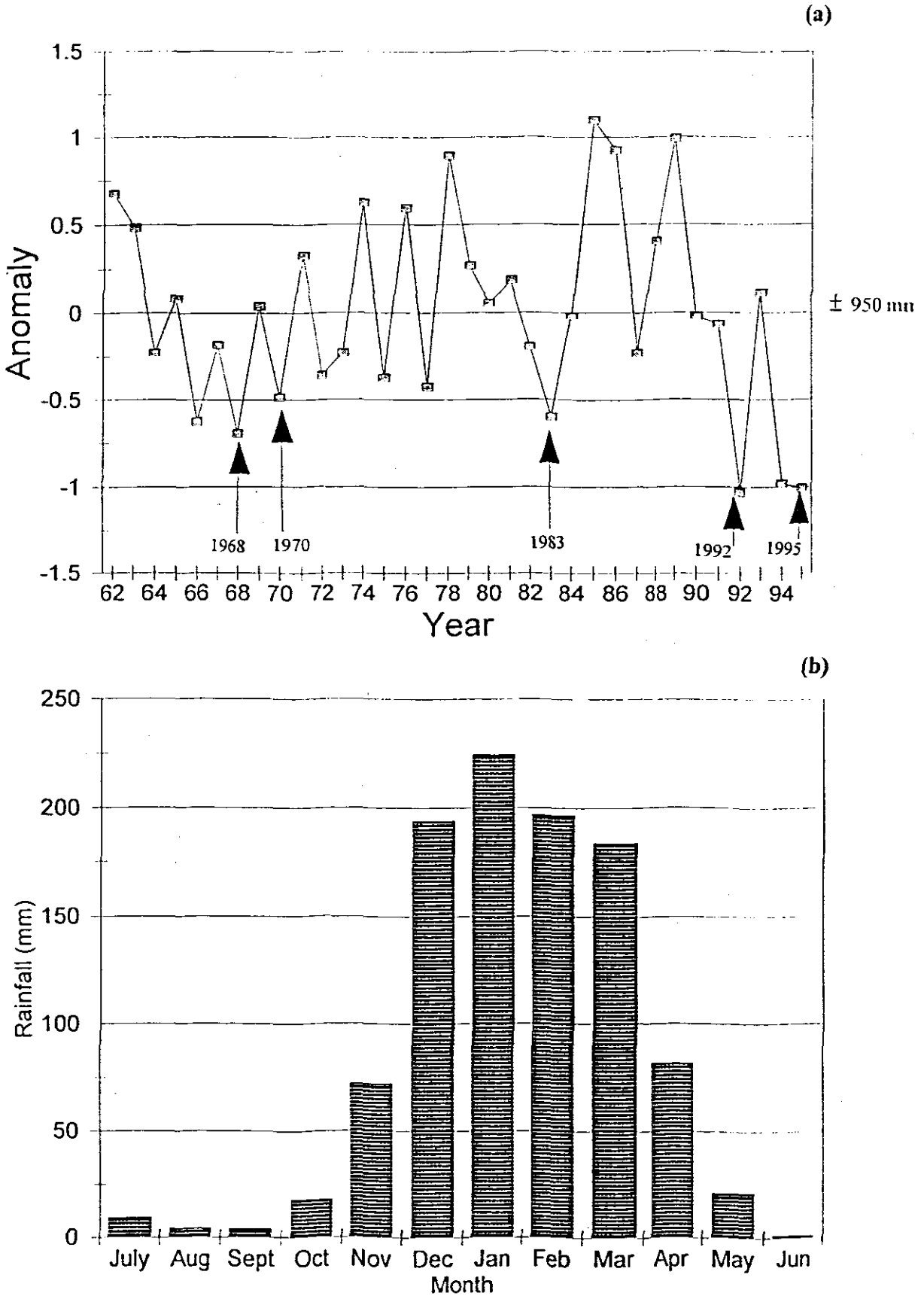

Figure 3.1: (a) Malawi rainfall index (normalised) 1962-1995. Arrows refer to dry years selected. (b) Malawi seasonal cycle for same period as (a).

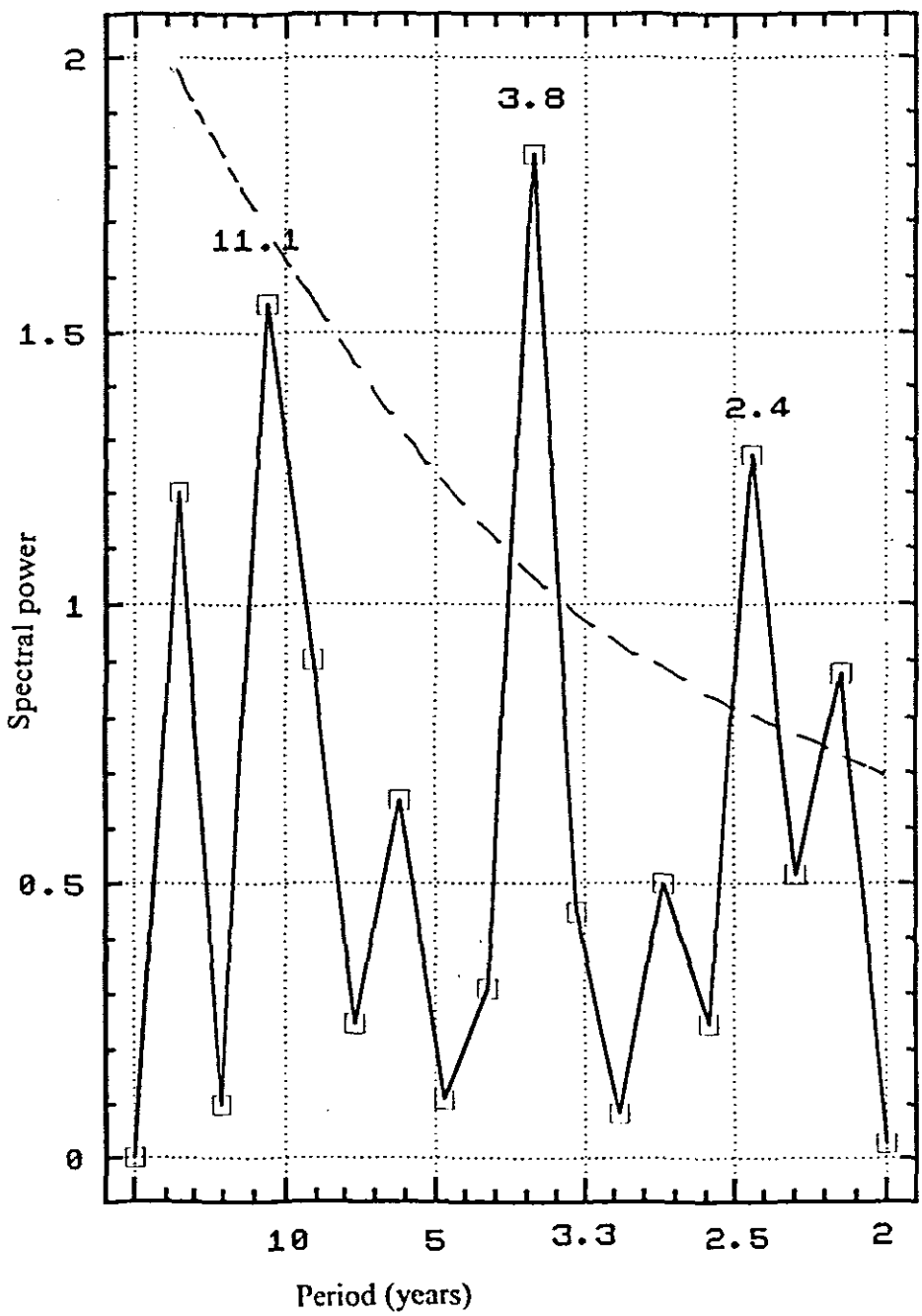

Figure 3.2: Spectral analysis of Malawi summer rainfall time series for the period 1962-1995. Dashed curve indicates 95% significant level.

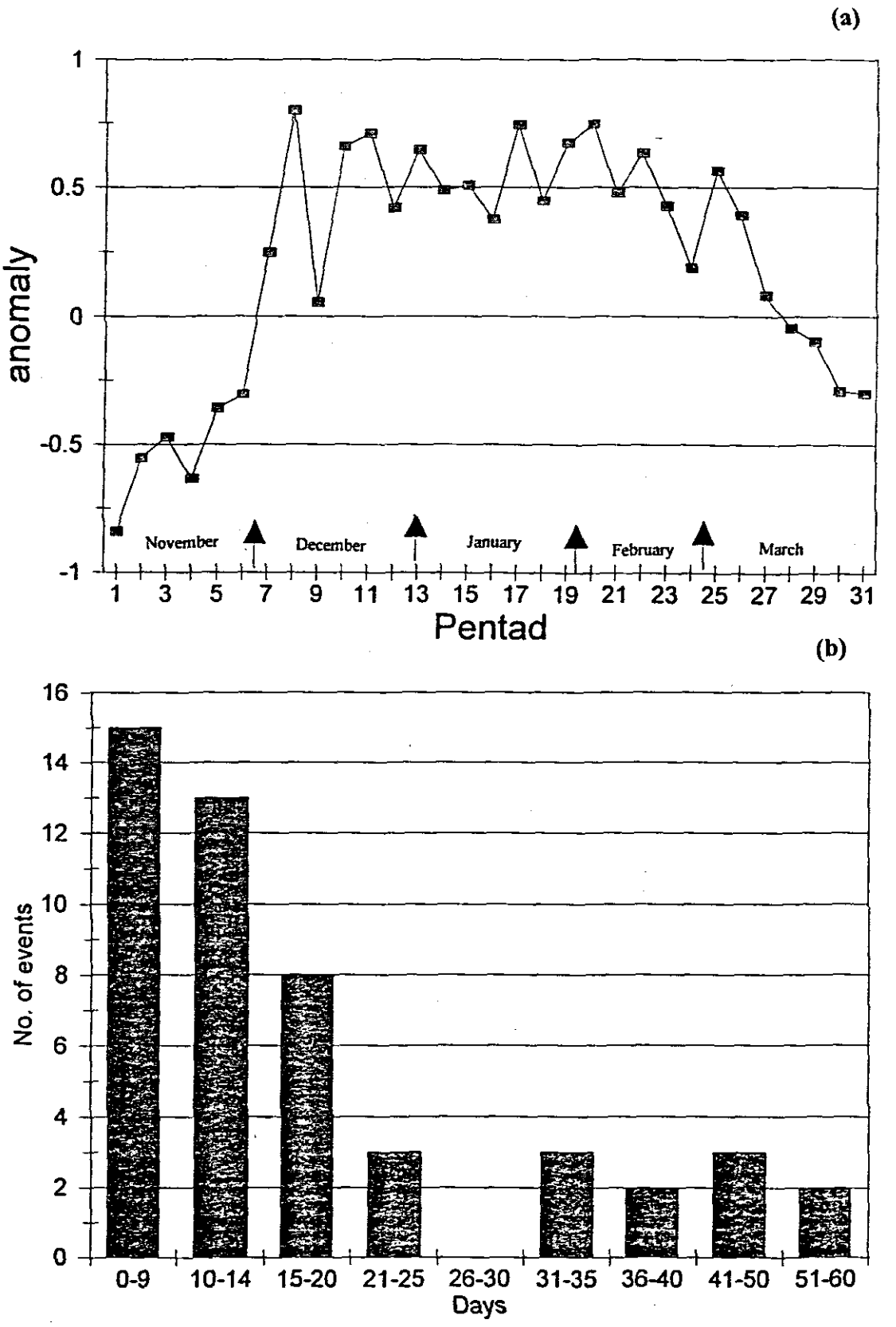

Figure 3.3: (a) Malawi long-term normalised seasonal pentad rainfall (1972-1993) time series. (b) frequency distribution of intra-seasonal oscillations identified in 1972-1993 daily rainfall. Arrows in top show division of months with respect to pentad.

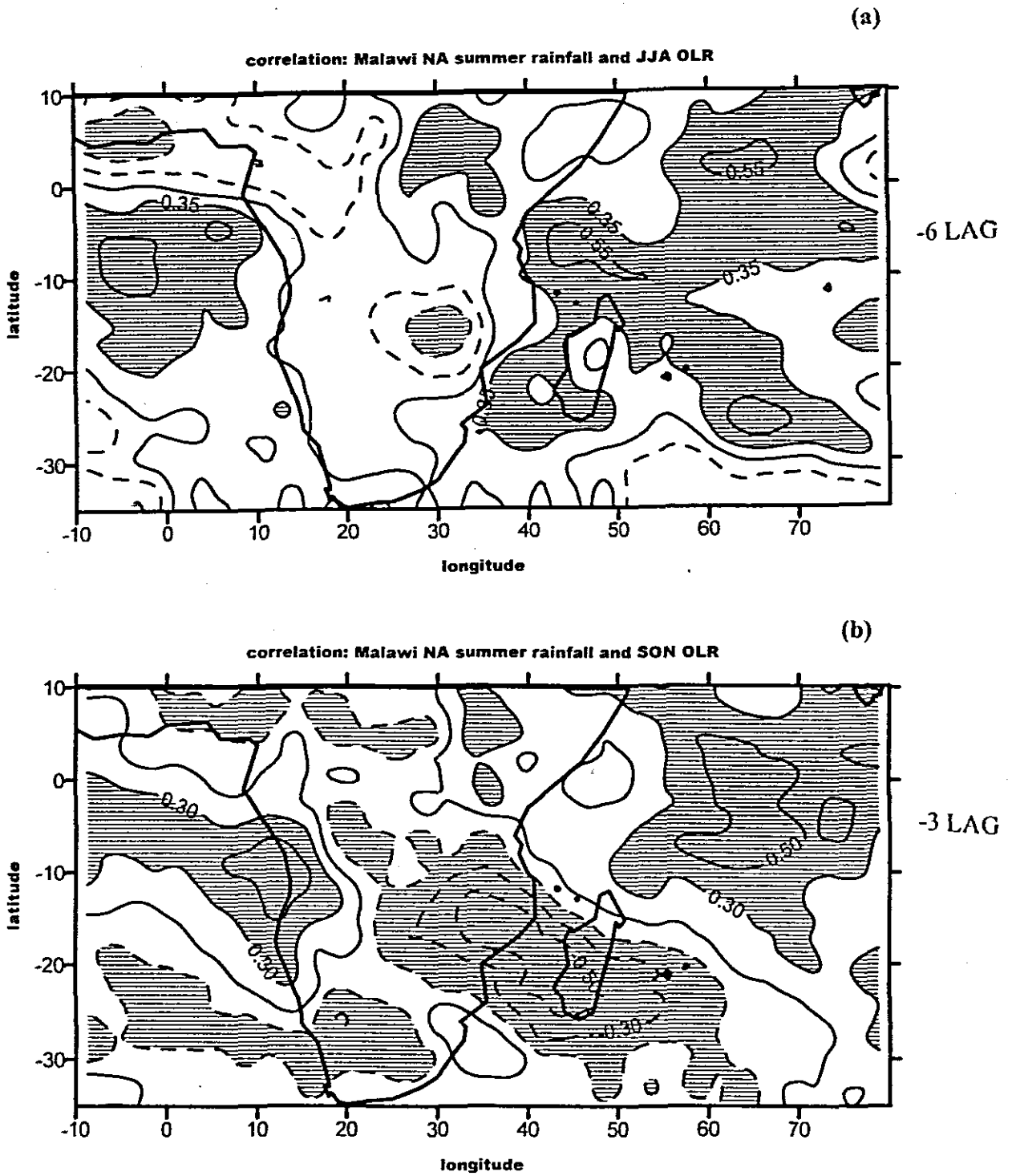

Figure 3.4: Correlations between the rainfall index (MRI) and OLR and lag (a) -6 (b) -3 months. Areas with largest correlations are shaded. Negative values are represented by dashed isolines, positive (solid). A value of 0.4 is significant at 95% significant with 20 degrees of freedom.

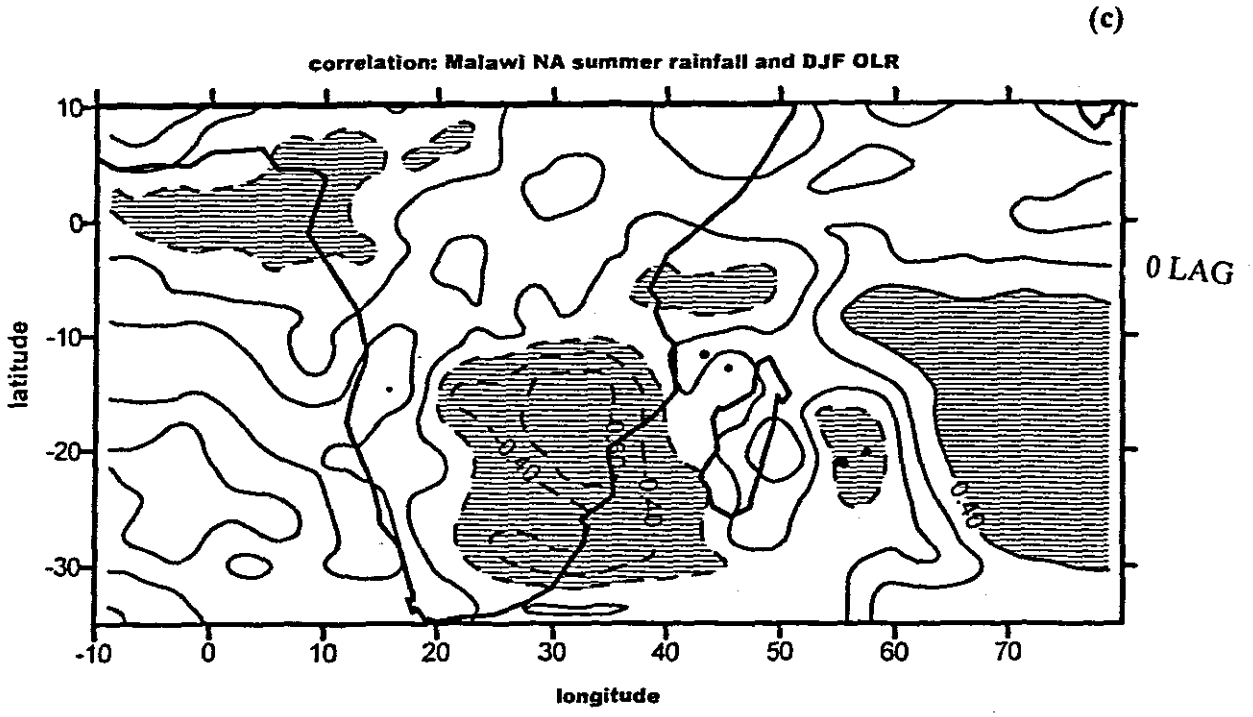

Figure 3.4 continued. Same as (a) but for (c) at 0 months lag.

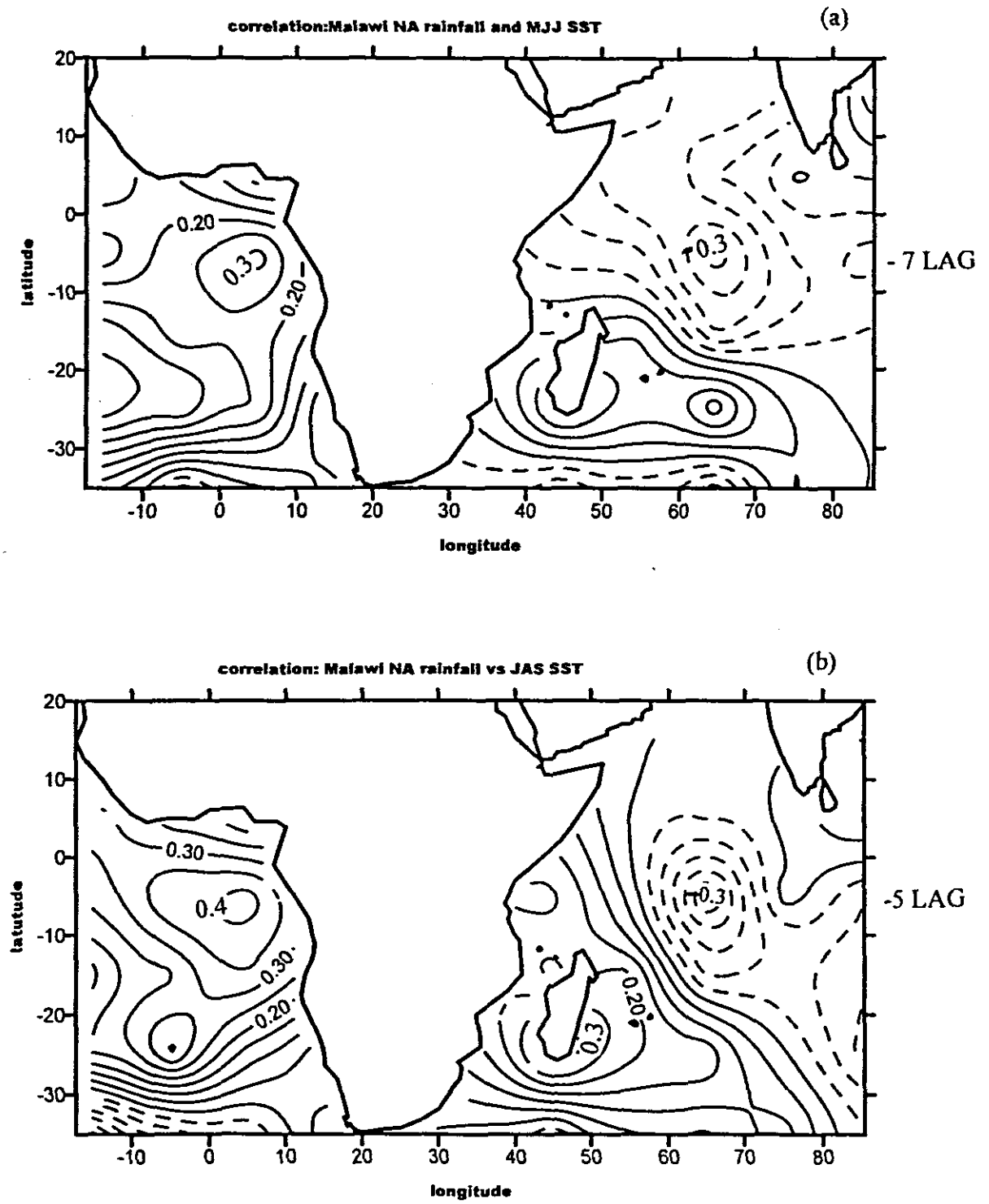

Figure 3.5: correlations between NA rainfall and Atlantic and Indian Oceans SST at lags (a) -7 and -5 months. Negative values are represented by dashed isolines, positive (solid). A value of 0.3 is significant at 95% significant level with 32 degrees of freedom.

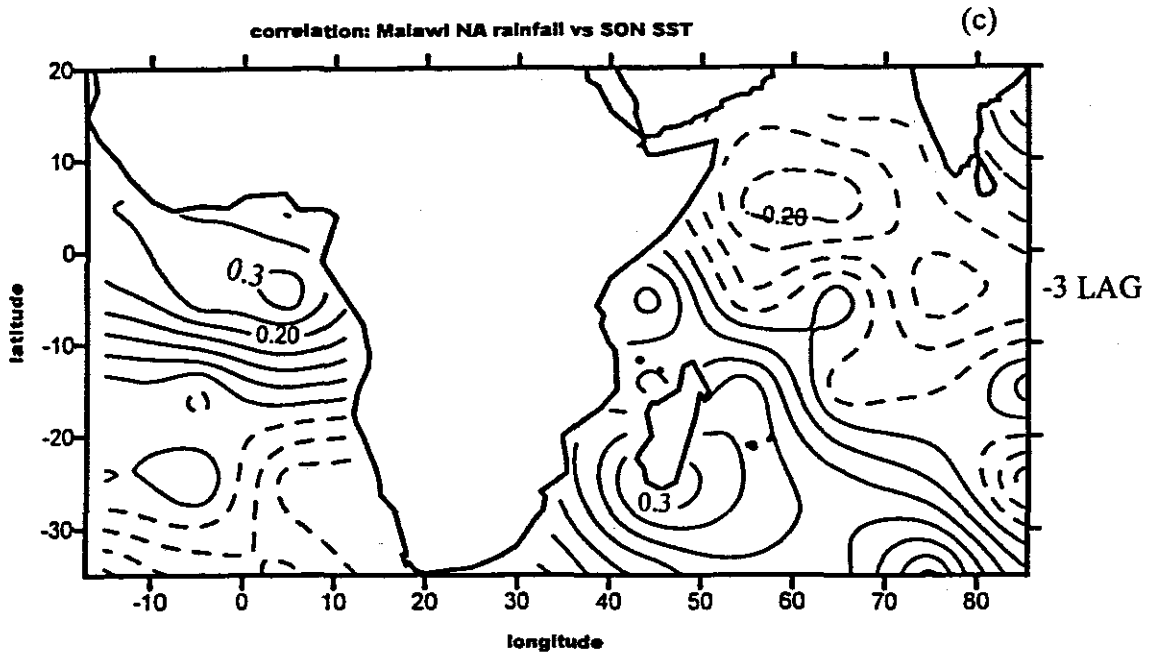

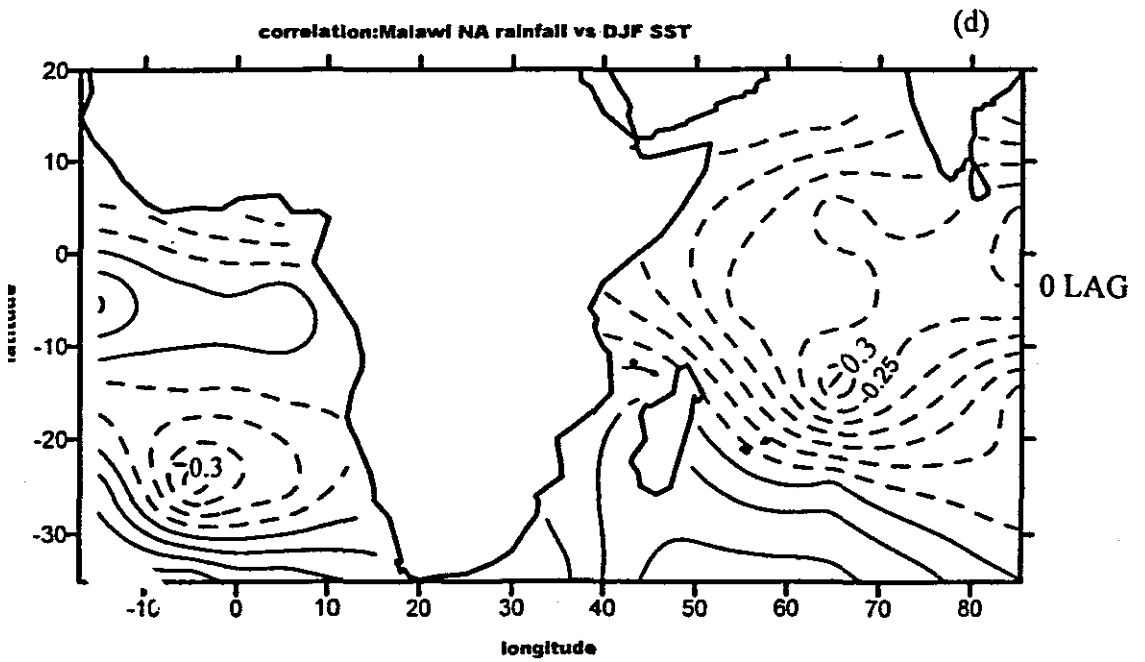

Figure 3.5 continued. Same as (a) but for (c) at -3 and (d) 0 months lags.

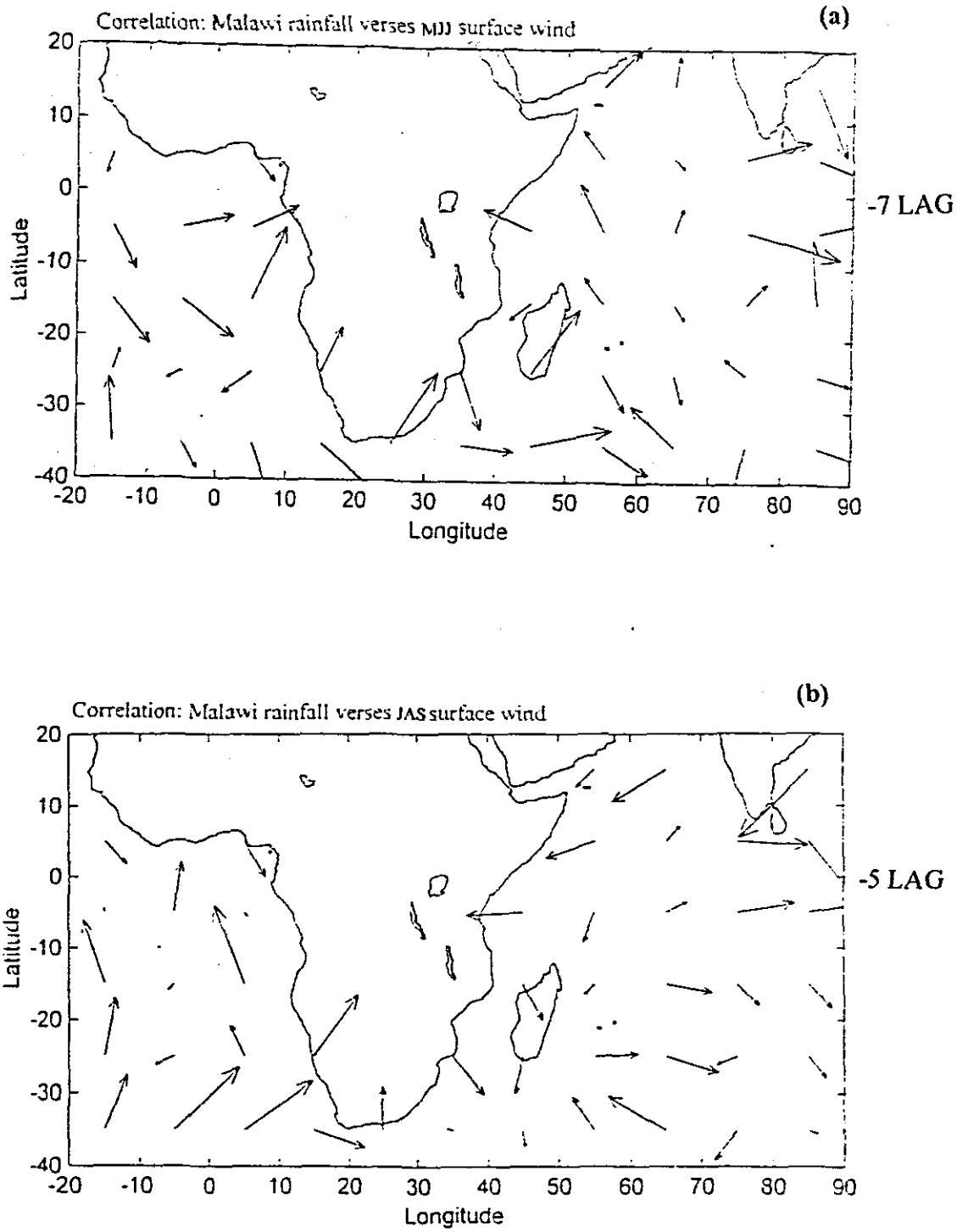

Figure 3.6: Vector correlation map of Malawi NA summer rainfall verses surface oceanic wind for lags (a) -7 and (b) -5 months. A length of 0.3 cm represents 95% significant level with 32 degrees of freedom.

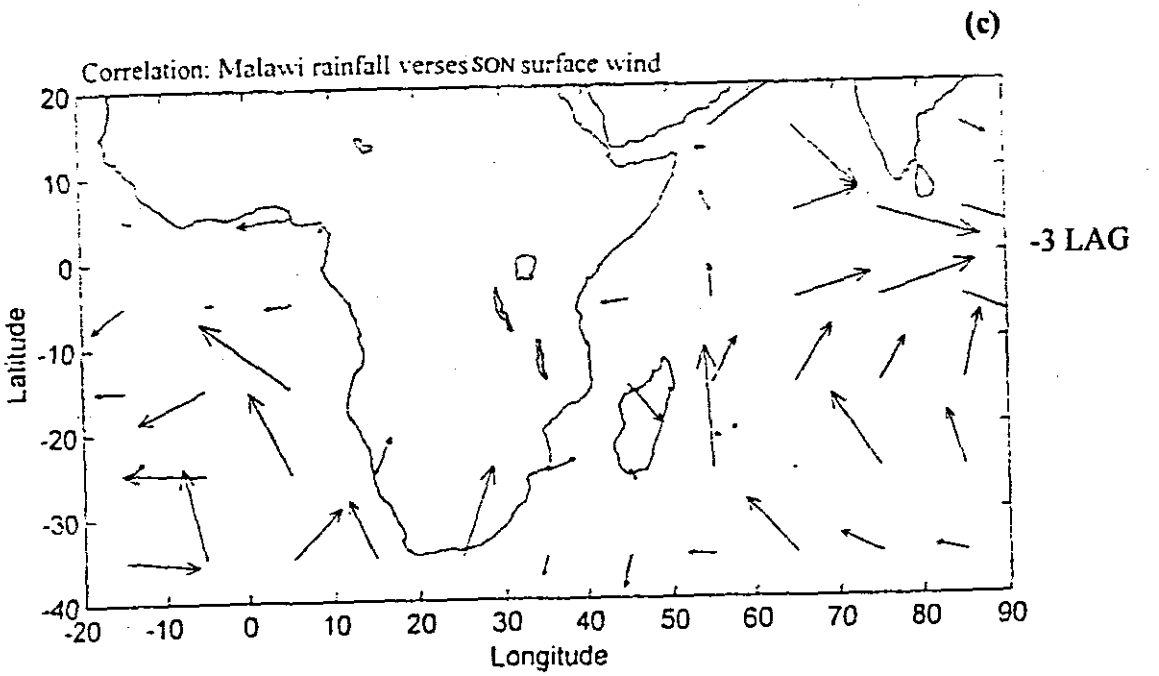

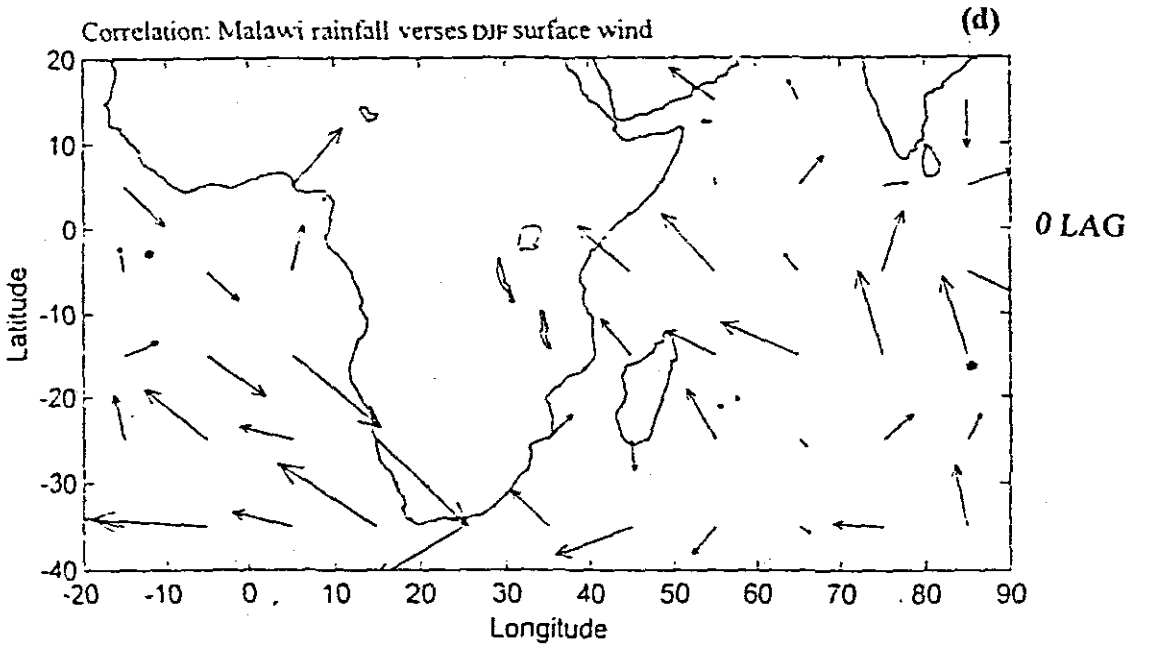

Figure 3.6 continued. Same as (a) but for (c) and (d) at lags -3 and 0 months.

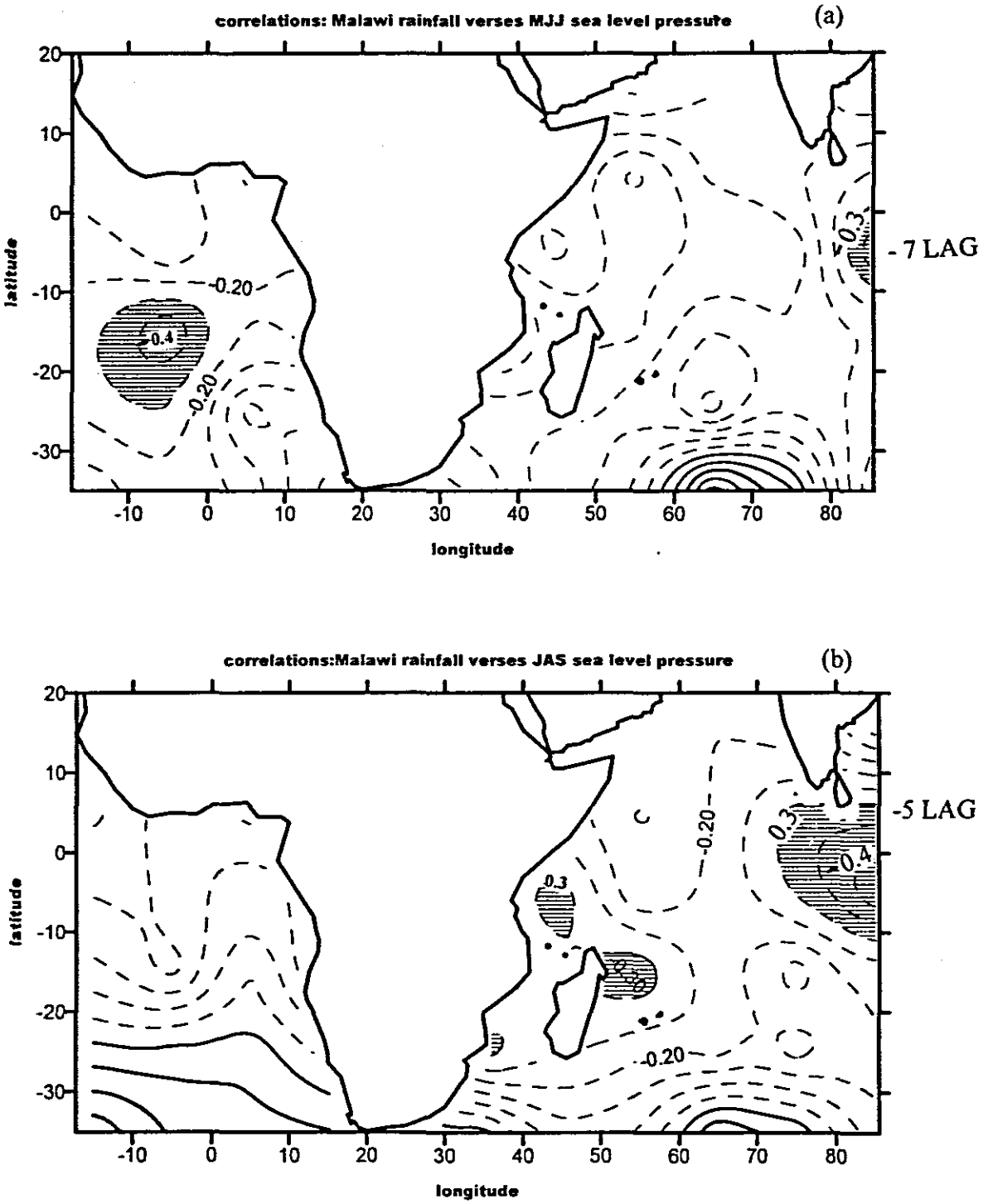

Figure 3.7: Correlations between NA rainfall and sea level pressure at lags (a) -7 and (b) -5 months. Negative values are represented by dashed isolines, positive (solid). Areas with largest correlations are shaded. A value of 0.3 is significant at 95% significant level with 32 degrees of freedom.

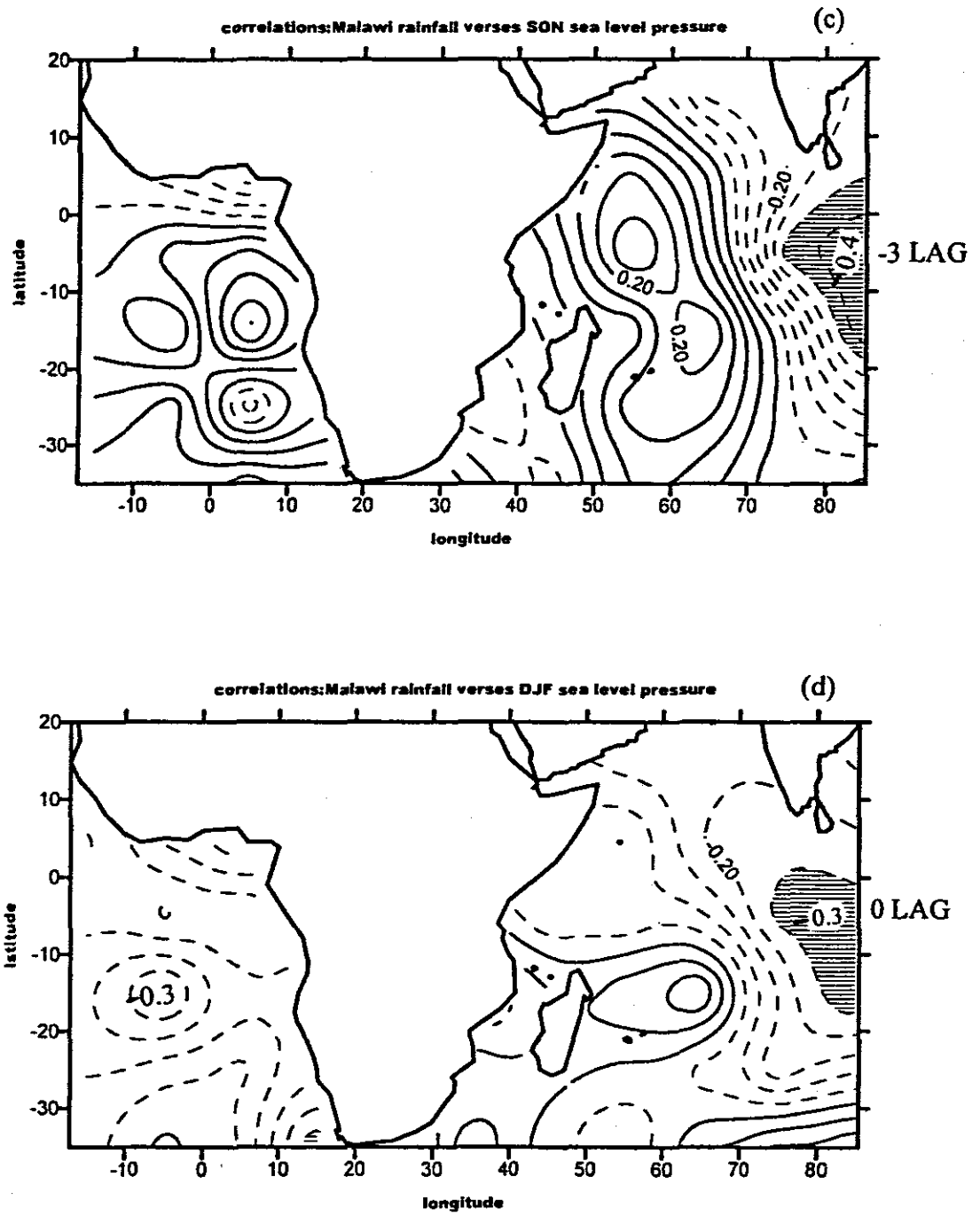

Fingure 3.7: continued. Same as (a) but for (c) at lags -3 and (d) 0 months.

Chapter 4

RESULTS OF COMPOSITE ANALYSES FOR DRY SEASONS AND THEIR PRECURSORS

4.1 Introduction

The main aim of this chapter is to investigate characteristics of dry conditions during summer and the winter season spring preceding it. The analysis is undertaken with the hypothesis that the circulation patterns and embedded weather systems some months before dry seasons behave differently. The study will also identify whether composite dry conditions over Malawi are related more to circulation patterns south of 10°S than those north of it. The summer period is from November to April while the precursor period is from May to October, taken as -6 months lag in the study. The precursor period May-October is important because climatic fluctuations taking place before the season may be captured and used for predictive purposes.

The objectives are achieved through interpretation of composite anomaly patterns of selected meteorological parameters, namely sea level pressure, geopotential height, vector winds, model-derived outgoing longwave radiation (OLR), precipitable water, sea surface temperature, air temperature, streamfunction and velocity potential from NCEP reanalysis. The patterns are observed at levels 850 hPa, 500 hPa and 200 hPa for geopotential height, vector wind but at sigma levels 0.995 and 0.210 sigma levels for streamfunction and velocity potential. Precipitable water is an integrated value between 1000 and 300 hPa. The 850 hPa and 200 hPa are chosen to represent lower and upper level circulation. These levels are routinely analysed in global diagnostic bulletins and then utilised for forecasting purposes (Jury and Pathack, 1993). The mid level is represented by 500 hPa nearest to the level of non-divergence. Circulation patterns during composite dry summers and the precursor period are analysed in the section below and important findings from the analyses are listed at the end of the chapter. The prior period May-October will be considered again in chapter six to identify common predictors.

4.2 Results of seasonal composites and precursors for dry years

4.2.1 Sea level pressure (SLP)

The anomaly pattern at lag -6 months (figure 4.1a) is dominated by high pressure to the south of Madagascar (47°S, 43°E) with a ridge into Malawi and another high pressure cell over the Atlantic Ocean (30°S, 20°W). Negative values are found northeast of Madagascar.

The composite anomaly pattern of sea level pressure (figure 4.1b) during the driest 5 summers indicates high pressure over Malawi extending into the Southern Mozambique Channel. Pronounced negative values are found over the ocean east of Madagascar and have extend into the Southern Ocean. The negative values extend westwards up to longitude 20°W, south of 38°S in the South Atlantic Ocean. Marked positive anomalies are observed over the Sahel. The pattern suggests that low pressure east of Madagascar is maintained but intensified at zero lag preceding dry summers.

4.2.2 Geopotential height: 500 hPa and 200 hPa

Anomalies of geopotential height at lag -6 months at 500 hPa level are indicated in figure 4.2a. An anticyclone in the south Indian Ocean is centred at about 45°S, 35°E and another anticyclone is centred at about 35°S, 25°W in the Atlantic Ocean. Figure 4.2b indicates the anomaly pattern of geopotential height at 500 hPa during composite dry seasons. The pattern reveals the dominance of an anticyclone over the subregion centred over Southern Namibia covering Botswana and South Africa. Marked negative values are observed over southern Oceans south of 40°S from the Atlantic to the Indian Ocean with a pronounced trough extending east of Madagascar. Large positive values that are observed south of 25°S at -6 lag are replaced with negative values at 0 lag months.

Figure 4.3a shows anomalies of geopotential height at 200 hPa during the preceding period (-6 months lag). The pattern is dominated by positive values with marked centre at approximately 40°S, 42°E in the South Indian Ocean ridging into Madagascar. Another pronounced centre of positive values is observed near 35°S, 30°W over the South Atlantic Ocean. The anomaly pattern of geopotential height at 200 hPa (figure 4.3b) during composite dry summer shows negative values along an axis near 45°S from the Atlantic to Indian Ocean. A zonal ridge is positioned over East Africa.

Variable	-6 months lag MO	0 month lag NA	Key area
SLP	+ 0.9	- 0.7	38°S, 55°E
SLP	- 0.3	- 0.7	15°S, 60°E
SLP	+ 1.0	+ 0.4	30°S, 20°W
500 GPM	+ 11.0	- 8.0	38°S, 30°E
200 GPM	+ 20.0	- 22.0	35°S, 45°E
850 wind	- 2.8	- 2.0	3°N, 85°E
200 wind	- 0.6	+ 1.0	10°S, 10°E
OLR	- 12.0	- 8.0	10°S, 50°E
	- 3.0	+ 5.0	20°S, 35°E
Precipitable water (PW)	+ 2.5	+ 1.5	20°S, 60°E
SST	+ 0.4	+ 0.6	15°S, 70°E
SST	- 0.4	- 0.5	35°S, 70°E
SST	- 0.1	- 0.9	35°S, 10°W
Temperature at 850 hPa	- 0.6	- 0.4	20°S, 65°E
Streamfuction 0.995 sigma level	-7×10^5	-8×10^5	7°S, 85°E

Table 4.1: Climatic memory of anomaly patterns over areas of strong signals at lags -6 and 0 months extracted from composite analysis (dry years) of selected meteorological parameters. Note that the mid-latitude change in sign of geopotential field could be an artifact of the different cases or a real predictor.

Lack of climatic memory is observed when there is a change in sign of a value from -6 months lag to 0 months lag. Several cases are consistent in table 4.1(e.g., SST, OLR, winds and SLP at two locations). However a sharp change is found in the upper level geopotential, hence zonal wind in the mid-latitudes.

4.2.3 Wind vectors: 850 hPa, 500 hPa and 200 hPa

Figure 4.4a shows anomalies of vector wind at 850 hPa at a lag of -6 months. Cyclonic flow, with a centre north of Madagascar controls the wind flow over most parts of the western Indian Ocean. Strong easterly winds are observed over the equator, east of 75°E to the south of India. These are persistent up to 0 lag months.

In the anomaly pattern of vector wind at 850 hPa level (figure 4.4b) during composite dry summer, easterlies are moderately strong south of India spreading along the equator causing Ekman divergence in the surface ocean. The flow resembles an El Nino

situation type where a cool tongue of SST is found west of Malaysia favouring sinking motion and divergence near Indonesia. Westerly winds north of Madagascar flow towards warmer SST in the central Indian Ocean and reduce moist inflows to Malawi and surrounds.

The pattern of vector wind at -6 months lag at 500 hPa (figure 4.5a) shows a cyclonic flow centred over the border between Angola and Namibia and extends a trough into southern half of Mozambique through Zimbabwe and Botswana. Marked anticyclonic flow is found off east coast of Madagascar. The centre of an anticyclonic flow is at about 45°S, 30°E and extends into the Republic of South Africa. Winds are generally onshore in the Atlantic Ocean within latitudes band 5-15 °S but offshore north and south of this band. Winds are easterly and stronger in the Atlantic Ocean south of 20°S than in the Indian Ocean.

The anomaly pattern of vector wind at 500 hPa (figure 4.5b) indicates an s-curve pattern of westerly wind anomalies from the Atlantic Ocean (35°S) to Malawi through southern South Africa (15°S). A pronounced trough is found to the east of South Africa and a ridge to the west while marked equatorward flow is found between South Africa and Malawi. There is a change in latitude hence coriolis parameter. The effect of latitude change has been analysed by calculating omega (section 7.2.2). Results indicate sinking motion associated with the mid-tropospheric circulation pattern.

Anomaly patterns for vector wind at 200 hPa at lag -6 months are presented in figure 4.6a. Pronounced anticyclonic flow, with centre south of Madagascar, is observed over Indian Ocean south of Madagascar. It extends a ridge inland up to Angola. Wind regimes in the Atlantic Ocean show the dominance of easterlies in the Atlantic Ocean north of the equator but westerly over the Indian Ocean over the same latitudes and winds are generally easterly over southern Africa.

The anomaly pattern of vector wind at 200 hPa (figure 4.6b) during composite dry summer indicates westerly equatorial Atlantic flow which extends over Malawi. SW flow from the South Atlantic reaches Madagascar thus causing confluence with the westerly equatorial flow from the Atlantic. Winds are generally westerly over the Atlantic and the subcontinent. The flow over the Indian Ocean is a dipole structure, anticyclonic to the northeast of Madagascar and cyclonic to the south. Wind anomalies are strong in the Atlantic Ocean north of 15°S but in the Indian Ocean strongest westerlies are within 15-30°S band over southern Madagascar.

4.2.4 Outgoing Longwave Radiation (OLR)

Anomaly field of OLR (figure 4.7a) at -6 months lag shows the dominance of negative values over much of the domain with lowest negative values just north of Madagascar. Figure 4.7b indicates the anomaly pattern of model-derived OLR during composite dry summer. Positive values are found in a NW-SE axis over Zimbabwe, southern Malawi and Southern Mozambique. Marked negative values are found over the Congo basin extending eastwards through East Africa. Marked negative values are also observed over Northern Madagascar and east of Mauritius.

4.2.5 Precipitable water

The anomaly pattern of precipitable water (figure 4.8a) at -6 months lag is dominated by positive values mainly over the Indian Ocean. Maximum positive values are centred north east of Madagascar.

The anomaly field of precipitable water (figure 4.8b) during composite dry summer indicates negative values south of Madagascar, Malawi and over South Africa. Positive values are observed over the western Congo and East Africa. Maximum positive values, with centre near 20°S, 65°E, occur east of Mauritius. This suggests that dry spells over Malawi 'spill over' from the southern Mozambique Channel, and occur when convection is increased in the south Indian Ocean.

4.2.6 Sea Surface Temperature (SST)

Anomalies of SST (figure 4.9a) at lag of -6 months shows pronounced negative values in the Atlantic Ocean from latitude 5°N to about 40°S with lowest value off the Angola coast. Weaker positive values are observed in the central Indian Ocean south of India. Hence tropical east Atlantic and central Indian Ocean SST are anti-phase with the onset of drought conditions.

Figure 4.9b indicates the anomaly pattern of SST during composite dry summer. Marked negative values are observed southeast of Madagascar (37°S, 65°E) and over the Atlantic Ocean centred at about 37 °S, 10°W. Negative values are found from the equator to latitude 20°S in the Atlantic from 30°W to 10°E. Marked positive values are found north east of Madagascar centred at about 15°S, 70°E. The pattern shows the importance of positive SSTs over the central Indian Ocean to the dry conditions not only

over Malawi but also to other countries of southern Africa as indicated elsewhere by other researchers. The westerly wind transport moist air away from tropical southern Africa towards convective area over central Indian Ocean.

4.2.7 Temperature at 850 hPa

Temperature is very useful parameter in the determination of extreme climatic conditions and is usually negatively correlated with rainfall. Therefore temperature may be a proxy indicator of drought severity. Temperature has been used by Chang (1998) to study teleconnections between droughts and spatial patterns which might be responsible for the drought producing mechanism during the Northern hemisphere summer with time scales on the order of at least a month.

Anomaly pattern of temperature at 850 hPa (figure 4.10) at -6 months lag shows marked positive values northeast of Madagascar (20°S, 55°E).

The anomaly pattern of air temperature at 850 hPa (figure 4.10b) during composite dry summer indicates highest temperature anomalies over southern Africa with a centre over Botswana consistent with the anticyclonic gyre at 500 hPa (figure 4.5b). Marked positive anomalies are also found east of Madagascar over the central Indian Ocean. Negative values are observed over the Eastern Sahel.

4.2.8 Streamfunction at 0.995 and 0.210 sigma levels

Streamfunction is a useful derived parameter in identifying large-scale rotational circulation. Positive values indicate cyclonic circulation while negative values shows anticyclonic circulation in the Southern Hemisphere. Cyclonic circulation is associated with low geopotential height (thus maximum positive stream function). In the Northern Hemisphere negative streamfunction and cyclonic circulation are associated with low geopotential heights.

Figure 4.11a shows anomalies of streamfunction at lower level (0.955 sigma level) at lag -6 months prior to composite dry summers. Marked anticyclonic circulation (negative values) is found in the Atlantic Ocean south of latitude 15°S with centre at 35°S, 22°W. In the Indian Ocean an anticyclonic circulation is observed east of longitude 50 °E from Arabian Sea with centres at 10°S, 85°E and 45°S, 55°E. There is marked band of positive anomaly from Madagascar to East Africa.

Anomaly field for streamfunction (figure 4.11b) at lower level (0.995 sigma level) during composite dry summers shows marked rotational trajectory from the dry SE Atlantic Ocean into eastern sub-region with centre of cyclonic circulation east of Madagascar during composite dry years. The pattern indicates change in sign of rotational flow from anticyclonic flow at lag -6 month to cyclonic flow 0 months lag south of 20°S and east of 55°E.

The anomaly pattern of streamfunction (figure 4.12a) at higher level (0.210 sigma level) at -6 months lag period prior to composite dry summer indicates anticyclonic circulation southeast of Madagascar with an axis extending to the Atlantic Ocean through Angola. Anomaly pattern for streamfunction in the upper atmosphere (0.210 sigma level) is presented in figure 4.12b.The pattern indicates the splitting of equatorial flow over 0°E. The pattern suggests confluence of tropical and subtropical westerlies near 40°E. An anticyclonic centre southeast of Madagascar (-6 months) shifts to north of Madagascar at 0 lag. The rotational flow lacks memory.

4.2.9 Velocity potential at 0.955 and 0.210 sigma levels

Velocity potential is a useful parameter to identify large-scale mass flux divergence. The parameter describes the circulation pattern, especially thermally forced direct circulations, which undergoes the north-south or east-west overturnings in the troposphere of the tropical region. The flow is from negative area to positive and perpendicular to contours with divergence proportional to contour gradient. Negative anomalies of velocity potential are associated with divergence while positive values are associated with convergence, hence sinking or rising motion depending on level of occurrence.

Anomaly pattern of velocity potential (Figure 4.13a) at lower level (0.955 sigma level) during period prior to composite dry summer (-6 months lag) shows strong convergence north of Madagascar and divergence east of 65°E. Moderate positive values are centred over Cameroon and Sahel region.

Anomaly pattern of velocity potential (figure 4.13b) at lower level (0.995 sigma level) during composite dry summer shows persistence of positive anomalies near Madagascar from -6 lag months to lag 0 months. Monsoon convection is enhanced north of Madagascar at first, then east of Madagascar at 0 lag by convergent flow.

The anomaly pattern for velocity potential (Figure 4.14a) at higher level at lag -6 months shows maximum positive values in the Atlantic Ocean (28°S, 25°W) and Indian Ocean (35°S, 80°E) and lowest negative values centred over Eastern Tanzania.

Figure 4.14b indicates the anomaly pattern of velocity potential at higher level (0.210 sigma level) during composite dry summer. The pattern shows upper convergence centred over Zimbabwe and divergent axis at ± 60°E. The pattern is generally dominated by positive anomalies over the entire domain.

4.3 Discussion and Summary

The study was undertaken with the hypothesis that the circulation patterns and embedded weather systems some months before a dry season behave differently. The study was also to discover whether dry conditions over Malawi were related more to circulation patterns south of 10°S than to the north of it. The main objectives of the study have been achieved through the interpretation of selected meteorological variables and summary of results are presented below.

Based on results of the analysis, dry conditions over Malawi are due to ridging of anticyclone from either southern Mozambique or from high pressure cell in the Atlantic Ocean and deep low pressure cell to the east of Madagascar in the lower levels. An anticyclone prevails over Botswana and Namibia at 500 hPa level. Marked positive SSTs are observed over the central Indian Ocean and are in phase with SSTs to the south of South Africa but anti-phase with SSTs in the tropical east Atlantic Ocean during dry summer. The pattern is well supported by velocity potential fields at lower and upper levels and as well as streamfunction at lower level. OLR shows negative composite anomalies to the north of Madagascar in a southeast-northwest axis. This represents the position of the Inter-Tropical Convergence Zone during dry years. Positive OLR is found over Mozambique and Zimbabwe and related more to circulation patterns to the south of 10°S. When drought affects Malawi, it also appears in Zimbabwe, Mozambique, the adjacent Channel and southern Madagascar. Malawi dry summers have been associated with circulation pattern at 500 hPa level (figure 4.5b).

The precursors for dry summers are summarised below:

(a) SST anomalies are negative over the Atlantic Ocean north of 38°S and east of 20°W with a pronounced centre off Angola in anti-phase with positive SST anomalies over areas northeast of Madagascar.

(b) Anticyclone south of Madagascar ridges up to Malawi/Zambia through southern Mozambique and low pressure cell is found to the northeast of Madagascar.

(c) Pronounced positive velocity potential (hence convergence) over southern Africa with centre over Zimbabwe in the upper level.

(d) Largest positive values of temperature over Botswana and east of Madagascar at lower levels.

(e) Anticyclonic circulation of streamfunction to the east of 40°E with centre at 7°S, 85°E in lower level (0.995 sigma level) and over southern Madagascar at upper level (0.210 sigma level).

(f) Marked anticyclonic flow south of Madagascar at 200 hPa.

The composite analysis of circulation patterns shows that the wet circulations (not shown) are almost opposite to those of dry years. The circulation patterns of these differences of precursor period will be investigated in chapter 6 in order to identify common predictors for both dry and wet years. Composites fields will assist in establishing long-range forecast models for rainfall over southeastern Africa, thus helping reduce the risk of drought impacts on food and other resources.

The analyses in the next chapter investigate circulation patterns of selected dry spells at intra-seasonal time scales.

(a)

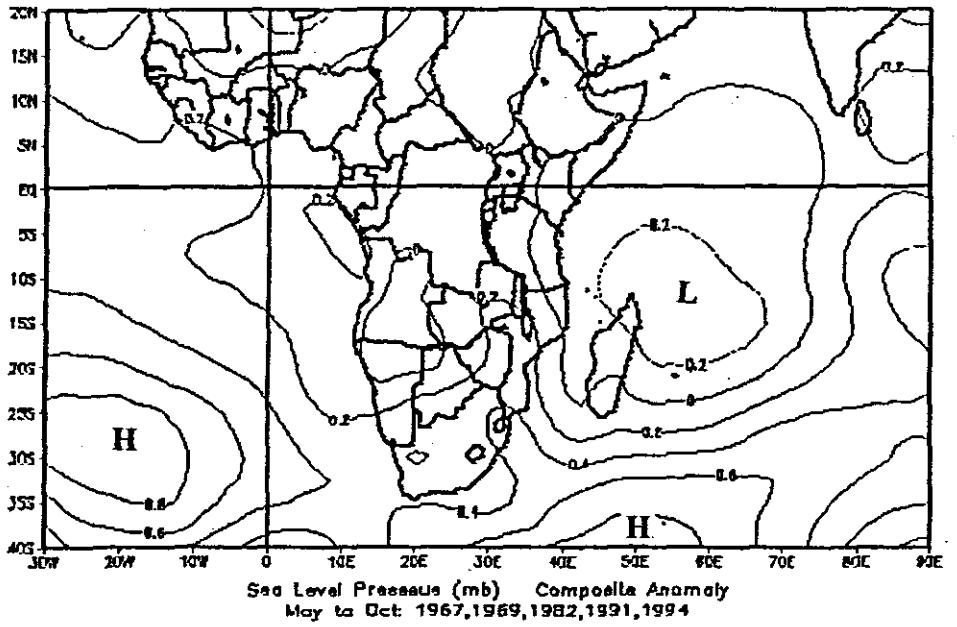

(b)

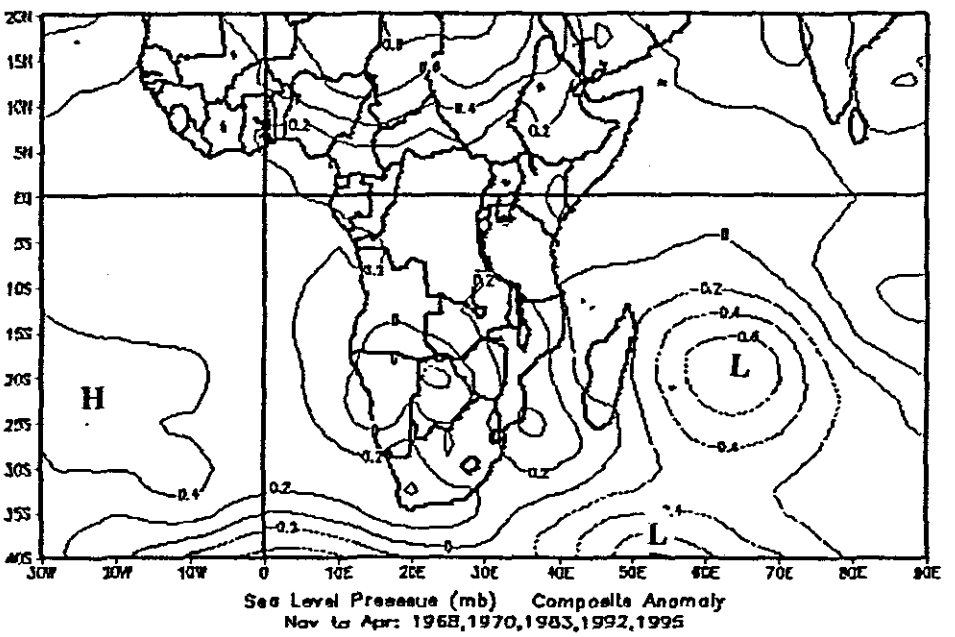

Figure 4.1: Sea level pressure composite anomaly (a) during preceding period may-October (b) during dry summer. Negative values are represented by dashed isolines, positive (solid). Contour interval is 0.2 hPa.

(a)

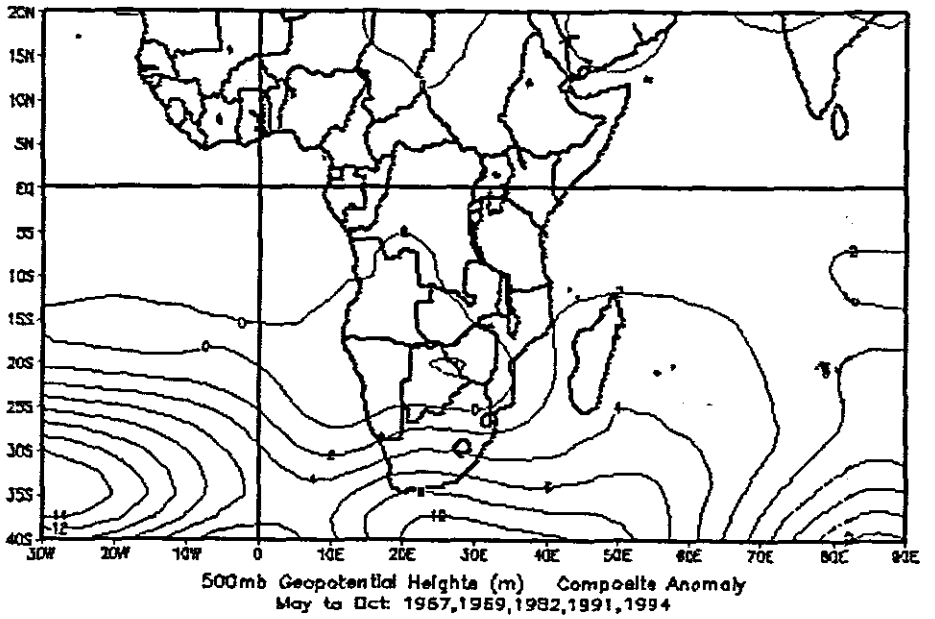

(b)

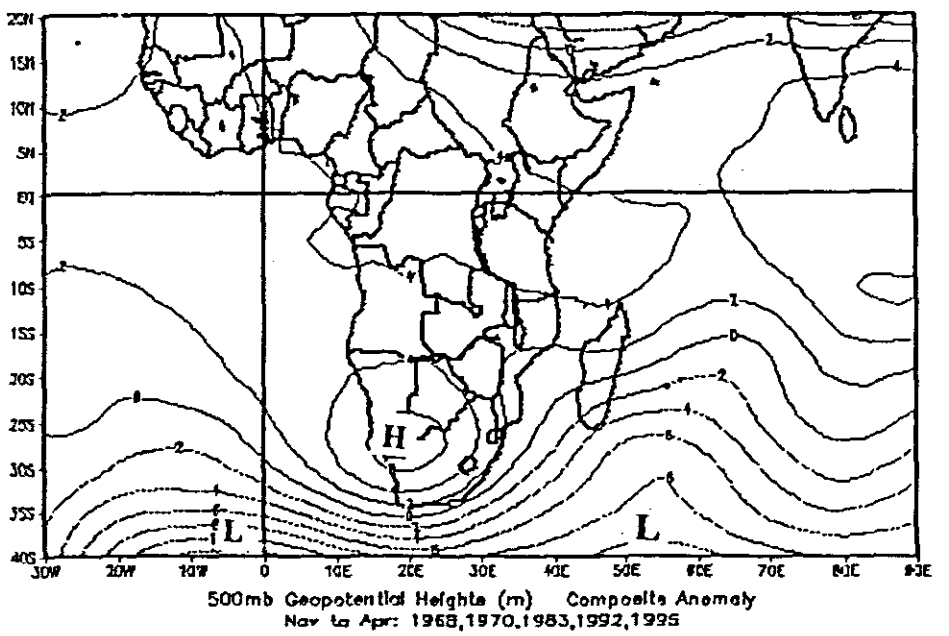

Figure 4.2: Geopotential height composite anomaly at 500 hPa (a) during preceding period May-October. (b) during dry summer Negative values are represented by dashed isolines, positive (solid). Contour interval is 2 m.

(a)

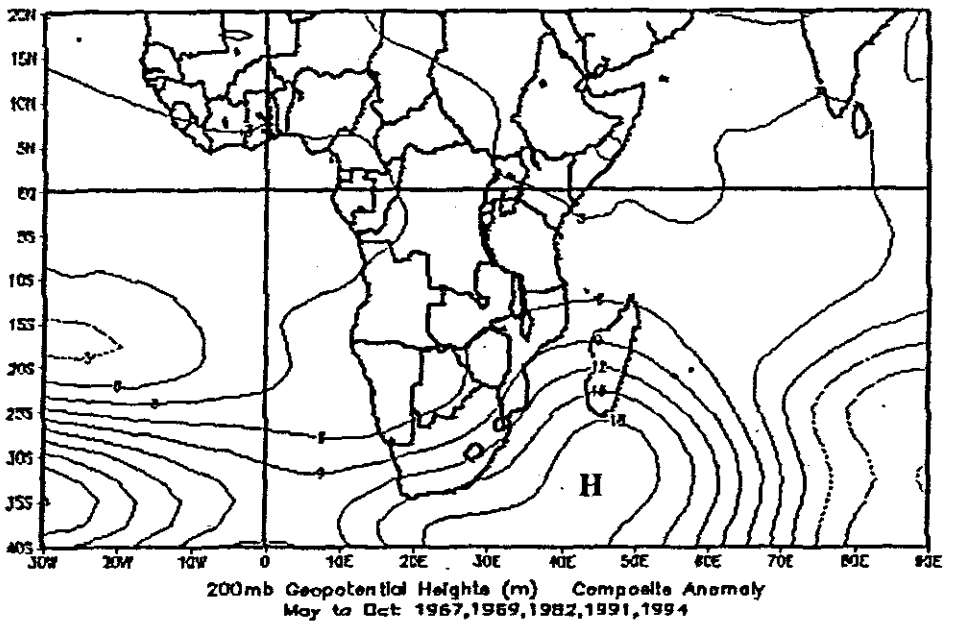

(b)

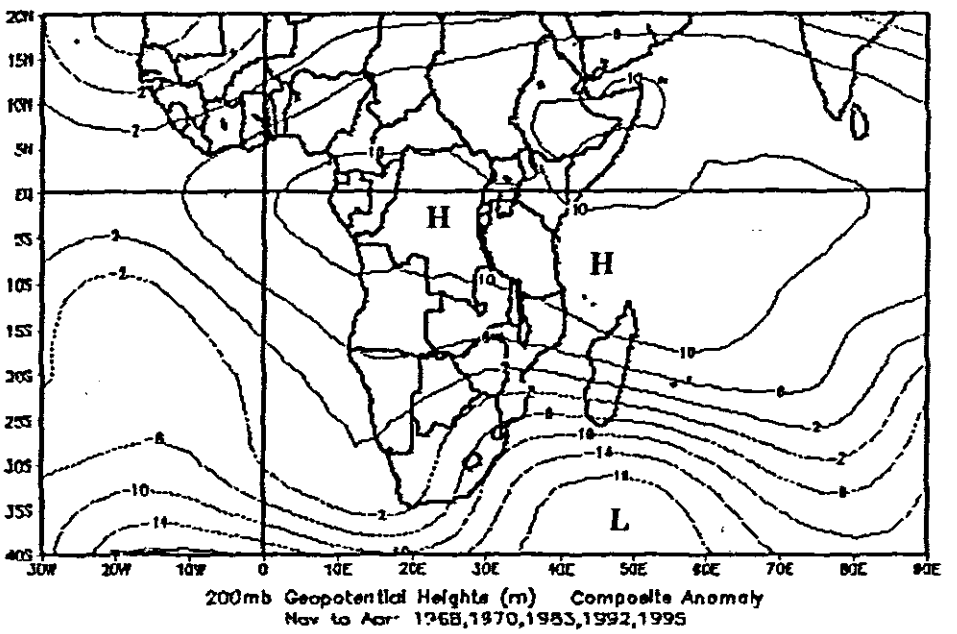

Figure 4.3: Geopotential height composite anomaly at 200 hPa (a) during preceding period May-October. (b) during dry summer. Negative values are represented by dashed isolines, positive (solid). Contour interval is 4 m.

(a)

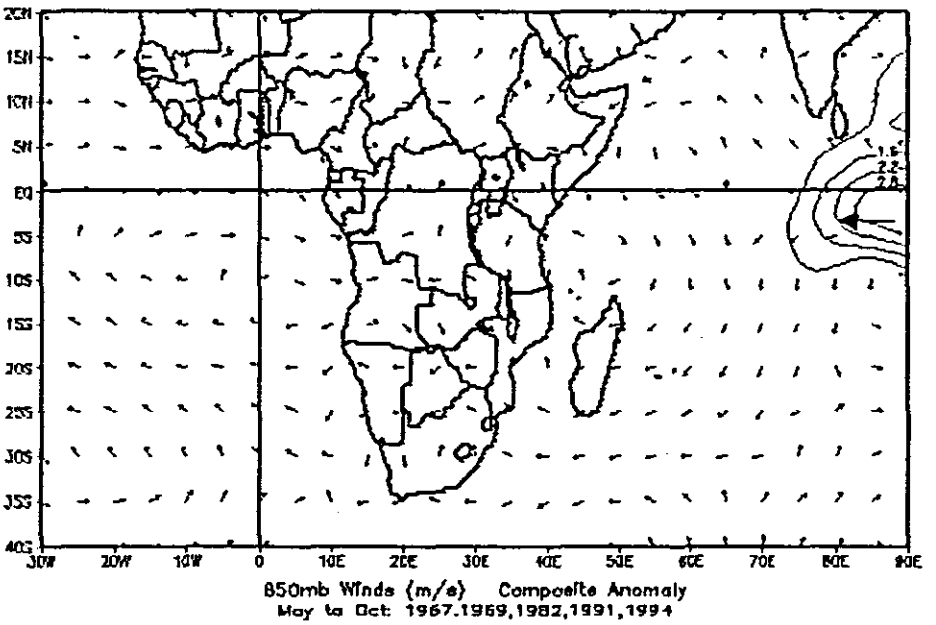

(b)

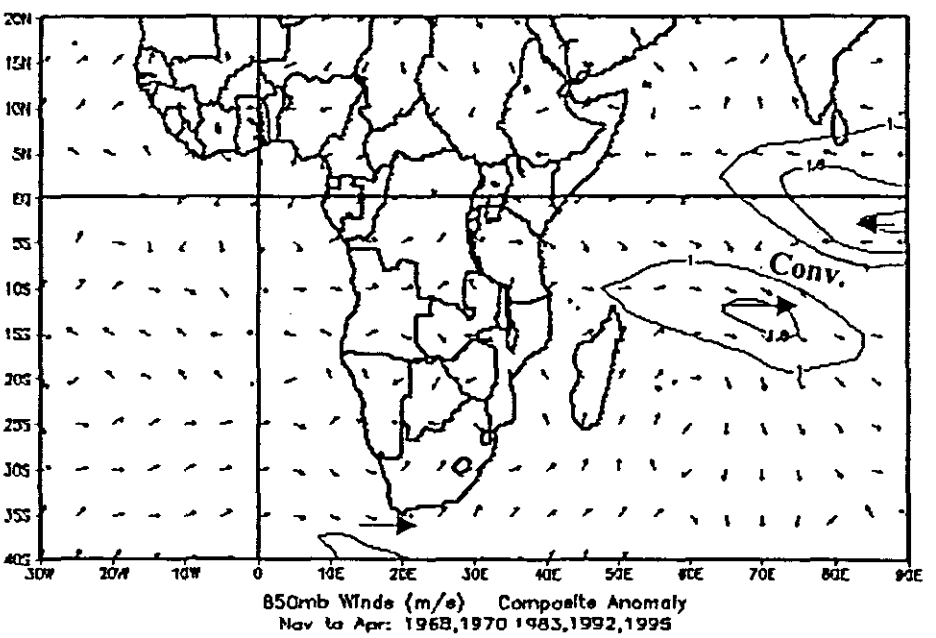

Figure 4.4: Vector wind composite anomaly at 850 hPa (a) during preceding period May-October. (b) during dry summer. Contour interval is 0.6 m/s.

(a)

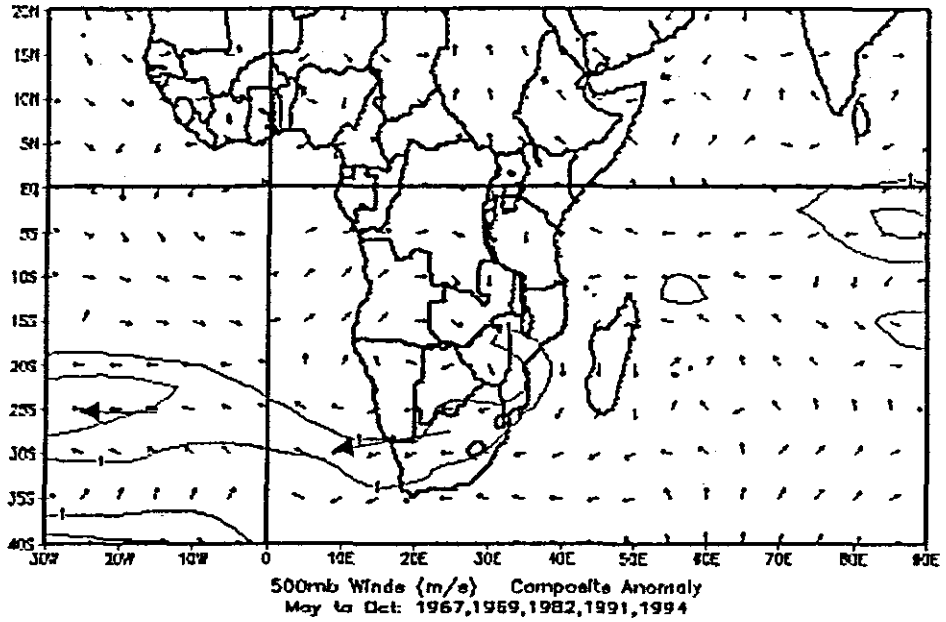

(b)

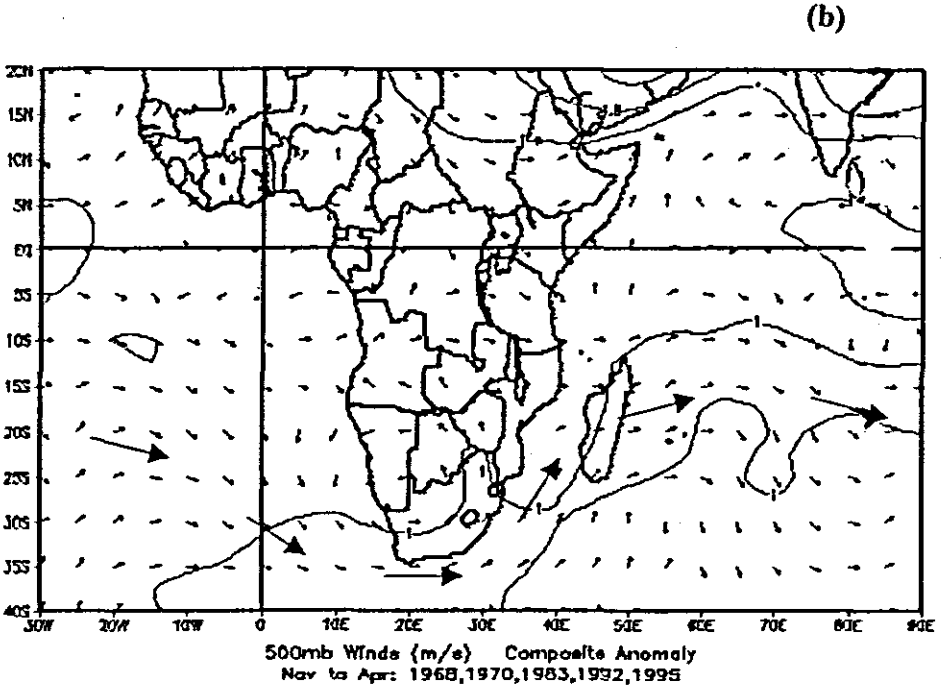

Figure 4.5: Vector wind composite anomaly at 500 hPa (a) during preceding period May-October. (b) during dry summer. Contour interval is 0.5 m/s.

(a)

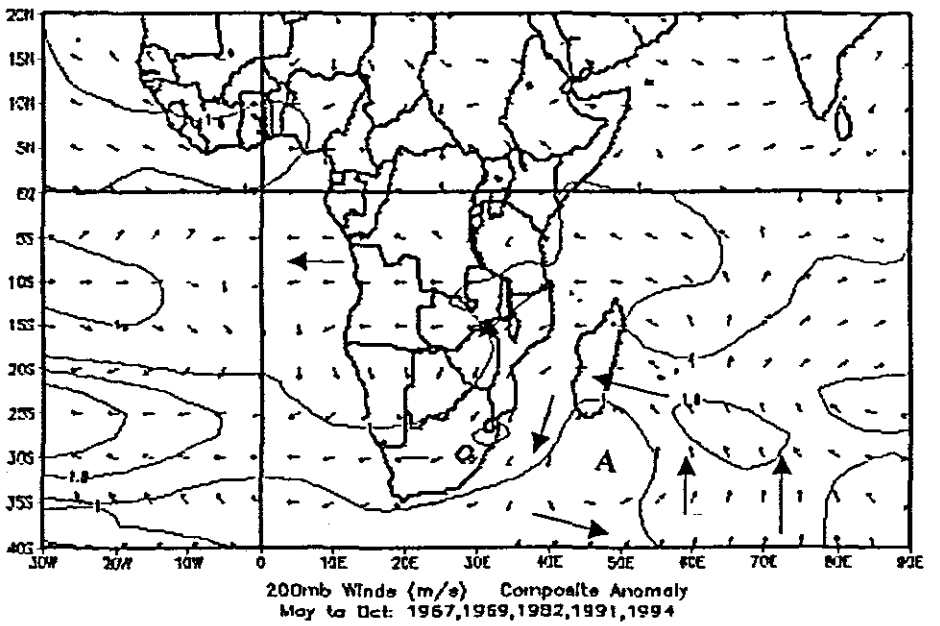

(b)

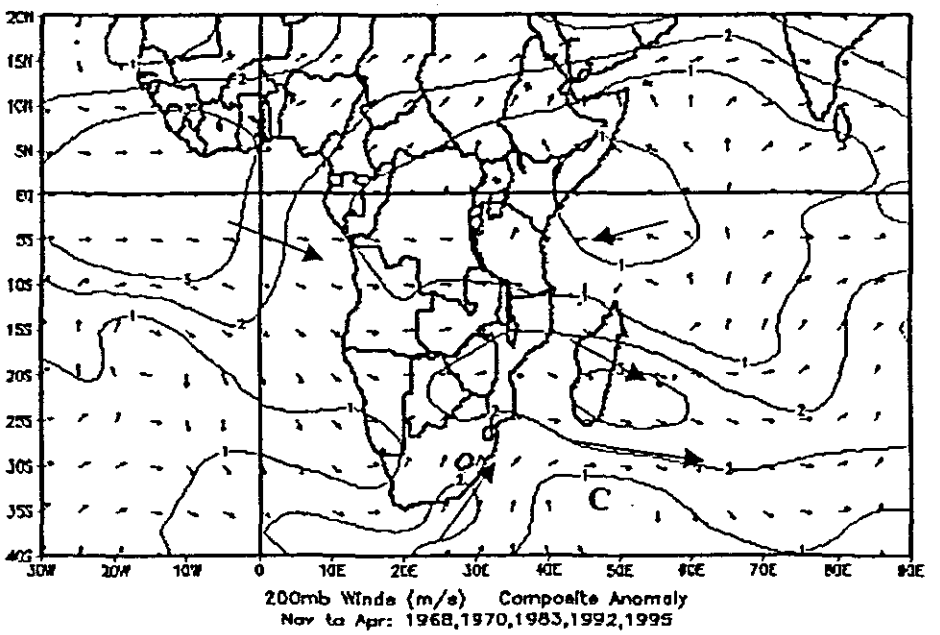

Figure 4.6: Vector wind composite anomaly at 200 hPa (a) during preceding period May-October. (b) during dry summer. Contour interval is 0.6 m/s.

(a)

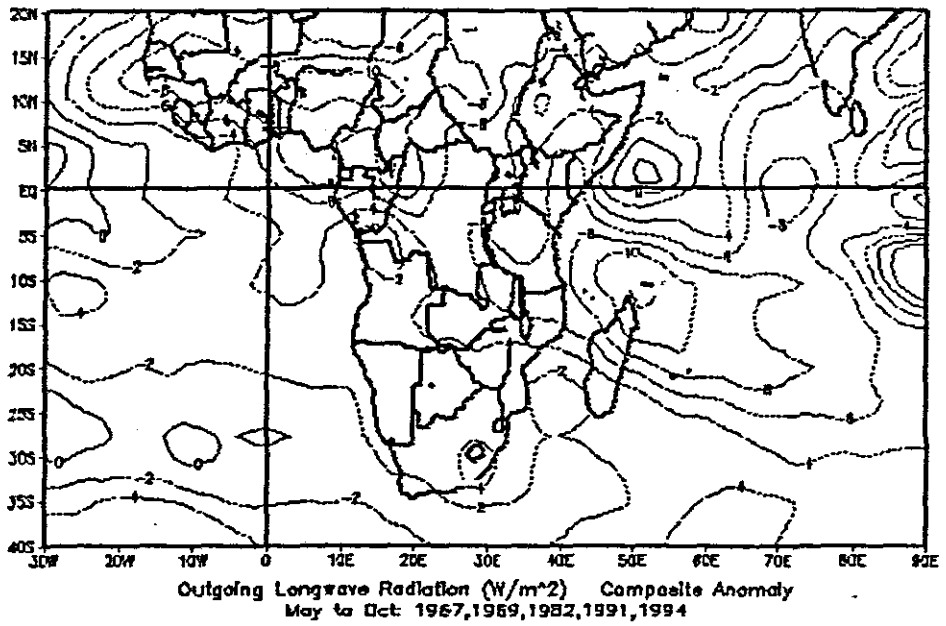

(b)

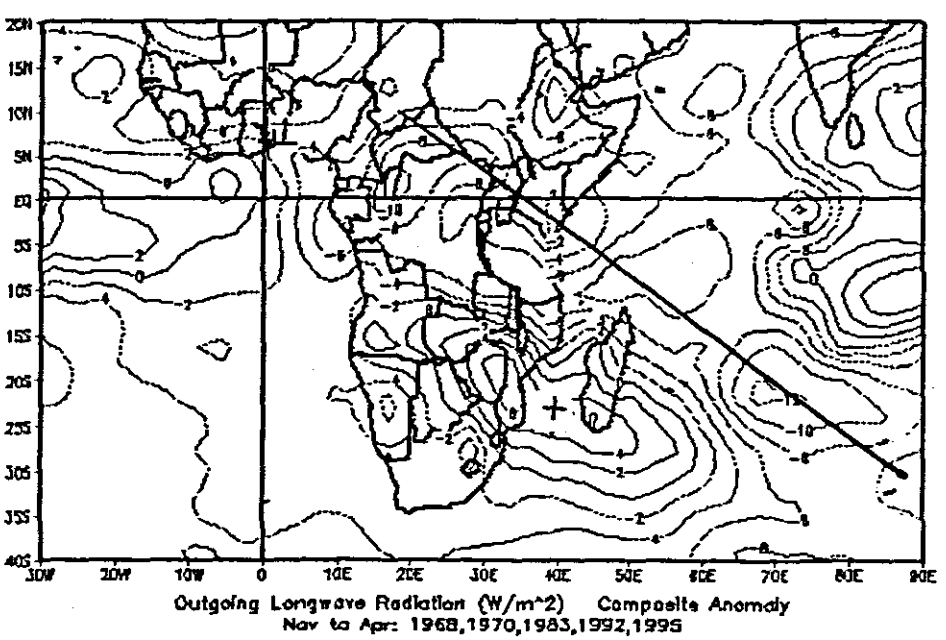

Figure 4.7: OLR composite anomaly pattern (a) during preceding period May-October. (b) during dry summer. Negative values are represented by dashed isolines, positive (solid). Contour interval is 2 w m^{-2}.

(a)

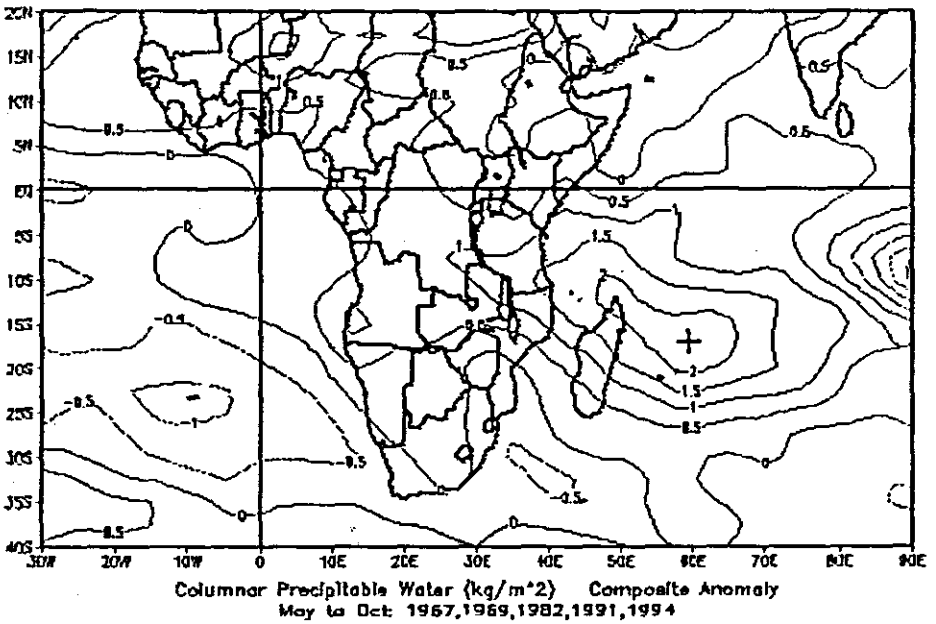

(b)

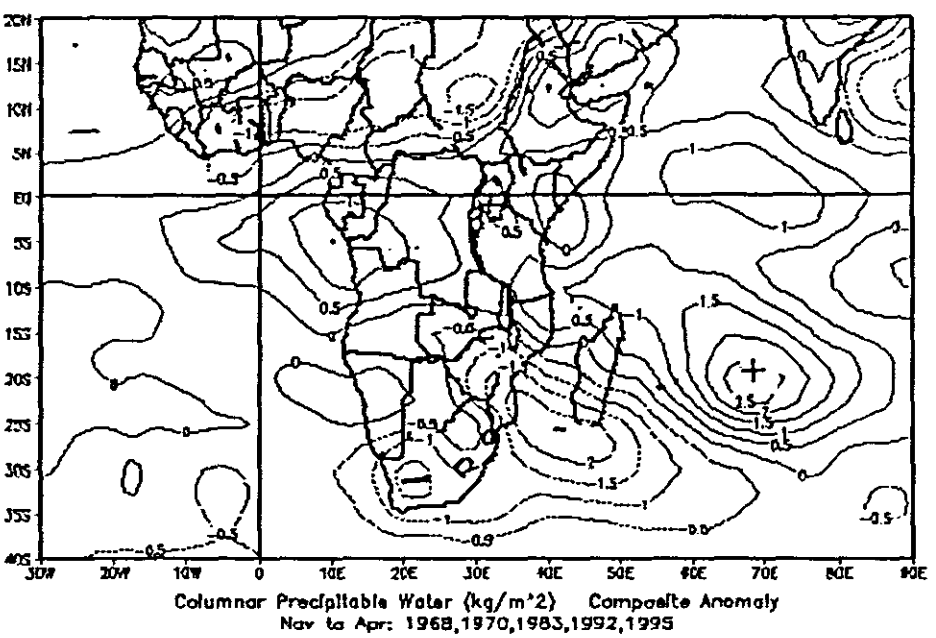

Figure 4.8: Precipitable water composite anomaly (a) during preceding period May-October. (b) during dry summer.(a) during dry summer. Negative values are represented by dashed isolines, positive (solid). Contour interval is 0.5 kg m^{-2}.

(a)

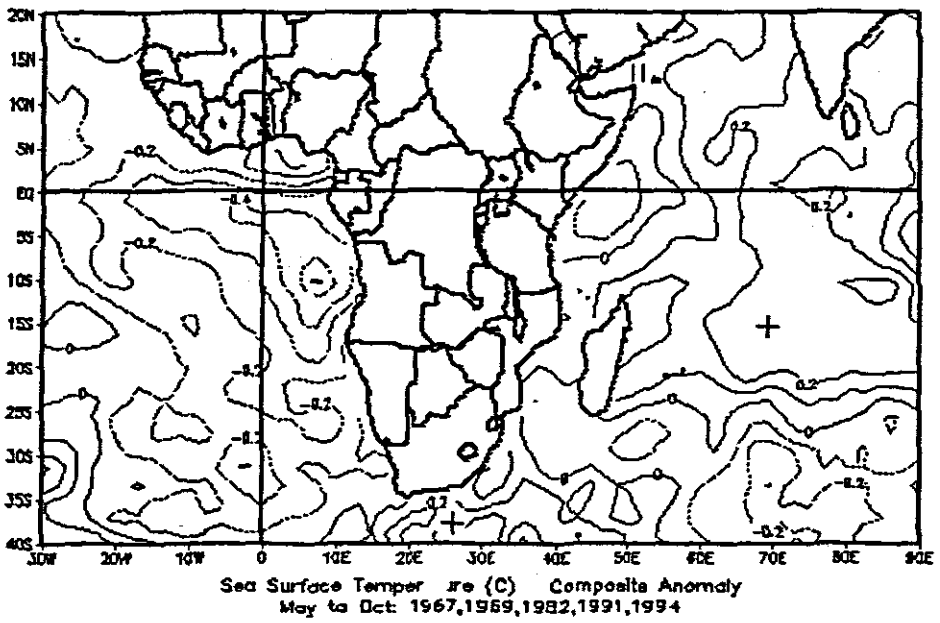

(b)

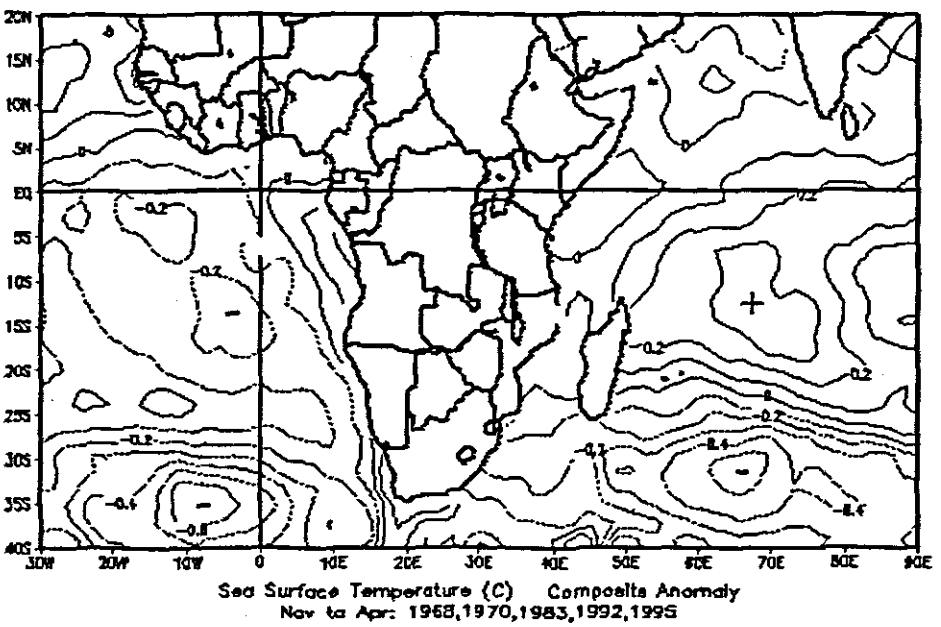

Figure 4.9: SST composite anomaly (a) during preceding period May-October. (b) during dry summer. Negative values are represented by dashed isolines, positive (solid). Contour interval is 0.1 °C.

(a)

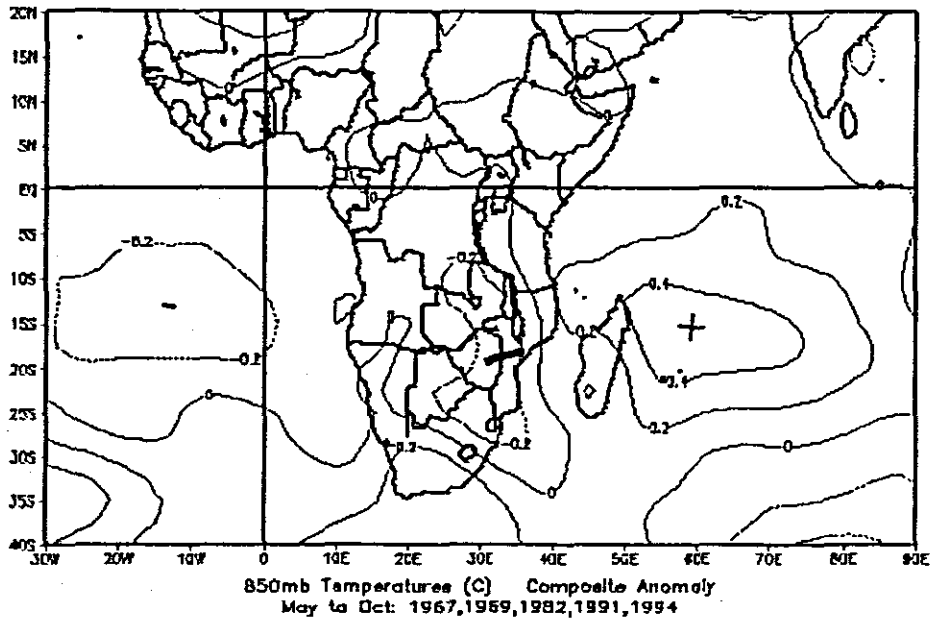

(b)

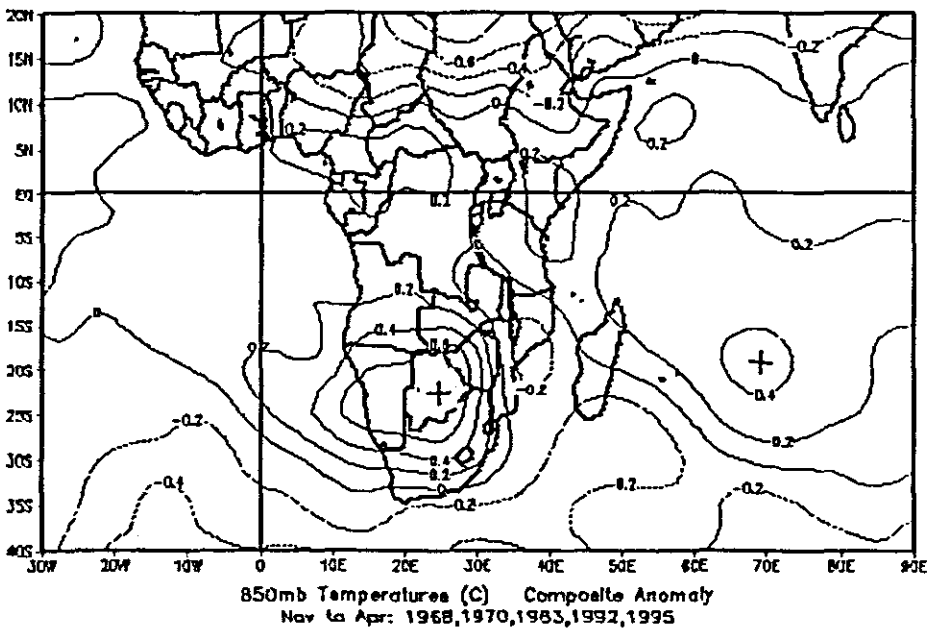

Figure 4.10: Air temperature composite anomaly at 850 hPa (a) during preceding period May-October. (b) during dry summer. Negative values are represented by dashed isolines, positive (solid). Contour interval is 0.2 °C.

(a)

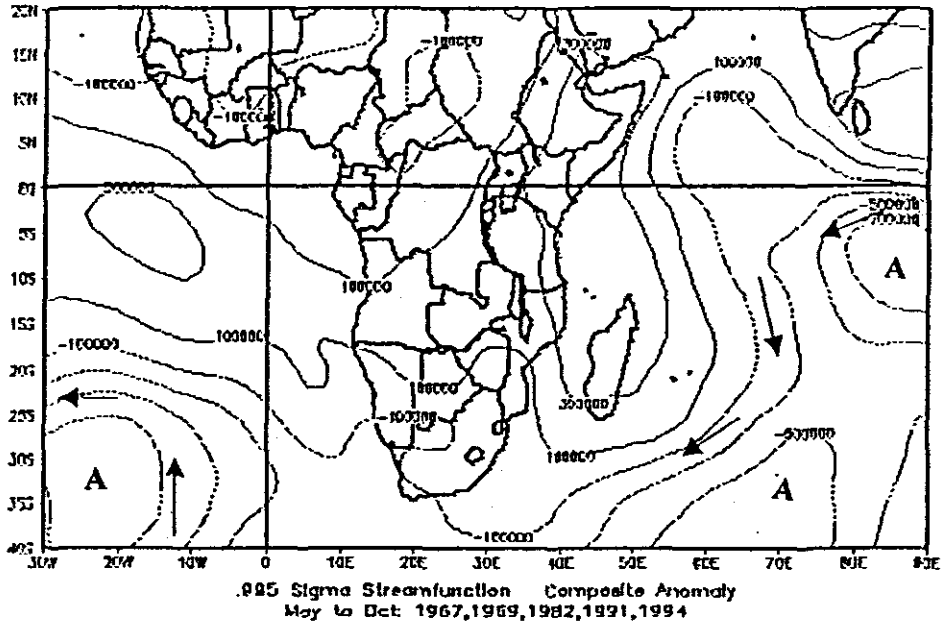

(b)

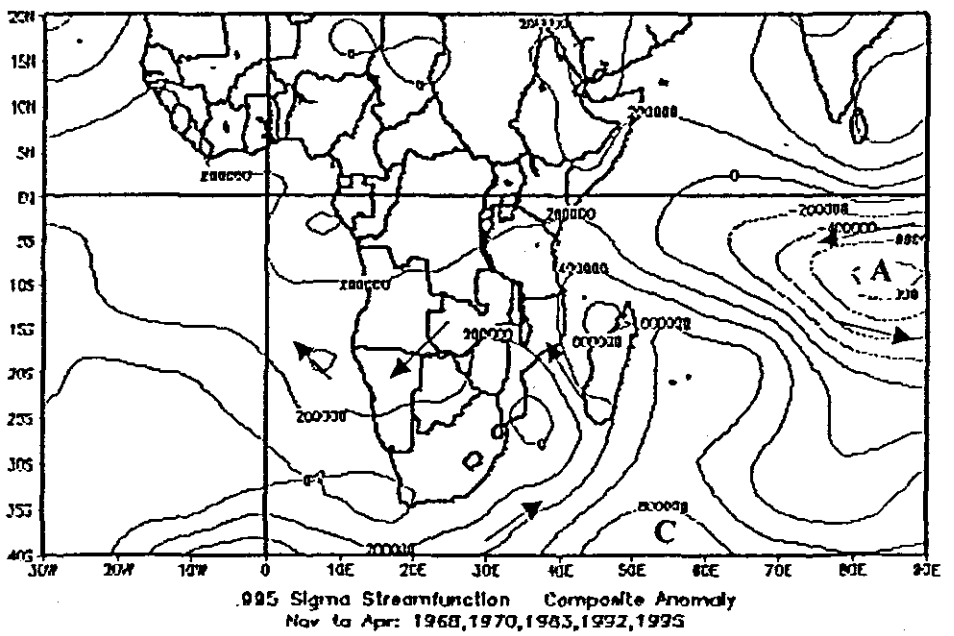

Figure 4.11: Streamfunction composite anomaly at lower level. (a) during preceding period May-October. (b) during dry summer. Negative values are represented by dashed isolines, positive (solid). Contour interval is 2 x 10^{+5} m^2 s^{-1}

(a)

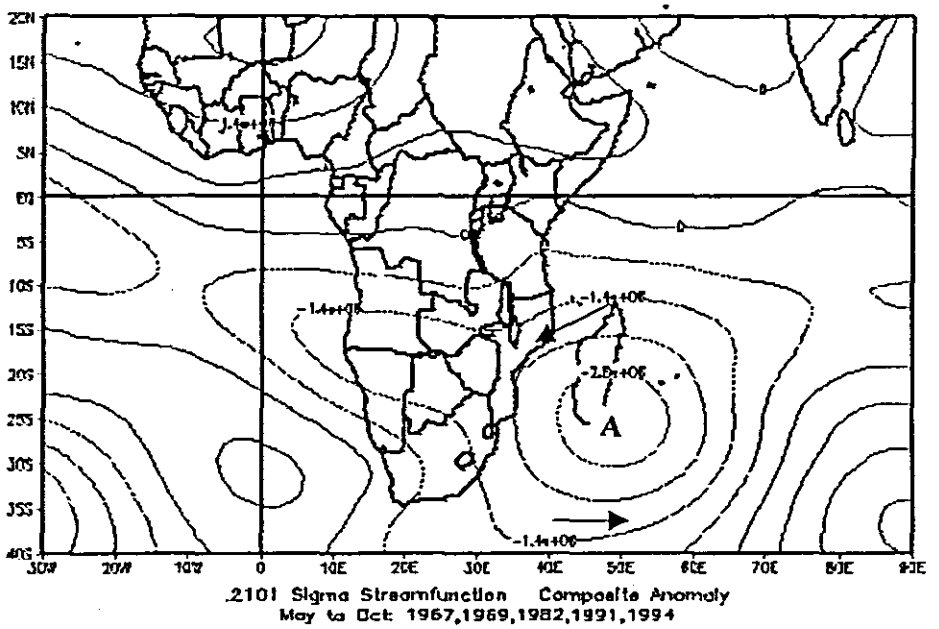

(b)

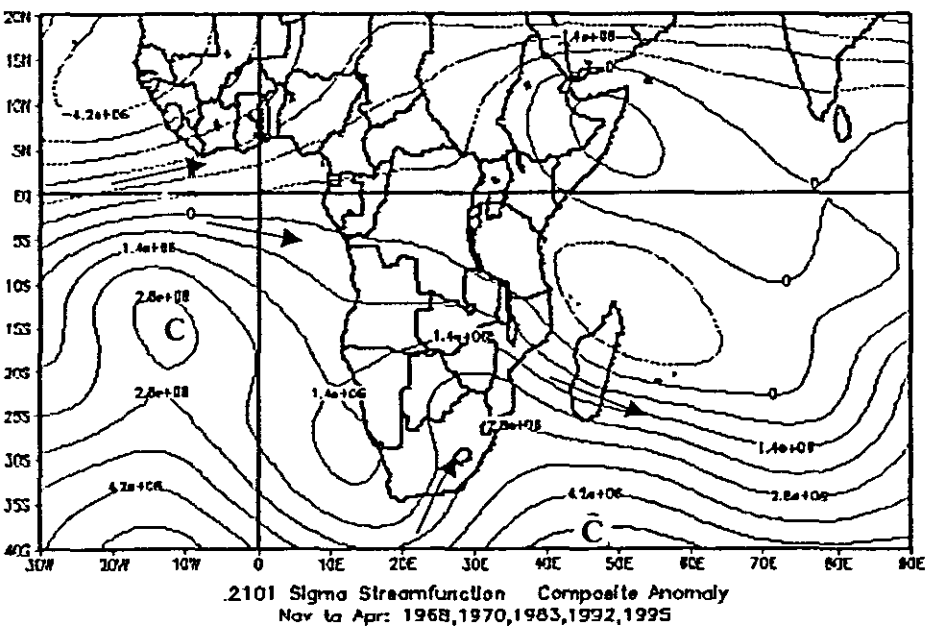

Figure 4.12: Streamfunction composite anomaly at upper level (a) during preceding period May-October. (b) during dry summer. Negative values are represented by dashed isolines, positive (solid). Contour interval is $0.7e^{+06}$ m^2 s^{-1}

(a)

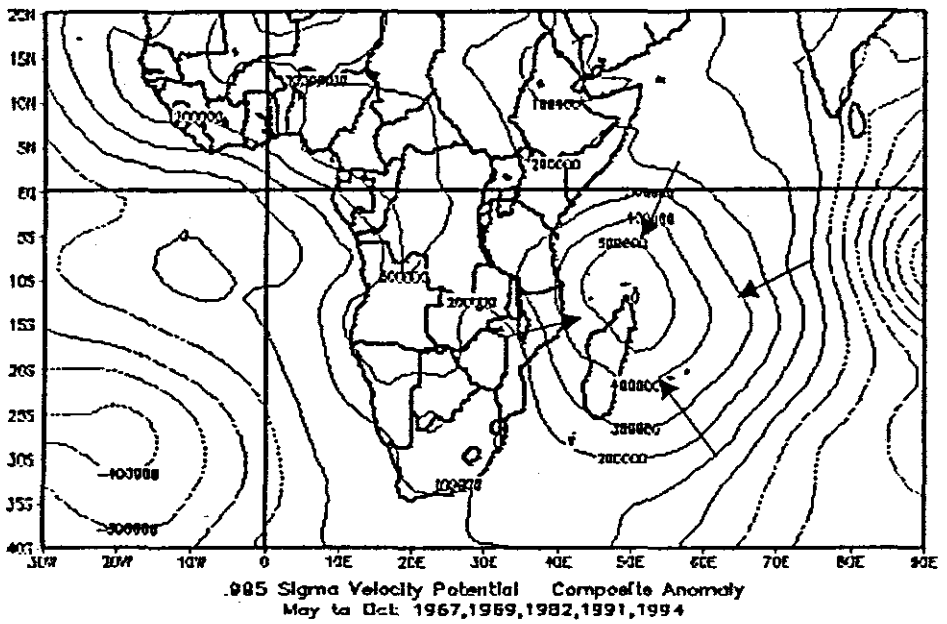

(b)

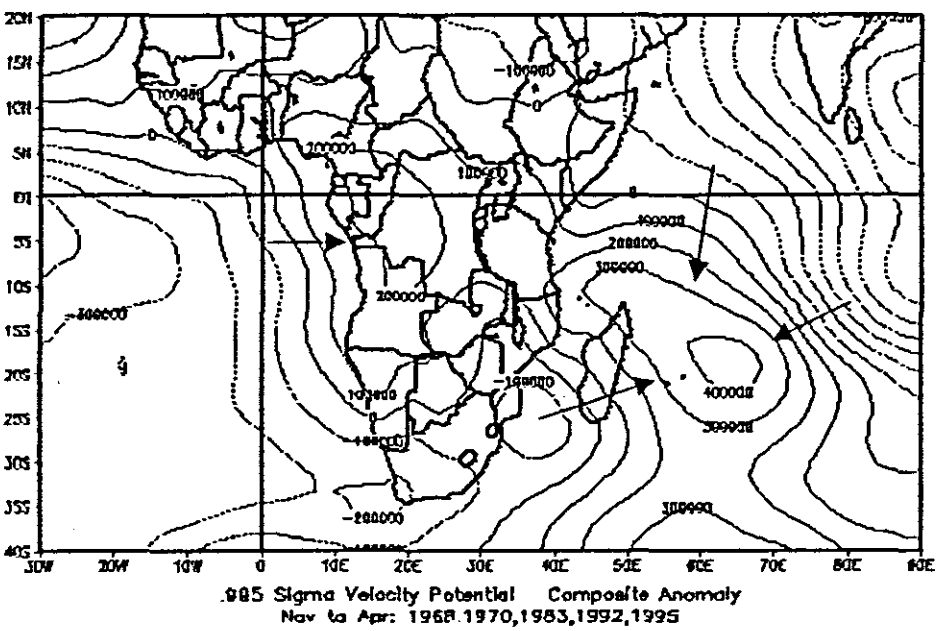

Figure 4.13: Velocity potential composite anomaly at lower level (a) during preceding period May-October. (b) during dry summer. Negative values are represented by dashed isolines, positive (solid). Contour interval is 8 x 10^{+4} m^2 s^{-1}

(a)

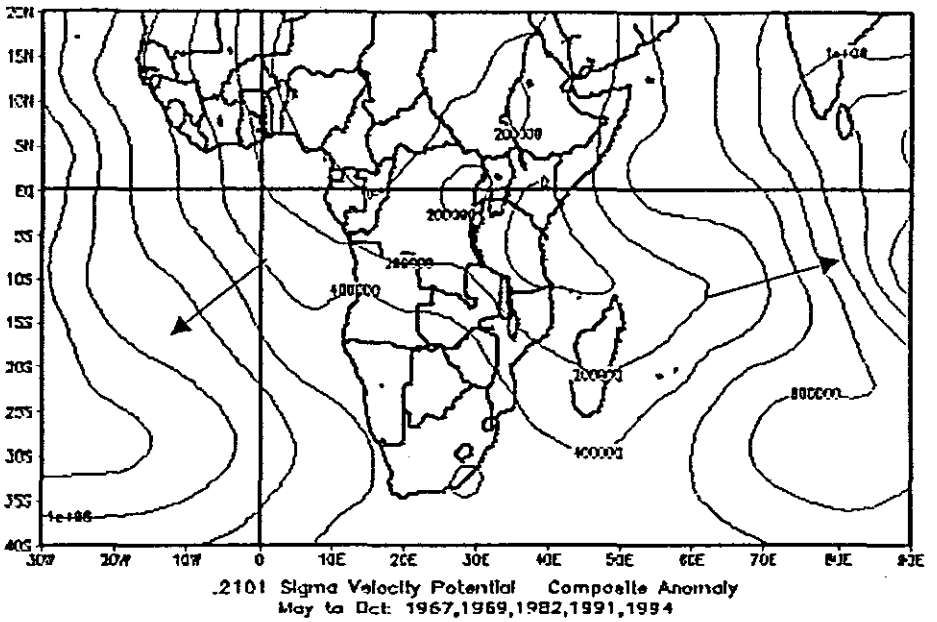

(b)

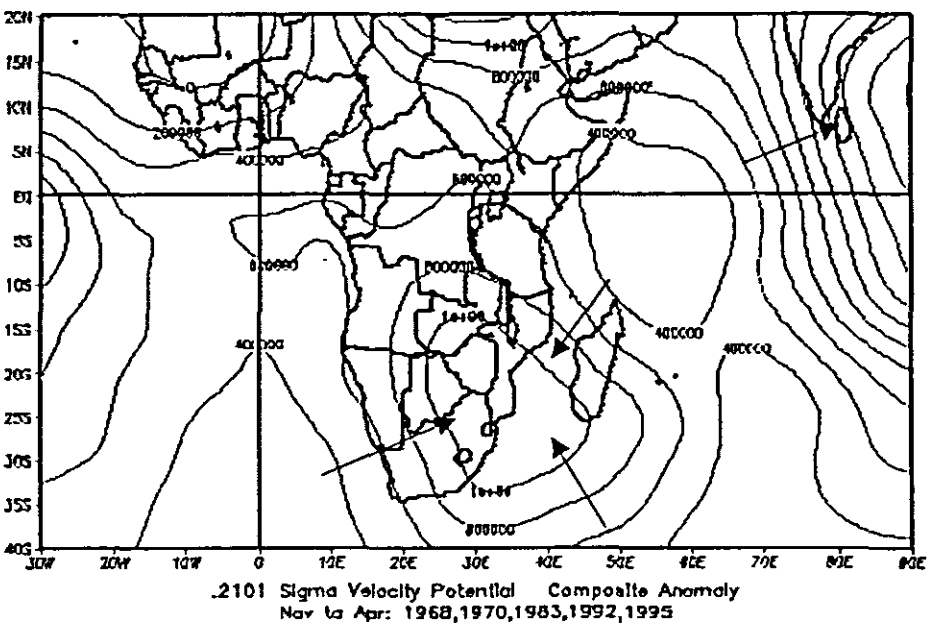

Figure 4.14: Velocity potential composite anomaly at upper level. (a) during preceding period May-October. (b) during dry summer. Negative values are represented by dashed isolines, positive (solid). Contour interval is 2 x 10^{+5} m^2 s^{-1}

Chapter 5

CASE STUDIES OF SELECTED DRY SPELLS

5.1 Introduction

This objective of this chapter is to investigate the circulation patterns that are specific to dry spells over tropical Southern Africa. It is hypothesised that each dry spell has specific circulation patterns. Case studies are important since specific processes and mechanisms may be identified which might otherwise be obscured by compositing over many months and years. As also noted by Matarira (1990) diagnostic studies of event-scale phenomena are important as the frequency of isolated severe weather systems usually determine the difference between a dry and wet summer. This study will contribute a better understanding of the mechanisms responsible for dry spells.

Malawi experienced one of the longest and driest spells in1992 when the country received below normal rainfall. The 40-day drought in1992 (February 2- March 12) is followed by a second case study of 17 days of dry weather in 1980 (January 11-January 27). The dry periods have been identified from Malawi daily rainfall as the period when the average accumulated rainfall for each day for ten stations considered in the investigation falls below the long-term average for 10 consecutive days based on the 1971 to 1992 study period as defined in chapter 2. The rainfall for the two selected dry spells are presented in figure 5.1. Historical maximum temperature departures and seasonal cycle for the same stations are presented (figure 5.2). These are required to confirm if dry conditions are associated with large positive anomalies and to indicate the period when Malawi registers highest temperatures. It should be noted that the years 1992 and 1980 are El Nino and non-El Nino years respectively. Therefore findings from circulation analysis may give further insight to whether dry spells originate from different centres of action.

In this study, the NCEP reanalysis data set are used to understand the circulation modes for predictive purposes. These are in terms of anomaly fields of outgoing longwave radiation (OLR), relative humidity (RH), temperature, zonal and meridional wind components, vector wind and geopotential heights. Moisture sources and sinks are identified from moisture advection of water vapour flux (figure 5.25).

The first part of the chapter concentrates on hovmoller and vertical cross- sections of the selected dry summers. These analyses identify the fluctuations with time using

longitude-time plots (hovmoller diagrams) for selected meteorological variables. The longitude-time plot for each map is averaged over latitudes 10-17.5°S from November to April, 10°W to 70°E. The fluctuations of each variable with time are in terms of anomalies obtained from the long-term mean of period 1968-1996. The variables include zonal (u) and meridional (v) wind components, geopotential height, temperature and precipitable water. Vertical structure of the atmosphere is also studied in order to have a proper picture of the circulation patterns. Vertical-cross section plots are height-longitude and latitude plots for each variable averaged over latitudes (longitudes) 10-17.5°S (30-37.5°E) and spanning November-April of each dry summer season for the vertical layer from 1000 hPa to 100 hPa plotted from 10°W to 70°E (10°N to 40°S) in the horizontal. The changes taking place in the vertical and horizontal within the vertical band are revealed.. Vertical cross-section studies are not new in southern Africa. For example, Harangozo (1989), using monthly data, has analysed vertical cross-sections in detail over southern Africa.

Finally the analysis considers the general circulation patterns that are associated with each dry spell during the identified periods. Water vapour fluxes and flow at 850 and 200 hPa for both dry spells are studied. A layout of results is as follows:

Results are shown for each dry spell, starting with the 17 days dry spell of 1980. Results of hovmoller analysis are shown first, followed by height-longitude and height-latitude plots. Thereafter the circulation patterns are indicated. The results of the 40-day dry spell of 1992 are similarly presented and discussion of the findings end the chapter.

5.1.1 Results of maximum temperature analysis

Figure 5.2a shows the seasonal cycle of maximum temperature of the stations to be investigated . The pattern indicates that highest temperature are registered in November (about 31°C). Lowest temperatures are obtained in July (about 24°C). The maximum temperature anomaly series (figure 5.2b) shows that low temperatures were registered in the 1970's. An oscillation of low and high temperatures occurs through 1989, whereafter a steady upward trend is maintained. Dry years are generally associated with high temperatures and lowest temperatures with wet summers. For example, the indicated years show high positive temperature departures in 1980 and 1992. Based on 20 years data, November-April summer, temperature are negatively correlated ($r < -0.4$)

with Malawi rainfall index (MRI) during the rainy season as expected. Spring-time temperatures at lags from -5 to -4 months are positively correlated ($r > +0.5$) with the summer rainfall (MRI). Hence a hot (cool) spring precedes a wet (dry) summer. Dry spells within these dry years are analysed below.

5.2 Results of Hovmoller analysis for 1980 dry spells

5.2.1 Zonal (u) wind component at 850 hPa and 200 hPa

The u-wind anomaly pattern at 850 hPa (figure 5.3a) shows a predominance of easterlies within 0-35°E . These winds show largest values during mid- season over Malawi and the Atlantic Ocean with a marked centre near 5°E and 30°E. Westerlies are dominant to the east of 40°E throughout the season. These winds are strongest in December with a marked centre near 50°E. Together these create divergence over Malawi and Mozambique.

The pattern at 200 hPa (figure 5.3b) level shows the dominance of easterlies during early part of the period (November-December) extending up to 30°E. Thereafter westerly airflow prevails and extending up to Malawi during January-February period.

5.2.2 Meridional (v) wind component at 850 hPa and 200 hPa

The pattern of v-wind (figure 5.4a) anomaly at 850 hPa level shows the dominance and persistence with time of southerly winds within 20°- 40°E. Hence Malawi is under the influence of these stable winds. Northerlies are observed near 60°E during early part of the season (November-December).

The anomaly pattern at 200 hPa (figure 5.4b) shows the persistence of southerly winds from early to mid-summer over Malawi (November-February) then northerlies thereafter. Marked southerly wind anomalies are found to the east of 40°E towards the end of the season.

5.2.3 Geopotential height at 850 hPa and 200 hPa

The anomaly pattern of geopotential height at 850 hPa is presented in figure 5.5a. The anomaly values indicate the persistence with time of positive anomalies to the east of 30°E with strong ridge extending up to 40°E during the mid-season (January and

February). Similarly negative values are dominant throughout the period east of 40°E with deep low pressure within 50-60°E during mid- season. The pattern indicates that Malawi was under the influence of high pressure hence subsidence. The anomaly pattern at 200 hPa (figure 5.5b) shows the persistence and dominance of positive anomalies throughout the season over the area east of 40°E.

5.2.4 Precipitable water and air temperature at 850 hPa

The anomaly pattern (figure 5.6a) shows a centre of lowest negative anomalies over Malawi during mid-season (December-February). It is interesting to note that the season starts wet in November and ends wet toward March. Pronounced positive anomalies are found east of 40°E in the Indian Ocean. The pattern indicates a lack of moisture over Malawi in mid-season. The anomaly pattern of air temperature at 850 hPa (figure 5.6b) shows the dominance of positive values to the west of 35°E from January to the end of period with a marked centre at zero meridian in January. The pattern shows that the dry spell over the country was associated with high temperatures to the west.

5.3 1980 dry spell Longitude-height analysis

5.3.1 Zonal (u) and meridional (v) wind components

Figure 5.7a indicates the anomaly pattern of cross- section of zonal wind component. The pattern shows the predominance of easterly wind below 300 hPa over Malawi and all east of 38°E. Pronounced westerly winds are found near 50°E below 300 hPa level. The pattern suggests Malawi was under divergence, caused by monsoonal westerlies over Madagascar.

The pattern for meridional wind component (figure 5.7b) indicate the predominance of southerly wind over Malawi with marked centre at 250 hPa level. Pronounced northerly wind is found near 10°E at 200 hPa level. The pattern indicates Malawi dry spells are associated with deep southerly wind influence.

5.4 1980 dry spell Latitude-height analysis

5.4.1 Zonal (u) and meridional (v) wind components

An anomaly pattern of zonal wind component (figure 5.8a) shows the dominance of anticyclonic flow over Malawi with centre of easterlies at 250 hPa. Pronounced westerlies are found within 20-25°S with centre at 250 hPa extending through a deep layer. The pattern suggest subsidence over Malawi.

The anomaly pattern of meridional wind (figure 5.8b) indicates the predominance of southerly winds from 30-40°S in the 700-100 hPa layer.

5.5 Results of 1980 dry spell circulation patterns

5.5.1 Outgoing Longwave Radiation (OLR)

OLR anomalies have been utilized in estimating area-rainfall on intra-seasonal time scales (Jury and Pathack, 1991; Lyons, 1991). Figure 5.9 presents OLR anomalies. The pattern shows maximum positive anomalies (non-convective) over Malawi, Zambia and central Mozambique. Another positive centre is found near 5°S, 60°E forming dipole pattern pattern with the one over Malawi/Mozambique. Lowest negative values are found just east of Madagascar. The pattern demonstrates dry conditions over Malawi and wet conditions east of Madagascar.

5.5.2 Sea level pressure (SLP)

Sea level pressure anomaly pattern (figure 5.10) shows pronounced tropical cyclone Hyacinthe east of Madagascar. According to Jury (1993) the cyclone persisted from 15 to 27 February 1980 causing excess rainfall of over 500 cm on the Reunion Island. The pattern is in sympathy with OLR. As a result of this tropical cyclone, tropical southern Africa is denied steady moisture from Indian Ocean.

5.5.3 Geopotential height at 850 hPa and 200 hPa

Figure 5.11a indicate the geopotential anomalies at 850 hPa during the 17 day dry spell in 1980. The pattern shows that Malawi is under the influence of a ridge of high pressure from an anticyclone south of Madagascar. Some marked positive values are observed over southern South Africa. Lowest negative values are centred east of

Madagascar. The pattern is generally in sympathy with OLR and sea level pressure patterns.

An anomaly pattern at 200 hPa (figure 5.11b) shows the dominance of negative anomalies over southern Africa with lowest values centred over southern Namibia and southern Mozambique channel. The combined patterns, lower and upper levels, were conducive to dry conditions over Malawi. The convergence in the upper level was associated with divergence in the lower level.

5.5.4 Wind vector at 850 hPa and 200 hPa

The wind anomaly pattern at 850 hPa (figure 5.12a) shows diffluence over Malawi with anticyclonic flow centred over Botswana and a deep tropical cyclone at 25°S, 52°E, east of Madagascar. Wind anomalies are generally easterly over southern Africa and the Atlantic Ocean. The wind anomaly at 200 hPa (figure 6.12b) indicates cyclonic flow over southern Africa with a centre over northern South Africa. The combined patterns show divergence and convergence in lower and upper levels respectively.

5.5.5 Relative Humidity at 850 hPa and 500 hPa

The anomaly pattern for relative humidity at 850 hPa (figure 5.13a) indicates lowest negative anomalies in northeast- southwest direction from northeast of Madagascar to South Africa through Malawi. Largest positive values are found southeast of Madagascar, southern Somalia and in the Atlantic Ocean. The anomaly pattern at 500 hPa (figure 5.13b) indicates a centre of lowest negative values over Zambia which extends to Malawi and Angola. The pattern shows the lack of moisture over Malawi in low and mid-levels was a contributing factor to the dry spell of 1980.

5.5.6 ECMWF water vapour flux

As pointed out by Chen and Tzeng (1990), a closer association to convection is achieved if dynamics and moisture fields are considered together rather than in isolation. Figure (5.25a) shows the anomaly pattern of water vapour flux during the 1980 dry spell. The pattern indicates the NE monsoon feeds a westerly axis around 15°S. The water vapour flux is observed to flow from south of Madagascar with pronounced cyclonic circulation just east Madagascar. An anticyclonic flow is centred over Botswana. The pattern shows

divergence over Malawi thus supporting dry conditions.

5.6 Results of Hovmoller analysis 1992 dry spell

5.6.1 Zonal (u) wind component at 850 hPa and 200 hPa

The anomaly pattern of zonal wind component at 850 hPa (figure 5.14a) show the persistence of easterly wind over Malawi. These are pronounced during the mid season. Westerly winds are persistence east of 45°E.

The anomaly pattern at 200 hPa (figure 5.14b) is dominated by westerly winds. The combined pattern indicates that Malawi was under the influence of divergence through out the period hence dry conditions.

5.6.2 Meridional (v) wind component at 850 hPa and 200 hPa

The anomaly pattern of meridional wind component at 850 hPa (figure 5.15a) indicates that Malawi is at the edge of southerly wind from the start of the season to mid January. Thereafter, northerly wind becomes dominant. The pattern shows the persistence of cyclonic flow at 200 hPa (figure 5.15b) and is strong from start of the season to February. The pattern also demonstrates independent circulations over the Atlantic and Indian Oceans. the combined pattern suggest that convergence aloft and divergence at lower levels supported dry conditions.

5.6.3 Geopotential height at 850 hPa and 200 hPa

The anomaly pattern at 850 hPa (figure 5.16a) shows that Malawi was under the influence of positive anomalies (high pressure) during the entire season. Anomaly pattern at 200 hPa (figure 5.16b) shows the persistence of large positive anomalies from mid-December. The combined pattern suggests the dominance of subsidence of air over Malawi during the entire period.

5.6.4 Precipitable water and air temperature at 850 hPa

Anomaly pattern of precipitable water (figure 5.17a) indicates lowest negative anomalies over Malawi during a peak period of the season (December-February). Persistent pattern of negative values is observed over Indian Ocean east of 40°E. The

dry spell over Malawi was supported by lack of moisture.

Negative precipitable water over Malawi is associated with positive air temperature (figure 5.17b) from end of December to the end of the season. However, the temperature pattern puts the centre of maximum temperature anomaly at 20°E during February. Positive anomalies are also observed east of 45°E throughout the season.

5.7 1992 dry spell longitude-height analysis

5.7.1 Zonal (u) and meridional (v) wind components

The anomaly of zonal wind (figure 5.18a) shows the predominance of westerly airflow at all levels with tight gradient above 500 hPa centred at around 200 hPa. Marked divergence is observed below 500 hPa over Malawi with easterly wind.

The meridional wind component (figure 5.18b) shows that Malawi is under the influence of convergence aloft and divergence in low levels. The pattern shows an interesting four way pattern of Hadly cells. The combined pattern indicates that dry spell over the country was associated with subsidence of air.

5.8 1992 dry spell Latitude-height analysis

5.8.1 Zonal (u) and meridional (v) wind components

The anomaly pattern of zonal wind(figure 5.19a) shows pronounced westerly near 15°S above 600 hPa with centre at 200 hPa. Easterlies are observed within 10°N-10°S band with main centre near 650 hPa at 7°S.

The anomaly pattern of meridional wind (figure 5.19b) shows southerly wind above 800 hPa within 12-35°S with maximum value near 300 hPa near 27°S. The combined pattern indicates that dry spell over Malawi in 1992 was associated with easterly and southerly wind regimes.

5.9 Circulation patterns of 1992 dry spell

5.9.1 Outgoing Longwave Radiation (OLR):

An anomaly pattern of OLR (figure 5.20) shows pronounced positive values over all areas from South Africa to Malawi (maximum +30 w m^{-2} over Malawi). A centre of negative values are observed over central Indian Ocean. Marked positive values are

observed to the south of Madagascar. The pattern indicates widespread drought over Southern Africa.

5.9.2 Sea level pressure (SLP)

Sea level pressure anomaly pattern (figure 5.21) shows deep low pressure with tight gradient to the east of Madagascar. Moderate low pressure is observed over southern Angola and Malawi is found on the peripherical of the trough and a ridge. An anticyclone to the south east of Madagascar has extended into southern Mozambique. The pattern is inducive to diverging winds over Malawi hence dry conditions.

5.9.3 Geopotential Height: 850 hPa and 200 hPa

An anomaly pattern of geopotential heights at 850 hPa (figure 5.22a) shows Lowest negative values (low pressure) east of Madagascar. An anticyclone south east Madagascar has extended a ridge to Malawi. Another marked anticyclone is observed over western South Africa. The pattern suggest that dry conditions over Malawi were supported by widespread air subsidence over southern Africa.

Figure5.22b shows the geopotential anomalies at 200 hPa. The feature that is significant to the investigation is negative values over southern Africa with lowest value centred over southern Mozambique. The combined pattern shows dry spell was supported by convergence aloft and divergence in low levels.

5.9.4 Vector wind at 850 hPa and 200 hPa

Wind vector anomaly pattern at 850 hPa (figure 5.23a) indicates pronounced Indian Ocean westerlies over central Indian Ocean. Cyclonic flow is observed over northern South Africa while anticyclonic flow is found along the coast of Namibia. Winds tend to be mainly westerly over the entire southern Africa.

The wind anomaly pattern at 200 hPa (figure 5.23b) indicates the prevalence of westerly winds over southern Africa and Atlantic Ocean, north of 20°S. Marked cyclonic flow is observed over southern Mozambique Channel. A belt of strong winds passes over Malawi to South Africa from central Indian Ocean. The combined pattern suggests that jet streams were further north than normal position. Rain-bearing systems were held further north of jet streams hence dry conditions.

5.9.5 Relative Humidity 850 hPa and 500 hPa

The pattern of relative humidity at 850 hPa (figure 5.24a) indicates lowest negative anomalies from South Africa to Malawi and Zambia with centre over Botswana. Figure 5.24b shows the relative humidity anomalies at 500 hPa. The pattern shows dipole with negative centre over southern Africa, from Malawi to South Africa, and positive centre to the east of Madagascar which is similar to the one over western Angola.

5.9.6 Water vapour flux: 1992

The anomaly pattern of water vapour flux (figure 5.25b) shows centre of convective centre to the east of Madagascar. Westerly axis of the flow of water vapour flux, fed by northeast monsoon, is found at 15°S. Anticyclonic flow is observed over South Africa.

5.10 Discussion and summary

The principal aim of this chapter was to increase the understanding of characteristics of dry spell conditions over tropical southern Africa. The hypothesis was that each dry spell has certain circulation patterns associated with it. The objective has been achieved by investigating the kinematic and thermodynamics properties of dry spells of 1992 and 1980. Cross section analyses and circulation patterns have been presented for selected meteorological variables from NCEP data set. Common features between two dry spells have been identified from the study. Tropical cyclones and associated cyclonic flow in low and middle levels east of Madagascar are prominent for both dry spells. These cyclones divert monsoonal moisture from tropical southern Africa. Within the dry spell period of 1980, tropical cyclone Hyacinthe was persisted east of Madagascar from 15-27 January 1980 (Jury, 1993). Consequently tropical cyclone Hyacinthe was the major factor causing the 17 days dry spell in 1980 over Malawi. Tropical cyclone Hyacinthe has been studied by Jury (1993) and has reported that this cyclone was quasi-stationary to the east of Madagascar causing rainfall in excess of 500 cm on Reunion Island from 15-27 January 1980. The cyclone was spawned in association with an eastward moving convective wave and reached a maximum OLR anomaly of < -92 w m^{-2} and radius of > 1000 km from 21 to 26 January 1980. Tropical cyclone Hyacinthe was rated as a historic peak, considering all tropical cyclones over the region (SW Indian Ocean) from 1964 to 1991 (Jury, 1993). Within the dry spell period of 1992, about six tropical

cyclones were reported over the tropical cyclone region (Meteo France-Reunion, 1992). These tropical cyclones were usually co-existing on the same period. The cyclones of significance during the dry spell period were Celesta (8-12 February); Davilia (16-25 February); Elizabeth (22-25 February); Farida (23 February-3 March); Gerda (24 February-4 March) and Heather (1-7 March). Pressure east of Madagascar remained low during the period. The occurrences of these cyclones were enhanced by favourable westerly monsoons over the region during the period. Sea surface temperature were usually > 28°C . Pronounced outflow aloft (200 hPa level) combined with cyclonic flow in low levels (Meteo France-Reunion, 1992). As a result of these cyclones moisture was transported towards the convective area thus leaving tropical southern Africa dry. In both dry spells pronounced negative relative humidity in lower and mid levels are oriented in the northeast-southwest direction. Easterly and southerly wind regimes are dominant, in both dry spells, in low levels and westerlies in the upper troposphere. The above discussion indicates that generally the circulation features of dry spells are similar but their severity may be different.

Findings, amongst others, from the analysis of both dry spells are listed below starting with 17 days dry spell of 1980. Table 5.1 below summarises dominant features of both dry spells.

5.10.1 1980 dry spell

Dry spell of 1980 have the following characteristics::

(a) It is associated with tropical cyclone Hyacinthe east of Madagascar. This cyclone caused moisture to be diverted away from tropical southern Africa.

(b) It is associated with high pressure cell over Botswana.

(c) It is associated with maximum positive OLR anomalies over Malawi extending into Zambia and Mozambique Channel (figure 5.9a).

(d) It is associated with low negative precipitable water over Malawi (figure 5.6a) or low negative relative humidity in low and mid-levels (figure 5.24).

(e)The pattern is dominated by easterly and southerly wind regimes in lower levels.

Conditions over Malawi during the1980 dry spell (generally over most countries south of 10°S) are associated with deficiency in moisture due to the tropical cyclone east of Madagascar.

5.10.2 1992 dry spell

The brief summary below gives the characteristics of 40 days dry spell of 1992. The dry spell is associated with:

(i) Several episodes of tropical cyclone disturbances east of Madagascar. These were diverting monsoonal moisture from tropical southern Africa.

(ii) Maximum positive OLR anomalies over Malawi, central Mozambique extending to South Africa and southern Madagascar.

(iii) Easterly and southerly wind regimes in low levels and westerlies in the upper levels.

(iv) High pressure cell over western South Africa and a strong ridge over Malawi extended from an anticyclone south of Madagascar.

(v) Pronounced negative precipitable water and marked positive temperature anomalies.

Overall the 1992 dry spell over Malawi (and most countries south of 10°S) was associated with tropical cyclones east of Madagascar which diverted moisture. The chapter has revealed that generally similar mechanisms are at work controlling day-to-day characteristics of dry weather.

Significant features of both dry spells are presented in table 5.1 below.

Parameter	1980 dry spell	1992 dry spell
Horizontal wind	Easterlies are dominant in low levels and westerlies in the upper level.	Easterlies are dominant in low levels and westerlies in the upper level
Geopotential height & Sea level pressure	Marked positive values are found in low and upper levels and lowest negative values east of Madagascar in low levels. Tropical cyclone Hyacinthe east of Madagascar.	Marked positive values are found in low and upper levels and lowest negative values east of Madagascar in low levels. Tropical cyclones east of Madagascar.
Precipitable water	Lowest negative precipitable water centred over Malawi.	Lowest negative precipitable water centred over Malawi.
Air temperature	Pronounced positive temperature.	Pronounced positive temperature.
OLR	Lowest values centred just east of Madagascar. Largest positive values extending from Malawi to South Africa.	Lowest anomalies centred east of Mauritius. Largest positive anomalies over Malawi, Zambia and Mozambique.
Water vapour flux	Tropical cyclone east of Madagascar fed by advection from south of Madagascar. NE monsoon feeds westerly axis around 15°S.	Tropical cyclone east of Madagascar. fed by advection from south of Madagascar. NE monsoon feeds westerly axis around 15°S.

Table 5.1: Summary of dominant features identified from case studies of 1980 and 1992 dry spells.

The study has contributed in revealing the association between dry spells over tropical southern, using Malawi in the analyses, and spatial/temporal structure of selected meteorological variables. It should be noted that similarity in patterns of different dry spells does not necessarily mean their impacts are the same.

Common precursors and possible predictors for dry and wet conditions are investigated and statistical forecast models are developed for predicting Malawi summer rainfall in the next chapter.

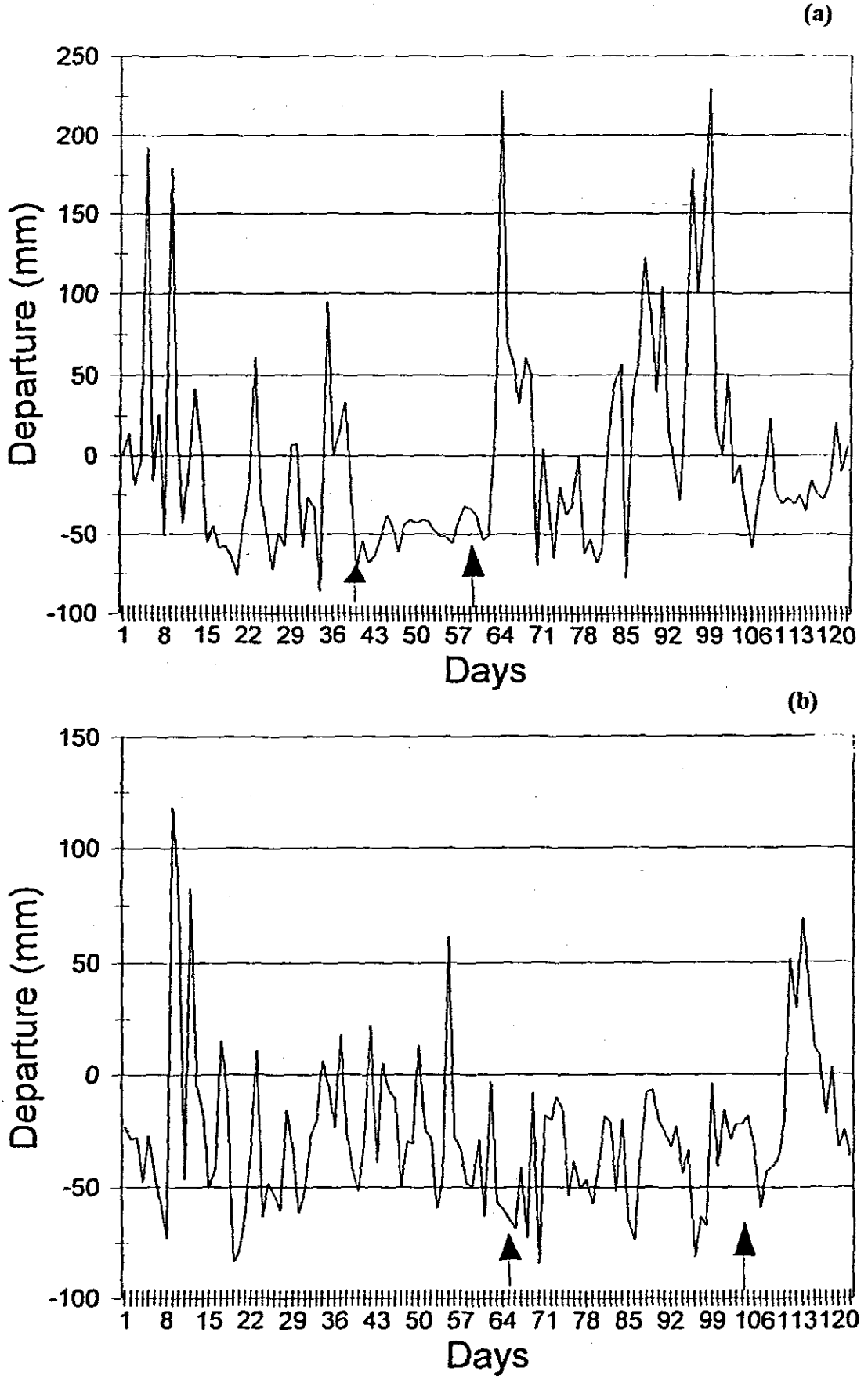

Figure 5.1: (a) *Unstandardised daily rainfall time series for 1980 November-March.* (b) Same as (a) but for 1992. Dry spells between arrows are analysed.

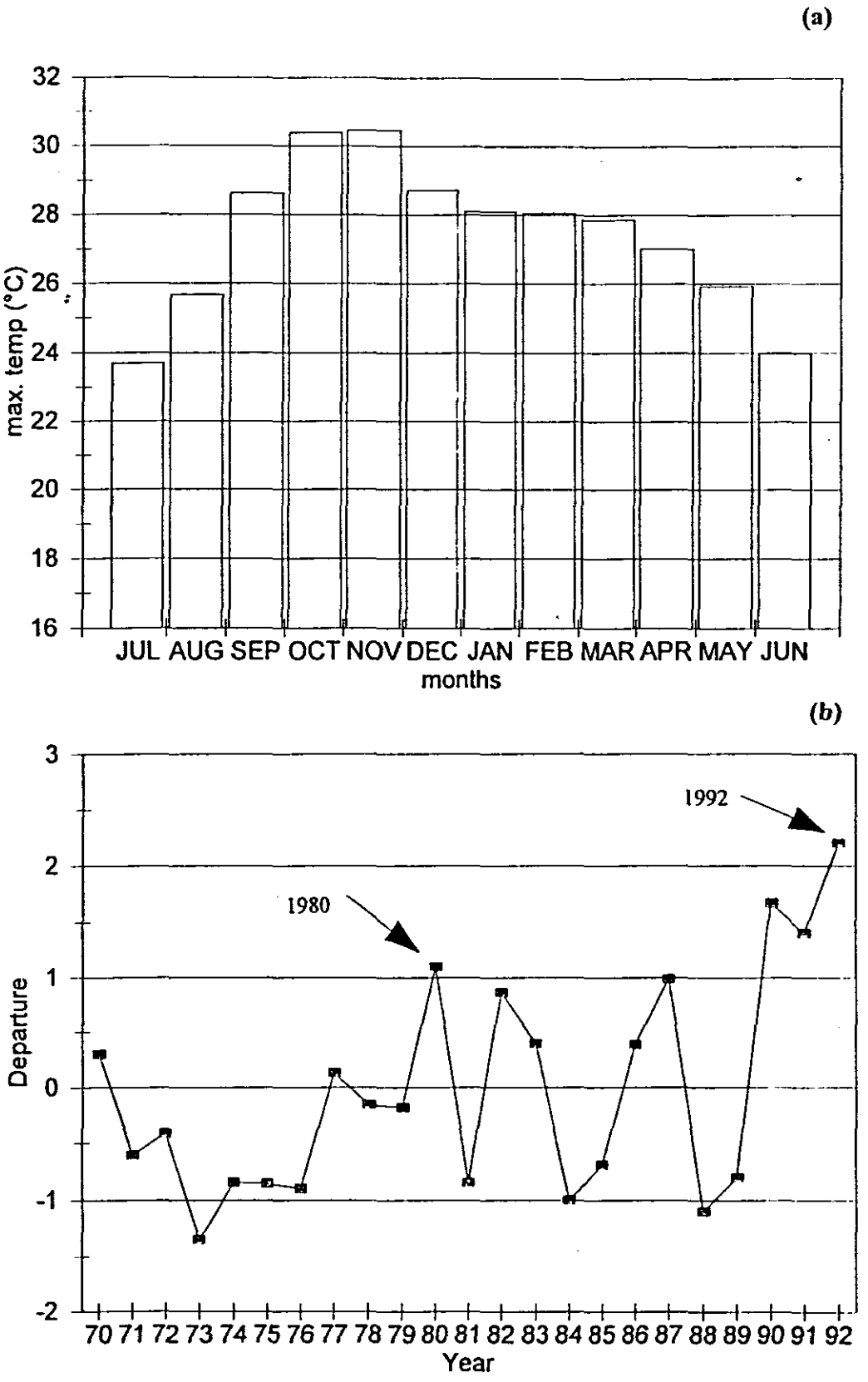

Figure 5.2:(a) Seasonal cycle of Maximum temperature for ten stations. (b) Normalised maximum temperature anomalies for same stations used to study dry spells over Malawi. Data based on 1970-1992 from November to March. Years to be investigated are indicated by an arrow (1980 and 1992).

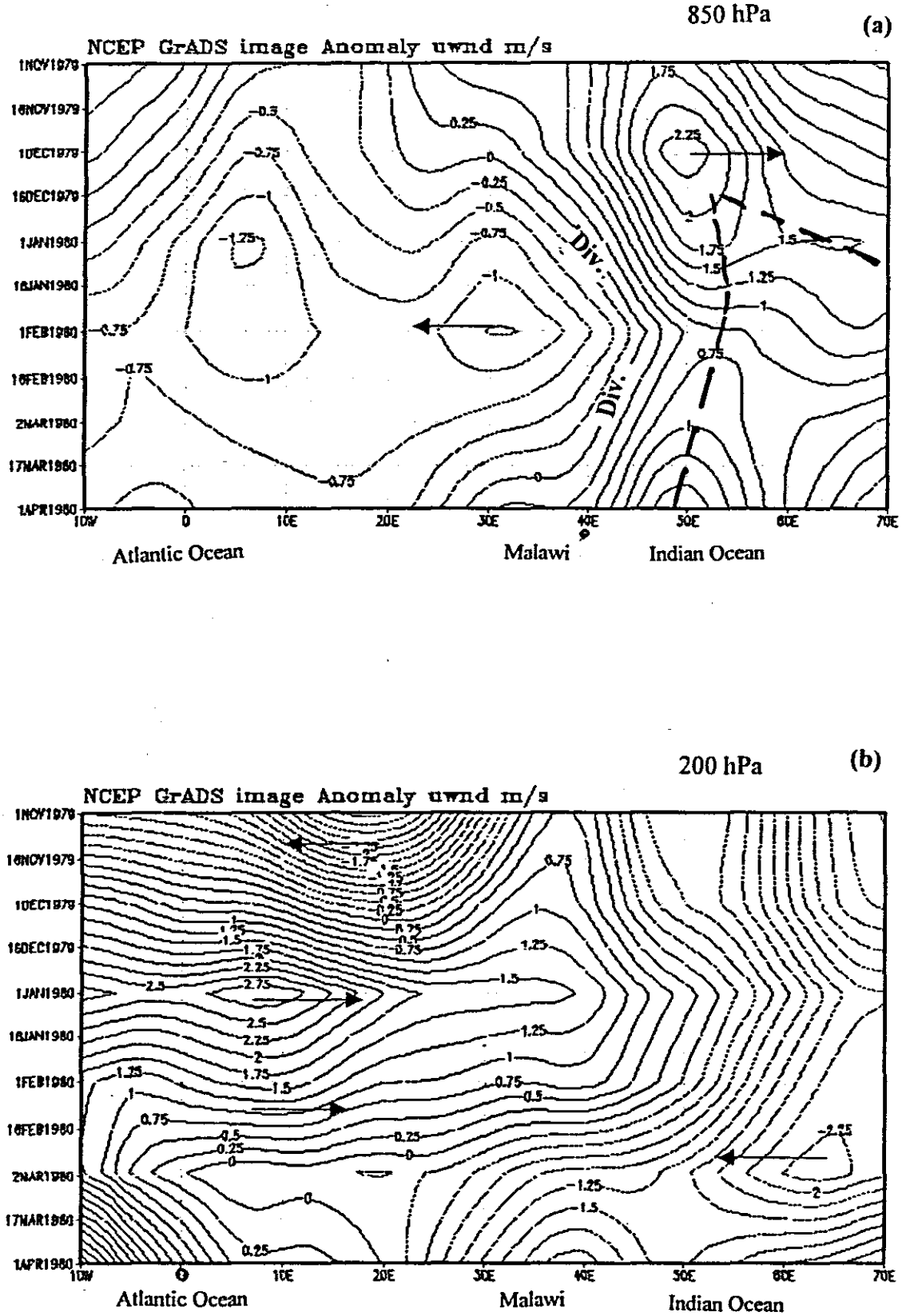

Fig. 5.3: Hovmoller diagrams for u- wind component anomaly averaged over latitudes 10-17.5°S, for 1980 season from 10°W to 70°E at (a) 850 hPa and (b) 200 hPa. Negative values are represented by dashed isolines, positive (solid). Contour interval is 0.25 m/s.

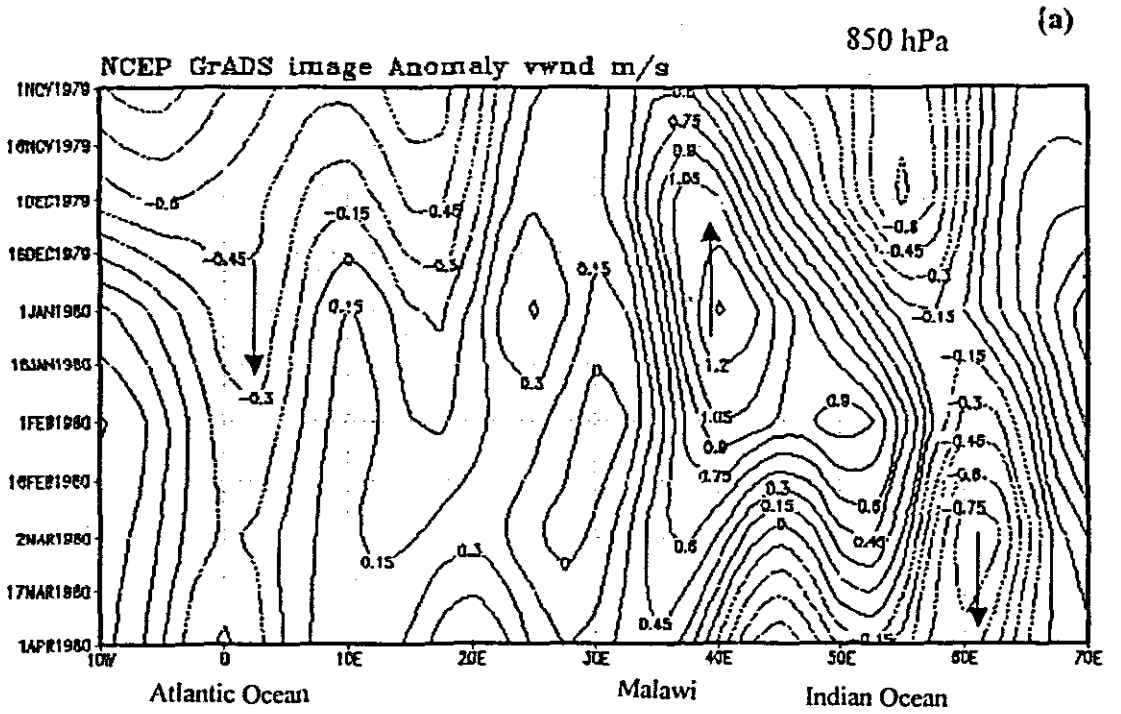

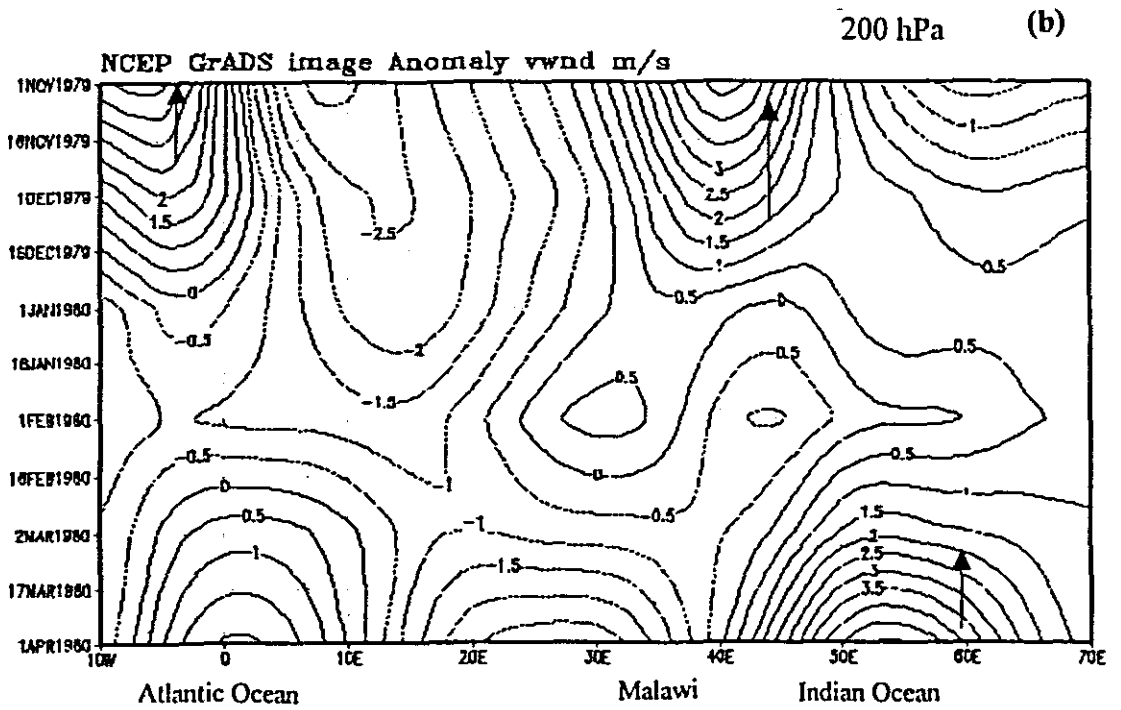

Fig. 5.4: Hovmoller diagrams for v- wind component anomaly averaged over latitudes 10-17.5°S, for 1980 season from 10°W to 70°E at (a) 850 hPa and (b) 200 hPa. Negative values are represented by dashed isolines, positive (solid). Contour intervals are 0.15 m/s and 0.5 m/s respectively.

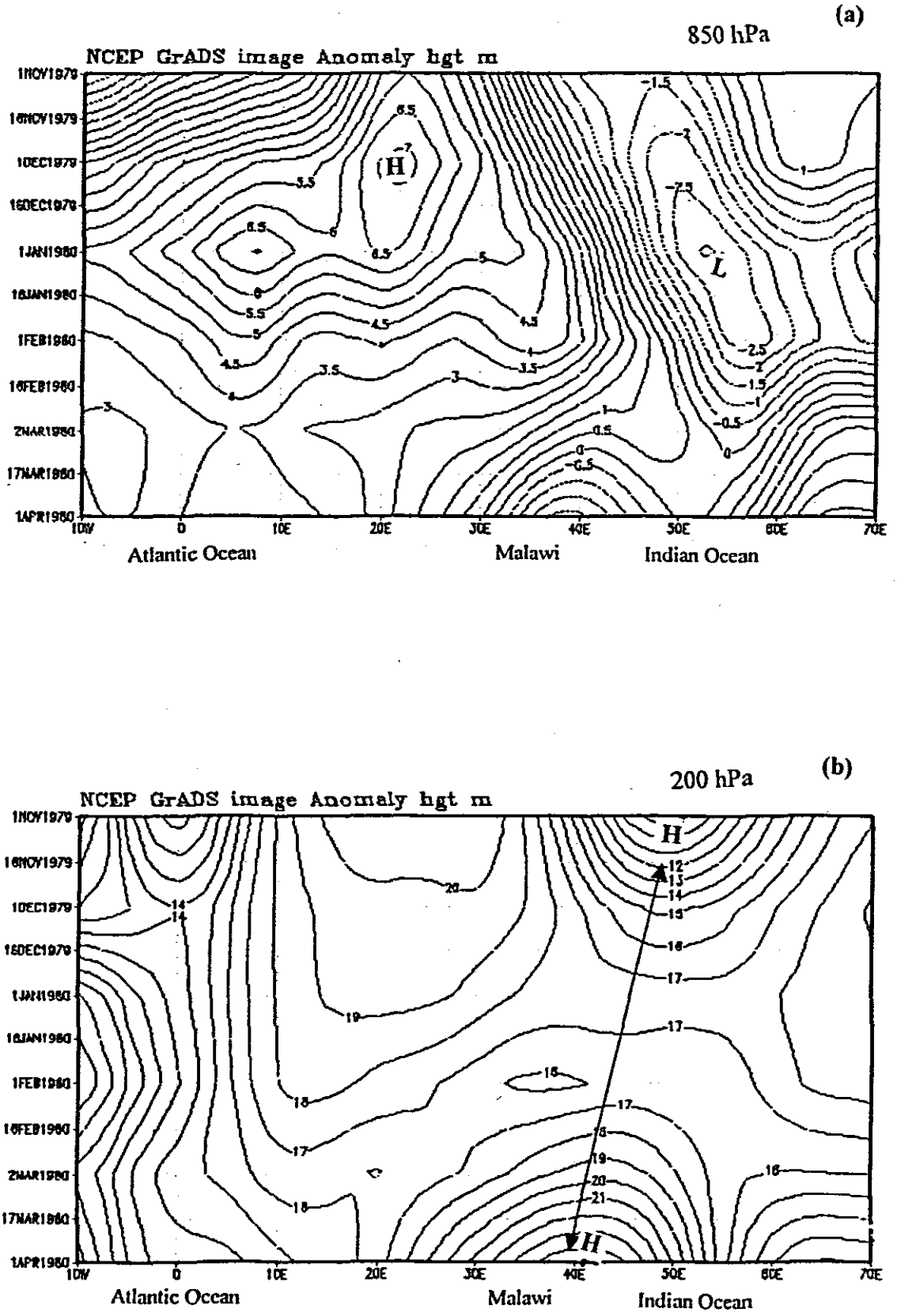

Fig. 5.5: Hovmoller diagrams for geopotential height anomaly averaged over latitudes 10-17.5°S, for 1980 season from 10°W to 70°E at (a) 850 hPa and (b) 200 hPa. Negative values are represented by dashed isolines, positive (solid). Contour intervals are 0.5 gpm and 1.0 respectively.

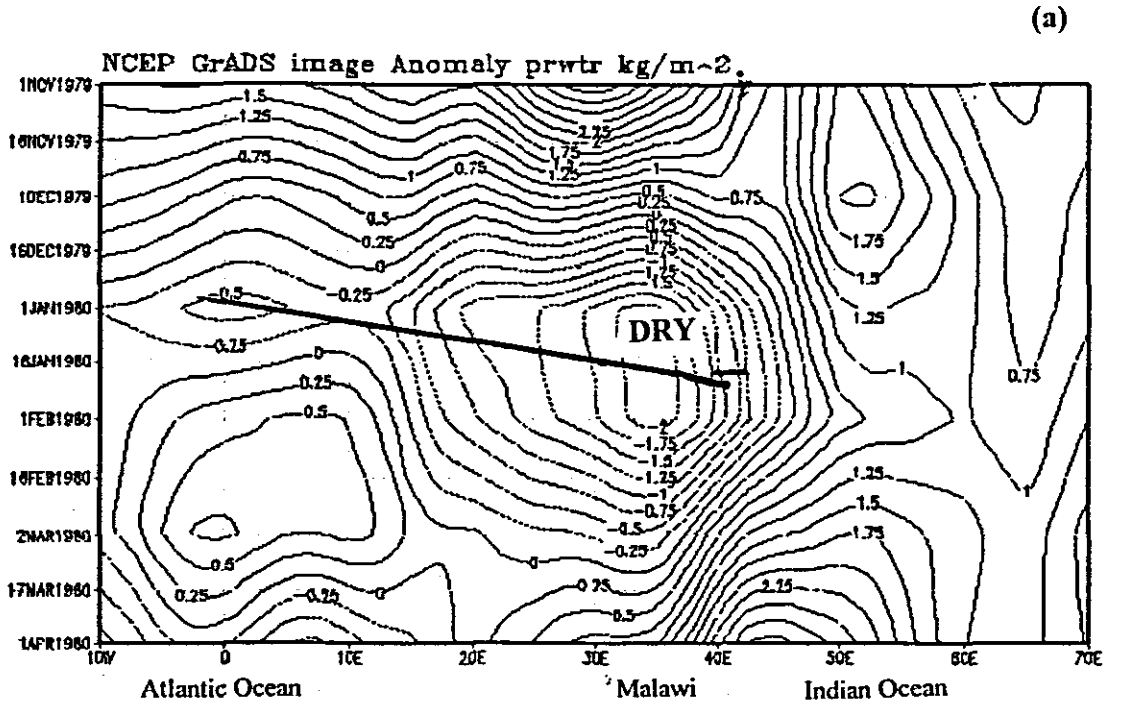

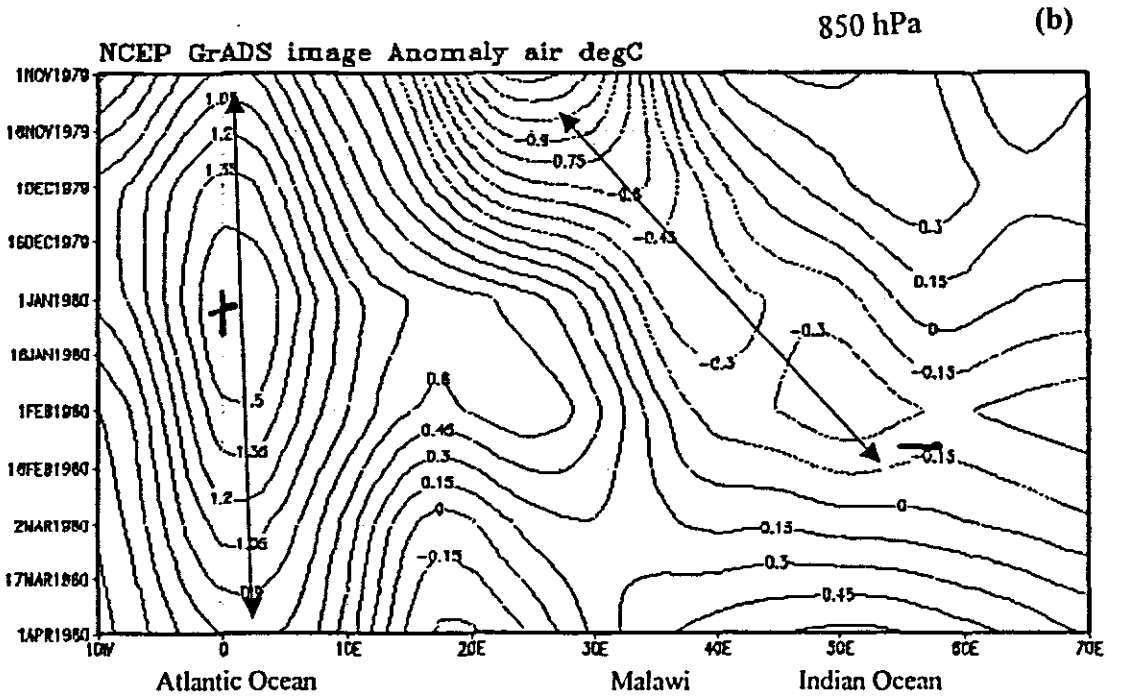

Fig. 5.6: (a) Hovmoller diagram for precipitable water (1000-300 hPa) anomaly averaged over latitudes 10-17.5°S, for 1980 season from 10°W to 70°E Negative values are represented by dashed isolines, positive (solid). Contour interval is 0.25 kg m^{-2}.(b) Anomaly pattern of air temperature over the same area but at 850 hPa level and contour interval is 0.15°C.

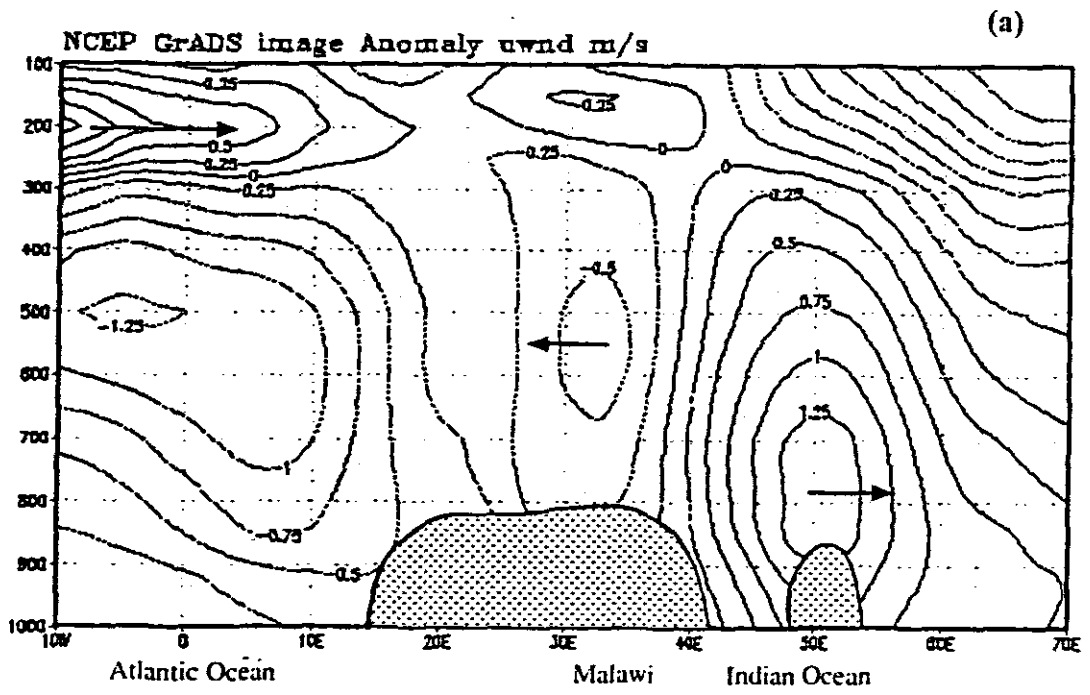

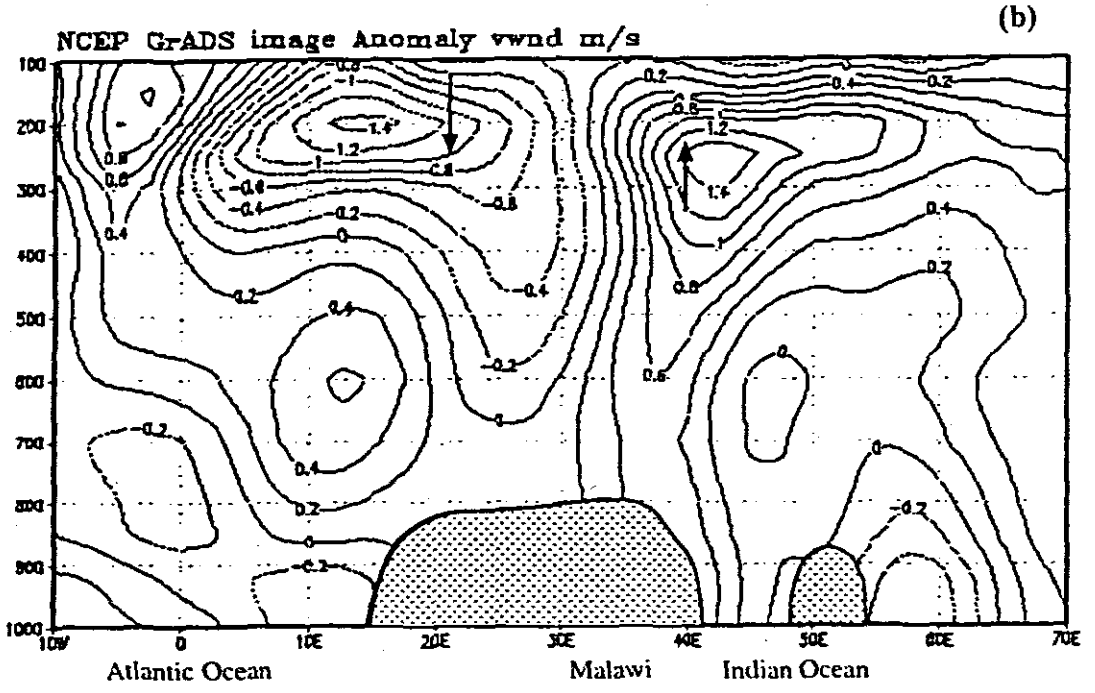

Figure 5.7: (a) Longitude-height diagram for u-wind anomaly field averaged over latitudes 10-17.5°S, for 1980 season from 10°W to 70°E and from 1000-100 hPa. Negative values are represented by dashed isolines, positive (solid). Contour interval is 0.25 m/s. (b) Same as (a) but for v-wind anomaly field and contour interval 0.2 m/s.

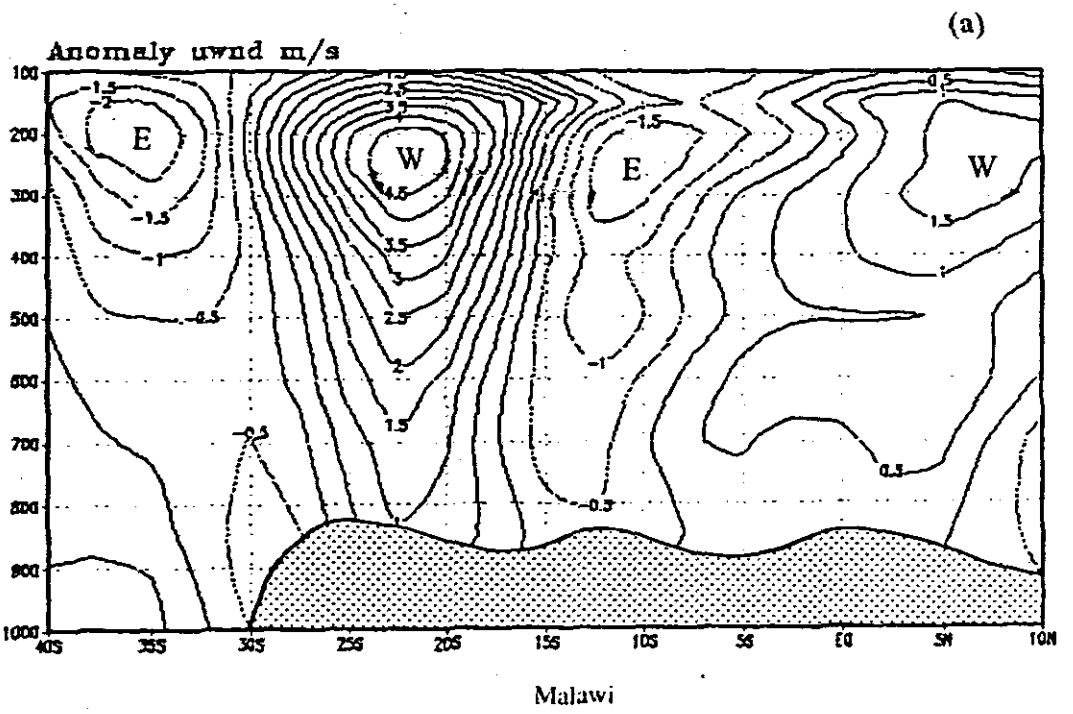

MAX = 5.03871
MIN = -2.55544

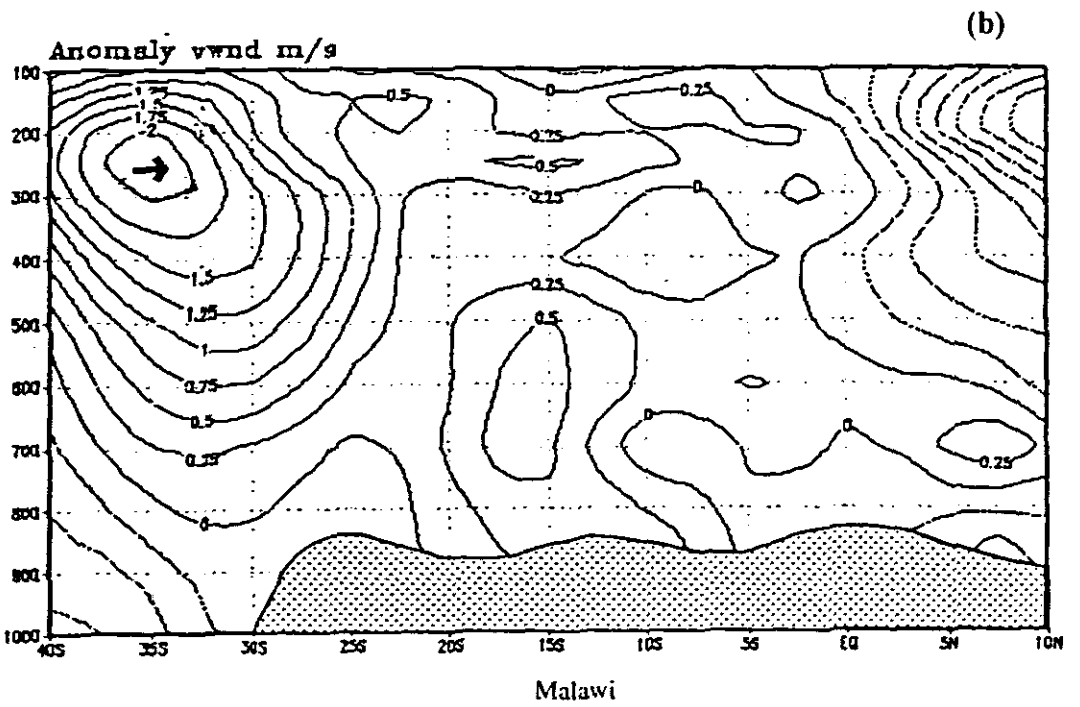

MAX = 2.16447
MIN = -2.2429

Figure 5.8: (a) Latitude-height diagram for u-wind anomaly field averaged over longitudes 30-37.5°E for 1980 season from 10°N to 40°S and from 1000-100 hPa. Negative values are represented by dashed isolines, positive (solid). Contour interval is 0.5 m/s. (b) Same as (a) but for v-wind anomaly field and contour interval 0.25 m/s.

(a)

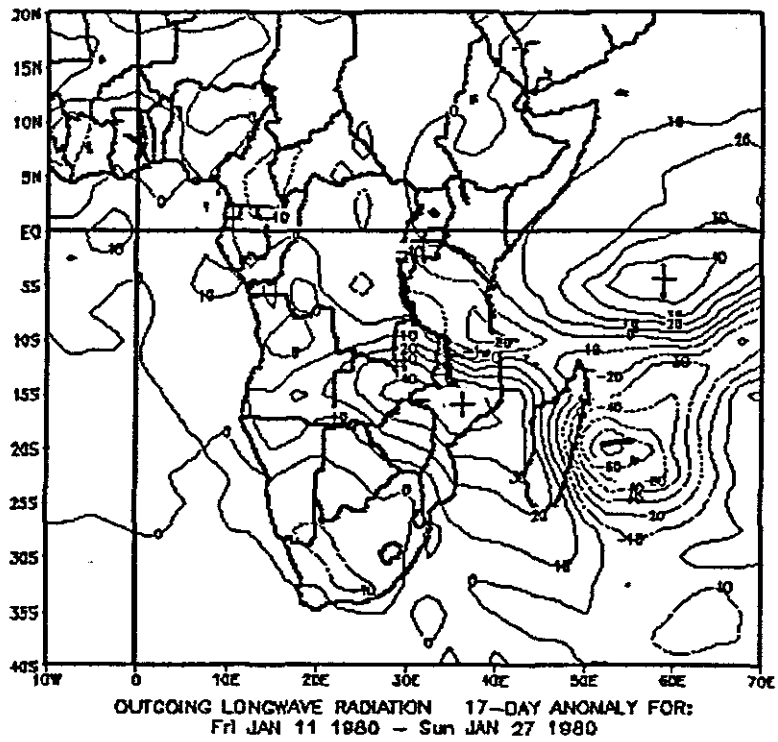

Figure 5.9: (a) Outgoing longwave radiation anomaly field for 1980 dry spell. Negative values are represented by dashed isolines, positive (solid). Contour interval is 10 w m^{-2}.

(b)

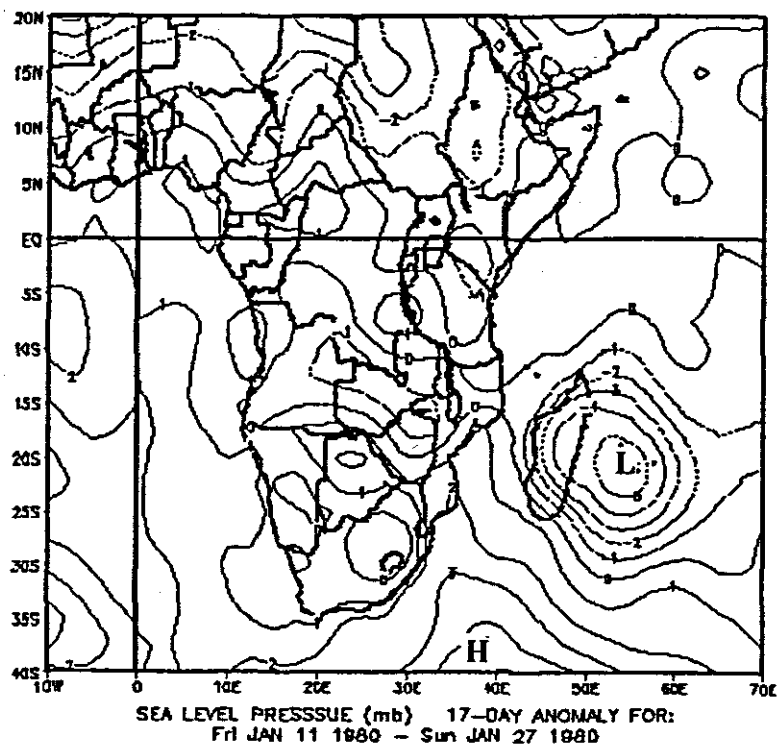

Figure 5.10: (b) Sea level pressure anomaly field for 1980 dry spell. Negative values are represented by dashed isolines, positive (solid). Contour interval is 1.0 hPa.

(a)

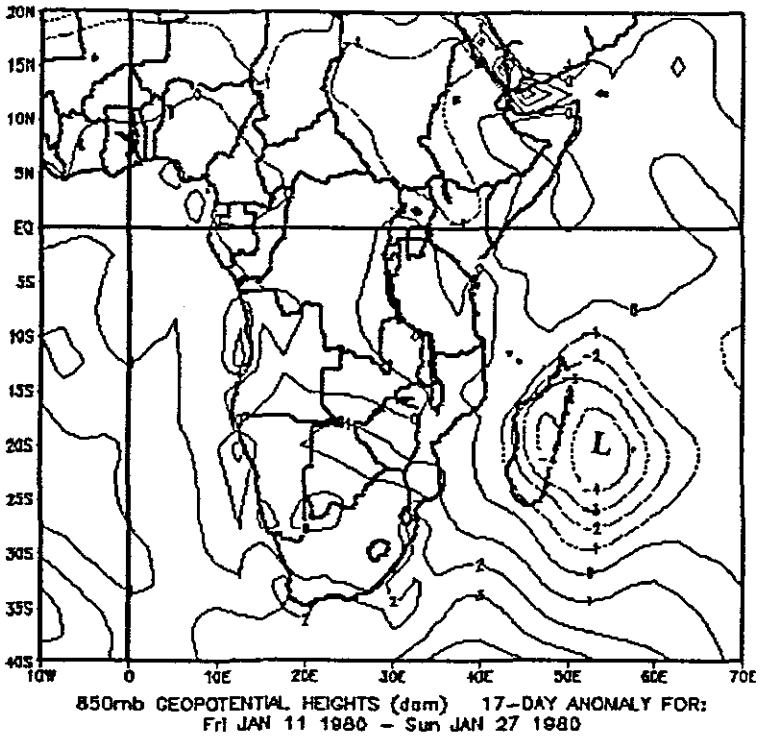

(b)

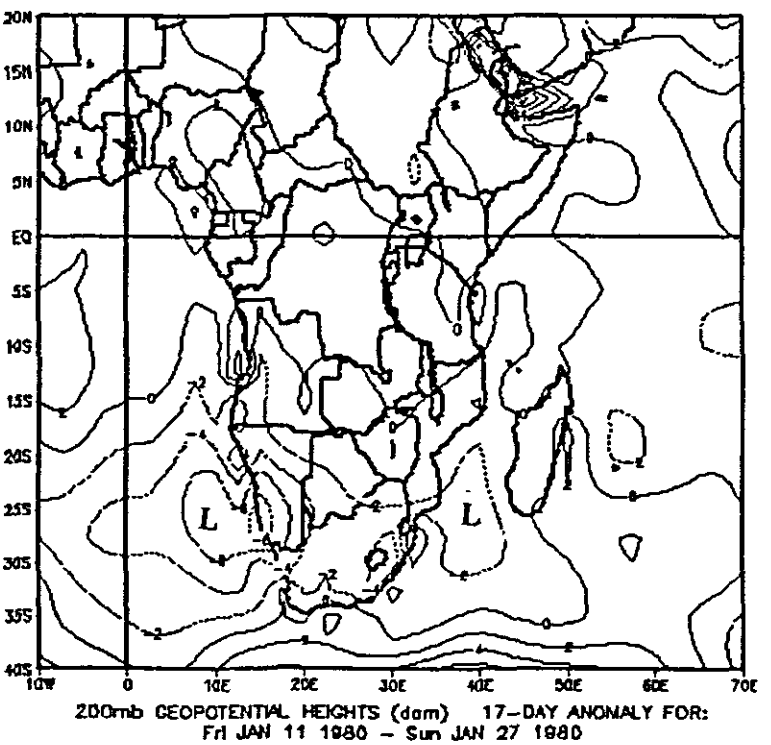

Figure 5.11: Geopotential height anomaly for 1980 dry spell at (a) 850 hPa and (b) 200 hPa. Negative values are represented by dashed isolines, positive (solid). Contour interval is 1.0 gpm and 2.0 gpm respectively.

(a)

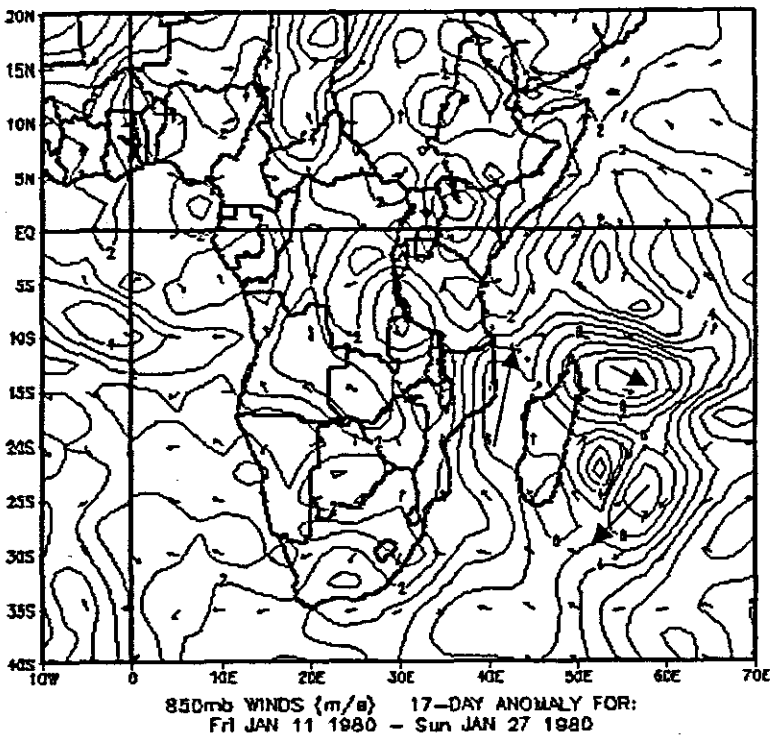

(b)

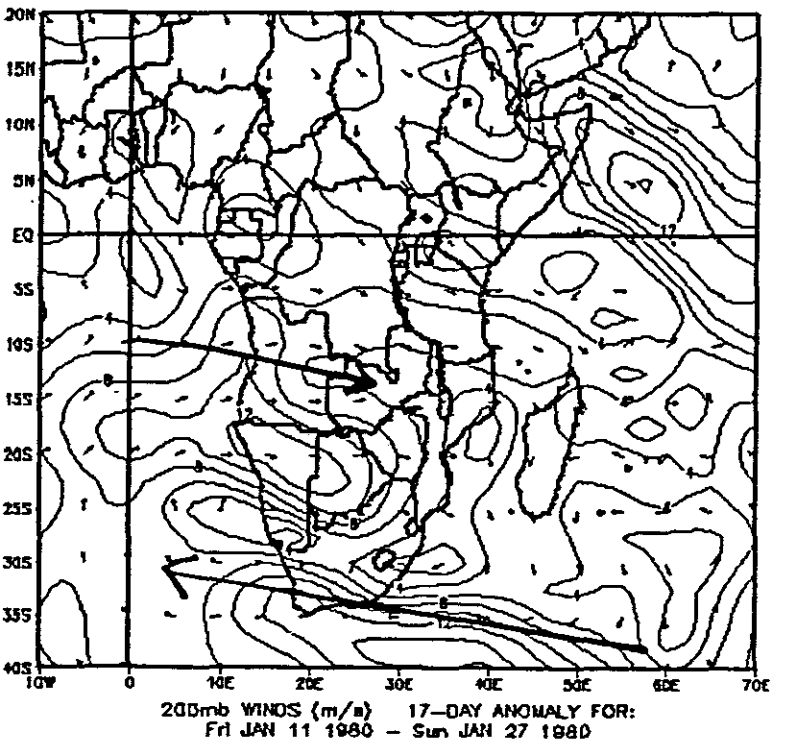

Figure 5.12: Wind vector anomaly for 1980 dry spell at (a) 850 hPa and (b) 200 hPa. Contour interval is 2.0 m/s.

(a)

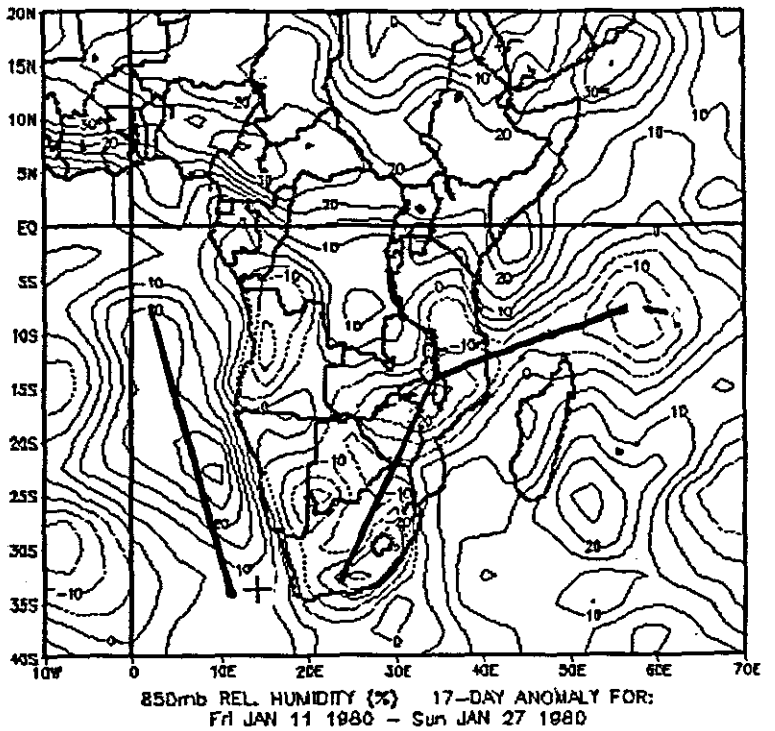

(b)

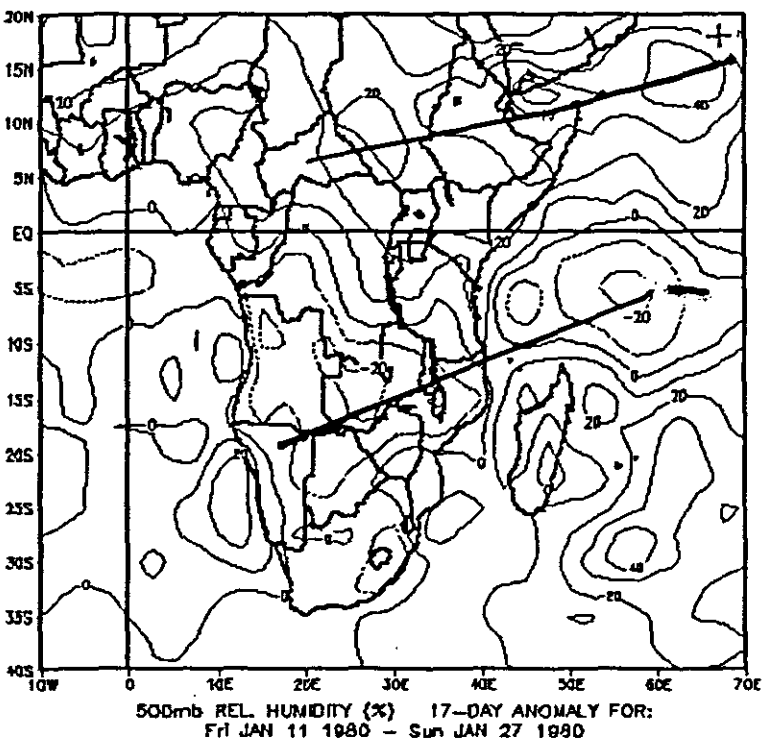

Figure 5.13: Relative humidity anomaly for 1980 dry spell at (a) 850 hPa and (b) 500 hPa. Negative values are represented by dashed isolines, positive (solid). Contour interval is 10%.

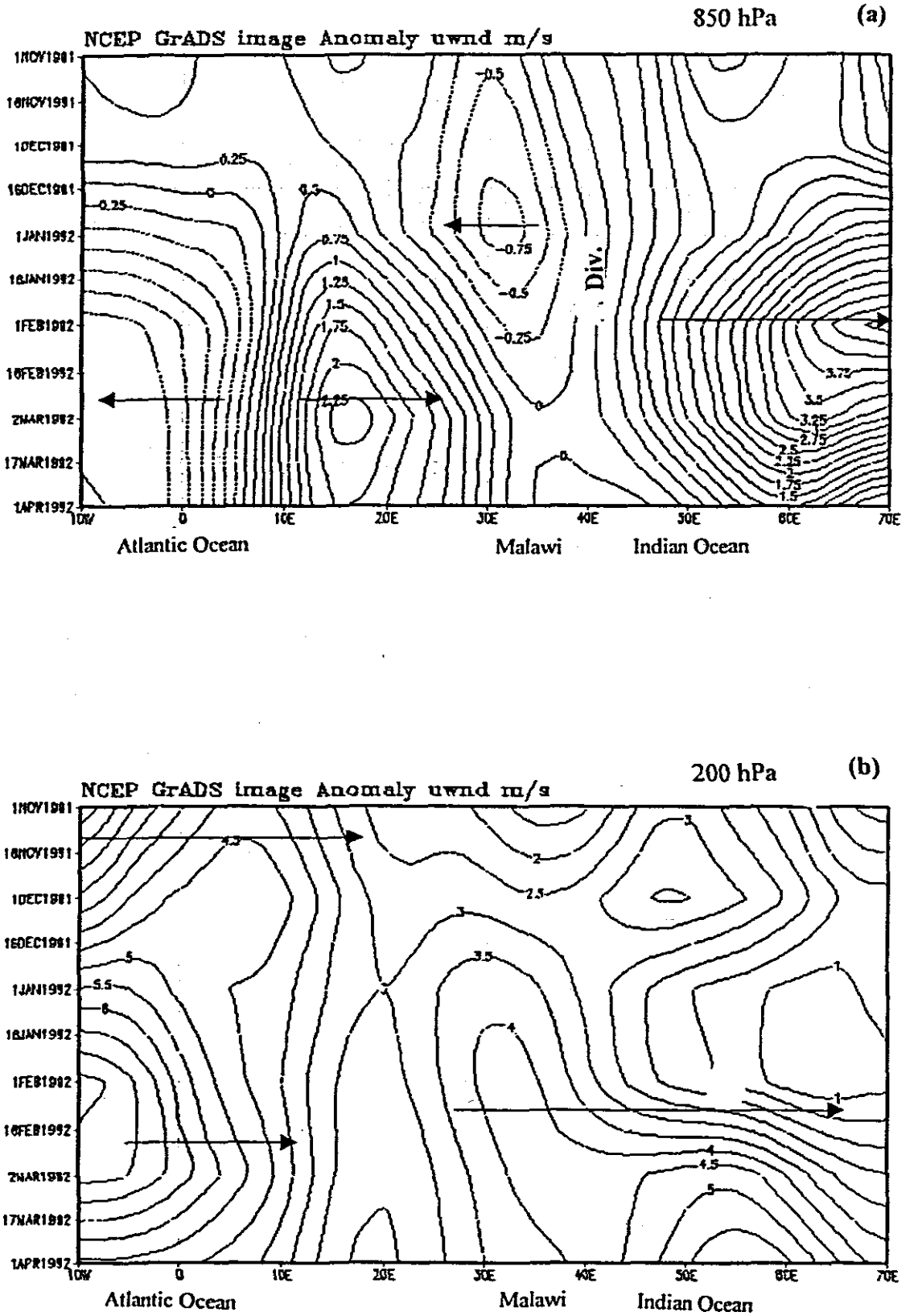

Fig. 5.14: Hovmoller diagrams for u- wind component anomaly averaged over latitudes 10-17.5°S, for 1992 season from 10°W to 70°E at (a) 850 hPa and (b) 200 hPa. Negative values are represented by dashed isolines, positive (solid). Contour intervals are 0.25 m/s and 0.5 respectively.

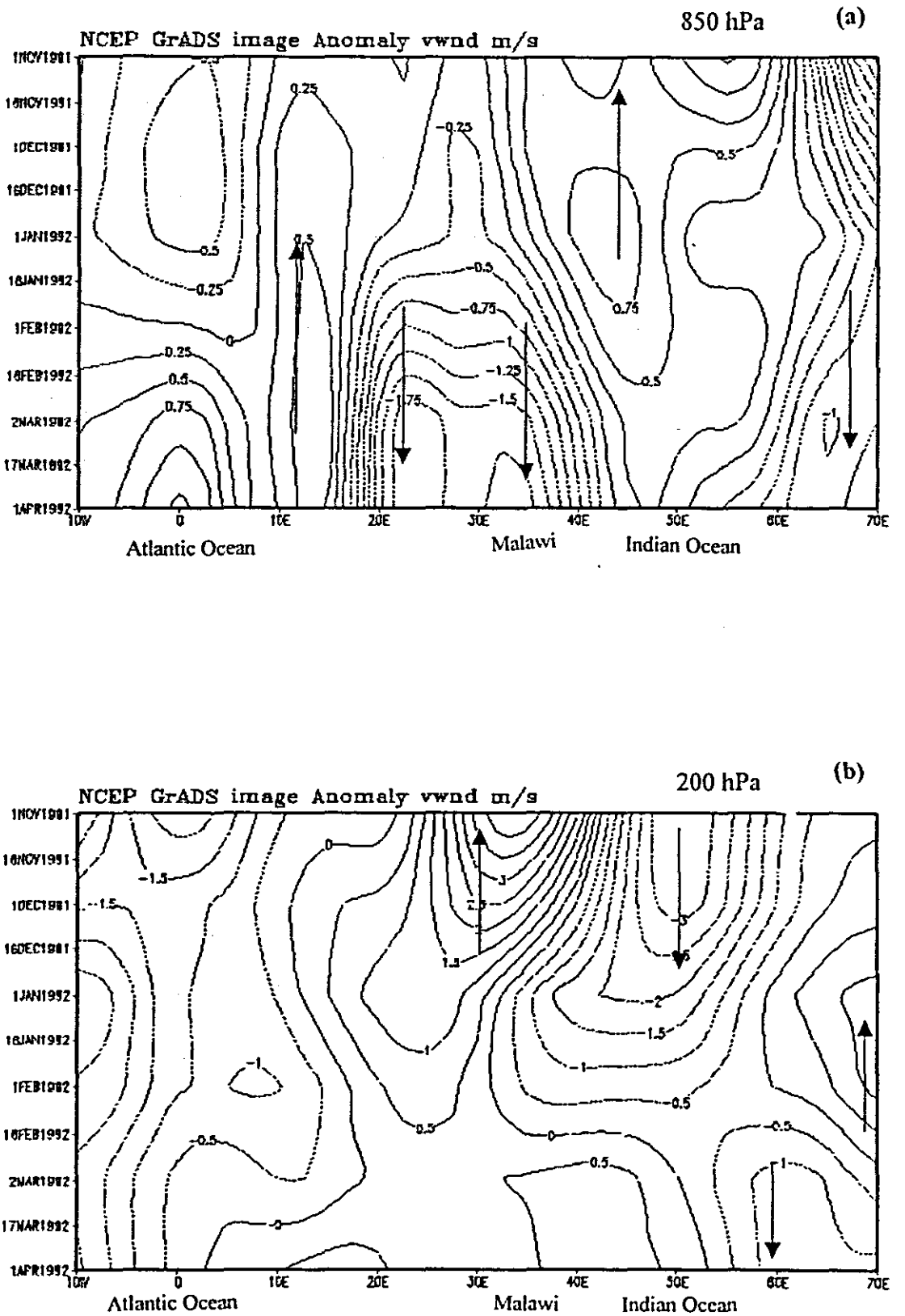

Fig. 5.15: Hovmoller diagrams for v- wind component anomaly averaged over latitudes 10-17.5°S, for 1992 season from 10°W to 70°E at (a) 850 hPa and (b) 200 hPa. Negative values are represented by dashed isolines, positive (solid). Contour intervals are 0.25 m/s and 0.5 m/s respectively.

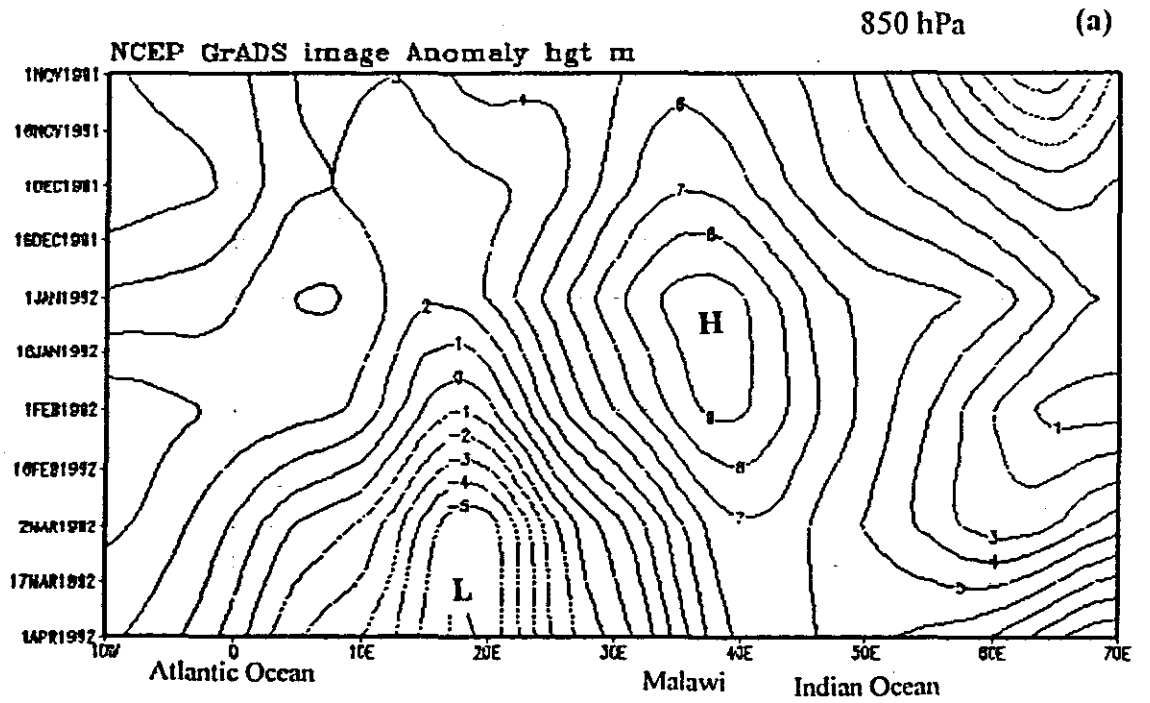

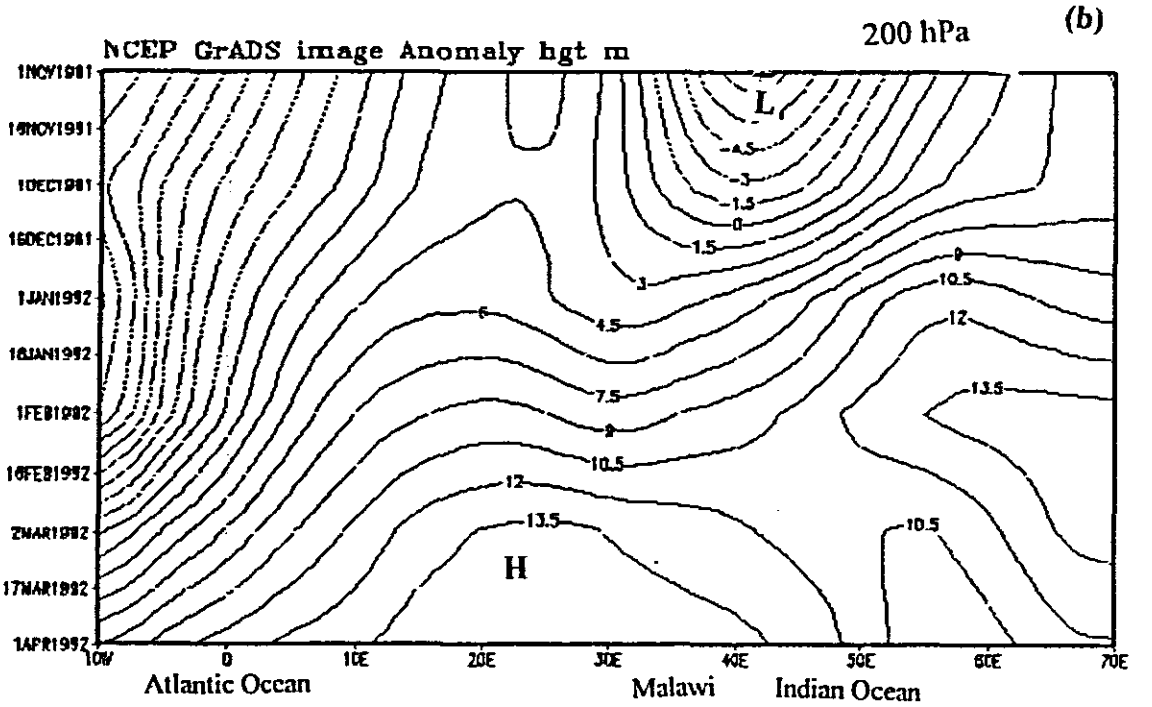

Fig. 5.16: Hovmoller diagrams for geopotential height anomaly averaged over latitudes 10-17.5°S, for 1992 season from 10°W to 70°E at (a) 850 hPa and (b) 200 hPa. Negative values are represented by dashed isolines, positive (solid). Contour intervals are 1.0 gpm and 1.5 gpm at (a) and (b) respectively.

(a)

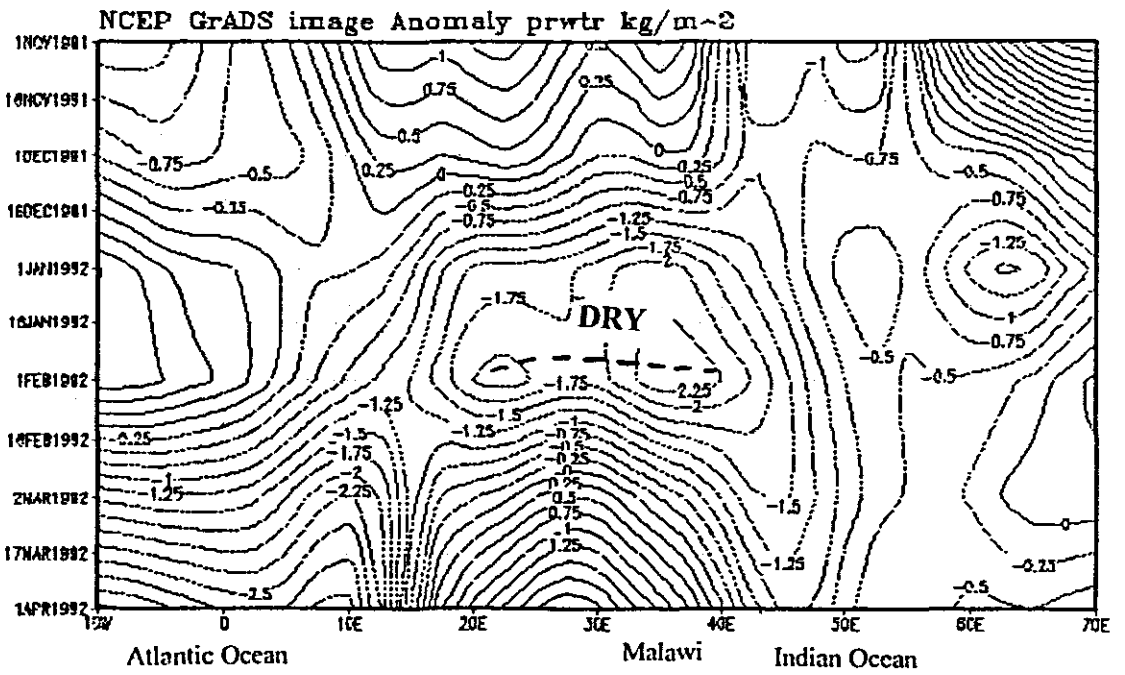

850 hPa (b)

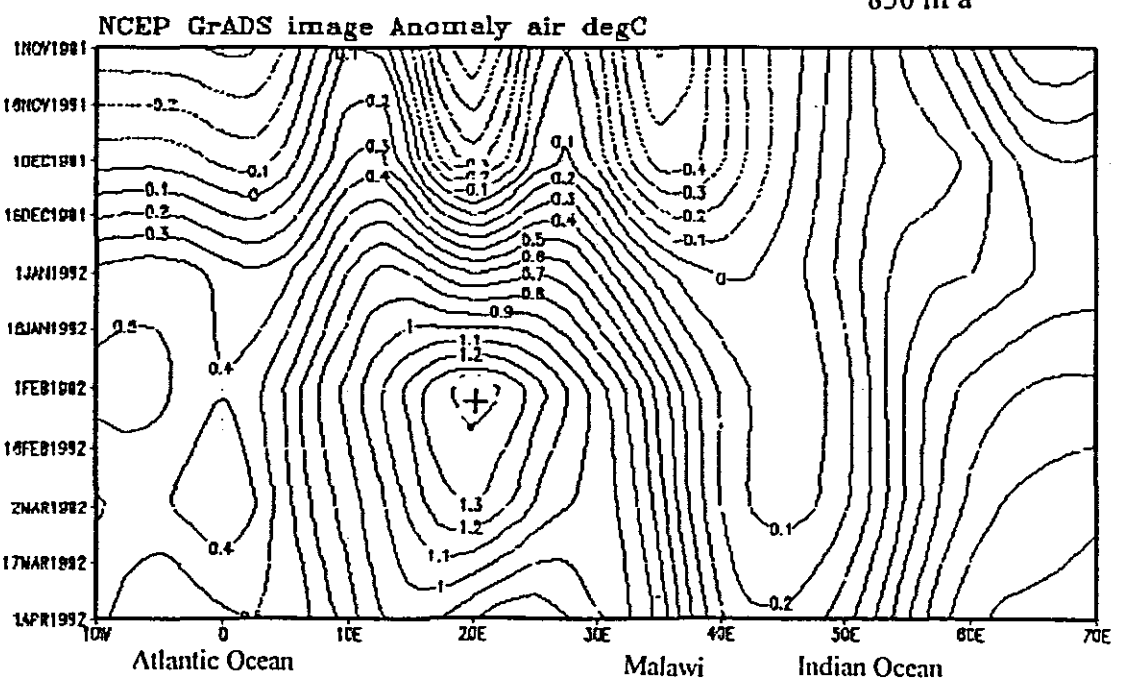

Fig. 5.17:(a) Hovmoller diagram for precipitable water (1000-300 hPa) anomaly averaged over latitudes 10-17.5°S, for 1992 season from 10°W to 70°E. Negative values are represented by dashed isolines, positive (solid). Contour interval is 0.25 kg m^{-2} (b) Anomaly pattern of air temperature over the same area but at 850 hPa level and contour interval is 0.1 °C.

(a)

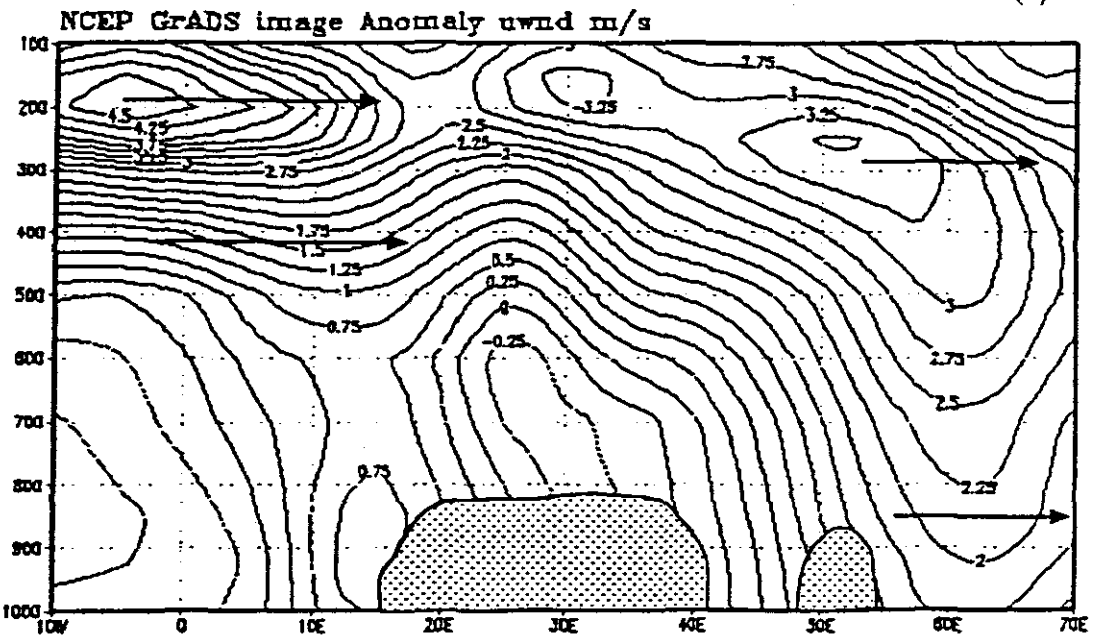

MAX = 4.72154
MIN = 0.638091

(b)

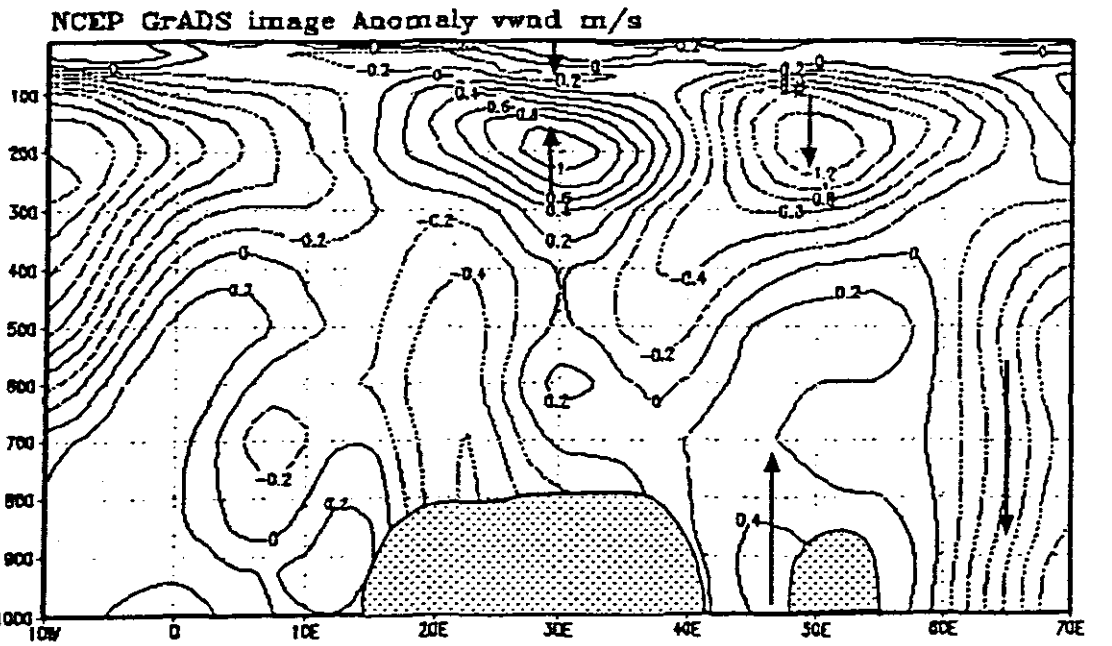

MAX = 1.17405
MIN = 1.90748

Figure 5.18: (a) Longitude-height diagram for u-wind anomaly field averaged over latitudes 10-17.5°S, for 1992 season from 10°W to 70°E and from 1000-100 hPa. Negative values are represented by dashed isolines, positive (solid). Contour interval is 0.25 m/s. (b) Same as (a) but for v-wind anomaly field and contour interval is 0.2 m/s.

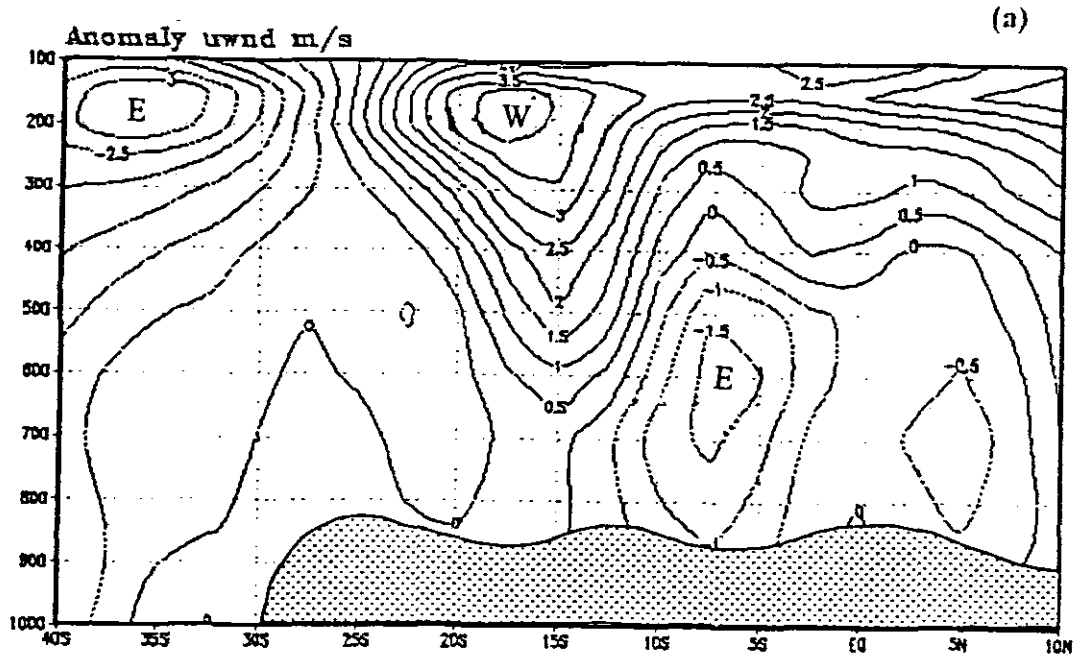

MAX = 4.27215
MIN = -3.45312

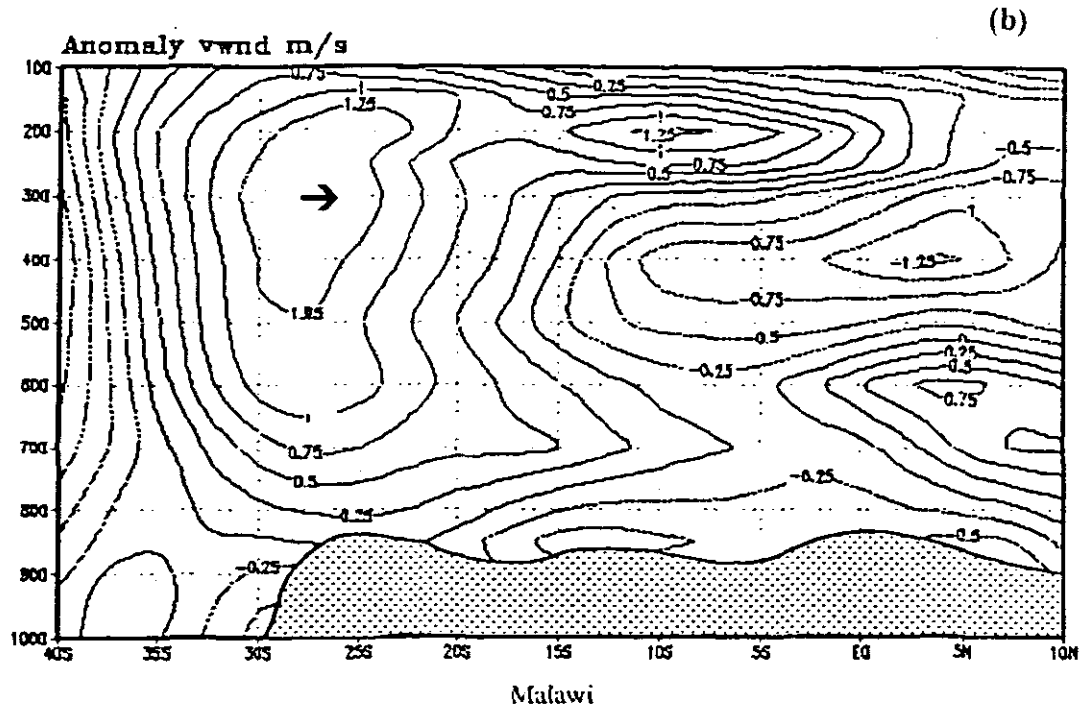

MAX = 1.53672
MIN = -1.31293

Figure 5.19: (a) Latitude-height diagram for u-wind anomaly field averaged over longitudes 30-37.5°E for 1992 season from 10°N to 40°S and from 1000-100 hPa. Negative values are represented by dashed isolines, positive (solid). Contour interval is 0.5 m/s. (b) Same as (a) but for v-wind anomaly field and contour interval is 0.25 m/s.

(a)

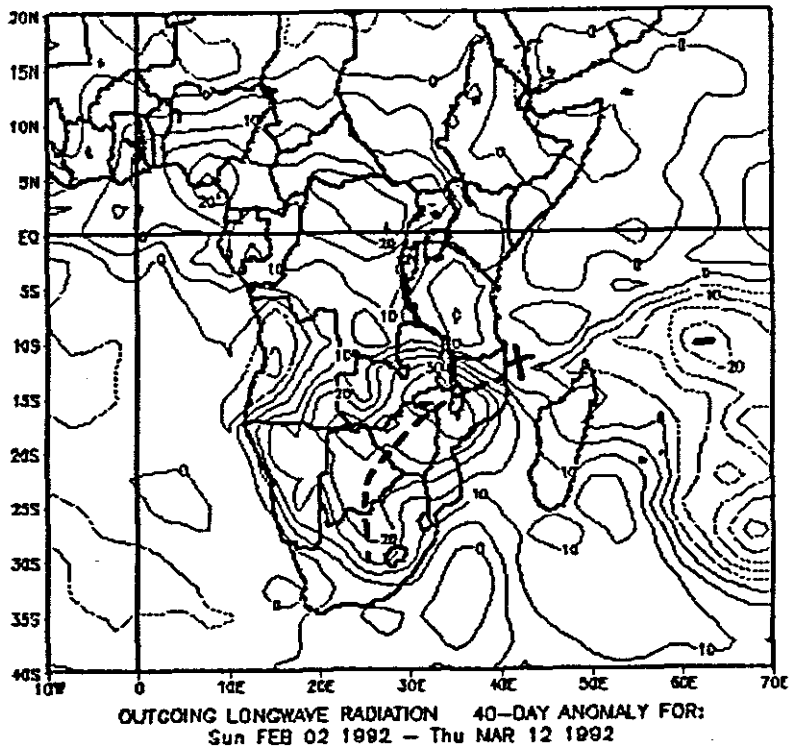

Figure 5.20: (a) Outgoing longwave radiation anomaly field for 1992 dry spell. Contour interval is 5.0 w m^{-2}. Negative (dashed isolines), positive (solid).

(b)

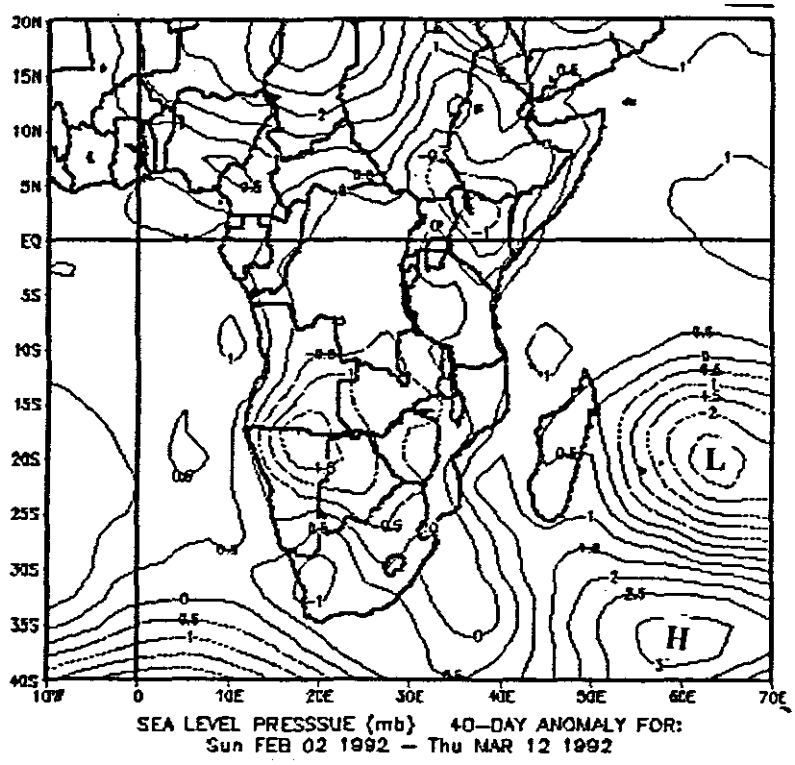

Figure 5.21: (b) Sea level pressure anomaly field for 1992 dry spell with contour interval of 0.5 hPa. Negative values are represented by dashed isolines, positive (solid). Contour interval is 0.5 gpm.

(a)

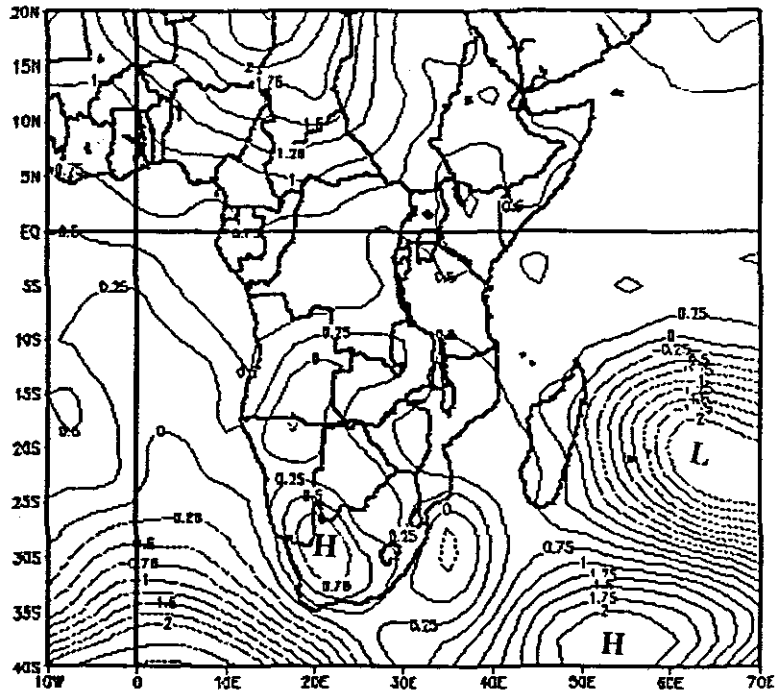

850mb GEOPOTENTIAL HEIGHTS (dam) 40-DAY ANOMALY FOR:
Sun FEB 02 1992 – Thu MAR 12 1992

(b)

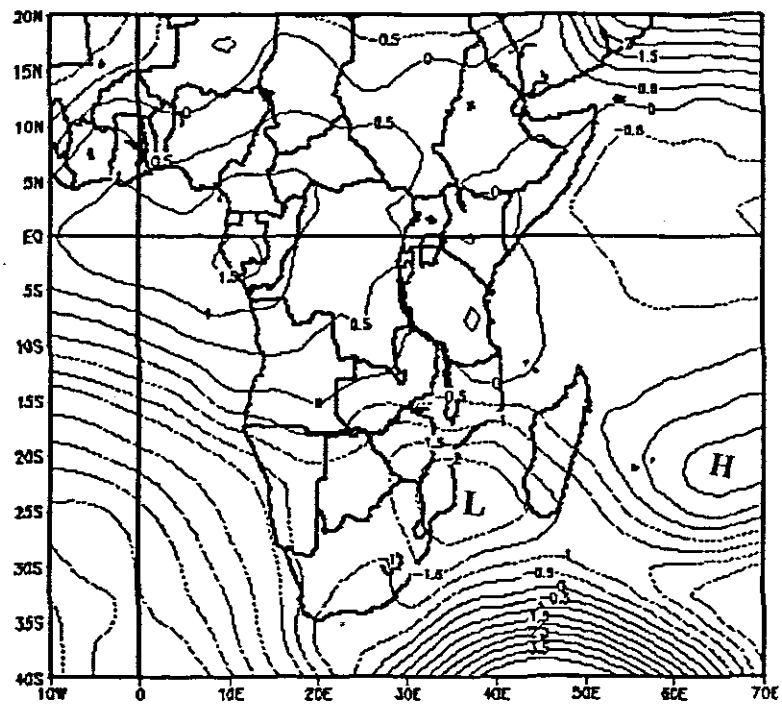

200mb GEOPOTENTIAL HEIGHTS (dam) 40-DAY ANOMALY FOR:
Sun FEB 02 1992 – Thu MAR 12 1992

Figure 5.22: Geopotential height anomaly for 1992 dry spell at (a) 850 hPa and (b) 200 hPa. Negative values are represented by dashed isolines, positive (solid). Contour interval is 0.25 and 0.5 gpm respectively.

(a)

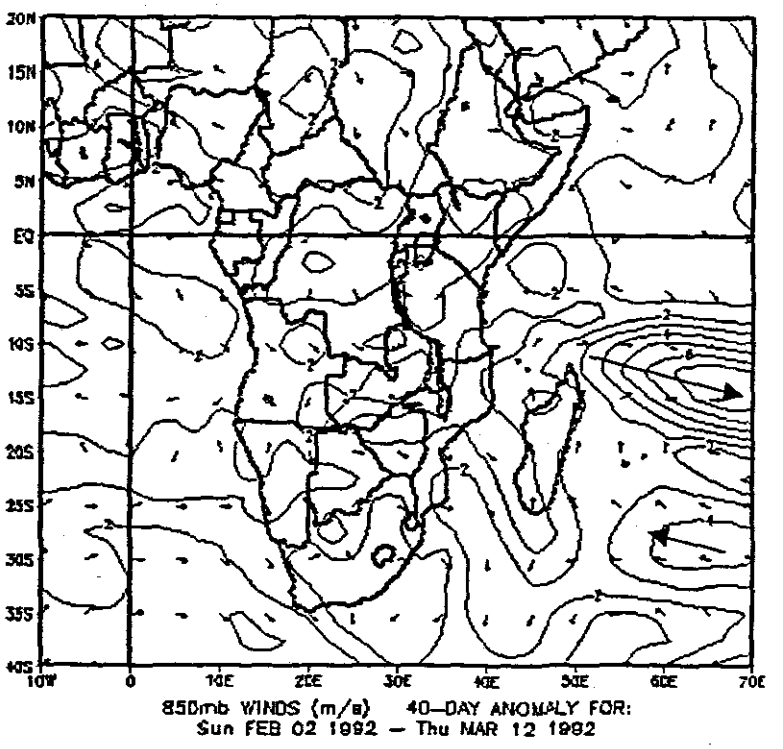

(b)

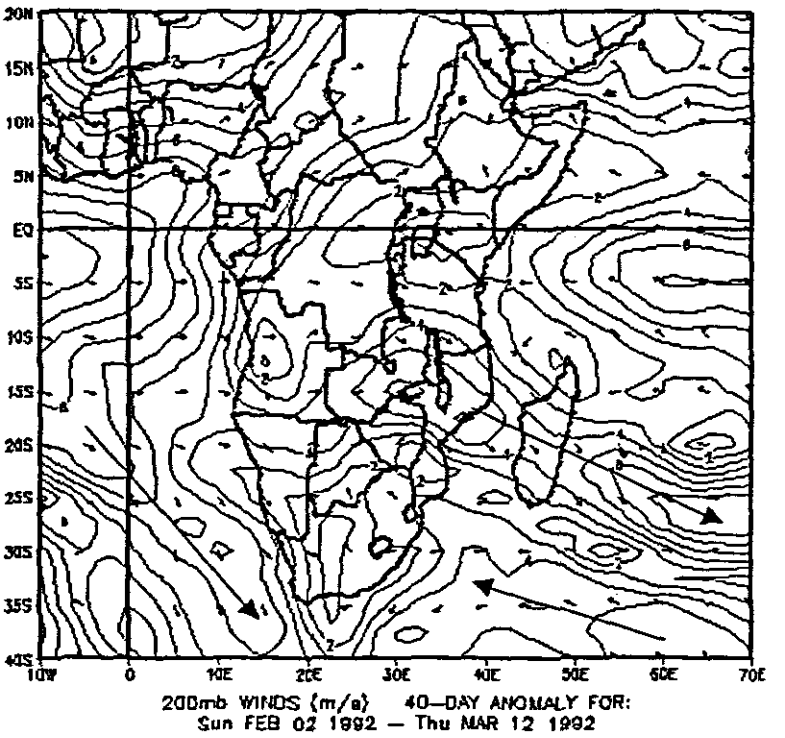

Figure 5.23: wind vector anomaly for 1992 dry spell at (a) 850 hPa and (b) 200 hPa. Contour interval is 2.0 m/s.

(a)

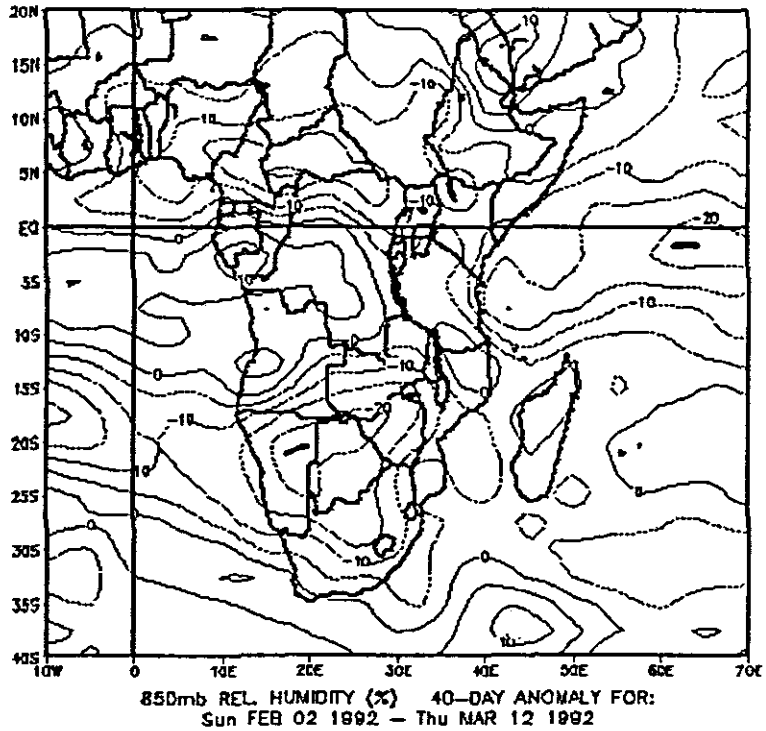

(b)

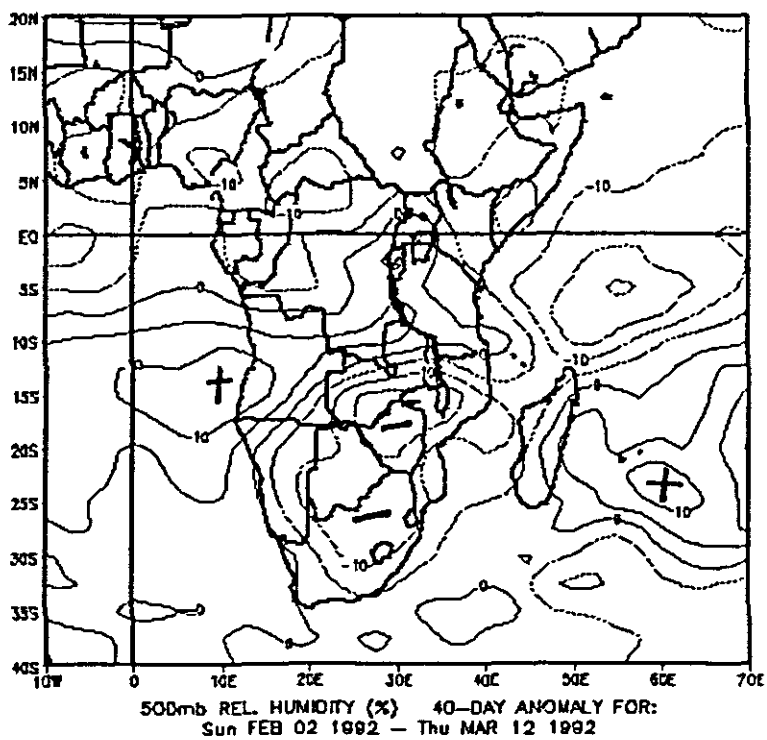

Figure 5.24: Relative humidity anomaly for 1992 dry spell at (a) 850 hPa and (b) 500 hPa. Negative values are represented by dashed isolines, positive (solid). Contour interval is 5%.

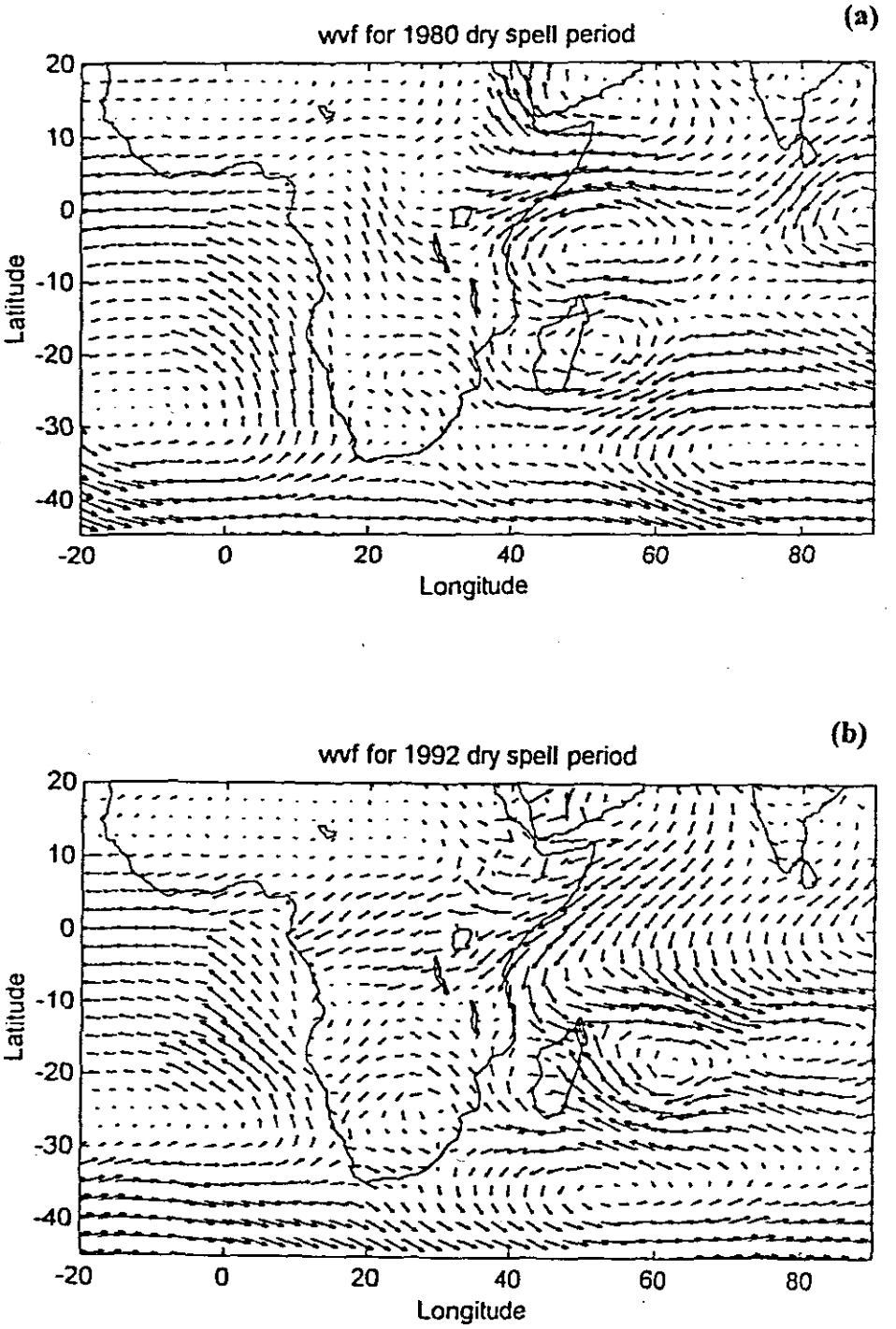

Figure 5.25: ECMWF water vapour flux anomaly field integrated from 1000-500 hPa (a) averaged over 17 days from 11 January 1980 to 27 January, 19980. (b) averaged over 40 days from 02 February 1992 to 12 March, 1992.

Chapter 6

PREDICTABILITY AND MODELLING OF MALAWI SUMMER RAINFALL

6.1 Introduction

It is imperative that objective tools are identified to predict summer rainfall over tropical southern Africa. The principal aim of this chapter is to identify possible predictors and subsequently to develop statistical forecast models. The identification of reliable predictors will enable further development of statistical models in future. Possible predictors are identified from composite analysis of May-October seasons prior to dry and wet summers. The NCEP parameters considered in the analysis are: sea level pressure, geopotential height, wind vector, OLR, precipitable water, SST, air temperature, streamfunction and velocity potential.

This chapter is divided into two sections. In section one, a summary of 'dry minus wet' composites is presented from maps of wet years subtracted from composites of dry years as identified by Malawi Rainfall Index (MRI). This is a useful method of identifying linear precursors. Indices can be formed over key locations for the variables with strong signals and correlated with Malawi summer rainfall.

Predictors have been assembled from correlation and composite differences analyses and other indices. Only those indices which are statistically significant at 95% significant level are retained as input to step-wise regression analysis.

Formulation of statistical forecasting models is presented in section 2. Discussion and general summaries are given at the end of the chapter.

6.2 Summary of composite mean analysis (dry minus wet)

The aim of this section was to identify common precursors/predictors for dry and wet years. The precursor period was May-October and composite mean of wet was subtracted from that of dry. The characteristics of the circulation features prior to dry summers have been investigated and identified (e.g., figure 6.1). The key areas over which indices for identified variables could be formed have been identified. These indices can be used in multi-variate regression analysis in formulating statistical forecast

models for Malawi summer rainfall. The significant findings from this section are listed below.

(a) Mid-level circulation is dominated by a cyclonic gyre over southeastern Angola, Zambia, Namibia and Botswana.

(b) Cool upwelling in the tropical east Atlantic precedes dry years.

(c) The Inter-Tropical Convergence Zone (ITCZ) over the eastern Sahel is weaker than usual.

(d) The low-level velocity potential shows that maximum positive anomalies occur over northern Madagascar preceding dry years.

(e) The upper velocity potential is positive over the central Ocean basins east of 70 °E and to the west of 10°E.

(f) The upper streamfunction is cyclonic in the subtropics prior to dry summers due to the westerly (easterly) wind anomalies over the equator (in the mid-latitudes).

(g) A prominent feature is below normal geopotential heights south of Africa and east of Madagascar, and corresponding westerly wind anomalies during dry pears.

(h) When drought affects Malawi, it also appears in Zimbabwe, Mozambique, the adjacent Channel and southern Madagascar.

(i) SSTs are below normal across the South Atlantic, but above normal in the central Indian Ocean, a pattern typical of El Nino conditions.

6.2.1 Locations of strong signals from 'dry-wet' analysis

The development of statistical forecasting models may be realised from indices formed from areas of strong signals. The following are the summaries of areas with significant signals that have been identified from dry-wet analysis. Indices may be created from the following atmospheric fields over the identified areas (Table 6.1) below.

Parameter	Level (hPa)	Area
Mean sea level pressure	surface	35-45°S, 20-70°E
Geopotential height	850, 500, 200	35-45°S, 20-70°E
Zonal wind	850	5-10°N, 40-70°E
Zonal wind	500	5-10°N, 0-60°E
Zonal wind	500	30-40°S, 20-60°E
Zonal wind	200	10°N-10°S, 30°W-0°E
OLR	surface	5-15°N, 10-80°E
Precipitable water	surface to 300	5-15°N, 10-80°E
SST	1000	0-10°S, 20°W-10°E
Stream function	200	20°S, 30°W-90°E
Air temperature	850	15-30°S, 20-35°E

Table 6.1: Parameters and locations of strong signals including their levels as identified from 'dry minus wet' analysis.

The knowledge and results from the study can be utilised to identify possible predictors from the identified key areas, and establish long-range forecast models for rainfall over southeastern Africa, thus helping to reduce the risk of drought.

The aim in all above sections was to identify possible predictors for forecasting Malawi summer rainfall and then subsequently attempt to develop statistical forecast models which are the topic of the final section. The study lays the foundation for future development of more objective tools for predicting summer rainfall over Malawi. Different methods have been applied in the study. Summary of potential predictors are listed in the subsequent section.

6.3 Formulation of Statistical forecast models

6.3.1 Introduction

Significant findings have been revealed in the study up to this point. The circulation patterns associated with dry summer at inter-annual and intraseasonal time scales have been studied. Precursors associated with dry conditions over Malawi have been identified by using composite analysis. Possible predictors for Malawi summer rainfall have been revealed and key areas where strong signals are associated with Malawi dry conditions have been identified. Major cycles in Malawi summer rainfall at inter-seasonal and intraseasonal time scales have been identified in the spectral analysis. The question that remains to be addressed is how to project future atmospheric conditions. Southern Africa could benefit considerably from skillful forecasts of rainfall (Mason *et al.*, 1996) since most countries in the region depend heavily upon rain-fed agriculture. The damage from droughts or floods could be alleviated if the frequency and magnitude of future droughts or floods events can be forecasted so that feasible relief measures which are economical can be planned and warning systems developed. For example, the prediction of a below normal rainy season would assist decision makers to put up measures that could reduce water usage in domestic, industrial and agricultural sectors to levels that are consistent with predicted levels of water availability (Allan, 1995).

An attempt is made in this final section to develop some statistical forecasting models for Malawi summer rainfall. The study also lay a foundation for future intensive research in formulation of forecasting models in Malawi and contributes to current CLIVAR Africa programmes in Southern Africa.

This section will concentrate on statistical method to approximate the future state of the atmosphere. The other method of approximating the future conditions of the atmosphere is based on the current state of the atmosphere and uses thermodynamic equations. The models developed based on this approach are generally called general Circulation Models (GCMs). One of the disadvantages of the statistical method is that models could not respond to atmospheric changes caused by a new climate regime because of their dependence on past data.

Statistical methods are used to formulate forecasting schemes that may be utilised to forecast Malawi summer rainfall. Hastenrath (1995) has reviewed recent advances in tropical climate prediction, pointing out the predictability of summer rainfall in the

eastern part of southern Africa. The weather forecast that is given some months in advance may be very useful to countries of southern Africa plagued by recurring drought. The advance information on the quality of a summer season may be used for planning and operational purposes by policy makers, water resource managers and agricultural institutions.

Malawi rainfall index, created from 21 Malawi stations as described in chapter 2, are influenced by several climate factors. Malawi monthly summer rainfall is grouped into November-January (NDJ), December-February (DJF), January-March (JFM), February-April (FMA) and the whole period November-April (NA) to reduce 'noise'. These groups are the target predictand. These divisions are useful for operational purposes as they cater for needs at different times of the rainy season. Weather information may be required on the expected onset date of rainfall or quality of rainfall during early summer, mid summer and late summer. These divisions may also capture different climatic signals as dominant weather systems are generally different during these periods. Generally early summer rainfall is controlled by baroclinic westerly wind perturbations while late summer is dominated by barotropic convective instability (Makarau, 1995; Mason *et al.*, 1996).

Several candidate predictors are used as inputs into step-wise multivariate linear regression equations using statgraphics version 6 software. The models are developed for optimum hindcast fit, deflated for degrees of freedom. The predictors (~ 13) that are included as inputs, using forward step-wise selection, in the regression equations are Pacific Nino3, Atlantic Ocean SST (0-10°S, 10°W-10°E), SOI, QBO, surface and upper winds, and several others from NCEP as explained in chapter 2 (see table 6.2). The multiple regression models are mainly based on a 32 year training period. The number of predictors are restricted to three. This is to prevent artificial skill and over-fitting the models. Each model requires input of three parameters for target seasonal rainfall, thus maintaining a degrees of freedom df >28. Models are formulated using July to September (JAS) predictors. This period is routinely used in southern Africa in forecasting summer rainfall over the region. Forecasts are required to be issued in spring.

Candidate predictor 13	Key area	Correlation coefficient (r) w.r.t. (MRI)
3AI	SST at 5°S-5°E plus SST at 25°S-45°E minus SST at 5°S-65°E in the Indian Ocean.	0.52
QBO-1	Singapore zonal wind at 30 hPa	0.33
SOI	Tahiti-Darwin pressure	0.47
CIst	SST over central Indian Ocean 2°S, 62°E	0.19
WIu	Western Indian Ocean Zonal wind; 0-10°S, 40-55°E	-0.28
WIv	Western Indian Ocean meridional wind, 0-10°S, 40-55°E	0.26
Nino3st	Pacific SST within 5N°-5°S, 150-90°W	-0.44
ATs	Atlantic Ocean SST; 0-10°S, 10°W-10°E	0.43
EIp	10°N-10°S, 70-90°E centred at 5°, 85°E	0.43
NIu	Zonal wind components 5-15°S, 55-85°E	0.23
EIst	SST; 0-10°S, 85-100°E	-0.09
AtIw	Upper zonal wind (200 hPa); central Atlantic Ocean	0.29
MAURp	Surface pressure, Mauritius region 20°S, 62°E	-0.25

Table 6.2: Candidate predictors used in the formulation of multi-variate algorithms. Predictors are averaged over JAS months, except for QBO which is the previous years's SON value.

Models are tested for reliability and the predictors are analysed for co-linearity as explained in chapter two (see section 2.3.1.4).

The relationship (the independence) that is available in the residuals left from model fitting is measured by the Durbin-Watson statistic. It should be noted that the value of

student t statistic is also examined to isolate important predictors. This statistic shows whether the predictor should be removed from the regression equation if it has a small coefficient. The predictor is retained in the regression if the t statistic is greater than two in magnitude at 95% significance level.

6.3.2 Model formulation Results

The regression models below are presented in two periods. The seasonal rainfall based on 32 years data and the whole summer based on 34 years data from 1962-1995. The model reveals the following features which are summarised in table 6.3:
Model (i), NArain34, gives the adjusted coefficient of determination of 55% and Durbin-Watson statistic of about 1.9 Model (ii), NDJrain32, indicates adjusted r^2 hindcast fit of 41% and Durbin-Watson Statistic of 2.1. Model (iii), FMArain32, shows coefficient of determination of 47% and Durbin-Watson Statistic of about 1.9.
The multi-variate algorithms for Malawi summer rainfall, with at most 3 predictors, based on the available data are shown below: The predictors are with respect to increased summer rainfall in the predetermined target predictand.

The multi-variate algorithms

(i) NArain34 = +0.48(3AI) - 0 .32(EIp) - 0.26(QBO-1)

(ii) NDJrain32 = +0.46(EIst) - 0.66(WIu) - 0.6(Nino3st) -0.12

(iii) FMArain32= +0.63(WIv) - 0.61(MAURp) - 0.24(QBO-1) +0.23

Predictand Malawi rainfall	predictors Times all JAS	Adjusted r^2 (%) Hindcast fit	Durbin-Watson statistic
(i)NArain34 Nov-Apr	3AI, EIp and QBO-1	55	1.9
(ii) NDJrain32 Nov-Jan.	Nino3st, WIu and EIst	41	2.1
(iii) FMArain32 Feb-Apr.	MAURp, QBO-1 and WIv	47	2.2

Table 6.3: Predictors in the multi-variate algorithms (for meaning of abbreviation see text below).

The reliability of the models is assessed by performing prediction experiments (figures 6.2- 6.4) on seven years independent data. The experiments show how the model would have predicted a particular seasonal rainfall in an operational situation. These experiments are done on early and later portions of the entire data. A solid line on each map shows the observed time index and dashed line indicates the predicted values. The vertical dashed line demarcates the portion used to develop a model that was used to predict the other portion. The length and test period is the same for seasonal models based on 32 years data and 34 years for NA rainfall.

Figure 6.2 presents test forecasts for NA seasonal rainfall based on 34 years data (1962-1995). The model is associated with a westerly phase of QBO at 30 hPa over Singapore previous year SON value negative, hence current year positive. SST at 5°S-5°E plus SST at 25°S-45°E minus SST at 5°S-65°E, (3AI), and sea level pressure (Elp) in the east Indian Ocean (10°N-10°S, 70-90°E). The test forecasts, figure 6.2a, shows fairly good fitting although at times it slightly underestimates or overestimates. The performance of predictions experiment in the later portion is similar to earlier portion (figure 6.2b). In general, the entire model display optimal fitting compared to other models.

The NDJ rainfall model is associated with JAS zonal wind over the Western Indian Ocean (WIu); Pacific JAS Nino3 and JAS SST over the Eastern Indian Ocean (EIst) within an area 0-10°S, 85-100°E. The test forecasts for NDJ seasonal rainfall (figure 6.3a) show good hits in 1987 and 1990. In other seasons, the model underestimates. The test forecasts for the earlier portion, figure 6.3b, indicate underestimation from 1966 and overestimation in 1962. the model performance in the 1960's is better than the 1990's. In general, the entire model fitting appears poorer than the NA model. The rather poor skill in NDJ rainfall (early summer over southern Africa) may be due to the influence of temperate rainfall-producing systems while the higher skills for rainfall prediction in other periods are due to mostly tropical atmospheric circulation influence during this summer peak period (Mason *et al.*, 1996).

Figure 6.4a shows test forecasts for FMA seasonal rainfall. The model is associated with a westerly phase of QBO at 30 hPa over Singapore, surface pressure (MAURp) over Mauritius region (20°S, 62°E) and meridional wind (WIv) over the western Indian Ocean(2°S, 47°E). The test forecasts show good hits. For example, the 1992 drought is fairly well predicted. The earlier portion, figure 6.4b, of the test forecasts shows poor fitting especially from 1964 to 1966. The entire model fitting is generally better than the

NDJ model. In general, the models based on 32 years data indicate highest predictability for FMA season. Both yield a Durbin-Watson statistic of at least two. The study has revealed the validity and reliability of two to three month lead- time forecasts and the validation is acceptable. The predictors are mainly atmospheric, but obtain 'memory' through ocean coupling in tropical monsoon regions.

6.4 Summary and discussion

The overall objective of this chapter was to develop statistical forecasting models for Malawi summer rainfall. The study first touched on common precursors for dry and wet summers and possible predictors for Malawi summer rainfall using different techniques. The common precursors for dry and wet summers have been identified and key areas which show association with Malawi summer rainfall have been revealed and presented. Possible predictors for Malawi summer rainfall have been identified, with respect to the available data.

The multi-variate algorithms have been developed for Malawi and results mainly based on 32-34 years data have shown that models could be operationally useful. Lowest predictability is revealed in seasonal forecast for November-January while highest predictability is found for the whole season November-April and late summer February-April. Generally results suggest that there is need to search for more predictors using up-to-date data. The training period of the models could be increased in order to give higher statistical confidence. This may result in increased predictability of Malawi summer rainfall. The models need to be updated because they could become gradually obsolete due to climate change, being based on past data. There is also a need for skill to be assessed operationally to observe performance. Depending on the reliability of the models operationally, these models could assist in giving advance warning on the prospects of seasonal rainfall. Contingency plans could be put in place for water and food security in the region. Results have generally shown that, according to current available data, Malawi rainfall is associated with July-September period of Nino3 SST over eastern Pacific ocean, SST in Atlantic and Indian Ocean, wind flow in the Indian Ocean, and the stratospheric QBO phase.

The next chapter summaries and concludes the entire thesis.

(a)

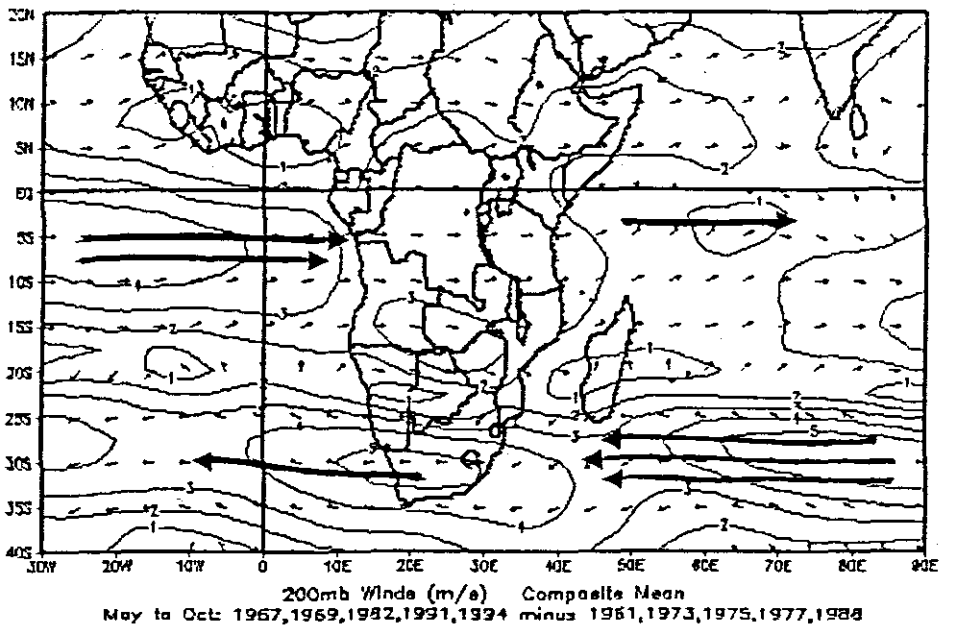

(b)

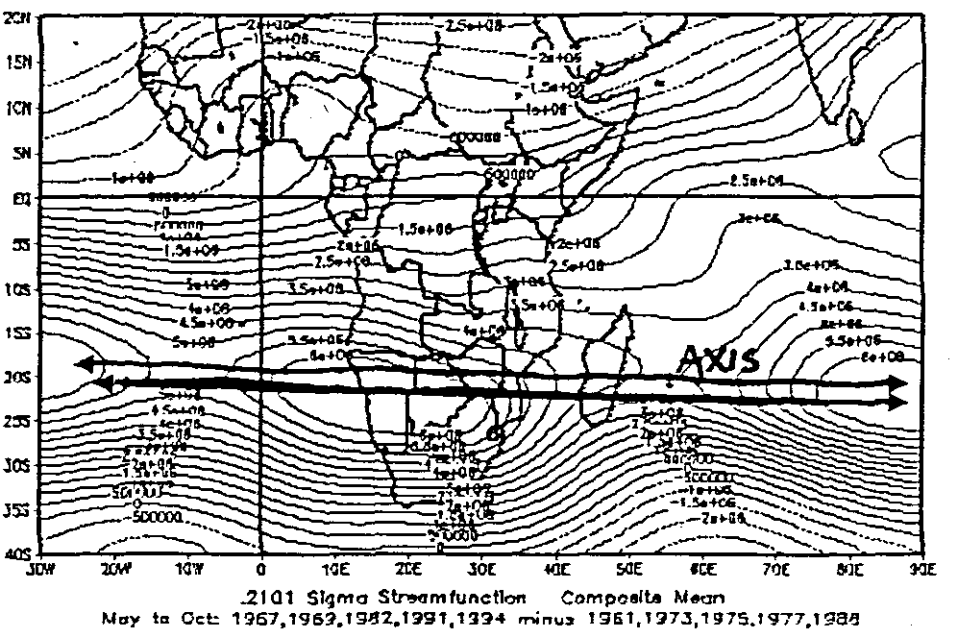

Figure 6.1: (a) Composite mean dry-wet vector wind showing axis of strong wind at about 30°S prior to dry summer in Malawi.
(b) Composite mean dry-wet streamfunction at 0.210 sigma level showing main axis at about 20°S with negative value (dashed) and positive value (solid).

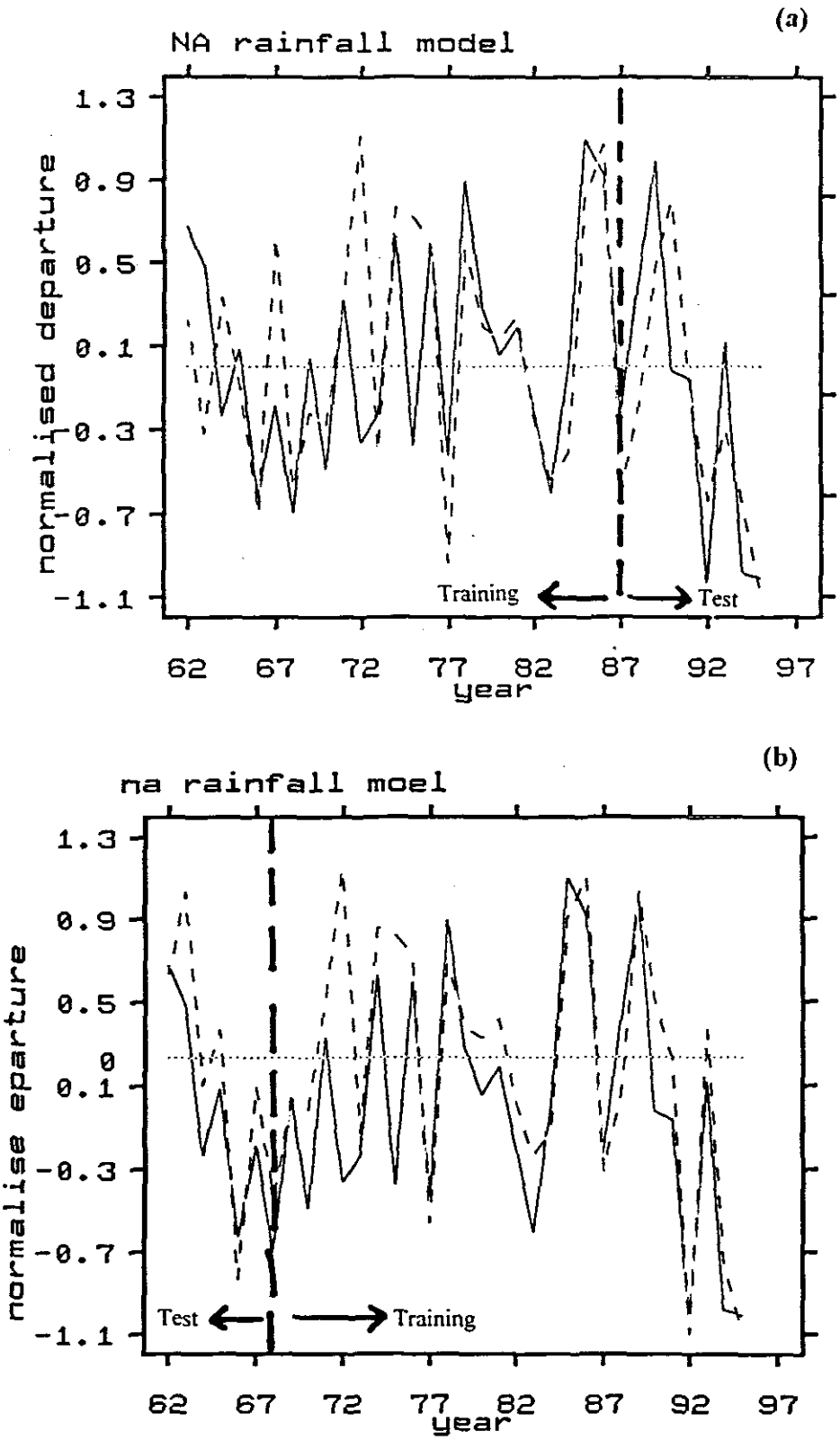

Figure 6.2: Hindcast model fitting for November-April (NA) seasonal rainfall forecast based on observed (solid) and predicted (dashed) values using (all JAS) 3AI, Elp and QBO using 34 yrs data. Test periods are (a) 1987-1995 and (b) 1962-1968.

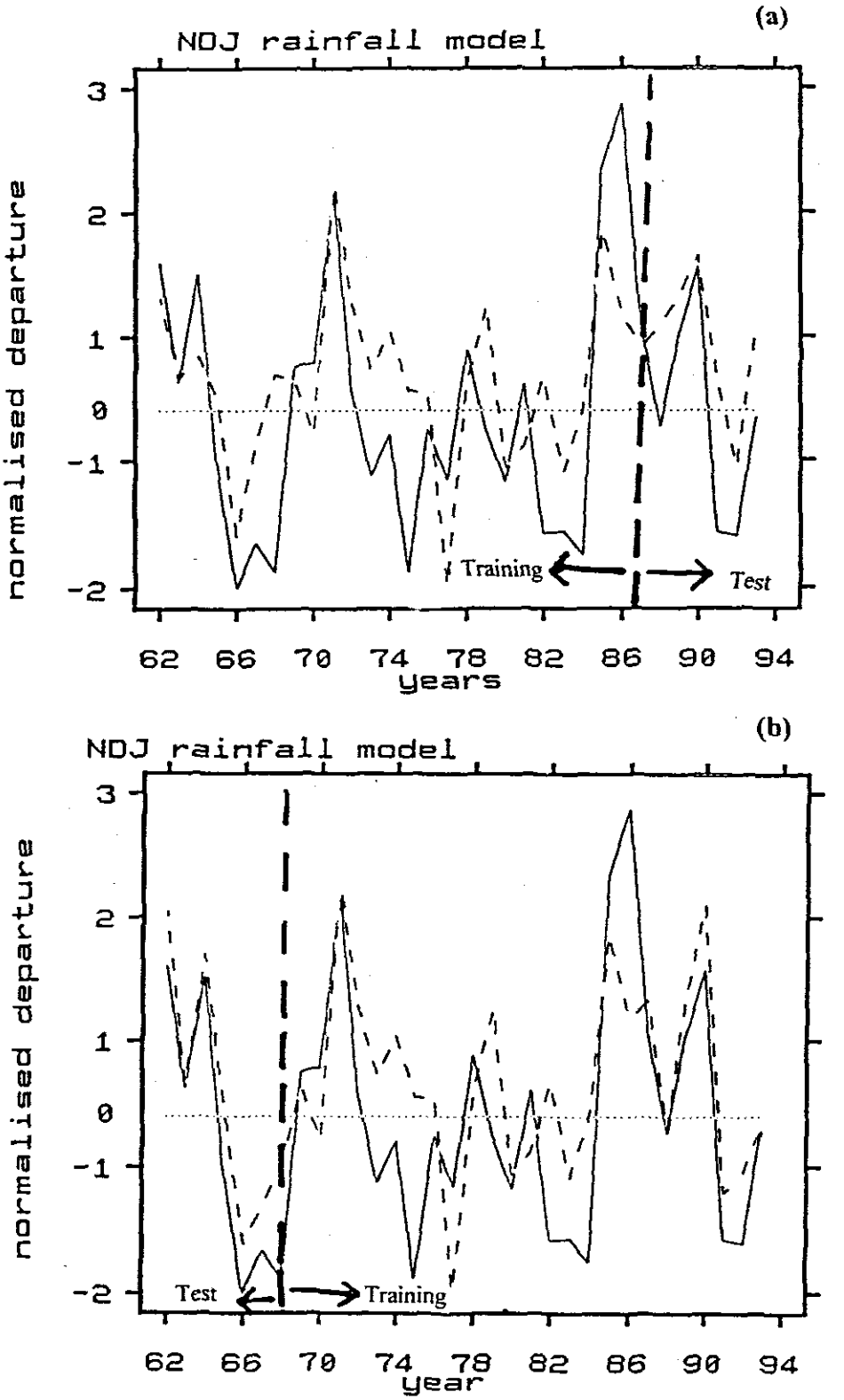

Figure 6.3: Hindcast model fitting for November-January (NDJ) seasonal rainfall forecast based on observed (solid) and predicted (dashed) values using (all JAS) Nino 3, WIu and EIst. Test periods are (a) 1987-1993 and (b) 1962-1968.

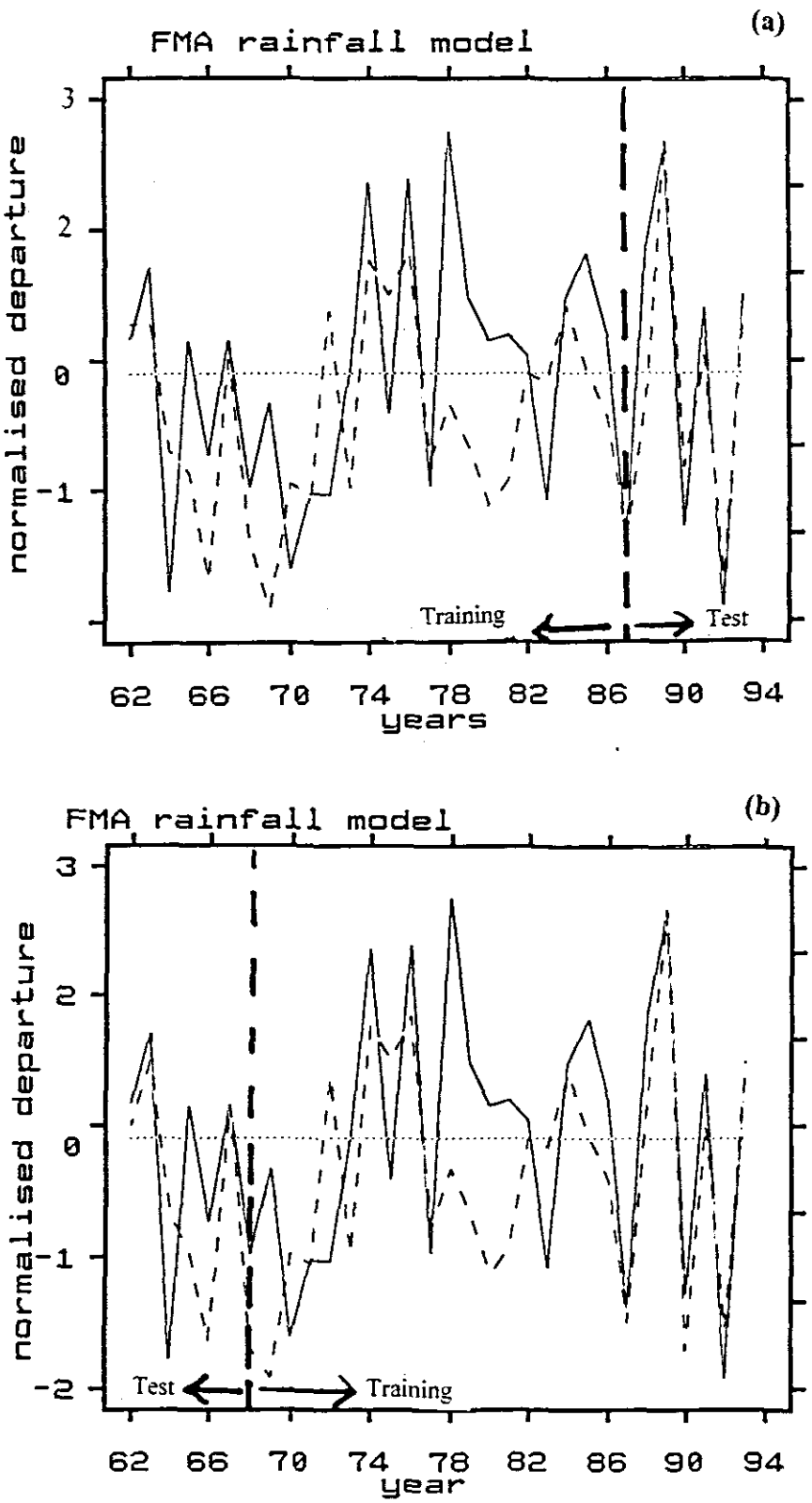

Figure 6.4: Hindcast model fitting for February-April (FMA) seasonal rainfall forecast based on observed (solid) and predicted (dashed) values using (all JAS) MAURp, QBO and WIv. Test periods are (a) 1987-1993 and (b) 1962-1968.

Chapter 7

SUMMARY AND CONCLUSIONS

7.1 Introduction

The economy of Malawi varies according to climate variability and few attempts have been made to understand rainfall variability and associated atmospheric circulation patterns. The precursors for dry and wet years for Malawi summer rainfall are unknown and operational statistical forecasting models applied in the prediction of seasonal precipitation in the country are unverified. Few detailed studies (Nkhokwe, 1996) on relationships between Malawi summer rainfall and other distant meteorological variables have been done. Therefore this study has sought to address these problems by investigating climate variability and its predictability mainly at seasonal time scale.

Regionally however, a number of studies have been done and links have been established between, for example, southern African summer rainfall and ENSO as well as SST over the Atlantic and Indian Oceans. Some characteristics of rainfall variability studies have been elucidated in southern Africa by comparing contrasting atmospheric circulation patterns associated with extreme weather/climate conditions. These studies have mainly concentrated on early, middle and late summers (NDJ, DJF, JFM) periods and at times from November to March. The circulation patterns associated with the extreme conditions for the whole summer period November to April have rarely been investigated in southern Africa. Likewise, for predictive purposes, the entire preceding period May to October has not often been studied as a block This study focusses on these periods. Consequently, at regional level, the thesis is intended to contribute towards better understanding of climate variability and its predictability over tropical southern Africa using Malawi as the representative country in the study. The focus is mainly on dry climatic conditions. The overall objective is to investigate circulation patterns associated with dry summers and to identify precursors and possible predictors for forecasting Malawi summer rainfall and subsequently develop some statistical forecasting models.

One of the stated objectives of the study was to increase the understanding of the summer rainfall variability over tropical southern Africa by examining temporal and spatial characteristics of Malawi summer rainfall at seasonal and intraseasonal time scales. This has been achieved in chapters 3 and 5 by analysing seasonal and pentad

Malawi summer rainfall. The characteristics of Malawi summer rainfall since the 1960's has been revealed and spectral analysis has identified major cycles in Malawi seasonal and pentad summer rainfall. Spectral analysis on Malawi November-April rainfall shows a highest peak at 3.8 years followed by 2.4 years and 11.1 years in descending order of significance associated with ENSO, QBO and the solar cycle respectively.

The other stated objective of the study was to try to identify and establish statistical relationships between Malawi summer rainfall and other meteorological variables such as ENSO (in terms of Southern Oscillation Index); Quasi-Biennial Oscillation (QBO); sea surface temperature (SST) and outgoing longwave radiation (OLR). This has been achieved (chapter 3) by employing correlation analysis. Malawi summer rainfall has been associated with several meteorological parameters and some of the results have been presented. The aim of the analysis was to find possible predictors for forecasting the quality of the summer season over Malawi.

The third objective was to investigate the characteristics of dry conditions before and during summer. The objective has been achieved (chapter 4 and 6). The objective was undertaken with the hypotheses that the circulation patterns and embedded weather systems some months before dry season behave differently and the dry summer over Malawi is related more to the circulation features south of 10°S than north of it. In order to identify circulation features associated with dry conditions, a November to April (NA) rainfall index was created. This index was then used to isolate dry and wet years following pre-determined criteria. Composite analysis was done for the season and preceding period May to October. The circulation features, in terms of selected meteorological variables (chapter 4) before and during were identified. The focus was mainly on the winter to summer transition for predictive purposes.

The fourth aim of the study was to increase the understanding of circulation controls over tropical southern Africa associated with dry spells, as identified in Malawi daily rainfall, at intraseasonal time scale. The aim has been achieved (chap 5) by investigating circulation modes of selected dry spells in a season. The objective was achieved under the hypothesis that each dry spell has unique circulation patterns associated with it. The forty day dry spell in 1992 and seventeen day dry spell in 1980 have been used in the study. The circulation patterns associated with these dry conditions over tropical southern Africa in general have been identified. Results have revealed that dry spells have similar circulation controls, a tropical cyclone east of Madagascar.

The fifth specific objective of the study was to attempt to develop some statistical models for forecasting Malawi summer rainfall. This has also been achieved (chapter 6). The statistical forecast models have been developed and prediction experiments have been performed to test their reliability. Candidate predictors (~13) were used as input to forward step-wise regression. The number of predictors for each seasonal rainfall (target) was restricted to at most three to maintain degrees of freedom to not less than 28 for the period of 32-34 years.

Some of the main findings of the entire study are listed in table 7.1, 7.2, 7.3, 7.4 and 7.5. below and are discussed in conjunction with hypotheses and objectives mentioned. The study lays a groundwork for future studies to formulate more statistical models for predicting Malawi summer rainfall. This may subsequently contribute toward mitigating the negative effects resulting from climate variability.

7.2 Summary

7.2.1 Chapter 3

Subject	Characteristics
inter-annual rainfall	Malawi rainfall shows a 4-5 year fluctuations with low values from 1979 to 1984 and after 1989 (figure 3.1a).
Pentad rainfall	-Malawi rainfall mean onset date of the first highest peak is pentad 2-6 December. Malawi rainfall shows two major cycles: the 10-20 day and 30-60 day cycles.
rainfall spectral analysis	The 3.8, 2.4 and 11.1 year cycles have been identified in Malawi summer rainfall (figure 3.2).
Malawi NA rainfall correlations	-Strong correlations with 3 area SST index from -7 to -3 months lags (table 3.1). -Significant correlation with sea level pressure (Elp) at -7 months lag (table 3.1). - Significant correlations with SOI from -5 to 0 months lags (table 3.1). -Significant correlation with Atlantic Ocean SST (0-10°S, 10°W-10°E) at -5 months lag (table 3.1). Significant correlation with NE monsoon at -5 months lag (figure 3.6). -Significant positive correlations with OLR north east of Madagascar at -3 months lag (figure 3.4 b)

Table 7.1: Summary of major findings from Malawi summer rainfall analysis and correlations.

7.2.2 Chapter 4

Malawi dry summers (November-April) have been associated with circulation pattern at 500 hPa level (figure 7.1). The pattern shows the effect of latitudinal change that has contributed to the marked subsidence from South Africa to Malawi (see results from vertical motion analysis below). Main findings from composite analysis of dry years with focus on period prior to dry years, for predictive purposes, are listed in table 7.2.

Parameter (precursor)	Characteristics prior to dry years
SST	Negative anomalies over the Atlantic Ocean north of 38°S and east of 20°W with pronounced centre off Angola are in anti-phase with positive anomalies over areas northeast of Madagascar (figure 4.9a).
Wind	Marked westerly confluence over southern Angola at 500 hPa (figure 4.5a).
Geopotential height	Pronounced positive anomalies south of Madagascar at 200 hPa.
Velocity potential	Pronounced positive anomalies (hence convergence) over southern Africa with centre over Zimbabwe in the upper level.
Streamfunction	Anticyclonic circulation to the east of 40°E with centre at 7°S, 85°E in lower level and over southern Madagascar at upper level (figures 4.11a and 4.12a).
Temperature	Largest positive values east of Madagascar.

Table 7.2: Characteristics of selected meteorological variables during the precursor period May-October prior to dry years based on composite analysis.

Characteristics of vertical motion during composite dry summer may be elucidated by using the quasi-geostrophic vorticity equation. The effect of latitudinal change is investigated from figure 7.1 at 500 hPa level. An s-curve pattern of westerly wind anomalies is observed from the Atlantic Ocean (35°S) to Malawi through southern South Africa (15°S). A pronounced trough is found to the east of South Africa and a ridge to the west while marked subsidence is found between South Africa and Malawi. There is a change in latitude hence coriolis parameter. The latitudinal change, assuming constant pressure gradient, of a parcel of air may create different patterns of convergence in rotating systems. The vertical motion is estimated by calculating omega, ω , through 700-300 hPa layer from the quasi-geostrophic vorticity equation (Holton, 1979).

$$\frac{\partial \zeta}{\partial t} = -V.\nabla(\zeta + f) + f_o \frac{\partial \omega}{\partial p} \quad \text{.....Eq 7.1}$$

where $\frac{\partial \zeta}{\partial t}$ = the local rate of change of relative vorticity

$-V.\nabla(\zeta + f)$ = the horizontal advection of absolute vorticity

For steady conditions, $\frac{\partial \zeta}{\partial t} = 0$; ζ and f_o are constants and negative in the southern hemisphere, $V = 2$ m $^{-1}$ at 500 hPa level.

$$f_o \int_{P1}^{P2} \frac{\partial \omega}{\partial p} dp = \int_{P1}^{P2} V.\nabla(\zeta + f) dp \quad \text{.....Eq 7.2}$$

But $\frac{\partial \omega}{\partial p} dp$ may be approximated to $d\omega$ then integrating from ω_1 (at p_1) to ω_2 (at p_2) the above equation becomes

$$f_o \int_{\omega 1}^{\omega 2} d\omega = \int_{P1}^{P2} V.\nabla(\zeta + f) dp \quad \text{.....Eq 7.3}$$

Simplifying the right-hand side of the equation by ignoring changes in x-direction then integrating between pressure levels 700 hPa (p_1) and 300 hPa (p_2). Substitute values

$f_o = 10^{-4} s^{-1}$; $\partial f = (-0.53)\ 10^{-5}\ s^{-1}$; $\partial y = (2)10^{6}$m (distance from 35°S to 15°S latitude); and taking $\omega_1 = 0$; $\zeta = -10^{-5}\ s^{-1}$; V (observed) = 2 m s $^{-1}$; $dp = 4\ (10^{4})$ pascal. Then $\omega_2 \cong 0.02$ Pa s $^{-1}$ (in isobaric coordinate system). The positive omega

value shows sinking motion over the region. In the x, y, z system the vertical motion may now be estimated from equation

$\omega_2 = -\rho g w$.....Eq 7.4

Where ρ is the mean density ~ 1 kg m^{-3} ; g is an acceleration due to gravity = 9.8 m s^{-2} and w is vertical velocity. Solving for w and substituting into equation w = -0.002 m s^{-1} = -0.2 cm s^{-1} (sinking motion). The sinking motion is relative to a horizontal flow of 2 m s^{-1} , and in agreement with observations (figure 4.5b).

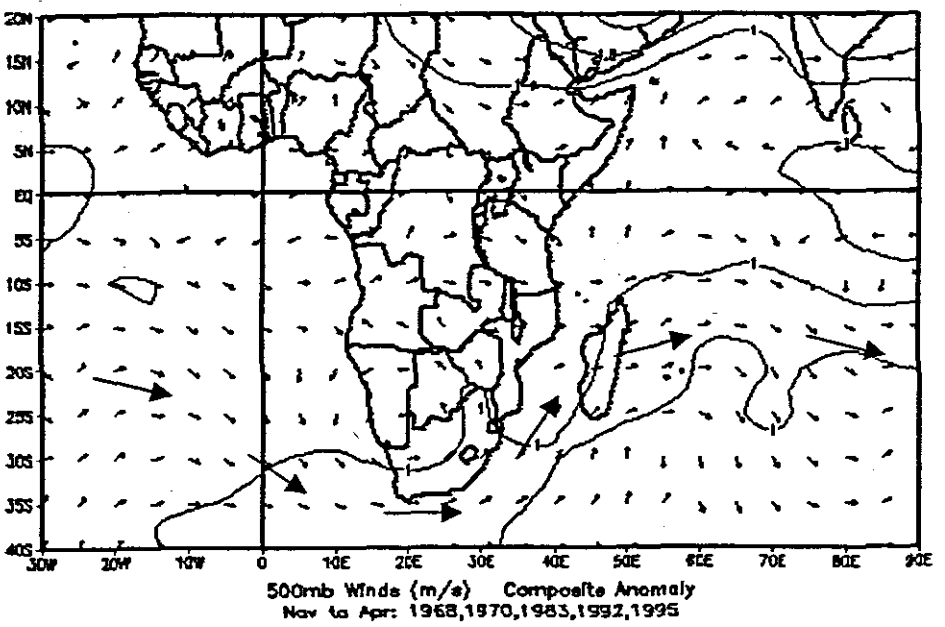

Figure 7.1: Wind circulation pattern at 500 hPa level during Malawi dry summers.

7.2.3 Chapter 5

The aim of the chapter was to investigate the kinematic and thermodynamics properties of dry spells of 1992 and 1980. These dry spells display common features. Main findings are presented in table 7.3 below:

Parameter	1980 dry spell	1992 dry spell
Sea level pressure	Associated with tropical cyclone Hycinthe east of Madagascar, resulting in moisture deficiency over tropical southern Africa. Moisture is transported towards tropical cyclone area.	Associated with several episodes of tropical cyclone activities east of Madagascar, resulting in moisture deficiency over tropical southern Africa.
Horizontal wind	Easterlies are dominant in low levels and westerlies in the upper level.	Easterlies are dominant in low levels and westerlies in the upper level
Precipitable water	Lowest negative precipitable water centred over Malawi.	Lowest negative precipitable water centred over Malawi.
Air temperature	Pronounced positive temperature.	Pronounced positive temperature.
OLR	Lowest values centred just east of Madagascar. Largest positive values extend from Zambia to southern Mozambique Channel through Malawi.	Lowest anomalies centred east of Mauritius. Largest positive values observed from Malawi to South Africa.
Water vapour flux	Tropical cyclone east of Madagascar fed by advection from south of Madagascar. NE monsoon feeds westerly axis around 15°S.	Tropical cyclone east of Madagascar fed by advection from south of Madagascar. NE monsoon feeds westerly axis around 15°S.

Table 7.3: Summary of dominant features identified from case studies of 1980 and 1992 dry spells.

In both dry spells water vapour flux is transported towards a convective region east of Madagascar. Tropical southern Africa is denied moisture and the results are in agreement with the findings by other researchers (Tyson, 1986; Harrison, 1986; D'Abreton, 1992). Jury *et al.* (1996) found that convection over southern Africa are

modulated by common climatic processes. The summaries of two dry spells has revealed that generally similar mechanisms are at work controlling day-to-day characteristics of weather. The study has contributed in revealing the relationship between dry spells over tropical southern using Malawi in the analyses and spatial/temporal structure of selected meteorological variables.

7.2.4 Chapter 6

From the dry minus wet analysis common predictors were identified by analysing characteristics of the circulation features prior to dry summers of selected meteorological variables. Table 7.4 highlights the locations of strong signals. Predictors in the multi-variate regression models are presented in table 7.5.

Locations of strong signals from 'dry-wet' analysis may assist in the development of statistical forecast models. Indices may be created from the following atmospheric fields over the identified areas:

Parameter	Level (hPa)	Area
Mean sea level pressure	surface	35-45°S, 20-70°E
Geopotential height	850, 500, 200	35-45°S, 20-70°E
Zonal wind	850	5-10°N, 40-70°E
Zonal wind	500	5-10°N, 0-60°E
Zonal wind	500	30-40°S, 20-60°E
Zonal wind	200	10°N-10°S, 30°W-0°E
OLR	surface	5-15°N, 10-80°E
Precipitable water	surface to 300	5-15°N, 10-80°E
SST	1000	0-10°S, 20°W-10°E
Stream function	200	20°S, 30°W-90°E
Air temperature	850	15-30°S, 20-35°E

Table 7.4: Parameters and locations of strong signals including their levels as identified from 'dry-wet' analysis.

The analysis has revealed important key areas from which possible predictors may be created in order to establish long-range forecast models for rainfall over southeastern Africa. This will help reduce the risk of drought impacts on food and other resources.

Results from formulation of statistical forecasting models show highest predictability in NA Malawi summer rainfall followed by FMA rainfall. Lowest predictability is observed in NDJ summer rainfall. Low predictability in NDJ summer rainfall is associated with the influence of baroclinic westerly wind perturbations while highest predictability in other periods are due to barotropic convective instability (Mason *et al.* 1996; Makarau and Jury, 1997). The predictability of Malawi summer rainfall is contributed mostly by Nino3 SST, sea surface pressure in the Atlantic and Indian Oceans, QBO and wind flow in the Indian Ocean. Predictors and characteristics of multi-variate regression models are presented below:

Predictand Malawi rainfall	predictors Times all JAS	Adjusted r^2 (%)	Durbin-Watson statistic
(i)NArain34	3IA, EIp and QBO-1	55	1.9
(ii) NDJrain32	Nino3st, WIu and EIst	41	2.1
(iii) FMArain32	MAURp, QBO-1 and WIv	47	2.2

Table 7.5: Predictors in the multi-variate algorithms.

7.3 Conclusion and recommendation

Dry summer conditions over Malawi are associated with strong convective system to the east of Madagascar at both inter-annual and intra seasonal time scales. Characteristics of the circulation pattern during dry conditions are associated with atmospheric circulation to the south of 10°S (e.g., figure 4.5b). It also appears that centres of action of weather systems are not generally anchored over Malawi. Malawi is generally found in a peripheral area of climatic anomalies from different sides. Correlation analysis between Malawi station rainfall (not shown) and the Southern Oscillation Index shows

that correlation coefficients decrease from south to north. East Africa rainfall is positively correlated with El Nino while southern Africa is negatively correlated. Most of Malawi's climatic anomalies occur in sympathy with southern Africa, particularly during extreme phase of ENSO. It is recommended that local ENSO indices should be investigated further. The effort will enable Malawi to have predictors which may explain most of the variations in Malawi summer rainfall. The causes of circulation patterns revealed by the study can be investigated further using numerical models.

References

Abu-Zeid, M.A. and A.K. Biswas, 1992: Climate fluctuations and water management. *Billings and Sons Ltd,* Worcester, UNEP, IWRA, WRC.

Allan, J.A. 1995: The Irelo of drought in determining the reserve water sector in Israel. *Drought network News*, 7, 21-23.

Asnani, G.C., 1993: Tropical meteorology. *Noble Printers, Pune-India.*

Barclay, J.J., 1992: Wet and dry troughs over southern Africa during early summer. *Msc. Thesis, University of Cape Town*, South Africa.

Barclay, J.J., M.R. Jury and W. Landman, 1993: Climatological and structural differences between wet and dry troughs over southern Africa in the early summer. *Meteorology and Atmospheric Physics*, 51, 41-51.

Barry, R.G. and A.H. Perry, 1973: Synoptic Climatology: Methods and Applications. *William Clowes & Sons, Ltd.*, London, U.K.

Bjerknes, J., 1966: A possible response of the atmospheric Hadley circulation to equatorial anomalies of ocean temperature. *Tellus*, 18, 820-829.

Bjerknes, J., 1969: Atmospheric teleconnections from the equatorial Pacific, *Monthly Weather review*, 97, 163-172.

Bluestein, H.B., 1992: *Synoptic-Dynamic Meteorology in Midlatitudes* Vol., 82-152.

Byers H.R., 1974: General Meteorology, Fourth Edition, *McGraw-Hill Book Company, Inc.*, New york, p. 110.

Cane, M.Z., S.E. Zebiak and S.C. Dolan, 1986: Experimental forecasts of El Nino. *Nature.* ,321, 827-832.

Cavalcanti, I.F.A and V.B. Rao, 1998: Atmospheric characteristics over tropical South America during dry and wet years of the Southern Hemisphere summer and autumn seasons. *Proceedings of the first WCRP International Conference on Reanalyses*, 27-31 October 1997, Silver Spring, Maryland, USA. *WMO/TD-No. 876*, 195-198.

Chatterjee, S., and B. Price, 1977: Regression Analysis by examples. *Willey*, 228pp.

Cayan, D.R. and L.G. Riddle, 1993: The influence of precipitation and temperature on seasonal streamflow in California. *Water Resources Research.* Vol. 29, 4, 1127-1140.

Chen, T.C and R.Y. Tzeng, 1990: Global scale intreseasonal and annual variation of divergent-water vapour flux, *Meteorology and Atmospheric Physics*, 44, 133-151.

CLIVAR, World Climate Research Programme, *Initial Science Plan, Draft, January, 1995.*

D'Abreton, P.C., 1992: Water Vapour fluxes and kinematic forcing of South African summer rainfall. Department of geography and Environmental Studies. *PhD thesis University of Witwatersrand,* Johannesburg, South Africa.

D'Abreton, P.C., and J.A. Lindesay, 1993: Water vapour transport over southern Africa during wet and dry early and late summer months. *International Journal of climatology,* 113, 151-170.

Dent, M.C., R.E. Schulze, H.M. Wills, and S.D. Lynch, 1987: Spatial and temporal analysis and the recent drought in the summer rainfall region of southern Africa. *Water SA. Vol.* 13. No. 1 January 1987.

Diaz, H.F. 1996: Precipitation monitoring for climate change detection, *Meteorological Atmospheric Physics.* 60, 179-190.

Dilley, M., 1996: Usefulness of climate forecasting information for drought mitigation and response from a Donor's standpoint. *Workshop in Reducing Climate-Related Vulnerability in southern Africa, 1-4 October 1996,* Victoria falls, Zimbabwe, p.30-37.

Dyer, T.G. J., 1979: Rainfall along the east coast of southern Africa, the Southern Oscillation and the latitude of the subtropical high pressure belt. *Quarterly Journal of Royal meteorological Society.,* 105, 445-451.

Dyer, T.G.J., 1981: Apparent absence of the quasi-Biennial Oscillation in sea level pressure in the south Indian and South Atlantic Oceans. *Royal Quarterly Journal of Meteorology.* pp. 461-467.

Ebisuzaki, W., M. Chelliah and B. Kistler, 1998: NCEP/NCAR Reanalysis: Caveats. *Proceedings of the first international conference on Reanalysis,* Silver Spring, Maryland, USA, 27-31 October 1997, *WMO/TD-No. 876,* 81-94.

ECMWF, 1989: The description of the ECMWF/WMO global analysis data sets.

Folland, C.K., T.N. Palmer and E.D. Parker, 1986: Sahel rainfall and worldwide sea temperatures 1901-1985. *Nature,* 320, 602-607.

Folland, C.K., D.E. Parker, and D.E. Jones, 1987: Experiments in the prediction of African rainfall. *Proc. First Technical Conference on Meteorological Research in Eastern and Southern Africa, 6-9 January 1987.* Nairobi, Kenya.

Gondwe, M.P. and M.R. Jury, 1997: Sensitivity of vegetation (NDVI) to climate over southern Africa: relationship with rainfall and OLR, *SA Geogr Journal.*

Gray, W.M., J.D. Sheaffer, and J.A.Knaff, 1991: Hypothesised mechanism for stratospheric QBO influence on ENSO variability. *5th Conference on Climate variation,* Denver, Colorado, U.S.A.

Hargraves, R., and M.R. Jury, 1997: Composite meteorological structure of flood events over the eastern mountains of South Africa. *Water SA,* Vol. 23, No.4, 357-363

Harangozo, S.A., and M.S.J. Harrison, 1983: On the use of synoptic data in indicating the presence of the cloud bands over southern Africa, *South African Journal of Science,* 79, 413-414.

Harangozo, S.A., 1989: Circulation characteristics of some South African rainfall systems. *MSc. Dissertation, University of Witwatersrand.*, South Africa.

Harrison, M. S.J., 1984: A generalised classification of South African summer rain-bearing synoptic systems. *Journal of Climate*, 4, 567-560.

Harrison,M.S.J., 1986: A synoptic climatology of south African rainfall variability. *PhD Thesis, University of the Witwatersrand, 341pp.*

Hastenrath, S.,A. Nicklis and L.Greishar, 1993: Atmospheric hydrospheric mechanisms of climate anomalies in the western Indian ocean. *Journal of Geophysical Research . Res.*, 98, 20219-20235.

Hastenrath, S., 1995: Recent advances in Tropical prediction. *Journal of Climate*, 8, 1519-1532.

Hastenrath, S., L. Greishar, and J. Van heerden 1995: Prediction of the summer rainfall over South Africa. *Journal of climate,* 8, 1511-1518.

Hirst, A.C. and S. Hastenrath, 1983: Atmosphere-Ocean mechanisms of climate anomalies in the Angola-tropical Atlantic sector, *Journal of Phys. Oceanogr.*, 13, 1146-1157.

Hofmeyer, W.L., and V.Gouws, 1964: A statistical and synoptic analysis of wet and dry conditions in the northwestern Transvaaal, Notos, *South African Weather Bureau,* 13, 37-48.

Holton, J.R., and R.S. Lindsen, 1972: An updated theory for the Quasi-biennial Oscillation of the tropical stratosphere. *Journal of Atmospheric Science*, 29, 1076-1080

.Holton, J.R., 1979: An Introduction to Dynamic Meteorology, second edition. *Academic press,* New York, Vol 23, pp 130-139.

Horel and J.M. Wallace, 1981: Planetary scale atmospheric phenomena associated with the Southern Oscillation, *Monthly Weather Review,* 109, 813-829.

Hsu, C.P.F. and J.M. Wallace, 1976: The global distribution of the annual and semi-annual cycles in precipitation. *Monthly Weather Review*, 104, 1093-1101.

Hulme, M. (ed.), 1996: Climate Change and southern Africa. An exploration of some potential impacts and implications in the SADC region. *Norwich, U.K: Climatic Research Unit, University of East Anglia.*

Janowiak J.E. 1988: An investigation of inter-annual rainfall variability in Africa. *Journal of Climate,* 1, 240-255.

Jarnal, B., 1993: Synoptic Climatology in Environmental Analysis. *Belhaven Press,* p. 48-130.

Jury, M.R. and J.A. Lindesay, 1991: Atmospheric circulation controls and characteristics of a flood event in central South Africa, *Journal of Climatology,* 11, 609-627.

Jury, M.R. and B. Pathack, 1991: A study of climate and weather variability over the tropical southwest Indian Ocean, *Meteorology and Atmospheric Physics,* 47, 37-48.

Jury, M.R., B. Pathack and D.M. Legler, 1991: Structure and variability of surface atmospheric circulation anomalies over the tropical South-West Indian Ocean in the austral summer. *South Africa Journal of Marine Science,* 11, 1-14.

Jury, M.R., 1992: A climatic dipole governing the inter-annual variability of convection over Southwest Indian Ocean and Southeast Africa region. *Trends in Geophysical research,* 1, 165-172.

Jury, M.R., B. Pathack and B.J. Sohn, 1992: Spatial structure and international variability of summer convection over southern Africa and the SW Indian Ocean, *South African Journal of Science,* 88, 275-280.

Jury, M.R. and S.W. Lyons, 1992: Contrasting synoptic events over South Africa in the dry summer of 1983., *South African Geographical Journal.*

Jury, M.R. and C. McQueen, 1993: Climate atlas of climatic determinants for Tanzania.

Jury, M.R. and K. levey 1993: The climatology and characteristics of drought in the eastern Cape of South Africa. *International Journal of climatology,* 13, 629-649.

Jury, M.R., and J.R.E Lutjeharms, 1993: 'The structure and possible forcing mechanisms of the 1991-1992 drought over southern Africa', *S. Afr. Tydskr. Nat. Tech.,* 12, 8-16.

Jury, M.R. and B. Pathack, 1993: Composite climatic patterns associated with extreme modes of summer rainfall over southern Africa: 1975-1984. *Theoretical and Applied Climatology,* 47, 137-145.

Jury, M.R., B. Pathack, D. Waliser, 1993: satellite OLR and microwave data as a proxy for summer rainfall over sub-equatorial Africa and adjacent oceans. *International Journal of Climatology,* 13, 257-269.

Jury, M.R., C. Mc Queen and K. Levey, 1994: SOI and QBO Signals in the African region. *Theoretical and Applied and Climatology,* 50, 103-115.

Jury, M.R., B.A. Parker, Raholijao and A. Nassor, 1995: Variability of summer rainfall over Madagascar: Climate determinants at inter-annual scales. *International Journal of climatology*, 15, 1323-1332.

Jury, M.R., 1995: A review of research on ocean-atmosphere interactions and South African climate variability. *South African Journal of Science*, Vol 91 of June 1995.

Jury, M.R., 1996: Regional teleconnection patterns associated with summer rainfall over South Africa, Namibia, and Zimbabwe.*International Journal of Climatology*, 16,135-153.

Jury, M.R., B. Pathack, C.J. DE W Rautenbach and J. Vanheerden, 1996: Drought over South Africa and Indian Ocean SST: Statistical and GCM results. *The Global Atmosphere and Ocean System*, Vol. 4, 47-63.

Jury, M.R., 1997: Inter-annual climate modes over southern Africa from satellite cloud OLR 1975-1994. *Theoretical and Applied Climatology*, 57, 155-163.

Jury, M.R., 1998: Statistical Analysis and Prediction of Kwazulu-Natal Climate. *Theoretical and Applied Climatology*, 60, 1-10.

Jury, M.R., 1998: Forecasting water resources in South Africa. *Water resources variability in Africa during the XXth century (Proceeding of the Abijan'98 Conference held at Abijan, Cote d'Ivoire).*

Kalnay, E., and et al., 1996: The NCEP/NCAR reanalysis 40-year project. *Bulletin of the American Meteorological Society*, 77, 437-471.

Kamdonyo, D., 1993: Use of the percentiles in delineating the spatial and temporal extent of Malawi's great droughts. *Proceedings of the forth annual scientific conference of the the SADC-Land and Water Management Research Programme*, Windhoek, Namibia.

Kidson, J., 1977: African rainfall and its relation to the upper air circulation. *Quarterly Journal of the Royal Meteorological Society.*, 103, 441-456.

Kilonsky, B.J., and C.S. Ramage, 1976: A technique for estimating tropical ocean rainfall from satellite observations. *Journal of Applied Meteorology.* ,15, 972-975.

Knaff, J.A., W.M. Gray, and J.D. Sheaffer, 1991: Evidence for an association between the stratospheric QBO and ENSO. *5th Conference on Climate variation*, Denver, Colorado., U.S.A.

Knutson, T,R. And K.M. Weickmann, 1987: 30-60 day atmospheric circulations. Composite life cycles of convection and circulation anomalies. *Monthly Weather Review.*,115, 1407-1436.

Kousky, V.E., M.T. Kayano and I.F.A. Cavalcanti, 1984: A review of the southern Oscillation ocean-atmospheric circulation changes and related rainfall anomalies. *Tellus,* 36a, 490-504.

Kumar, S., 1978: Interaction of upper westerly waves with the Inter tropical convergence zone and their effects on the weather over Zambia during the rainy season, *Government printer, Lusaka,* Zambia.

Levey, K.M. 1993: Intra-seasonal oscillations of convection over southern Africa. *MSc. Thesis, University of Cape Town,* South Africa. 236pp.

Levey, K.M., and M.R. Jury, 1996: Composite Intra-Seasonal Oscillations of Convection over southern Africa. *Journal of Climate,* Vol. 9, 8, 1910-1920.

Liebmann, B. and D.L. Hartmann, 1982: Interannual variation of outgoing IR associated with tropical circulation changes during 1974-78, *Journal of Atmospheric Sciences,* 39, 1153-1162.

Liebmann, B., and C.A. Smith, 1996: Description of a complete (interpolated) Outgoing Longwave Radiation Dataset. *Bulletin of the American meteorological Society,* 77, 1275-1277.

Lindesay, J.A. and M.S.J. Harrison, 1986: The southern Oscillation and South African rainfall, *South African Journal of Science,* 82, 196-198.

Lindesay, J.A., 1987: Relationships between the Southern Oscillation and atmospheric circulation changes over southern Africa, 1957 to 1982. *PhD. Thesis, University of Witwatersrand,* South Africa.

Lindesay, J.A., 1988: South African rainfall, the Southern Oscillation and a southern hemisphere semi-annual cycle. *International Journal of Climatology,* 8,17-30.

Lindesay, J.A. and C.H. Vogel, 1990: Historical evidence for Southern Oscillation-Southern African rainfall relationships, *International Journal of Climatology,* 10, 679-689.

Lindesay, J.A., and M.R. Jury, 1991: Atmospheric circulation controls and characteristics of flood events in central South Africa. *International Journal of Climatology,* 11, 609-627.

Lough, J.N., 1986: Tropical Atlantic sea surface temperatures and rainfall variations in sub-Saharan Africa, *Monthly Weather Review.* ,114, 561-570.

Lyons, S.W., 1991: Origins of convective variability over equatorial southern Africa during austral summer, *Journal of Climate, 4, 23-39.*

Madden, R.A., and P.R. Julian, 1971: Detection of a 40-50 day Oscillation in the Zonal Wind in the Tropical Pacific. *Journal of the Atmospheric Sciences, Vol.* 28, 702-708.

Madden, R.A., and P.R. Julian, 1972: Description of Global-Scale Circulation cells in the Tropics with a 40-50 day period. *Journal of the Atmospheric Sciences. Vol.* 29,1109-1108.

Madden, R. A., 1986: Seasonal Variations of the 40-50 Day Oscillation in the Tropics. *Journal of the Atmospheric Sciences,* Vol. 43, 24, 3138-3157.

Madden, R.A. and P.R. Julian, 1994: Observations of the 40-50-day tropical oscillation- A review. *Monthly Weather Review,* Vol. 122, 813-837.

Majodina, M., 1995: Composite analysis of winter storms south of Africa, *Honours thesis, University of Cape Town,* South Africa.

Makarau, A., 1995: Intra-seasonal oscillatory modes of the southern Africa summer circulation. *PhD. Thesis, University of Cape Town,* South Africa.

Makarau, A., and M.R. Jury, 1997: Seasonal cycle of convective spells over southern Africa during Austral summer. *International Journal of Climatology,* Vol. 17, 1317-1332.

Malawi Ministry of Agriculture Report, 1993: Food situation in Malawi.

Mason, S.J. 1992: Sea surface temperature and south African rainfall variability. *Ph.D. Thesis, University of the Witwatersrand.* 235pp. South Africa.

Mason. S.J. and P.D. Tyson, 1992: The mudulation of sea surface temperature and rainfall associations over southern Africa with solar activity and the Quasi-biennial Oscillation. *Journal of Geophysical Research, res.,* 97, 5847-5856.

Mason, S.J., J.A. Lindesay, and P.D. Tyson, 1994: Simulating drought in southern Africa using sea surface temperature variations. *Water SA* Vol. 20, 15-22.

Mason, S.J., 1995: Sea surface temperature-South African rainfall associations, 1910-1989, *International Journal of Climatology,* 15, 119-135.

Mason, S.J. and A.M. Joubert, 1995: A note on inter-annual variability and water demand in the Johannesburg region. *Water SA Vol.* 21 No. 3 July 1995.

Mason, S.J. , A.M. Joubert, C. Cosjin, and S.J. Crimp, 1996: Review of the current state of seasonal forecasting techniques with applicability to southern Africa. *Water SA..* 22, 203-209.

Mason, S.J., 1997: Review of recent development in seasonal forecasting of rainfall. *Water SA,* 23, 57-62.

Mason, S.J., 1998: Seasonal forecasting of South African Rainfall using a non-linear discriminant analysis model. *International Journal of Climatology*, 18, 147-164.

Matarira, C.H., 1990: Drought over Zimbabwe in a regional and global context, *International Journal of Climatology*, 10, 609-625.

Matarira, C.H., and M.R. Jury, 1992: Contrasting meteorological structure of intra-seasonal wet and dry spells in Zimbabwe. *International Journal of Climatology*, Vol. 12, 165-176.

Miron, O. and J.A. Lindesay, 1983: A note on changes in airflow patterns between wet and dry spells over South Africa, 1963-1979, *South African Geographical Journal.* , 65, 141-147.

Miron, O. and P.D. Tyson, 1984: Wet and dry conditions and pressure anomaly fields over South Africa and the adjacent oceans, 1963-79, *Monthly Weather Review,* 112, 2127-2132.

Montgomery, R.B., 1940: Report on the work of G.T. Walker, *Monthly Weather Review*, 39 (supplement), 1-22.

Mo K.C. and R.W. Higgins, 1998: Atmospheric processes associated with precipitation variability in the Western United States of America. *Proceedings of the first WCRP International Conference on Reanalyses*, 27-31 October 1997, Silver Spring, Maryland, USA, *WMO/TD-No. 876*, 183-186.

Mpeta, E.J., 1997: Intra-seasonal convection dynamics over southwest and northeast Tanzania: An observatory study. *MSc. thesis. University of Cape Town*, South Africa.

Mukherjee, B., K. Indira, S.R. Reddy and R. Murty, 1985: Quasi-Biennial Oscillation of stratospheric zonal wind and Indian summer monsoon, *Monthly Weather Review.*, 113, 1421-1424.

Mulenga, H.M., 1998: Southern African climatic anomalies, summer rainfall and the Angola low. *PhD. Thesis. University of Cape Town,* South Africa.

Naeraa, M., and M.R. Jury, 1997: Tropical Cyclone Composite Structure and Impacts over Eastern Madagascar during January-March 1994. *Meteorology and Atmospheric Physics*, 65, 43-53

Nassor, A., 1994: Monsoon surges, tropical cyclones and extreme rainfall in NW Madagascar *Msc. Thesis, University of Cape Town,* South Africa.

Nassor, A., and M.R. Jury 1997: Intra-Seasonal Climate Variability of Madagascar, Part2: Evolution of Flood events. *Meteorology and Atmospheric Physics,* 64, 243-254.

Naujokat, B., 1986: An update of the observed quasi-biennial oscillation of the stratospheric winds over the tropics. *Journal of atmospheric Science*, 43, 1873-1877.

Newell, R.E., J.W.Kidson, D.G. Vincent and G.J. Boer, 1972: The general circulation of the tropical atmosphere and interractions with extratropical latitudes. *Vol. I, MT Press, Cambridge,* MA.

Nicholson S.E., 1985: Sub-Saharan rainfall 1981-84. *Journal of Climatology and Applied Meteorology,* 24, 1388-1391.

Nicholson S.E., 1986: Rainfall variability in southern and equatorial Africa. Its relation to Atlantic sea surface temperatures and the southern oscillation. *American Meteorological Society,* 657-676.

Nicholson, S.E. and D. Entekhabi, 1986: The quasi-periodic behaviour of rainfall variability in Africa and its relationship to the Southern Oscillation, *Archiv fur meteorologie, geophysik und bioklimatologie,* Ser. A., 34, 311-348.

Nicholson, S.E. and Entekhabi, D., 1987: rainfall variability in equatorial and southern Africa: relationships with sea surface temperature along the southwestern coast of Africa. *Journal of Climate and Applied Meteorology.,* 26, 561-578.

Nicholson, S.E., J. Kim and J. Hoopingarner, 1988: Atlas of African rainfall and its interannual variability, Department of Meteorology, *The Florida State University,* Tallahassee, 237pp.

Nicholson, S.E., 1989: African drought: Characteristics, casual theories and global teleconnections. In *'Understanding climate change'*, *American Geophysical Union,* Washington, DC., 79-101.

Nicholson, S.E., and B.S. Nyenzi, 1990: Temporal and spatial variability of SSTs in the tropical Atlantic and Indian Oceans, *Meteorology and Atmospheric Physics,* Vol. 42, 1-17.

Ngara, R., D.L. McNaughton, and S. Lineham, 1983: Seasonal rainfall fluctuations in Zimbabwe, *Zimbabwe Agriculture Journal,* 80, 47-53.

Nkhokwe, J.L., 1996: Predictability of inter-annual rainfall variability in Malawi. Unpublished, *Malawi Meteorological Department,* Malawi.

Nyenzi, B.S., 1988: Mechanism of East African rainfall variability. *PhD. Thesis, Florida State University,* 184pp.

Ogallo, L.J., 1987: Teleconnections between rainfall in East Africa and some global parameters. *Proc. First Technical Conference on Meteorological Research in Eastern and Southern Africa, 6-9 January 1987.* Nairobi, Kenya, 71-75.

Ogallo, L.J. and k.A. Suleiman, 1987: Rainfall characteristics in East Africa during the El Nino years. *Proc. First Technical Conference on Meteorological Research in Eastern and Southern Africa, 6-9 January 1987.* Nairobi, Kenya, 76-80.

Parker, B.A., 1994: Composite structure of tropical cyclones in the SW Indian Ocean, *Msc. thesis, University of Cape Town*, South Africa.

Parker, D.E., C.K. Folland, and M.N. Ward, 1988: Sea surface temperature anomaly patterns and prediction of seasonal rainfall in the Sahel region of Africa, in: *Recent climatic change. Ed: S. Gregory, Belhaven press, London*, 1666-1678.

Parker, D.E, C.K. Folland, and J.A. Owen, 1987: The influence of global sea surface temperature of African rainfall. *Proc. First Technical Conference on Meteorological Research in Eastern and Southern Africa, 6-9 January 1987.* Nairobi, Kenya, *46-47.*

Pathack, B. 1993: Modulation of summer rainfall over South Africa by global climatic processes. *PhD. Thesis. University of Cape Town*, South Africa.

Philander, S.G., 1989: El Nino, La Nina and the Southern Oscillation. *International Geophysical series*, 46.

Plumb, R.A., 1984: The quasi-Biennial Oscillation. In the "Dynamics of the Middle Atmosphere" edited by J.R. Holton and T. Matsumo: *terra Scientific Publishing Company.*

Preston-Whyte, R.A. and P.D. Tyson, 1988: The Atmosphere and weather of Southern Africa, *Oxford University Press, Cape Town*, South Africa, 374pp.

Rasmusson, E.M. and T.H. Carpenter, 1982: Variations in tropical sea surface temperature and surface wind fields associated with the El Nino/Southern Oscillation, *Monthly Weather Review*, 110, 354-384.

Rocha, A., 1992: The Influence of global SSTs on the Southern African summer climate, P*hD Thesis, University of Melbourne*, Australia.

Ropelewski, C.F. and M.S. Halpert, 1987: Global and regional scale Precipitation and temperature patterns associated with El Nino/Southern Oscillation. *Monthly Weather Review*, 115, 1606-1626.

Ropelewski, C.F., M.S. Halpert, 1989: Precipitation patterns associated with the high index phase of the Southern Oscillation. *Journal of Climate*. 2, 268-284.

Ropelewski, C.F., M.S. Halpert, and X. Wang, 1992: Observed tropospheric Biennial variability and its relationship to the Southern Oscillation. *Journal of Climatology*., 5, 594-616.

Rui, H., and B. Wang, 1990: Development Characteristics and Dynamics structure of Tropical Intraseasonal Convection Anomalies. *Journal of the Atmospheric Sciences*. Vol. 47, 3, 357-379.

Schulze, R.E., 1984: Hydrological simulation as a tool for agricultural drought assessment. *Water SA*, 10, 1, 55-62.

Taljaard, J.J., 1986b: Contrasting atmospheric circulation during dry and wet summers in South Africa, *South Africa Weather Bureau Newsletter*, No. 445, 1-5.

Taljaard, J.J., 1987: The anomalous climate and weather systems over South Africa during summer 1975-1976, *South Africa Weather Bureau technical paper*, No. 16, 80pp.

Theron, G.F. and M.S. J. Harrison,1990: Thermodynamic properties of the mean circulation over southern Africa. *Theoretical and applied Climatology*, 43, 75-89.

Torrance, J.D., 1972: Malawi, Rhodesia and Zambia, in *Climates of Africa*, Ed. Griffiths, J.F., *World Survey of Climatology*, Vol. 10, *Elsevier, Amsterdam*, 409-460.

Trenberth, K.E., 1980: Atmospheric Quasi-Biennial Oscillations, *Monthly Weather Review*, 108, 1370-1377.

Tyson, P.D., 1981: Atmospheric circulation variations and the occurrence of extended wet and dry spells over South Africa. *Journal of Climatology*, 1, 115-130.

Tyson, P.D., 1984: The atmospheric modulation of extended wet and dry spells over South Africa, 1958-1978. *Journal of climatology*, 4, 621-635.

Tyson, P.D., 1986: Climate Change and Variability in Southern Africa, *Oxford University Press*, Cape Town, South Africa.

Van den Heever, S.C., P.C. D'Abreton and P.D. Tyson, 1997: Numerical simulation of tropical-temperate troughs over southern Africa using the CSU RAMS model. *South African Journal of Science*. 93, 359-365.

Walker, G.T., 1924: Correlation in seasonal variations of weather, IX. A further study of world weather (World weather II), *Memoirs of the Indian Meteorological department, 24, 275-332.*

Walker, G.T. and E.W. Bliss, 1937: World Weather VI, *Memoirs of Royal Meteorological Society*, 4, 119-139.

Walker, N.D., 1989: Sea surface temperature-rainfall relationships and associated ocean-atmosphere coupling mechanisms in the southern Africa region. *Ph.D. thesis, university of Cape Town*, South Africa.

Walker, N.D. 1990: Links between South African summer rainfall and temperature variability of the Agulhas and Benguala Current systems. *Journal of Geophysical Research, Res.*, 95, 3297-3319.

Walker, N.D. and J.A. Lindesay, 1989: Preliminary observations of oceanic influences of the February-March 1988 floods in central South Africa, *South African Journal of science*, 85, 164-169.

World Climate Research Programme (WCRP), 1998: *Proceedings of the first WCRP International Conference on Reanalyses*, 27-31 October 1997, Silver Spring, Maryland, USA, *WMO/TD-No. 876.*

Xhu, B., and B. Wang, 1993: The 30-60 day convective seesaw between the tropical Indian and western pacific oceans. *Journal of Atmospheric Science*. 50, 184-199.

Zhakata, W., 1996: Impacts of climate variability and forecasting on agriculture (Zimbabwe experience). *Workshop in reducing Climate-related vulnerability in southern Africa*, 1-4 October 1996, Victoria falls, Zimbabwe.

APPENDIX

APPENDIX A1

Acronyms and abbreviations

AOH.....Atlantic Ocean High

IOH.....Indian Ocean High

ITCZ.....Inter-Tropical Convergence Zone

MRI.....Malawi rainfall index

MJJ.....May to July

JJA.....June to August

JAS.....July to September

ASO.....August to October

SON.....September to November

OND.....October to December

MO.....May to October

NA.....November to April

NDJ.....November to January

DJF.....December to February

JFM.....January to March

FMA.....February to April

QBO.....Quasi-Biennial Oscillation

SST.....Sea surface temperature

SOI.....Southern Oscillation Index

SO.....Southern Oscillation

ENSO.....El Nino-Southern Oscillation

KZ Natal.....Kwazulu/Natal

APPENDIX A2

List of NCEP data used in the study:

Parameter	Pressure levels (hPa)			**Units**
Sea level pressure	1000	********	********	hPa
Geopotential height	850	500	200	gpm (m)
Vector wind	850	500	200	$m\ s^{-1}$
Zonal wind	850	500	200	$m\ s^{-1}$
Meridional wind	850	500	200	$m\ s^{-1}$
Outgoing longwave radiation (OLR)	Surface	********	********	$w\ m^{-2}$
Air temperature	850	********	********	°C
Precipitable water	Between	1000-300	levels	kg m-2
Sea surface temperature (SST)	Sea Level 1000	********	********	°C
Streamfunction	0.995 sigma level	********	0.210 sigma level	$m^2\ s^{-1}$
Velocity potential	0.995 sigma level	********	0.210 sigma level	$m^2\ s^{-1}$
Relative humidity	850	500	********	%